UNIVERSIDADE FEDERAL DE MINAS GERAIS
Escola de Engenharia
Programa de Pós-Graduação em Saneamento, Meio Ambiente e Recursos Hídricos

Flávia Cristina Rodrigues Costa

ARSENIC REMOVAL FROM DRINKING WATER BY MEMBRANE TECHNOLOGY: a solution for small and large communities

Belo Horizonte
2024

Flávia Cristina Rodrigues Costa

ARSENIC REMOVAL FROM DRINKING WATER BY MEMBRANE TECHNOLOGY: a solution for small and large communities

Tese apresentada ao Programa de Pós-graduação em Saneamento, Meio Ambiente e Recursos Hídricos da Universidade Federal de Minas Gerais, como requisito parcial à obtenção do título de Mestre/Doutor em Saneamento, Meio Ambiente e Recursos Hídricos.

Área de concentração: Meio Ambiente

Linha de pesquisa: Caracterização, prevenção e controle da poluição

Orientador: Míriam Cristina Santos Amaral Moravia

Belo Horizonte
2024

Costa, Flávia Cristina Rodrigues.
C837a Arsenic removal from drinking water by membrane technology [recurso eletrônico] : a solution for small and large communities / Flávia Cristina Rodrigues Costa.- 2024.
1 recurso online ([202] f. : il., color.) : pdf.

Orientadora: Míriam Cristina Santos Amaral Moravia.

Tese (doutorado) - Universidade Federal de Minas Gerais, Escola de Engenharia.

Apêndices: f. [181]-[202].

Bibliografia: f. 165-180.

1. Engenharia sanitária - Teses. 2. Meio ambiente - Teses. 3. Membranas (Tecnologia) - Teses. 4. Água potável - Contaminação - Teses. 5. Arsênio - Teses. 6. Avaliação de riscos - Teses. 7. Água - Purificação - Coagulação - Teses. 8. Água - Purificação - Floculação - Teses. I. Amaral, Míriam Cristina Santos. II. Universidade Federal de Minas Gerais. Escola de Engenharia. III. Título.

CDU: 628(043)

Ficha catalográfica elaborada pelo bibliotecário Reginaldo César Vital dos Santos CRB/6 2165
Biblioteca Prof. Mário Werneck, Escola de Engenharia da UFMG

UNIVERSIDADE FEDERAL DE MINAS GERAIS

Escola de Engenharia
Curso de Pós-Graduação em Saneamento, Meio Ambiente e Recursos Hídricos

"Arsenic Removal From Drinking Water By Membrane Technology: A Solution For Small And Large Communities"

FLÁVIA CRISTINA RODRIGUES COSTA

Tese defendida e aprovada pela banca examinadora constituída pelos Senhores:

Profa MÍRIAM CRISTINA SANTOS AMARAL MORAVIA

Profa SONALY CRISTINA REZENDE BORGES DE LIMA

Profa MIRIA HESPANHOL MIRANDA REIS

Profa ARIUSKA KARLA BARBOSA AMORIM

Profa Camila Baldasso

Aprovada pelo Colegiado do PG SMARH

Prof. Eduardo Coutinho de Paula Santos Amaral Moravia
Coordenador

Versão Final aprovada por

Profª. Miriam Cristina
Orientadora

Belo Horizonte, 25 de outubro de 2024.

Documento assinado eletronicamente por **Ariuska Karla Barbosa Amorim**, **Usuário Externo**, em 24/10/2024, às 08:16, conforme horário oficial de Brasília, com fundamento no art. 5º do Decreto nº 10.543, de 13 de novembro de 2020.

Documento assinado eletronicamente por **Camila Baldasso**, **Usuário Externo**, em 25/10/2024, às 16:49, conforme horário oficial de Brasília, com fundamento no art. 5º do Decreto nº 10.543, de 13 de novembro de 2020.

Documento assinado eletronicamente por **Sonaly Cristina Rezende Borges de Lima**, **Professora do Magistério Superior**, em 10/02/2025, às 17:28, conforme horário oficial de Brasília, com fundamento no art. 5º do Decreto nº 10.543, de 13 de novembro de 2020.

Documento assinado eletronicamente por **Miriam Cristina Santos Amaral Moravia**, **Professora do Magistério Superior**, em 13/03/2025, às 14:04, conforme horário oficial de Brasília, com fundamento no art. 5º do Decreto nº 10.543, de 13 de novembro de 2020.

Documento assinado eletronicamente por **Miria Hespanhol Miranda Reis**, **Usuário Externo**, em 25/03/2025, às 07:55, conforme horário oficial de Brasília, com fundamento no art. 5º do Decreto nº 10.543, de 13 de novembro de 2020.

A autenticidade deste documento pode ser conferida no site https://sei.ufmg.br/sei/controlador_externo.php?acao=documento_conferir&id_orgao_acesso_externo=0, informando o código verificador **3671838** e o código CRC **9197CBFC**.

AGRADECIMENTOS

Agradeço primeiramente a Deus, pois do seu amor que foi possível o sustento em todas as dificuldades. Obrigada, Senhor, por guiar o meu caminho, por fazê-lo mais belo e por cuidar de mim através de tantas pessoas.

Agradeço de todo coração meu esposo, Diego, que além de todo companherismo, amor, paciência e incentivo, abraçou o meu sonho como se fosse o seu e fez um projeto pessoal se tornar um projeto da nossa família. Não caberia aqui tudo o que tenho a agradecer a você durante esse período.

Aos meus amores: João, Isabel e Letícia. Meus presentes recebidos ao longo dessa caminhada. A conclusão dessa etapa pode ter sido mais desafiadora com a chegada de cada um de vocês, mas tornou essa caminhada infinitamente mais bonita e digna de ser comemorada. O amor à vocês dá um novo sentido a tudo o que faço.

Aos meus pais, Vicente e Sandra, e meus irmãos, Daniel e Samuel. Obrigada por todo amor, carinho e incentivo.

Agradeço a família do meu esposo, em especial à dona Vani, por todo auxílio na reta final do doutorado.

Agradeço aos amigos de CL, minha companhia para a vida, em especial aos amigos que Brasília me trouxe, e a todos os amigos com os quais fui presenteada ao longo desses anos.

Agradeço a todos os professores que passaram em minha vida, que com empenho e dedicação, foram essenciais na minha trajetória.

Agradeço imensamente a minha orientadora, Profa. Dra. Míriam Amaral. Míriam, também não caberia aqui o quanto sou grata a você. Claro, te agradeço por toda experiência e conhecimento compartilhados, pela condução da pesquisa, por todo o apoio, compreensão, atenção, paciência e confiança. Mas minha gratidão vai muito além. Seria óbvio dizer à orientadora que “sem você isso não seria possível”. Mas quando digo isso a você, é por mil razões que fogem do óbvio. Toda vez que penso

em como você possibilitou que eu continuasse nesse caminho, me emociono. Que Deus a abençoe!

Agradeço a todos os colegas do GEAPs, pelas experiências compartilhadas. Em especial, sou muito grata ao Prof. Dr. Victor: muito obrigada pela parceria ao longo desse tempo! Agradeço também à Marina, pela parceria.

Agradeço à UFMG, ao DESA e ao PPG SMARH pela oportunidade e recursos oferecidos para a desenvolvimento da pesquisa e para minha formação. Agradeço à CAPES pela bolsa concedida.

Agradeço às professoras Ariuska, Camila, Miria e Sonaly por gentilmente aceitarem o convite para compor a banca de avaliação deste trabalho.

Por fim, agradeço a todos que, de alguma maneira, foram importantes para a minha formação e para a realização dessa pesquisa. A vocês, minha sincera gratidão!

“É justo que muito custe o que muito vale”

(Santa Teresa D’Ávila)

RESUMO

O arsênio (As) é um elemento que compõe a crosta terrestre e é liberado no meio ambiente naturalmente, mas também devido a atividades antropogênicas, como a mineração. Dessa forma, o As chega aos recursos hídricos e, em muitos países, tem sido detectado em águas subterrâneas, superficiais e potáveis em concentrações muito superiores às recomendadas pela OMS para consumo humano (10 µg/L). Isso representa um sério risco à saúde humana devido aos vários efeitos adversos que o consumo de água com As pode causar, como câncer de pele. Nesse contexto, esta tese teve como principal objetivo avaliar o tratamento de água superficial real contendo altas concentrações de arsênio (até cerca de 35 µg/L) usando ultrafiltração (UF) e osmose inversa (OI) em escala piloto. Primeiramente, avaliou-se a contribuição do tratamento prévio da água pelo processo convencional de tratamento de água (pré-oxidação, coagulação/floculação e decantação) na performance da UF e da OI no tratamento de águas com elevada concentração de As. O sistema de UF-OI gerou água de elevada qualidade (cor < 15 uH, turbidez < 0.1 NTU, ferro < 0.3 mg/L, manganês < 0.1 mg/L), atendendo os limites legais brasileiros para água potável, com ou sem pré-tratamento, porém o pré-tratamento aplicado foi importante para melhorar a permeabilidade da membrana de UF. Os resultados também evidenciaram a maior resiliência do sistema de tratamento com integração da UF-OI ao processo convencional. A OI foi essencial para que os padrões de potabilidade em relação a As fossem atingidos, assegurando um permeado com concentração inferior a 0.5 µg/L. Uma vez confirmada a viabilidade do uso do sistema UF-OI para remoção de arsênio de água superficial,o sistema foi operado por mais de 2000 horas, visando a avaliação da influência do modo de operação (Feed and Bleed e Full Drain), da vazão de retrolavagem e da variação da concentração de sólidos na alimentação no desempenho da UF. Foi avaliado ainda a estabilidade da OI na remoção de arsênio, simulando as condições de diferentes módulos de um sistema de duplo estágio. A operação no modo Full Drain favoreceu a maior permeabilidade da membrana, que foi 10,5% maior do que durante o modo de operação Feed and Bleed. Ademais, no caso de água com baixa concentração de sólidos (turbidez < 10 NTU), não há necessidade de adoção de elevada razão entre fluxo de retrolavagem/ fluxo de permeado. Uma razão de 0.91 foi suficiente para o controle da incrustação. A turbidez da alimentação teve impacto na permeabilidade da membrana A permeabilidade reduziu de 186.4 para 182.3 L/m^{2}h.bar quando a turbidez aumentou para valores > 10 NTU. A concentração de As no permeado de UF foi em torno de 8-30 µg/L, resultado esse influenciado pela especiação do As. A UF atua apenas na retenção de As associado a partículas e coloides. Para remoção de As dissolvido, a OI se faz necessária. A OI garantiu a produção de um permeado com concentração < 0.5 µg/L. Outra alternativa para remoção de As é o uso da dosagem de coagulante ($FeCl_3$) em linha na alimentação da ultrafiltração. A dosagem de coagulante em linha aumentou a eficiência da UF e a concentração de As no permeado foi reduzida de valores de até 23 µg/L para valores < 10 µg/L, tornando a UF adequada para remoção de arsênio. A adição do coagulante também promoveu o aumento do tamanho das partículas, aumentando a porosidade e permeabilidade da torta formada, melhorando a permeabilidade. Destaca-se que o concentrado da OI apresentou qualidade suficiente para seu enquadramento ao padrão de lançamento vigente. Recomenda-se a recirculação do concentrado da UF para o início do tratamento da ETA para aumentar a recuperação de água. Os resultados encontrados podem subsidiar o projeto de

sistemas que podem ser aplicados tanto como polimento de ETAs que recebem como afluente águas com elevadas concentrações de As, com um custo operacional total que varia entre 1.05 e 4.34 US$/$m^3$, quanto para comunidades menores com um custo operacional do sistema de membranas de 0.47-0.49 US$/$m^3$. Assim, a tese contribui para o alcance do Objetivo de Desenvolvimento Sutentável 6 da ONU: garantir disponibilidade e manejo sustentável da água e saneamento para todos.

Palavras-chave: contaminação por arsênio; tratamento de água potável; membranas. coagulação-floculação; avaliação de risco.

ABSTRACT

Arsenic (As) is an element that makes up the Earth's crust and is released into the environment naturally, but also due to anthropogenic activities, such as mining. In this way, As reaches water resources and in many countries, it has been detected in groundwater, surface water, and drinking water at concentrations much higher than those recommended by the WHO for human consumption (10 µg/L). It poses a serious risk to human health due to the various adverse effects that its consumption can cause, such as skin cancer. Therefore, it is necessary to apply technologies that efficiently remove arsenic. In this context, this thesis aimed to evaluate the treatment of real surface water containing high concentrations of arsenic (up to approximately 35 µg/L) using ultrafiltration (UF) and reverse osmosis (RO) on a pilot scale. First, the contribution of pretreatment of water by the conventional water treatment process (pre-oxidation, coagulation/flocculation, and decantation) on the performance of UF and RO in the treatment of water with high concentrations of As was evaluated. The UF-RO system generated high-quality water (color < 15 uH, turbidity < 0.1 NTU, iron < 0.3 mg/L, manganese < 0.1 mg/L), meeting the Brazilian legal limits for drinking water, with or without pretreatment, but the applied pretreatment was important to improve the permeability of the UF membrane. The results also demonstrated the greater resilience of the treatment system with the integration of UF-RO into the conventional process. RO was essential for achieving the potability standards concerning As, ensuring a permeate with a concentration below 0.5 µg/L. Once the feasibility of using the UF-RO system for arsenic removal from surface water was confirmed, the system was operated for more than 2000 hours, aiming to evaluate the influence of the operating mode (Feed and Bleed and Full Drain), backwash flow rate, and variation in solids concentration in the feed on the UF performance. The stability of the RO in arsenic removal was also evaluated, simulating the conditions of different modules of a two-stage system. Operation in Full Drain mode favored greater membrane permeability, which was 10.5% higher than during the Feed and Bleed mode. Furthermore, in the case of water with low solids concentration (turbidity < 10 NTU), there is no need to adopt a high backwash flow/permeate flow ratio. A ratio of 0.91 was sufficient for fouling control. Feed turbidity impacted membrane permeability. Permeability decreased from 186.4 to 182.3 $L/m^2h.bar$ when turbidity increased to values > 10 NTU. The As concentration in the UF permeate was around 8-30 µg/L, a result influenced by As speciation. UF acts only on the retention of As associated with particles and colloids. RO is necessary to remove dissolved As. RO ensured the production of a permeate with a concentration < 0.5 µg/L. Another alternative for As removal is dosing in-line coagulant ($FeCl_3$) in the ultrafiltration feed. In-line coagulant dosing increased UF efficiency, and the As concentration in the permeate was reduced from values up to 23 µg/L to values < 10 µg/L, making UF suitable for arsenic removal. The addition of the coagulant also increased the particle size, increasing the porosity and permeability of the cake formed, improving permeability. Notably, the RO concentrate presented sufficient quality to comply with the current discharge standard. It is recommended that the UF concentrate be recirculated at the beginning of the WTP treatment to increase water recovery. The results can support the design of systems that can be applied both as polishing for WTPs that receive water with high concentrations of As as influent, with a total operating cost ranging from US$1.05 to US$4.34/m^3. For smaller communities, the operating costs of the membrane system are US$0.47-0.49/$m^3$. Thus, the thesis contributes to achieving UN Sustainable

Development Goal 6: ensuring the availability and sustainable management of water and sanitation for all.

.

Keywords: arsenic contamination; drinking water treatment; membranes; coagulation-flocculation; risk assessment.
.

LIST OF FIGURES

Figure 2.1. Occurrence of arsenic in water resources of Latin-American countries: (a) groundwater, (b) surface water, and (c) drinking water……..37

Figure 2.2. (a) Lowest and (b) highest arsenic concentration in water from Latin American countries and their comparison with the MCL for plant irrigation (100 µg/L) and animal watering (200 µg/L)……..42

Figure 2.3. Non-carcinogenic risks to human health for the lowest (a) and highest (b) arsenic concentration reported…….43

Figure 2.4. Skin cancer risk for the lowest (a) and highest (b) arsenic concentration reported……...44

Figure 2.5. Risk of bladder and lung cancer in women for the lowest (a) and highest (b) arsenic concentration reported……..44

Figure 2.6. Summary of the procedure developed for arsenic analysis……50

Figure 2.7. Mean absorbance and linear adjustment of results for standards of different concentrations……..…….51

Figure 2.8. Correlation between arsenic concentration values obtained through the standard technique (ICP-MS) and the colorimetric method proposed (n=33)…….51

Figure 2.9. Difference between arsenic concentration values measured by the colorimetric method and the standard technique (ICP-MS) for different samples (n = 109)……..……51

Figure 2.10. Summary of consolidated technologies for arsenic control in water sources……54

Figure 3.1. Monitoring data (from the year 2023) on arsenic, iron, and manganese, provided by environmental agencies [22]……..64

Figure 3.2. Pilot-scale Ultrafiltration - ZeeWeed 500d modules…….67

Figure 3.3. Operational conditions during UF-RO test with (1) and without (2) pretreatment……69

Figure 3.4. (a) Turbidity and (b) color in the feed (F) stream, ultrafiltration permeate (UFp), and reverse osmosis permeate (ROp) in a scenario with and without pretreatment……..……..73

Figure 3.5. Arsenic concentration in the feed stream (F), ultrafiltration permeate (UFp) and reverse osmosis permeate (ROp) with and without pretreatment……..…75

Figure 3.6. Concentration of (a) iron and (b) manganese in the feed stream (F), ultrafiltration permeate (UFp) and reverse osmosis permeate (ROp) with and without pretreatment……76

Figure 3.7. Strategies (a) I and (b) II related to blend ratios in the treatment of waters with different initial arsenic concentrations in scenarios with (C/F-UF-RO) and without (UF-RO) pretreatment……79

Figure 3.8. Permeability and total resistance to filtration for ultrafiltration (UF) and reverse osmosis (RO) in scenarios with and without pretreatment……83

Figure 3.9. Operating Cost of the UF-RO plant treating the entire WTP flow (Membrane lifespan of 7 years)……90

Figure 3.10 CapEX of the UF-RO plant according to different treatment strategies plant according to different treatment strategies ……91

Figure 3.11. Costs for implementing UF-RO treatment systems considering different communities. Treatment of all estimated required flow was considered……92

Figure 4.1 Operational modes of UF: Feed and Bleed (a) and Full Drain (b)……101

Figure 4.2 Operation scheme of the reverse osmosis (RO) pilot plant. Qa: feed flow rate. Qp: permeate flow rate. Qc: concentrate flow rate.……103

Figure 4.3 Effect of operating mode on ultrafiltration membrane permeability ……106

Figure 4.4 Summary of comparison between feed and bleed and full drain operating modes ……111

Figure 4.5 Permeability (K) of UF membrane before (BBW), during (DBW), and after (ABW) backwashing and boxplots showing significant difference ($p<0.001$) between backwash strength practiced in each period. ……112

Figure 4.6 Permeability (K) of UF membrane before (BBW), during (DBW), and after (ABW) backwashing and boxplots showing significant difference ($p<0.001$) between the feed turbidity in each period……113

Figure 4.7 Scatter plots between actual and predicted values for Permeability BBW ……115

Figure 4.8 Contribution of each variable to the permeability value ……115

Figure 4.9 (a) Turbidity and (b) color in the feed and permeate from UF during the long-term operation……117

Figure 4.10. (a) Iron and (b) manganese in the feed and permeate from UF during during the long-term operation ……118

Figure 4.11. Arsenic concentration in the feed and permeate from UF during the long-term operation. ……..……119

Figure 4.12. Arsenic concentration in the feed and permeate from RO during the long-term operation ……..……..122

Figure 4.13. Flux (a), TMP (b) and Permeability (c) in the RO membrane during the simulation of different modules ……125

Figure 4.14. Scanning electron microscopy and elemental mapping (iron – Fe, manganese – Mn, arsenic – As, and aluminum – Al) of (a) ultrafiltration and (b) reverse osmosis membranes ……..……127

Figure 4.15. Excitation Emission Matrix (EEM) for the (a) ultrafiltration and (b) reverse osmosis membrane……128

Figure 5.1. Schematic of the surface water treatment setup, including the processes of coagulation-flocculation, sand filtration, and ultrafiltration……136

Figure 5.2. Normalized ultrafiltration permeate flux (J/J0) for experiments without and with an in-line dose of FeCl3. J: final permeate flux, J0: initial permeate flux. Transmembrane pressure 0.2 bar……..……..141

Figure 5.3. Analysis of particle sizes for two aqueous samples from ultrafiltration feed before (UF) and after (UF-FeCl3) the in-line dosing of FeCl3……142

Figure 5.4. Excitation Emission Matrix (EEM) for ultrafiltration feed samples (a) before and (b) after the in-line dose of FeCl3 (0.086 mg/L), and for ultrafiltration permeate of experiments (c) without and (d) with an in-line dose of FeCl3……..…144

Figure 5.5. Comparison between the parameters of (a) aluminum, (b) arsenic, (c) iron, and (d) manganese after the settling unit, UF permeate, and UF permeate aided by an in-line dose of FeCl3 (UF-FeCl3). Results refer to averages ± standard deviation (n = 3). Effect of concentrate recirculation: bench-scale……...146

Figure 5.6. Comparison of physicochemical characteristics at different stages of the treatment process along the four stages of ultrafiltration concentrate recycling. In-line dose of FeCl3 before ultrafiltration (UF): 0.086 mg/L……..……148

Figure 5.7. Excitation Emission Matrix (EEM) for samples collected after the settling unit and for ultrafiltration permeate……150

Figure 5.8. Comparison between the ultrafiltration (a) permeate flux (J) in L/m2h (LMH), (b) transmembrane pressure (TMP), and (c) normalized flux (J/J0) in pilot-scale operated without and with in-line dosing of FeCl3 (0.086 mg/L)……..……152

Figure 5.9. Comparison between the values of turbidity and color in ultrafiltration (UF) feed and permeate in pilot-scale operated without and with in-line dosing of FeCl3 (0.086 mg/L)……..……..154

Figure 5.10. Comparison between the concentrations of arsenic in ultrafiltration (UF) feed and permeate in pilot-scale operated without and with in-line dosing of FeCl3 (0.086 mg/L). MCL: maximum contaminant level according to national standards for drinking water……..……154

LIST OF TABLES

Table 1.1. Premises, Hypotesis, and specific objectives of the study……..……26

Table 2.1. Exposure parameters used as a single-point estimation values to calculate noncarcinogenic and carcinogenic risks……..……39

Table 2.2. Summary of different techniques used to determine arsenic concentration in aqueous samples……...48

Table 2.3. Costs break down for analyses of total and dissolved arsenic……..…53

Table 3.1. Characterization of water from the Velhas River (UF feed during period without pretreatment) and the settle water (UF feed during period with pretreatment)……..65

Table 3.2. Characterization of the WTP filtered water..……..……..70

Table 3.3. Values of the parameters considered for the economic analysis……71

Table 3.4. Additional physicochemical characterization of the feed stream, ultrafiltration permeate (UFp), and reverse osmosis permeate (ROp) during periods with pretreatment (C/F-UF-RO) and without pretreatment (UF-RO)……..77

Table 3.5. Effect of pretreatment on membrane area and specific energy consumed by the UF-RO system in each blending strategy. In the system without pretreatment, operation in the rainy season was considered, with feed with higher turbidity……..……81

Table 3.6. Physicochemical characterization of UF and RO concentrates……..85

Table 3.7. Characterization of RO concentrates in the C/F-UF-RO and UF-RO tests and comparison with the maximum values allowed for release (COPAM-CERH Resolution No. 08/2022) ……93

Table 3.8. Summary of the main findings of the present study, comparing UF-RO with and without pretreatment.……94

Table 4.1. Physicochemical characterization of the feed (UFF) and permeate (UFp) streams during Feed and bleed and Full Drain operation modes……108

Table 4.2. UF concentrate physical-chemical characterization. *Maximum contaminant level established by local guidelines for wastewater discharge in receiving bodies. **Maximum value allowed for iron ……110

Table 4.3. Additional parameters for characterization of UF permeate during the long-term operation ……..……..119

Table 4.4. Physicochemical characterization of reverse osmosis currents during the simulation of different conditions. Sample N is found in Table C1 of the supplementary material……..…121

Table 5.1. Descriptive statistics of the key physicochemical parameters obtained from the raw surface water within the basin where the water treatment plant is situated……..……137

Table 5.2. Physicochemical parameters during conventional water treatment. Results refer to averages ± standard deviation (n ≥ 3)……139

Table 5.3. Comparison between the parameters of turbidity, apparent color, pH, and conductivity after the settling unit, ultrafiltration (UF) permeate, and UF permeate aided by an in-line dose of FeCl3 (UF-FeCl3)……145

LIST OF ABBREVIATIONS, ACRONYMS AND SYMBOLS

As – Arsenic

WHO - World Health Organization

UF – Ultrafiltration

RO – Reverse Osmosis

BS - best scenario

WS – worst scenario

FAO - Food and Agriculture Organization

DD – Daily dose

DI - Daily water intake

CSF - Cancer slope factor

RfD - Oral reference dose

HQ – Hazard quotient

CR – Cancer risk

SCR - risk of developing skin cancer

BLCR – risk of developing bladder and lung cancer

MCL – Maximum concentration limit

C/F – Coagulation and Floculation

WTP – Water treatment plant

TDS – Total dissolved solids

W – pump’s work

SEC - specific energy consumptio

Qf – feed flow

Qp – Permeate flow

R – Resistance to filtration

FW – Filtered water

J_{BBW} – Flux before backwashing

J_{DBW} – Flux during backwashing

J_{ABW} – Flux after backwashing

SUMMARY

1 CHAPTER 1: GENERAL INTRODUCTION, OBJECTIVES, HYPOTHESES AND STRUCTURE OF THE DOCUMENT 22
1.1 Introduction 22
1.2 Objectives 24
1.2.1 General objective 24
1.2.2 Specific objectives 24
1.3 Document structure 25
2 CHAPTER 2 - ARSENIC IN NATURAL WATERS OF LATIN-AMERICAN COUNTRIES: OCCURRENCE, RISK ASSESSMENT, LOW-COST METHODS, AND TECHNOLOGIES FOR REMEDIATION 27
2.1 Introduction 27
2.2 Arsenic occurence 31
2.3 Risk assessment in Latin-American countries 37
2.3.1 Exposure assessment 38
2.3.2 Carcinogenic risk 39
2.3.3 Risks associated with the use of water for plant irrigation and animal watering 40
2.3.4 Human health risk assessment 41
2.4 Low-cost methods for arsenic quantification 45
2.5 Technologies for arsenic removal 53
2.6 Conclusions 56
3 CHAPTER 3: PRE-OXIDATION AND COAGULATION-FLOCCULATION AS A PRETREATMENT TO UF-RO APPLIED FOR SURFACE WATER TREATMENT AND ARSENIC REMOVAL 58
3.1 Introduction 58
3.2 Methodology 63
3.2.1 Surface water 63
3.2.2 Pilot-plant description 65
3.2.3 Pilot-plant operation 67
3.2.4 Blends 69
3.2.5 Statistical analysis 70
3.2.6 Economic analysis 70
3.3 Results and discussion 71
3.3.1 Membranes performance and compliance with potability standards 71
3.3.2 Membrane fouling 81
3.3.3 Concentrate management 83
3.4 Final considerations 92

4 CHAPTER 4: LONG-TERM PERFORMANCE OF PILOT SCALE UF-RO FOR ARSENIC REMOVAL FROM SURFACE WATER: IMPACT OF OPERATING CONDITIONS 93
Abstract 93
4.1 Introduction 94
4.2 Methodology 98
4.2.1 Feed water 98
4.2.2 Ultrafiltration description and operation 99
4.2.3 Reverse Osmosis description and operation 102
4.2.4 UF-RO Monitoring 103
4.2.5 Data modeling 104
4.2.6 Statistical analysis 104
4.3 Results and discussion 105
4.3.1 Impact of operating mode on UF performance 105
4.3.2 Long-term effects of operational variables in Full-Drain mode 110
4.3.3 Consistency of UF permeate quality in the long-term operation 116
4.3.4 Reverse Osmosis 120
4.3.5 Membrane fouling characterization and chemical cleaning effectiveness 126
4.4 Conclusion 129
5 CHAPTER 5: ULTRAFILTRATION WITH IN-LINE COAGULATION ($FeCl_3$) TO ENHANCE ARSENIC REMOVAL AND IMPROVE DRINKING WATER QUALITY: FROM BENCH TO PILOT-SCALE 131
Abstract 131
5.1 Introduction 131
5.2 Materials and methods 134
5.2.1 Water and sediments sampling 134
5.2.2 Pre-oxidation, coagulation-flocculation, and sand filtration 135
5.2.3 Ultrafiltration: Bench-scale 136
5.2.4 Pilot-scale ultrafiltration 137
5.2.5 Statistical analysis 139
5.3 Results and discussions 139
5.3.1 Coagulation-flocculation and sand filtration 139
5.3.2 Performance of ultrafiltration membranes: Bench-scale 141
5.3.3 Performance of ultrafiltration membranes: Pilot-scale 153
5.4 Final considerations 157
6 CHAPTER 6: GENERAL CONCLUSIONS 159

1 CHAPTER 1: GENERAL INTRODUCTION, OBJECTIVES, HYPOTHESES AND STRUCTURE OF THE DOCUMENT

1.1 Introduction

Arsenic (As) is an element that makes up the Earth's crust and is released into the environment naturally, but also due to anthropogenic activities, such as mining and burning fossil fuels. These activities deserve attention since exposure to inorganic arsenic for long periods can lead to many serious health problems (Howard, 2003). The main route of exposure to arsenic is through drinking water, ingestion, crop control, and food preparation with contaminated water, as several countries have naturally high concentrations of As in their waters (Litter et al., 2019; Tapia et al., 2022).

Given the growing knowledge about the effects of As consumption, the World Health Organization (WHO) reduced the maximum recommended value for arsenic in drinking water from 50 to 10 µg/L (WHO, 2011). However, adhering to the precautionary principle, WHO recommends that As concentrations be kept as low as possible (WHO, 2011). WHO suggests, among other measures, that:

I. Waters with high and low concentrations of arsenic can be distinguished, as those with low concentrations must be designated for drinking and irrigation purposes, while waters with high concentrations can be used for other purposes, such as washing clothes;
II. Water with low and high concentrations of As can be blended in order to obtain an acceptable concentration;
III. Treatment systems must be installed to remove arsenic effectively (Howard, 2003).

Conventional drinking water treatment can often be insufficient to provide safe water for consumption, with an arsenic concentration lower than 10 µg/L (Moreira et al., 2021a). Among the technologies capable of effectively removing arsenic from water, membrane technology stand out since the efficiency in arsenic removal can be greater than 99.95% (Moreira et al., 2021b; Amaral et al., 2018; Foureaux et al., 2020; Reis et al., 2018). Furthermore, this option is more robust to variations in the characteristics of the water to be treated compared to other processes (Moreira et al., 2021a).

Ultrafiltration (UF) is a membrane process option that becomes an additional barrier to colloids and precipitated species, including those containing arsenic, when integrated into conventional treatment. However, arsenic is commonly found in its dissolved species. As the primary separation mechanism of UF is size exclusion, high As removals by UF are not expected. Another membrane process is reverse osmosis (RO), a technology known for years to remove arsenic from water effectively (Ning et al., 2002; Abejón et al., 2015). However, the energy demand of RO is greater than that of UF. Furthermore, RO membranes are more susceptible to fouling.

To overcome the limitations of these technologies, an alternative is to integrate conventional treatment with the UF and RO systems, combining the advantages of each of these processes. In this configuration, UF can generate a less fouling feed for RO and, as the quality of the RO permeate is very high, mixtures of the permeates can be made (blending formulation), or even with the effluent from the sand filter, and still have a blend that meets potability standards. In addition to being in line with WHO guidelines, this option would be advantageous, as it would reduce the volume of water treated in RO and the energy costs related to this operation. Guimarães et al. (2022) evaluated this treatment configuration in a bench study and saw that coupling UF and RO to the conventional water treatment system could meet consumption standards, even with feeds containing high concentrations of arsenic. Given the promising results found, the main objective of this study is to investigate the performance of this system on a pilot scale, considering different forms of operation.

In brief, this thesis is part of a project already under development by the research group on treating surface water with high concentrations of arsenic. In a general context, the project considers conditions for a possible tailings dam rupture and, consequently, higher concentrations of arsenic, iron, and manganese, among other contaminants, in water that supply various populations. In this way, the conditions are assessed so that the population can continue to be supplied with safe water. After previously carrying out bench-scale studies, this thesis takes another step towards implementing membrane technology on a full scale, bringing together studies carried out on a pilot scale.

In addition, this thesis focus on conditions that do not occur only during environmental disasters but that are common in several locations that have higher arsenic concentrations in their waters, which can occur naturally, as a consequence of human activities, or be a seasonal condition, among other particularities. Thus, the results can be of great value to several communities, from the smallest ones not served by centralized treatment plants to large communities already supplied by WTPs, to reinforce treatment and guarantee safe drinking water to the entire population.

1.2 Objectives

1.2.1 General objective

Evaluate the treatment of water containing high concentrations of arsenic using ultrafiltration and reverse osmosis on a pilot scale.

1.2.2 Specific objectives

The specific objectives, hypotheses and premises are found in Table 1.1.

Table 1.1. Premises, Hypotesis, and specific objectives of the study.

ID	Premises	Hypotesis	Specific objectives	Chapter
1	The presence of Arsenic in water in concentrations greater than that recommended by WHO (10 µg/L) can lead to several health problems; however, several places do not have the necessary resources to carry out Arsenic monitoring and water treatment adequately.	Several places in Latin American countries have waters that pose risks to the population due to the presence of Arsenic. Knowledge of the occurrence and risks, as well as the proposition of feasible monitoring and treatment techniques in these countries, can guarantee water security and reduce the risks to which the population is exposed.	Conduct a survey of arsenic concentrations in water bodies in Latin American countries, calculate the risk associated with exposure to these concentrations, and propose monitoring and treatment solutions practicable in these countries.	2
2	Conventional water treatment faces limitations in ensuring water safety, considering: (i) the need to remove trace	The coupling of ultrafiltration and reverse osmosis (UF-RO) membranes to the conventional water treatment process	Compare the effect of pre-treatment by pre-oxidation, coagulation and flocculation on UF-RO performance in treating	3

	contaminants, such as arsenic; (ii) changes in the quality of the water entering the WTP.	increases the robustness of the process, promoting the effective removal of arsenic and maintaining high performance even with more critical quality feed.	water containing high concentrations of arsenic.	
3	Ultrafiltration and reverse osmosis membranes can increase the robustness of conventional water treatment and overcome the limitations of conventional technologies in removing trace contaminants such as arsenic.	Incorporating the UF-RO into the WTP increases its robustness and water quality during long periods of operation and guarantees water security for a long time.	Evaluate the long-term operation of the UF-RO system in treating water containing high concentrations of arsenic.	4
4	Conventional water treatment plants are often limited in removing trace contaminants like arsenic. Ultrafiltration increases the robustness of conventional treatment in general, but it is not expected to remove dissolved metal fractions and is subject to fouling formation.	An in-line coagulant dose improves UF performance, increasing arsenic removal, reducing fouling problems, and enhancing the resilience of the water treatment plant.	Evaluate the effect of coagulant dose in the UF feed in water treatment with a high concentration of arsenic.	5

1.3 Document structure

This document was divided into chapters that have already been or will be published as articles. In this way, some important points for the independent understanding of each chapter were repeated. Chapter 1 is a brief introduction to the topic and contains the objectives and document structure; Chapter 2 addresses specific objective 1, where a literature review was carried out regarding the occurrence of arsenic in the waters of Latin American countries. With these data, a risk assessment was carried out, and a feasible monitoring method was proposed when considering the reality of several locations in these countries. Chapter 3 is related to specific objective 2, and Chapter 4 to specific

objective 3. Chapter 5 addresses specific objective 4. Appendices A, B, C, and D refer to chapters 2, 3, 4, and 5. Finally, in Chapter 6, "General conclusions", it may be found the main achievements of this study.

2 CHAPTER 2 - ARSENIC IN NATURAL WATERS OF LATIN-AMERICAN COUNTRIES: OCCURRENCE, RISK ASSESSMENT, LOW-COST METHODS, AND TECHNOLOGIES FOR REMEDIATION

Abstract

This chapter presents an updated dataset analysis on arsenic occurrence in Latin American countries, along with the associated risks, both carcinogenic and non-carcinogenic. Arsenic was detected in various aqueous matrices at concentrations ranging from 0.009 to 32,000 µg/L. The study differs from previous ones as it provides an in-depth discussion of risks. Considering the minimum concentration values, the risk assessment revealed that most analyzed waters do not pose any non-carcinogenic or carcinogenic risks. However, the reported maximum concentrations suggested both environmental and human health risks. In most locations, the hazard index values for natural waters exceeded one (HQ > 1), which is classified as unacceptable in all locations. These results underscore the necessity of arsenic monitoring and control in water matrices, particularly those designated for human consumption. The challenges related to arsenic monitoring and removal by different processes and their feasibility in the context of Latin American countries were critically discussed. Filters and recycled membranes have been demonstrated to be effective in arsenic control in drinking waters. Overall, this review serves as a foundation for establishing more stringent legislation regarding the arsenic occurrence, emphasizing the urgent need for effective and low-cost processes that are adapted to the reality of these countries. In a broader context, the summarized results may further ensure water safety, particularly in cases where it is supplied for human consumption.

2.1 Introduction

Arsenic (As) composes the crust of the Earth at an average 2 mg/Kg concentration, and it is naturally released into the environment mainly through volcanic activity and volatilization. Around 33% of the arsenic flux in the atmosphere is estimated to have a natural origin (WHO, 2001a). Besides volatile, some arsenic species are soluble in aqueous solution, so its inorganic forms (arsenate and arsenite, for instance) are commonly found in water (WHO, 2001b). Argentina (Litter et al., 2019), Chile (Tapia et al., 2022), and Mexico (Alarcón-

Herrera et al., 2020) are examples of countries that have naturally high concentrations of arsenic in their groundwaters.

Indeed, arsenic is present in all environmental compartments: soil, air, water, and biota. In addition to natural occurrences, mining, fossil fuel burning, metallurgical processes, and the use of pesticides containing arsenic are examples of human activities that release arsenic into the environment (WHO, 2003a). Given the arsenic ubiquity, humans can be exposed to it through drinking water, crop irrigation, and food preparation with contaminated water (WHO, 2003b). However, it is widely known that human exposure to inorganic arsenic for long periods can lead to many serious health problems (WHO, 2003a).

Acute arsenic poisoning can cause symptoms such as vomiting and diarrhea. The first manifestations of arsenicosis on the skin initiate due to exposure for five to ten years (Rahman et al., 2009). An example of skin lesions caused by arsenic exposure is hyperkeratosis on the palms of the hands and soles of the feet, which can be skin cancer precursor (WHO, 2003b). Concerning the nervous system, it is known that exposure to As affects the brain. Acute and chronic exposure cause complications associated with the sensory nerves, so common symptoms involve paraesthesia and numbness in the soles of the feet. Arsenic can also induce neuronal apoptosis, impairing memory (Namgung and Xia, 2001; Vahidnia et al., 2007). Regarding the cardiovascular system, exposure to arsenic can lead to atherogenesis and other cardiovascular diseases (such as hypertension, arrhythmia, and ischemic heart disease).

Furthermore, arsenic can impair several other organ systems, and many diseases can appear. The organ systems affected by arsenic contamination and some related diseases are: respiratory (lung dysfunction and higher rates of death due to respiratory diseases (Parvez et al., 2011), reproductive (fertility problems in men and women, pregnancy, and fetal development complications), immunological (immune system suppression), endocrine (there is correlation between arsenic exposure and diabetes cases, since As accumulates in pancreas and reduces insulin secretion and cells viability (Lu et al., 2011), hepatic (hepatomegaly and cirrhosis), hematopoietic (anemia, hemolysis, and

erythrophagocytosis), and renal (degeneration of proximal tubule and cortical necrosis) (Abdul et al., 2015).

Arsenic is also classified by the International Agency for Research on Cancer (IARC) as carcinogenic (WHO, 2009). In addition to skin, bladder, and lung cancer (Smith et al., 1992; WHO, 2009), liver, kidney, and prostate cancer are also caused by exposure to arsenic in the long term (Abdul et al., 2015). However, Abdul et al. (2015) highlight that the cancer development mechanisms in the human body are still unclear and require more study.

The World Health Organization (WHO) reduced the maximum recommended value of arsenic in drinking water from 50 to 10 µg/L in 1993 due to the growing knowledge about the effects of consumption of drinking water containing arsenic (WHO, 2011). This value is considered provisional since lower values may not be achieved given the limited treatment conditions in some places. Adhering to the precautionary principle, the WHO recommends that As concentrations be kept as low as possible (WHO, 2011). Many countries have adopted the maximum value of 10 µg/L. However, some countries adopt lower values, in line with the precautionary principle, considering that there are indications that concentrations below 10 µg/L can cause injury to health. For example, Denmark, which adopts a maximum value of 5 µg/L, and the Netherlands, with a voluntary limit of 1 µg/L, can be mentioned (Ramsay et al., 2021).

In view of the matter of water contamination and the risks arising from the ingestion of arsenic, the WHO itself suggests, among other measures: that waters with high and low concentrations of arsenic may be distinguished since those with low concentrations must be designated for potable, cooking and irrigation use, while high concentrations waters may be intended for washing clothes; mix waters with low and high concentrations of As, so that an acceptable concentration is obtained; and install treatment systems that effectively remove As (WHO, 2003b). It is noticeable that it is essential to use methods to monitor the As concentration in water resources to make these proposals effective.

It is important to point out that in some locations, despite the waters that supply the population typically containing high levels of As, there may be difficulties in

carrying out this monitoring. For example, in some regions of Latin America, there are no conditions for monitoring techniques that require expensive materials and equipment or more specialized labor (Litter et al., 2019), even if it is a region in which the presence of arsenic in the water is noteworthy. There are countries where specific geological settings and climatic conditions, such as Argentina and Chile, mainly cause the contamination. In other locations, arsenic reaches water because of the deposit of solid waste and acid drainage, which is responsible for the contamination of several areas in Bolivia, Brazil, Colombia, Ecuador, and other countries (Bundschuh et al., 2012).

In this context, this review provides a survey of arsenic concentration in different aqueous matrices (groundwater, surface water, and drinking water) of several Latin American countries. The literature search was conducted in May 2023 using Web of Science, Google Scholar, Science Direct, and Scopus. One hundred twenty-two articles published since 2000 were selected. Risk assessment calculations were made using the arsenic concentrations reported in these studies. The main risk assessment objective was to evaluate the risks these concentrations may pose in populations that drink directly (or after simplified treatments) these waters. This paper also provides an overview of arsenic monitoring techniques, focusing on more viable methods for locations with logistical and resource difficulties and remediation technologies. Finally, an overview of arsenic remediation technologies is presented.

This paper is expected to favor a broad knowledge of arsenic risks in water resources of Latin American countries. There are countries where arsenic is already a well-known problem. However, some places require more studies since knowing the real risk to which people are exposed is essential. In this context, this manuscript serves as a foundation for competent organizations to reevaluate the limits of arsenic in waters permitted by law, enabling it to be considered practicing more stringent legislation. In addition to focusing on the problem, other authors have already addressed (Bundschuh et al., 2020; Osuna-Martínez et al., 2021), the relevance of this manuscript lies in proposing viable practices to guarantee the safety of drinking water concerning arsenic, considering the reality of several locations in Latin America that face logistical difficulties and lack of

resources. In this sense, this paper discusses the urgent need for effective and low-cost technologies and methods adapted to the realities of these countries. Thus, methods that can enable frequent monitoring of arsenic (several places may face difficulties in carrying out this monitoring using techniques such as ICP/MS) and efficient and viable technologies for its removal to guarantee the population's safety are presented. Overall, the summarized results may contribute further to ensuring water safety, particularly in cases where it is supplied for human consumption.

2.2 Arsenic occurence

Figure 2.1 (Table A1) presents the arsenic (As) concentration range found in the water resources of 17 Latin American countries. Almost 120 papers published from 2000 onwards were selected to investigate the occurrence of As and, subsequently, calculate the associated risk. Until then, some countries, such as some localities of the Altiplano-Puna volcanic complex (made up of regions of Argentina, Chile, Bolivia, and Peru) and Mexico, received more attention from researchers, which will be discussed in this topic. The time water contamination with As has been known is one of the reasons why some countries are studied more than others. In Argentina, arsenic contamination due to ingestion of water containing As was first reported in 1913 (Ayerza, 1918). In Mexico, Chile, and Peru, arsenic in groundwater and surface water was confirmed in 1958, 1962, and 1975, respectively. These countries have much more reported data than Colombia and Guatemala, for example, where As occurrence in water was discovered in 2007, or Costa Rica, where As in water was reported only in 2017 (Bundschuh et al., 2021). Besides, much information concerning As in Latina American waters was presented in documents at a regional level and is written in Spanish, making it difficult to spread information. However, it is important to emphasize that this does not mean that poorly or uninvestigated places are arsenic-free. It is necessary to perform studies to confirm with an assurance that the population is free of the risks inherent in the consumption of water with high concentrations of As.

In Argentina, many investigations were conducted concerning arsenic in waters, mainly groundwater. Geochemical investigations of soils and sediments in this

country try to explain the frequent presence of arsenic in Argentine groundwater. These studies indicate that volcanic glass in Cenozoic sediments, which were mobilized under aerobic and high pH conditions, may be one of the main reasons for high As concentrations in waters (Litter et al., 2019). A study financed by the Argentine National Health Ministry demonstrated how it is common to find water containing arsenic in this country. It investigated the concentration of arsenic in water in 167 departments and concluded that in only 50 departments, concentrations up to 10 µg/L were detected (Olmos et al., 2016).

Figure 2.1 (Table A1, apêndix A) shows that the Chaco-Pampean plain region (Córdoba, Santiago del Estero, Chaco, Salta, Tucumán, Santa Fe, and La Pampa provinces) is greatly affected by the presence of As. It is especially worrying considering that it is a densely populated region, and groundwater with a high concentration of As is the only source of water available all year round for many rural communities. Besides this practical situation, it is also worth mentioning that the maximum concentration of As allowed in the country is still under discussion. Values vary between provinces, being 10 µg/L (Chubut), 50 µg/L (Buenos Aires and Mendoza), or even 150-180 µg/L (La Pampa) (Litter et al., 2019), values sometimes well above those recommended by the WHO.

There is evidence that arsenic has affected the health of human populations for many years in some regions, such as in northern Chile and southern Peru, where the effects of As on humans date back to 7000 years (Bundschuh et al., 2012). According to Tapia et al. (2021), who studied the natural occurrence of As in the Altiplano-Puna, Chile, there is a hypothesis that in this locality, volcanism is a relevant source of As, and the continental crust can act as an extensive reservoir of As, which rising fluids can leach. The northern region of Chile, including Antofagasta City, still has high concentrations of As in its water bodies. By Chilean law, the maximum amount of arsenic allowed is 10 µg/L (NCH-409/1, 2005).

The contamination of water resources with As in Peru is mainly due to natural contributions, given the weathering in the Andean region, releasing As of geogenic origin, and mining activities (Bundschuh et al., 2012). Peru has always

been among the largest producers of arsenic in the world (George et al., 2014), and it has already been reported as one of the countries with the highest concentration of As in their surface waters (Kumar et al., 2023). However, it is necessary to know more about the extent of water contamination and its consequences for this country's population (George et al., 2014).

Another country where there are fewer assignments regarding arsenic in its waters is Bolivia. Among Bolivia's characteristics, it is remarkable that water is a scarce resource in the Altiplano-Puna plateau region, and As in water is also a problem (Tapia et al., 2021). The maximum permitted level of As concentration value in drinking water in Peru and Bolivia is also 10 µg/L (Ministerio de Salud, 2011; Gobierno de Bolivia, 2005).

Arsenic also poses a big challenge for Mexico. It is estimated that around 1.5 million people in Mexico consume water with more than 25 µg/L (Alarcón-Herrera et al., 2020), a value two and a half times greater than the national limit for As concentration in drinking water (Frisbie; Mitchell, 2022). The country's northern region is highlighted among the places in Mexico that face problems with As contamination: states of Sonora, Chihuahua, Durango, Zacatecas, San Luís de Potosí, Coahuila, and Baja California, besides localities of the central and southern regions such as Hidalgo and Guanajuato, as is evident in Figure 2.1 and Table A1. In the arid regions of Mexico, such as Zimapán, Hidalgo, and Chihuahua, which make up much of the desert in northern Mexico, groundwater becomes the main and sometimes the only source of water (Alarcón-Herrera et al., 2020).

The contamination of Mexican water resources, especially groundwater, occurs mainly through natural routes due to its geological formation, such as the formation of the Sierra Madre Occidental, active tectonic movements, and volcanic emissions and volcanic dust and glass from other regions, such as the Andes mountains. Although natural routes mainly cause the contamination of Mexican waters, there is also contamination of water resources close to mining areas (Armienta and Segovia, 2008), and there may be contamination because of industrial activity. For example, the contamination of the Salamanca aquifer

system, which is in a region with rocks containing As, shows signs of contamination due to the presence of pesticide industries and an oil refinery (Rodriguez et al., 2005).

In Brazil, many studies assessed As contamination associated with mining, industrial pollution, diffuse sources (such as agrochemicals), and geochemical anomalies (de Souza et al., 2019; Nascimento et al., 2023; Faria et al., 2023). The contamination associated with mining is one of the most recognized and investigated. An area that is greatly affected by it is the Quadrilátero Ferrífero region in Minas Gerais state (Figure 2.1 and Table A1). This region is responsible for over 50% of the country's gold production (Teixeira et al., 2020). The main natural source of As in this locality is related to rocks containing sulfide-gold (Souza et al., 2018). In Colombia, mining is also a relevant activity regarding the contamination of water bodies with As. The largest mining areas in the country are found in the Paramos, the ecosystem responsible for 70% of the water supply. However, even in these regions, although some samples have higher As concentrations, most samples tested have values below 10 mg/L (Alonso et al., 2014).

Figure 2.1. Occurrence of arsenic in water resources of Latin-American countries: (a) groundwater, (b) surface water, and (c) drinking water. Concentration range is expressed in mg/L. Data was not available for countries in grey. Quantitative data was presented as supplementary material along the references. Water classification was carried out according to the terminology used in each manuscript, including drinking water, regardless of the treatment route applied in individual cases.

(a)

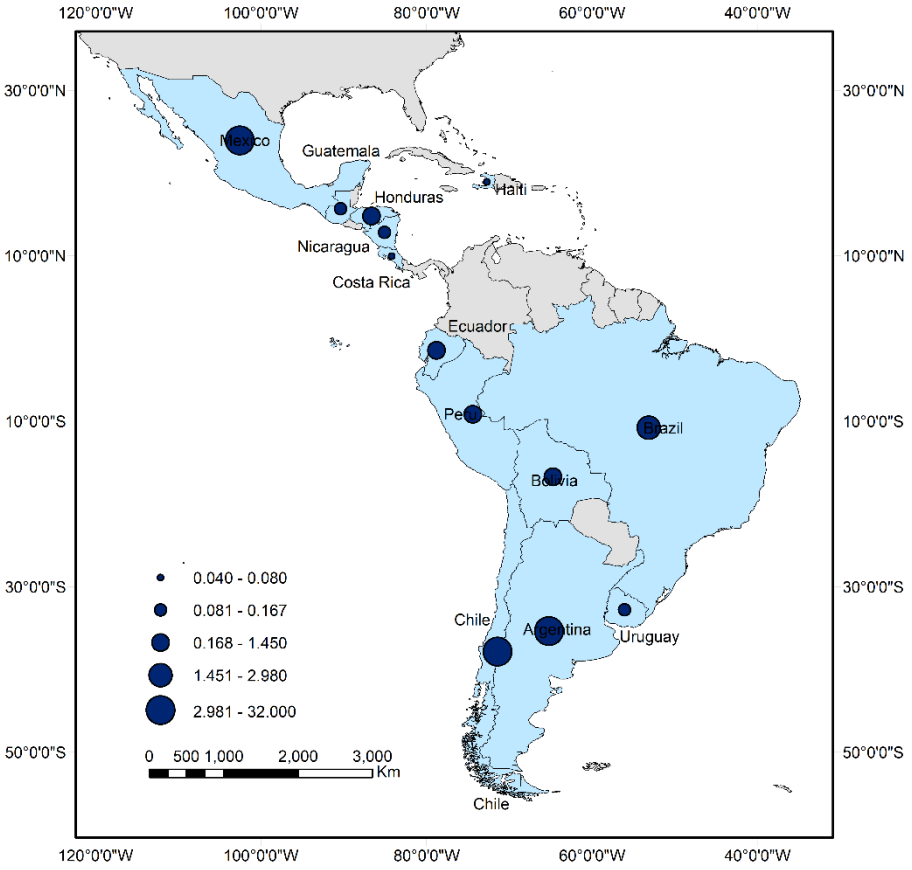
120°0'0"W
100°0'0"W
80°0'0"W
60°0'0"W
40°0'0"W
30°0'0"N
10°0'0"N
10°0'0"S
30°0'0"S
50°0'0"S
Mexico
Guatemala
Haiti
Honduras
Nicaragua
Costa Rica
Ecuador
Peru
Brazil
Bolivia
Chile
Argentina
Uruguay
0.040 - 0.080
0.081 - 0.167
0.168 - 1.450
1.451 - 2.980
2.981 - 32.000
0 500 1,000 2,000 3,000
Km

(b)

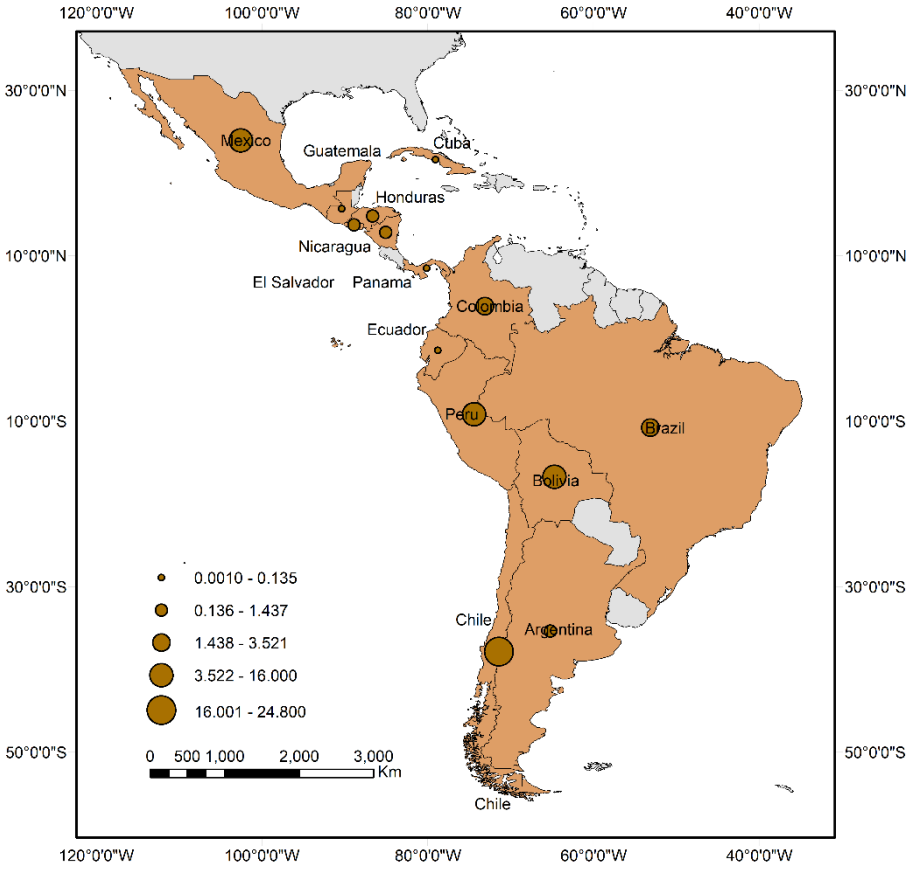
120°0'0"W
100°0'0"W
80°0'0"W
60°0'0"W
40°0'0"W
30°0'0"N
10°0'0"N
10°0'0"S
30°0'0"S
50°0'0"S
Mexico
Guatemala
Cuba
Honduras
Nicaragua
El Salvador
Panama
Colombia
Ecuador
Peru
Brazil
Bolivia
Chile
Argentina
0.0010 - 0.135
0.136 - 1.437
1.438 - 3.521
3.522 - 16.000
16.001 - 24.800
0 500 1,000 2,000 3,000
Km

(c)

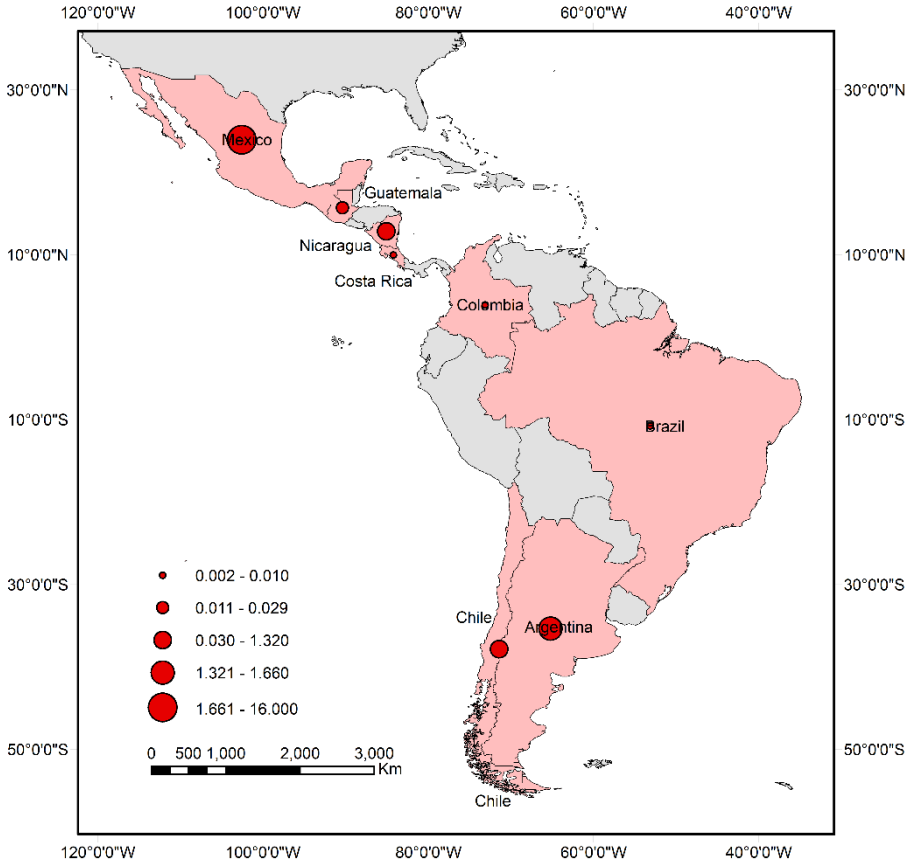

It is also possible to see in Figure 2.1 and Table A1 that, in some places, even drinking water is contaminated with As at levels much higher than 10 µg/L recommended by WHO. It may happen due to several factors: the socio-economic circumstances of the community, the population making direct use of the collected water, or a treatment that effectively removes arsenic is not applied - many times, only disinfection is carried out before consumption, as takes place in the rural community of San Rafael Las Flores, Guatemala (Marcillo et al., 2020). In eastern Guatemala, both volcanic geology that can leach arsenic and large-scale mining activity can increase the risk of arsenic exposure. In the study conducted by Marcillo et al. (2020), water samples were collected from homes, and in 13% of them, the arsenic concentration was greater than 10 µg/L. The research revealed a great distrust of the population concerning the water that reaches their homes: the majority either buy bottled water or collect it from untreated springs.

Another similar case is the rural population of Antofagasta, Chile. Although almost the entire urban population is served by treated water, about 42% of the rural

population is still not formally supplied with drinking water in a scenario where, at the entrances to water treatment plants, As concentrations reach 1240 µg/L (Ruffino et al., 2022). Therefore, Diaz et al. (2015) observed that, in a rural village of Antofagasta, the consumption of water that contains on average 276.5 µg/L of As caused the average intake of As via drinking water to be 359.1 µg/day, a value higher than indicated by FAO/WHO (149.8 µg of i-As·day−1).

Another factor that may contribute to human ingestion of arsenic is the difficulties in monitoring As concentration. Litter et al. (2019) point out that despite a wide distribution of laboratories throughout Argentina, 66% of the analytical capacity is concentrated in Santa Fe, Córdoba, and Buenos Aires provinces. In this way, it is crucial to develop and apply concentration monitoring tests that are simple and affordable to be feasible for their application in different locations with logistical, social, and economic restrictions. It would directly affect the population's safety since, with few technological and human resources, the safety of the water source could be attested. In addition, these tests could become tools that help plan the use of water resources since the same water source may be safe at one season of the year but at another season containing a high concentration of As (Tapia et al., 2019).

2.3 Risk assessment in Latin-American countries

Risks were evaluated to know the threats that arsenic concentrations from different water resources pose to plants, animals, and humans. For the calculations, two scenarios were considered, namely “best scenario (BS)”, where the minimum values of arsenic concentration found in water matrices of each locality were used, and “worst scenario (WS)”, where the maximum concentrations found were used. The concepts of "best" and "worst" scenarios are not alternatives to be chosen. The As concentrations varied for several reasons, such as the water source and the effect of seasonality. Thus, exposure to the conditions called "best" and exposure to the condition called "worst" in the same reported location occurs. For arsenic concentrations greater than 10 µg/L, calculations were performed as described in sections 2.3.1 and 2.3.2. No calculations were made for lower concentrations, as these waters are considered

safe by the World Health Organization. Therefore, risk values were assumed to be 0.

Arsenic concentrations found in waters were compared with the value established by The Food and Agriculture Organization (FAO), which recognizes that the toxicity of arsenic to plants is quite variable and recommends a maximum concentration of arsenic in irrigation water of 100 µg/L (Ayers and Westcot, 1994).

Regarding the safety of using water for animal watering, arsenic concentration in waters was compared with the maximum allowed value for use in livestock watering, also according to FAO, which is 200 µg/L. This criterion was adopted since the maximum permitted value of arsenic in water for this purpose varies considerably between countries: 50 µg/L for Venezuela, 67 µg/L for Argentina, and 100 µg/L for Peru, 33 µg/L for Brazil, and 200 for Colombia, Ecuador, and Mexico (Valente-Campos et al., 2014). This notable variation can be attributed to the different toxicological data (such as exposure conditions, different sensitivity for different species, study duration, and the chosen endpoint, among others). Therefore, selecting the Maximum Contaminant Level (MCL) recommended by FAO as the criterion for As in water for livestock in this study is reasonable.

2.3.1 Exposure assessment

The average daily dose (DD) of arsenic intake is estimated to assess exposure via direct ingestion. It can be calculated using equation 1 (IRIS, 1991a).

$$DD = (C \times DI)/BW \quad (1)$$

Where C is the concentration which was found (mg/L), DI is the daily water intake, and BW is the body weight (Alarcón-Herrera et al., 2020). The values used for each parameter to calculate potential noncarcinogenic and carcinogenic risks are shown in Table 2.1.

Table 2.1. Exposure parameters used as a single-point estimation values to calculate noncarcinogenic and carcinogenic risks

Parameter	Unit	Value	Reference
Body Weight (BW)	kg	70	Alarcón-Herrera et al., 2020

Cancer slope factor (CSF) for skin cancer	mg/kg/day	1.5	IRIS, 1991b
Cancer slope factor (CSF) for bladder and lung cancer in women	mg/kg/day	25.7	Rockafellow-Baldoni et al., 2018
Daily water intake (DI)	L/day	2	Alarcón-Herrera et al., 2020
Oral reference dose (RfD)	mg/kg/day	0.0003	IRIS, 1991b

Noncarcinogenic risks were calculated using the hazard quotient (HQ) expressed in equation 2:

$$HQ = DD/RfD \quad (2)$$

Where RfD is the oral reference dose (value in Table 2.1), below which no adverse effects are expected for a population exposed for a lifetime. For HQ < 1, it is considered that the population that consumes that water is safe (IRIS, 1991b).

2.3.2 Carcinogenic risk

According to the US EPA, drinking water containing high concentrations of arsenic can increase the mortality of several types of cancer (such as kidney, lung, and bladder) and increase the incidence of skin cancer. Therefore, the risk of consuming arsenic-containing water for human health in different locations was evaluated by calculating the risk of developing skin cancer (SCR) and developing bladder and lung cancer (BLCR) in women. The latter was assessed due to women's greater sensitivity to developing these types of cancer through the consumption of water contaminated with arsenic (Rockafellow-Baldoni et al., 2018). Cancer risks (CR) were calculated according to Equation 3 for bladder and lung cancer in women and skin cancer.

$$CR = DD \times CSF \quad (3)$$

Where CSF is the cancer slope factor. The same parameter values were used for the SCR and BLCR calculations, except for CSF, whose values are in Table 2.1.

Cancer risk was classified as follows: CR < $1x10^{-6}$ negligible risk (chance of contracting cancer through drinking water consumption of 1 per 1000000), $1x10^{-6}$ < CR < $1x10^{-4}$ moderate risk, and CR > $1x10^{-4}$ unacceptable risk (IRIS, 1991a). When the arsenic concentration was lower than the limit proposed by the WHO (< 10 µg/L), the risk was considered negligible.

2.3.3 Risks associated with the use of water for plant irrigation and animal watering

In the best scenario, water could be considered safe for agriculture in most assessed locations (Figure 2.2). The exceptions: 1 place in Argentina (Pinter et al., 2018), 1 in Brazil (Campos, 2002), 3 in Chile (Nicolau et al., 2014; Pérez-Carrera; Cirelli., 2010; Diaz et al., 2015), 1 in El Salvador (López et al., 2009), 1 in Guatemala (Hoyos et al., 2013), and 3 in Mexico (Flores et al., 2009, Armienta et al., 2014, Flores-Tavizón et al., 2003). Thus, 91.7% of the assessed locations have sources that can be safely used in agriculture.

In the worst scenario, only 39.7% of the assessed locations have their water in a safe condition to be used directly for irrigation without prior treatment to remove arsenic. Argentina, Bolivia, and Chile have the most severe conditions: 11.5, 11.1, and 8.3% of localities in each country are considered safe for irrigation. On the other hand, Brazil, Mexico, and Peru present a less serious situation, but which still deserves attention: 60.0, 52.6, and 44.4% of the locations in these countries have safe water sources for use in irrigation. Among the countries where fewer studies have been carried out, water could be considered safe (more than 60% of the assessed locations in each country) for agriculture in most countries, even in the worst scenario. With exceptions: Nicaragua (N=5, 20% of the locations have safe water), Uruguay, Honduras, and El Salvador (however, it is worth noting that the sample size of these countries is not representative).

Considering the best scenario, 96.7% of the water is safe for animal watering. The waters classified as unsafe for this purpose are only those of 2 locations evaluated in Chile (Nicolau et al., 2014; Diaz et al., 2015) and 2 in Mexico (Flores et al., 2009; Armienta et al., 2014). In the worst scenario, 50.4% of the water is considered safe for animal watering. Again, Argentina, Bolivia, and Chile stand

out, with, respectively, 15.4, 11.1, and 8.3% of the waters being classified as safe. Peru also has 44.4% of the waters considered safe, while the other countries have more than 60% of their waters in this classification, even in the worst scenario. Honduras and El Salvador (both N=1) have their waters classified as unsafe, emphasizing, once again, that this result is not representative for these countries.

Figure 2.2. (a) Lowest and (b) highest arsenic concentration in water from Latin American countries and their comparison with the MCL for plant irrigation (100 µg/L) and animal watering (200 µg/L).

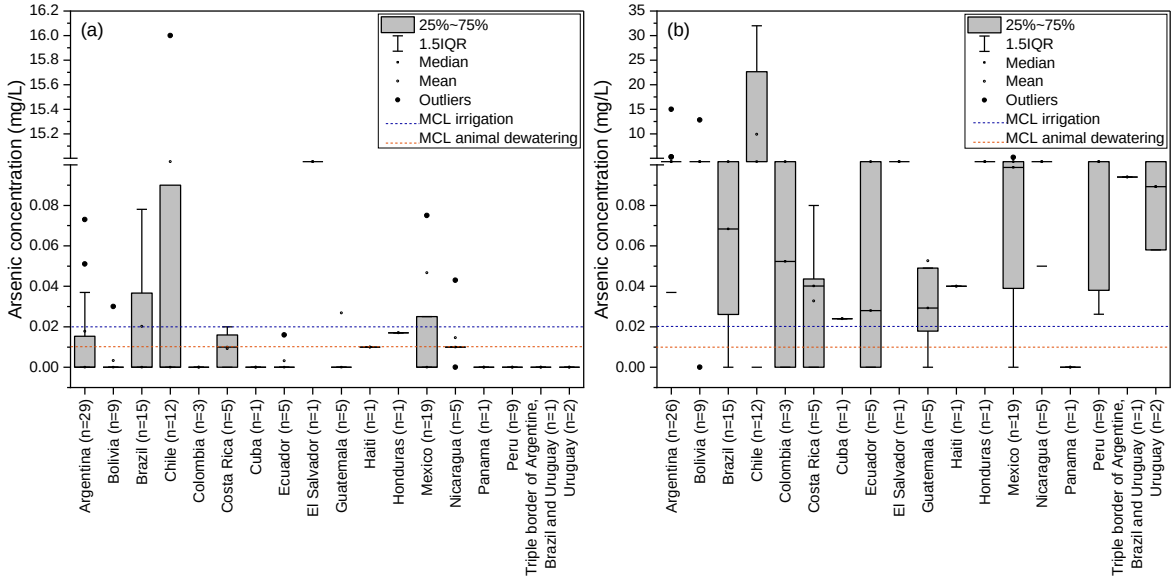

2.3.4 Human health risk assessment

Figure 2.3 shows the boxplot graphs for HQ in both evaluated scenarios. It is important to note that most data refer to As concentrations found in untreated water. Accordingly, the risk results refer to the consumption of these waters and reinforce the need to apply treatments that remove arsenic efficiently besides monitoring the concentration of As.

Figure 2.3. Non-carcinogenic risks to human health for the lowest (a) and highest (b) arsenic concentration reported. Note: Red = unacceptable risk, blue = negligible risk. *All arsenic concentrations are lower than 10 µg/L.

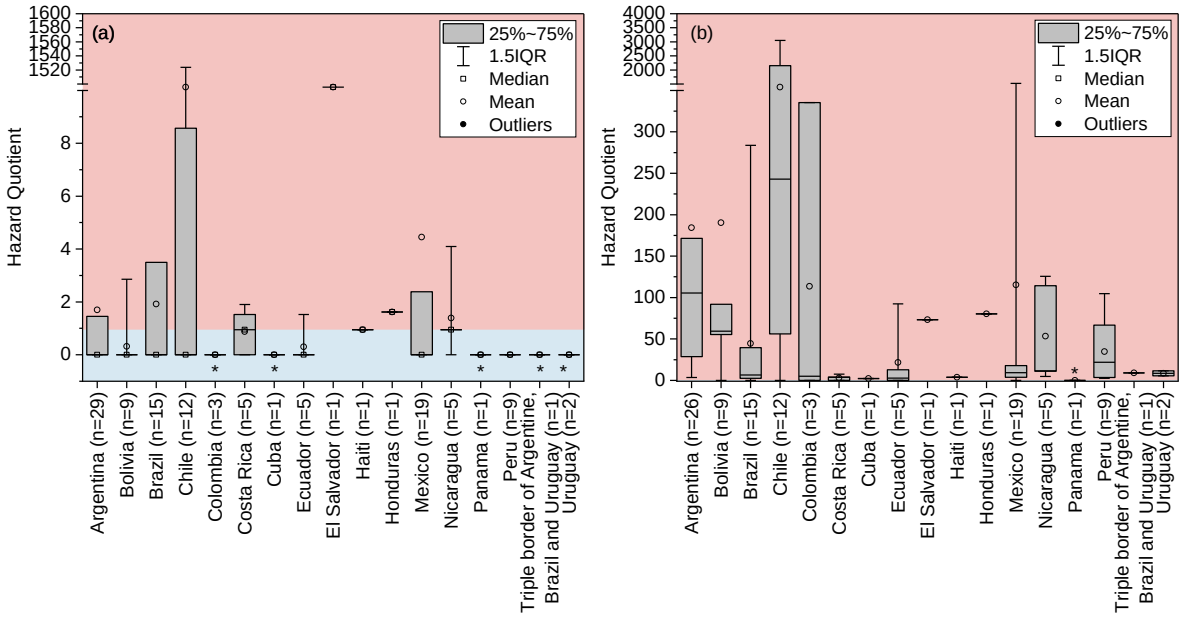

In the best scenario, most medians of HQ in all countries are lower than 1. In other words, in this case, most places in each country do not present a risk to the population that is exposed to their sources of water all their lives. All assessed locations in Colombia, Cuba, Panama, Peru, and Uruguay presented HQ < 1. Despite the maximum HQ in Bolivia being 2.86, more than 75% of the calculated HQs were considered safe. There is a similar situation in Ecuador. Although the maximum HQ was 1.52, 75% of the HQs were lower than 0.76.

Negatively attracting attention, Chile, in the best scenario, has locations with high concentrations of arsenic in water, as Nicolau et al. (2014) reported for the El Tatio geothermal field region, where the lowest concentration of As found was 16 mg/L. However, it is essential to understand some particularities of the region and its waters. Geothermal systems are expected in northern Chile along the Andes at high altitudes (>4,000 m). The thermal waters in the region naturally have high concentrations of silica, arsenic, boron, and antimony, with temperatures around 70-90 ^{o}C (Nicolau et al., 2014). Given these waters' characteristics, they are not expected to be used in irrigation, animal watering, or drinking water. Therefore, we do not expect these waters to pose a direct danger to animals, humans, and the environment.

In the worst scenario, median HQ values are higher than 1, indicating that most water consumption is dangerous to human health. Again, as the most critical location, there is Chile, whose calculated HQ median was 242.9. Following, with the highest values of HQ in the worst scenario evaluated, there are Argentina and Bolivia, with median values of 105.4 and 59.3. The results indicate that in these three countries, it is necessary to be very careful so that the population does not consume the water without ensuring a safe concentration of As or promoting adequate treatment.

Figures 2.4 and 2.5 show the boxplot graphs of the risk analysis for skin cancer (SCR) and lung and bladder cancer (BLCR).

Figure 2.4. Skin cancer risk for the lowest (a) and highest (b) arsenic concentration reported. Note: Red = unacceptable risk, yellow = moderate risk, blue = negligible risk. *All arsenic concentrations are lower than 10 µg/L.

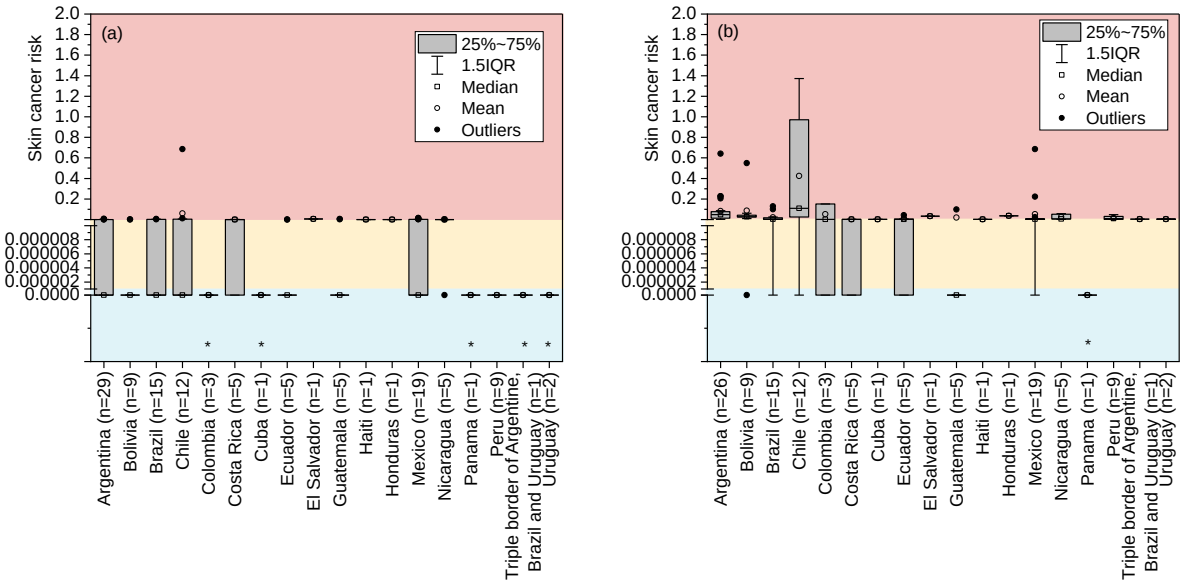

Figure 2.5. Risk of bladder and lung cancer in women for the lowest (a) and highest (b) arsenic concentration reported. Note: Red = unacceptable risk, yellow = moderate risk, blue = negligible risk. *All arsenic concentrations are lower than 10 µg/L.

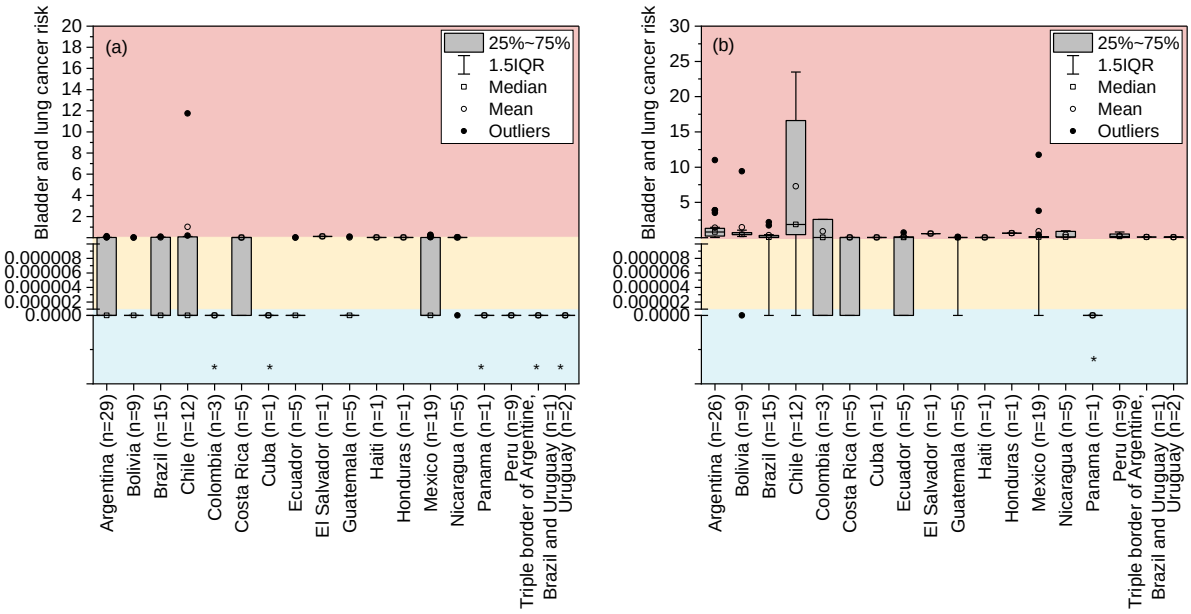

In the best scenario, the direct consumption of most water has no potential carcinogenic risks due to arsenic presence if consumed directly, including in Argentina, Brazil, Chile, and Mexico, where many studies were carried out. Only in Costa Rica, Nicaragua, Honduras, Haiti, and El Salvador did the results indicate that even in the best scenario, there is a moderate or unacceptable potential risk of developing cancer through the consumption of As in most water. Once again, it is relevant to notice that these countries have far fewer studies than others, such as Argentina and Mexico. More studies are needed to conclude whether this represents a real risk in various regions of these countries.

In the worst scenario, median carcinogenic risks values are classified as unacceptable in all locations, which once again highlights the need to be careful with the water that the population has access to, especially in regions of countries such as Chile and Argentina. The consequences of consuming contaminated water that is not adequately treated have great potential to harm human health.

HQ values for the best scenario are consistent with other studies. Varol (2019) assessed the non-carcinogenic risks of trace metals (including arsenic) exposure through ingestion and dermal contact at Keban Dam Reservoir (Turkey). HQ values were less than 1. As non-carcinogenic risks, the CR values were within the limits that define a moderate risk, between 1x10-6 and 1x10-4. In this way,

the author states that the reservoir does not put people at risk due to As and other trace metals. Fishing, irrigation, and recreation are safe activities in the reservoir.

Similarly, Varol and Tokatli (2022) investigated tap water samples collected from 10 houses in villages located in İpsala district in the northwest of Turkey. Groundwater from the agricultural area studied is a source of drinking water, and pesticides, which may contain arsenic, are widely used there. Nevertheless, the authors observed a low presence of arsenic in the study water, attributed to the low soil infiltration rate and its high clay content. Consequently, all HQ values were less than 1. Regarding carcinogenic risks, all were considered low or moderate (according to the nomenclature adopted in this review paper).

Conversely, Kumar et al. (2023) conducted a meta-analysis of toxic metals (including arsenic) in surface water, covering all continents. They reported HQ values for As contamination via ingestion were higher than 1 for all continents. Concerning carcinogenic risks, they could be classified as unacceptable. These results are consistent with the HQ and CR values calculated in the worst scenario evaluated in the present study, indicating potential harm to human health.

2.4 Low-cost methods for arsenic quantification

Currently, there are several procedures and equipment for arsenic quantification in aqueous matrices. Atomic absorption spectrometry (AAS), inductively coupled plasma atomic emission spectrometry (ICP-AES), and inductively coupled plasma mass spectrometry (ICP-MS) are increasingly common techniques to quantify arsenic. Although consolidated, they are techniques that demand robust equipment and complex sample preparation, factors that sometimes impede the analysis of arsenic in raw and drinking water in remote locations or small facilities. For analysis in AAS, the arsenic present in the sample must be initially reduced to arsine (AsH3), a gaseous hydride that must dissociate under high temperature once introduced to the equipment. The technique has low sensitivity (50 µg/L (Perkin-Elmer-Coorporation, 1996)) and requires additional equipment to reduce arsenic, namely quartz supports, gas/liquid separators, and cells for hydride analysis. This method quantifies total inorganic arsenic but may not detect all organic forms unless preceded by an acid digestion step. By operating with higher temperatures and more robust detectors, ICP-AES and ICP-MS techniques

present greater sensitivity, accuracy, and precision when compared to AAS. For this reason, they are also techniques recommended by standard procedures for arsenic analysis (method 3500-As), made available by Standard Methods for the Examination of Water and Wastewater (APHA, 2019). Even so, they have technical limitations, such as the loss of analytes by volatilization, interferences, high demand for consumables, and recurring maintenance. Interferences lead to changes (either positive or negative) in the analyte signal intensity and could be non-spectral and spectral. They are generally associated with emissions from oxides, undissociated molecules of the sample matrix that have a broad band absorption spectrum, unvaporized solvent droplets or molecular species in the flame which may scatter light over a wide wavelength region, sample viscosity, refractory elements (e.g., Ti, W, Zr, Mo, and Al, which form thermally stable oxides), and others (Skoog et al., 2013).

Techniques such as ICP-MS are essential for verifying compliance with the legal limits of As in water. However, these analyses require specialized labor and resources. They are also ex-situ techniques in which the quantification often occurs outside the place where the samples were collected. These characteristics may impede the frequent control of arsenic concentration in short-income locations or even laboratory units not equipped with such equipment. However, it is extremely necessary to regularly monitor As concentrations in places that have problems with high concentrations of As in water, especially in drinking water sources. The risks discussed in previous sections support the importance of arsenic monitoring in drinking water, and simpler techniques would be helpful for that purpose.

In this context, colorimetric techniques can be used. They are based on the ability of an element to produce color after a chemical reaction. This color is compared with a standard, and the sample’s concentration is determined based on the intensity of the color generated. The measurement requires a spectrophotometer, equipment capable of monitoring a specific wavelength associated with the color generated and ignoring those considered irrelevant to the analysis. A spectrophotometer is a portable equipment used in laboratories or the field. This type of method has disadvantages, such as relatively high detection limits and

more time required for these analyses compared to other techniques. Therefore, it is not suggested to replace ICP/MS to ensure compliance with legal limits. Colorimetric methods can be an alternative to enable frequent monitoring of As since their cost and accessibility align with the reality of several places in Latin American countries.

Dhar et al. (2004) described a colorimetric method of arsenic (III) and arsenic (V) quantification in the presence of phosphate. Despite the sensitivity (detection limit of 2 µg/L), the method requires several reagents to eliminate the presence of interferents during the quantification process, namely, potassium iodide, hydrochloric acid, sodium metabisulfite, sodium thiosulfate, sulfuric acid, ascorbic acid, ammonium molybdate, and potassium antimony tartrate. Moreover, according to the authors, the groundwater samples required about 45 minutes for the arsenic complexation reaction to occur completely. Like the study by Darh et al. (2004), other methods claimed to be simple and fast were presented in state of the art, summarized in Table 2.2.

Table 2.2. Summary of different techniques used to determine arsenic concentration in aqueous samples. Note: n.a.: information not available.

Technique	Linear range (µg/L)	Detection limit (µg/L)	Brief description	Reference
Total reflection X-ray fluorescence spectrometry	n.a.	50	The technique was developed for the quantification and speciation of arsenic in water samples using gold nanoparticles as an internal standard	(Sanyal et al., 2020)
Inductively coupled plasma mass spectrometry	n.a.	100 - 200	Inductively coupled plasma mass spectrometry is a type of mass spectrometry that can detect metals and various non-metals	(Zhang et al., 2007)
Hanging mercury drop electrode	4.5 – 180	0.3 - 0.5	Quantitative analysis of arsenic based on its reduction or oxidation on the electrode. The intensity of electrochemical signal is proportional to analyte concentration	(He et al., 2004)
Hanging mercury drop electrode	2.5 – 190	0.3 - 0.5	Quantitative analysis of arsenic based on its reduction or oxidation on the electrode. The intensity of electrochemical signal is proportional to analyte concentration	(He et al., 2007)

Vibrated gold (Au) microwire electrode	n.a.	0.2	Quantitative analysis of arsenic based on its reduction or oxidation on the electrode. The intensity of electrochemical signal is proportional to analyte concentration.	(Gibbon-Walsh et al., 2011)
Vibrated gold (Au) microwire electrode	0 – 0.75	0.005	Quantitative analysis of arsenic based on its reduction or oxidation on the electrode. The intensity of electrochemical signal is proportional to analyte concentration.	(Salaün et al., 2012)
E. coli based biosensor	8 – 78	<10	Utilize microorganism's defense against arsenite and arsenate for detection. Bacterial biosensors thus detect "bioavailable" arsenic	(Stocker et al., 2003)
Colorimetric method	n.a.	16.7	This method involves a reaction between arsenic and potassium iodate in acidic medium. Absorbances are measured at 515 nm	(Stocker et al., 2003)
Colorimetric method	1000 – 10000	1000	Selective detection of arsenate ions in water samples using a portable colorimeter. However, for concentrations below 1 mg/L, the concentrations are more difficult to measure due to the lack of instrument sensitivity	(Sidhu et al., 2014)
Field test kit/ Colorimetric method	0 - 50	0.5	Claimed to be low cost and convenient; it employes $AgNO_3$ as the colorimetric reagent in replacement to $HgBr_2$	(Kumar et al., 2022)
Colorimetric method	0 – 8630, 0 – 1100, and 0 - 110	1300, 530 and 30	It is based on the colour bleaching of methylene blue (MB) in anionic micellar medium. It is free from phosphate and silicate interferences and applicable for real sample analysis	(Kearns and Edson, 2018)
Smartphone-based kit for colorimetric detection of arsenic	710 – 1278	710	A smartphone platform was developed for point-of-care detection using surface plasmon resonance of gold nanoparticles. The simultaneous colorimetric detection of trace arsenic was performed using a new image processing application.	(Kundu et al., 2002)
Turbidimetric test to monitor microbial arsenic biotransformation	10000 - 100000	3000	This test is based on arsenate chelation with pyrrolidine dithiocarbamate followed by spectrometric measurement of absorbance	(Motalebizadeh et al., 2018)

Other authors considered a colorimetric method similar to the one described by Darh et al. (2004), validating its use in arsenic monitoring in surface and treated water samples. The data was made available in different studies intended to propose water treatment solutions in scenarios of arsenic contamination (Guimarães et al., 2022; Moreira et al., 2023b, 2023a; Moreira et al., 2021b, 2021a). As this method has already been used successfully, it will be presented here to illustrate how colorimetric methods can be easy, practical, and applicable in different realities with limiting factors, such as Brazil, the country of development and application of this method. Their protocol was summarized in Figure 2.6, and their data related to arsenic quantification is presented hereafter, exemplifying and validating the use of their colorimetric procedure for arsenic monitoring.

Figure 2.6. Summary of the procedure developed for arsenic analysis.

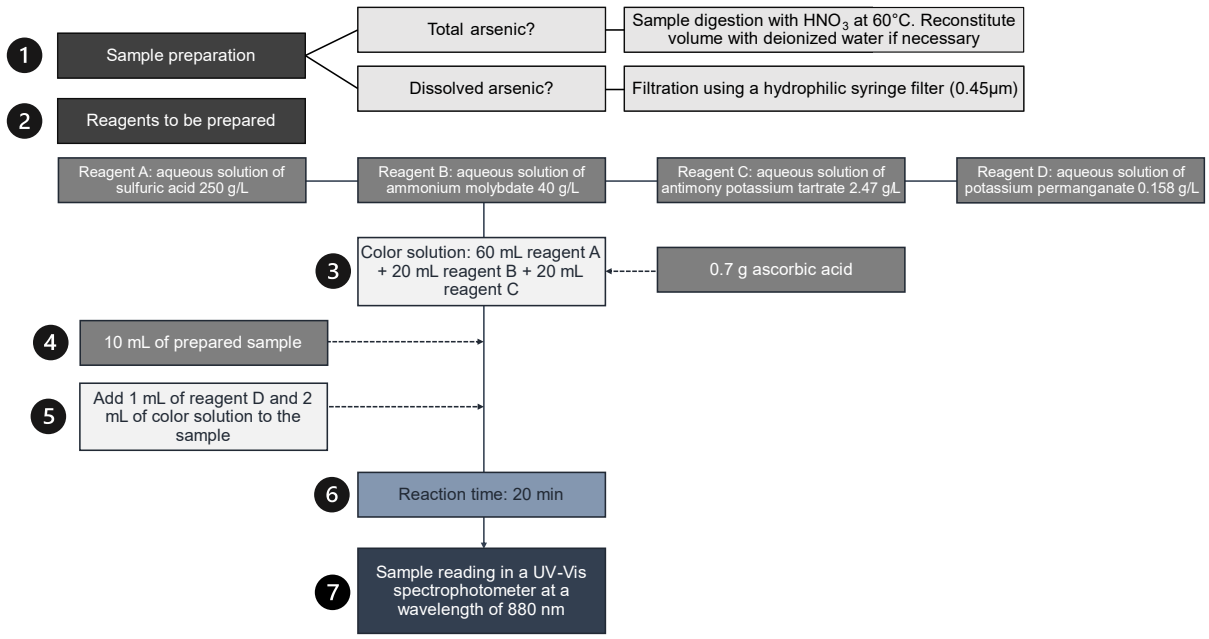

Source: Adapted from Guimarães et al., 2022; Moreira et al., 2023b, 2023a; Moreira et al., 2021b, 2021a

The results in Figure 2.7 indicate that the limit of detection and quantification for the method developed, which corresponded to 0.09 µg/L and 0.96 µg/L, respectively, are below the maximum value allowed by national and international agencies that limit the maximum value allowed in drinking water.

Figure 2.7. Mean absorbance and linear adjustment of results for standards of different concentrations. Red and grey bands represent the confidence limit at a 95% level.

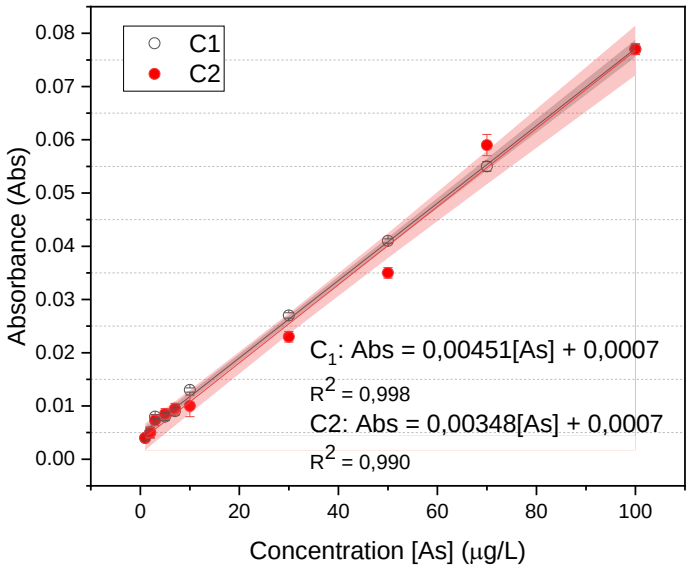

Source: Adapted from Guimarães et al., 2022; Moreira et al., 2023b, 2023a; Moreira et al., 2021b, 2021a

Their methodology was also validated by comparing the results obtained through the colorimetric technique and standard procedures (ICP-MS; results summarized in Figure 2.8). For that, real surface water samples spiked at different arsenic concentrations were used. High correlations were observed when the concentration values obtained from ICP-MS and the colorimetric protocol were compared. The adjusted r-square corresponded to R^2=0.835, which suggests that approximately 84% of the data obtained from the colorimetric procedure would match the results obtained from ICP-MS. In complement, Figure 2.9 presents these results, which show the difference between the concentration values obtained between the two techniques. The maximum and minimum values observed for residues were -4,991 – 4,004 µg/L, with a median of -2,466 µg/L. It is also observed that they are presented randomly and follow a normal distribution. Therefore, the expectation is that at least 68.3% of the analyses carried out present low residue values between -2.201 ± 1.967 µg/L. The normal distribution and randomness of the residuals meet the necessary requirements for validating the claimed methodology.

Figure 2.8. Correlation between arsenic concentration values obtained through the standard technique (ICP-MS) and the colorimetric method proposed (n=33).

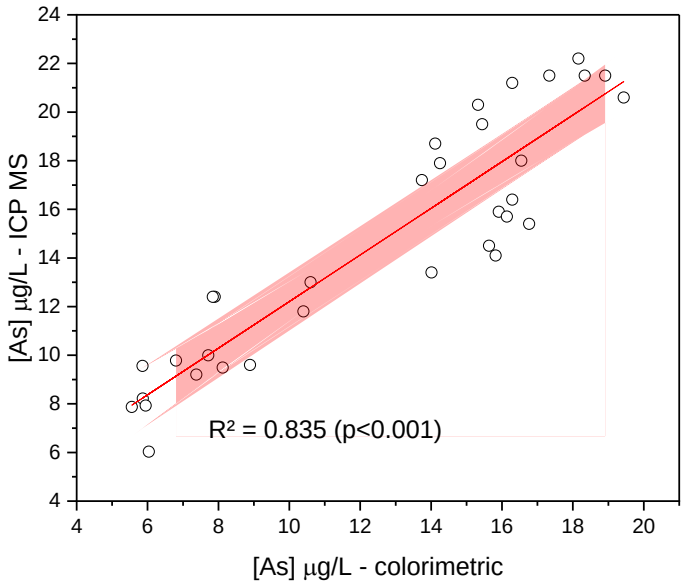

Source: Adapted from Guimarães et al., 2022; Moreira et al., 2023b, 2023a; Moreira et al., 2021b, 2021a

Figure 2.9. Difference between arsenic concentration values measured by the colorimetric method and the standard technique (ICP-MS) for different samples (n = 109).

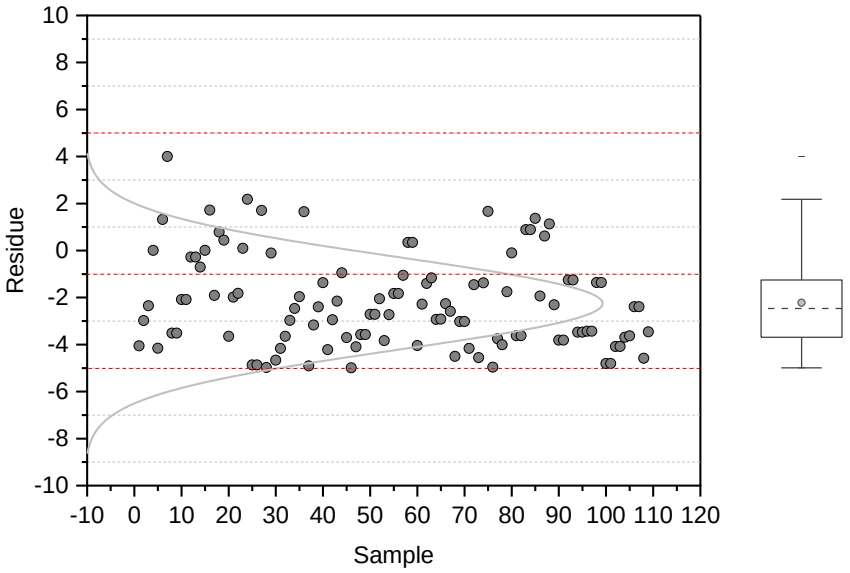

Source: Adapted from Guimarães et al., 2022; Moreira et al., 2023b, 2023a; Moreira et al., 2021b, 2021a

The parameters turbidity, iron concentration, and manganese concentration have little interference with the arsenic concentrations obtained by the colorimetric method. Randomness is observed when the residues are compared for different values of turbidity (Figure A1), iron concentration (Figure A1b), and manganese

concentration (Figure A1c). Figure A1 also shows the Spearman correlation coefficients when comparing the residuals and the variables mentioned, in all cases showing a low correlation (rSpearman close to zero) considered non-significant ($p>0.05$).

That is an important outcome, especially in the context of their study, in which iron and manganese are recurrent compounds in the basin where their studies were conducted. Investigations of water and sediment compositions suggested that arsenic, iron, and manganese could occur concomitantly since they derive from the same rock matrix (Borba et al., 2003; De C. Silva et al., 2018; Pinto et al., 2019). The same studies point out the potential for arsenic, iron, and manganese, detected in the bottom layers of the river, to be remobilized to aquatic environments, increasing the concentration of dissolved species. Even so, the results suggested that the method described could be a useful alternative for arsenic monitoring, free from interferences from iron and manganese.

The authors also raised the preliminary costs of their analysis, and the main cost data reported is presented in Table 2.3. The investment costs associated with the method would be mainly related to a new spectrophotometer, whereas the cost for each analysis would be lower than US$1, varying from US$0.31 for total arsenic and US$0.58 for dissolved arsenic. Despite being a preliminary estimation, the results suggest that the method would have a cost per sample analyzed lower than common practice for arsenic analyses via ICP-MS (~US$6.00; price informed by local laboratories). That represents an additional advantage to the method and reinforces its applicability for short-income locations and isolated and remote regions.

Table 2.3. Costs break down for analyses of total and dissolved arsenic.

Consumables and chemicals	Cost	Amount per sample	US$ per sample (total arsenic)	US$ per sample (dissolved arsenic)
Syringe filter	$57.00 (100 units)	1 unit	-	$0.57
Nitric acid	$15.13 (1L)	0.020 L	$0.30	-
Sulfuric acid	$19.20 (1L)	0.001 L	<$0.01	<$0.01
Ammonium molybdate	$112.65 (500 g)	0.016 g	<$0.01	<$0.01
Potassium tartrate	$25.12 (500 g)	0.001 g	<$0.01	<$0.01

Potassium permanganate	$15.03 (500 g)	0.158 g	<$0.01	<$0.01
Ascorbic acid	$14.44 (500 g)	0.014 g	<$0.01	<$0.01
Total costs			**$0.31**	**$0.58**

Source: Adapted from Guimarães et al., 2022; Moreira et al., 2023b, 2023a; Moreira et al., 2021b, 2021a

2.5 Technologies for arsenic removal

Given the high concentrations of arsenic found in various water courses and the negative effects that its consumption can cause, the need to apply proven-efficient technologies to remove As can be reaffirmed. Among the possibilities for removing As, it can be mentioned pre-oxidation (which is important for anoxic groundwater, where, at neutral pH, arsenic is found mainly in the form of As (III)), coagulation-flocculation, adsorption, ion exchange, and membrane separation processes (Moreira et al., 2021). Several recent studies highlight membrane separation processes as viable and effective technologies to treat arsenic-contaminated water, providing a safe permeate (Amaral et al., 2018; Foureaux et al., 2020; Reis et al., 2018) that can guarantee the safety of the water consumed by the population. These technologies were summarized in Figure 2.10.

Figure 2.10. Summary of consolidated technologies for arsenic control in water sources.

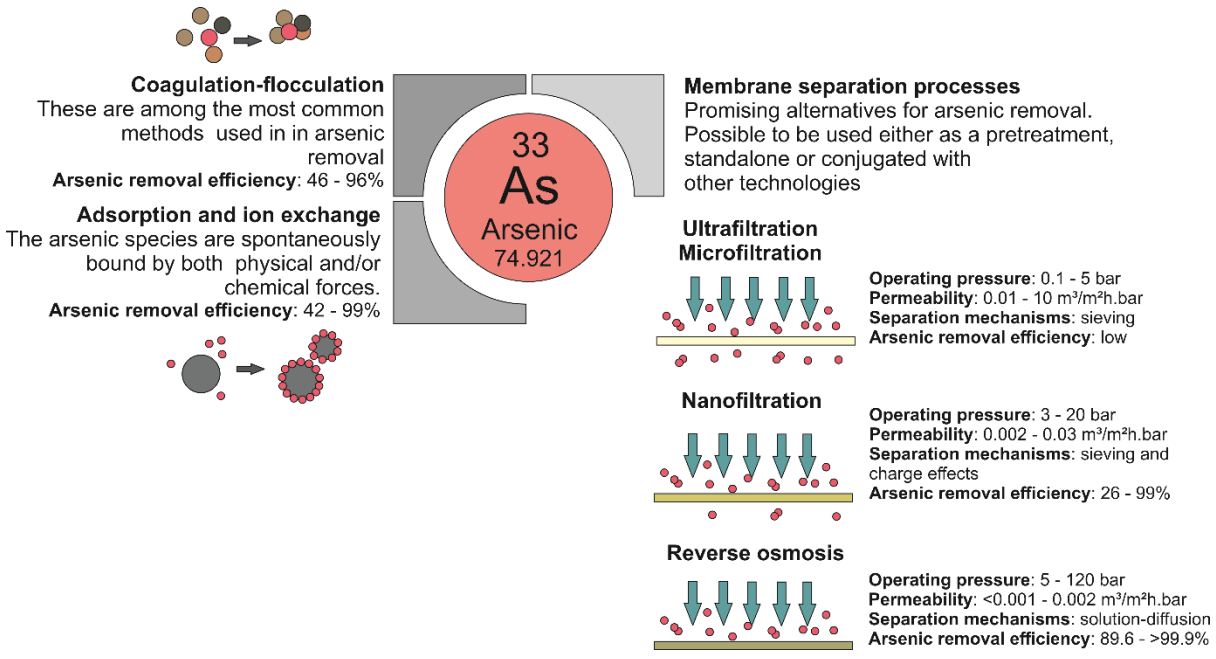

Source: Adpted from Moreira et al. (2021)

Pre-oxidation processes are intended to transform arsenite (arsenic III) into arsenate (arsenic V), the latter removed with greater efficiency by coagulation-flocculation, adsorption or even membrane separation processes. Studies suggest that the removal of arsenite is likely to be more affected by the surface water quality, specially by conventional technologies of coagulation-flocculation (Hering et al., 1997) and adsorption (Leupin and Hug, 2005) due to its poor mineral surface affinity. When arsenic and iron occur concomitantly, the pre-oxidation could contribute to the formation of insoluble precipitates, improving its removal rate (Hering et al., 1996; Krause and Ettel, 1989). In the Iron Quadrangle (Brazil) and the Altiplano-Puna volcanic complex (Argentina, Bolivia, Chille, and Peru), for example, the elements commonly derive from the same rock matrix, a scenario that could favor its removal in water treatment processes (de Figueiredo et al., 2007; Tapia et al., 2019). Another alternative is the use of iron-based coagulants during coagulation processes. To mention a few advantages of coagulation-flocculation are the lower costs and easily handle large water volumes; however, they required an additional process for flocs settling and removal from treated water, in addition to a safe sludge disposal due to its arsenic content.

Other alternatives are adsorption, ion exchange, and membrane separation processes, commonly employed as advanced technologies for water polishing. Adsorption and ion-exchange rely on a spontaneous interaction, whether physical or chemical, between the species of arsenic and the solid material. Their use to remediate arsenic is well documented accounts with the advantages of low chemical requirements; however, the costs could be higher than other technologies depending on the adsorbent or resin used and their regeneration process (Mohan and Pittman, 2007). In these processes, competitiveness also occurs for the active sites and the different pollutants present in water, directly impacting on the removal efficiency of a given specie (Moreira et al., 2019). Different than that, membrane separation processes are recognized for delivering a treated water with high quality regardless of the feed water composition (at higher or even trace concentrations of arsenic).

There are different membranes available for water treatment differing from their morphology, composition, and application. In Figure 2.10 are presented pressure driven processes (micro-, ultra-, nanofiltration, and reverse osmosis) and technologies that still require complementary studies to scale-up their usage (membrane distillation, electrodialysis, and forward osmosis). From the pressure driven process, nanofiltration and reverse osmosis presented the highest removal efficiency of arsenic with values >99%. These are generally non-porous membranes (with a few exceptions of nanofiltration membranes that still has pores on their structure) with potential to retain the dissolved fraction of divalent ions. The advancements in membrane materials also allowed their operation without pumps, but using the potential energy in a gravity driven process.

The subject was discussed by Pronk et al. (2019) which informed that total costs for gravity-driven systems can be lower than conventional processes and their operational stability and grid independence could extend their use to isolated and remote regions. That would be an important aspect and reflects the scenario faced by several regions and countries. The gravity-driven system presented by Moreira et al. (2022) showed a stable performance compatible with commercial membrane filters, attaining all 109 potable standards required by local environmental agencies, arsenic included.

In addition to the technologies mentioned, there are others specially developed for arsenic removal in low-income communities (Glade et al., 2021; Kabir and Chowdhury, 2017), rural and peri-urban areas (Kumar et al., 2019). In their review, Kumar et al. (2019) focused on low-cost adsorption methods with an implementation potential in Latin America. Glade et al. (2021), in turn, described a conventional iron electrocoagulation to treat arsenic contaminated drinking water in rural communities across the United States. The authors compared lab and field results and were able to reduce the arsenic concentration to values below 10 µg/L. Still, the process produced a hazardous sludge containing arsenic which requires attention for its proper disposal. It is a consensus among the studies the necessity for low-cost and easy-to-use technologies to attain the realities faced by these regions. Specially for low-income countries, Kumar et al. (2019) disclosed the advantages, disadvantages, and selection criteria for

different technologies. Despite the technology chosen and given the high arsenic concentration reported in Figure 2.1 (Table A1), it is important to guarantee and effective removal and the water safety to prevent risks related to arsenic exposure.

2.6 Conclusions

In this manuscript, a survey of arsenic concentration in the water resources from Latin American countries was carried out. The values reported in the literature were used in risk assessment calculations to enhance understanding of the consequences of arsenic occurrence in natural water sources. Analytical methods for arsenic quantification and technologies for its remediation were summarized, with particular attention given to the ones feasible in many places in these countries. The main conclusions of this study are highlighted below:

- Arsenic was often detected in waters from Latin American countries in concentrations above the safe limit (10 µg/L).

- Many studies were carried out in Argentina and Chile. They revealed the high concentrations of arsenic in their water resources.

- Only a few studies have been conducted in several countries, such as El Salvador, Honduras, Cuba, Haiti, Panama, and Colombia. There needs to be better knowledge about the real risks their water resources offer.

- In the best scenario, most water sources can be considered safe for irrigation and animal watering. In the worst scenario, 39.7% of the assessed locations have safe water to be used directly for irrigation, and 50.4% is considered safe for animal watering without prior treatment for As removal.

- In the worst scenario, high As levels might put the population at risk if the water is consumed without efficient treatment. Most waters offer non-carcinogenic risks (HQ>1) if directly consumed, and median carcinogenic risk values were classified as unacceptable.

- Simpler tests for arsenic monitoring carried out in situ and without expensive equipment are emphasized as attractive alternatives for enabling operational monitoring in locations with economic, logistical, and labor limitations. Colorimetric methods stand out in this context.

- Removing arsenic from water, especially drinking water sources, is imperative in many Latin American countries. Techniques such as pre-oxidation, coagulation-flocculation, adsorption, ion exchange, and membrane technologies can be used according to the location context.

Given the results, this review clarifies reasons for establishing more stringent legislation regarding arsenic occurrence. It highlights the need for further development, study, and application of effective and low-cost processes for monitoring and removing arsenic, considering the resources restrictions of many locations in Latin American countries. It is strongly recommended to carry out more studies concerning As in waters in some countries in Latin America so that the actual situation of these countries can be known. The summarized findings are expected to have broader implications, contributing further to ensuring water safety in Latin America.

3 CHAPTER 3: PRE-OXIDATION AND COAGULATION-FLOCCULATION AS A PRETREATMENT TO UF-RO APPLIED FOR SURFACE WATER TREATMENT AND ARSENIC REMOVAL

Abstract

In this chapter, the effects of applying pre-oxidation, coagulation, and flocculation (C/F) as pretreatment of an ultrafiltration (UF) - reverse osmosis (RO) system treating water containing arsenic were assessed. For this, the performance of a pilot scale – with a maximum treatment capacity of 2.25 m^3/h - UF-RO system with and without pretreatment was evaluated. The membranes were able to generate high-quality permeates, even when the feed presented a remarkable increase in color (>2100 uH) and turbidity (>300 NTU) due to the beginning of the rainy season. UF was not efficient for arsenic removal, so RO was essential to guarantee safe water, generating permeates with concentrations below 0.5 µg/L of arsenic. The effective removal of iron and manganese, among other ions, was verified using membranes. Given the high quality of the permeates, blend formulation strategies were carried out, mixing filtered water from the conventional water treatment plant and RO permeate (Strategy I) and mixing filtered water, UF permeate, and RO permeate (strategy II). Strategy II was viable for arsenic concentrations in filtered water of 13 and 15 µg/L. Pretreatment was important in maintaining a higher membrane permeability and ensured a more stable performance in the face of variations in feed quality, which may be seasonal in some places, as in the present case, where feed quality is significantly altered by the rainy season. Overall, although UF and RO membranes are effective processes for treating surface water containing arsenic, the results suggested that pretreatment, which is already part of the treatment of several water treatment plants, guarantees more robustness to the treatment concerning a higher and more stable membrane permeability, directly impacting operational expenses with membranes operation.

3.1 Introduction

Several countries have naturally high concentrations of arsenic (As) in their water resources (Litter et al., 2019; Tapia et al., 2022; Alarcón-Herrera et al., 2020). However, some anthropogenic activities, such as mining and metallurgical

processes, may also release arsenic in environmental compartments. Exposure to arsenic occurs mainly through water ingestion, use of contaminated water for irrigation, and use in food preparation (WHO, 2003). Vomiting, diarrhea, and death may happen in extreme cases of acute arsenic poisoning. In the long term, high concentrations of arsenic through ingestion can cause many effects, including cancer (Smith et al., 1992; WHO, 2009). Applying efficient technologies for arsenic removal from water is crucial to promote favorable health conditions in several places since it is estimated that around 140 million people in more than 70 countries consume water containing arsenic in concentrations higher than the World Health Organization (WHO) guidelines, 10 µg/L (WHO, 2022).

Coagulation-flocculation can be mentioned among the technologies applied to remove As, given its low costs and relatively simple operation for treating large water volumes. However, large amounts of arsenic-containing sludge are generated and, given the low As removal, may require an earlier pre-oxidation step. Adsorption also deserves to be mentioned, given its good acceptance in the market. However, its efficiency can be strongly impacted by the presence of other ions (Moreira et al., 2021).

In more critical water quality conditions, such as during rainy periods or when water treatment plants experience operational issues that compromise the quality of treated water, the water treatment plant resilience is crucial and could be provided by membrane processes. They are physical treatment processes that can produce high-quality water irrespective of the initial feed water conditions. It, in turn, ensures a safer and higher-quality water distribution to the population, even under adverse conditions.

Ultrafiltration (UF) is a reliable membrane process for treating surface water, as it is a barrier to bacteria, viruses, colloids, and precipitated species (Shen et al., 2020). Consequently, the application of full-scale UF has increased dramatically in recent decades (Yu et al., 2020). For example, the capacity of full-scale UF in drinking water treatment plants in China reached 10 million m^3/d in 2020 (Chang et al., 2022).

The main UF separation mechanism is size exclusion. Therefore, UF is not expected to be able to remove arsenic effectively, removing only the particulate fraction. In fact, in the studies by Hsieh et al. (Hsieh et al., 2008), UF removed between 1 and 14% of the total arsenic in real groundwater. However, there is evidence that a considerable amount of the total arsenic concentration in natural waters can be removed when it is associated with particulate or colloidal material that acts as a carrier (Bradhuber; Amy, 2001, Guimarães et al., 2022). Guimarães et al. (2022) observed arsenic removal efficiencies by UF that varied between approximately 14 and 80%. The highest removal efficiencies found in this study are due to the high percentage of arsenic (up to around 80%) in its colloidal form in the treated water.

Reverse osmosis (RO) can be applied to improve As removal since it is a well-known technology capable of removing arsenic from water effectively (Ning, 2002; Abejón et al., 2015). Yoon et al. (2009) compared different membranes for arsenic removal. While the UF membrane removed ions, including arsenic, with efficiencies varying between 3 and 47%, the RO membrane had a rejection of all ions greater than 90%. However, the energy demand for RO operation is higher, and RO membranes are more susceptible to fouling than UF. Given the limitations of UF and RO systems, these processes can be integrated to combine the advantages of each membrane process and overcome their respective drawbacks. When comparing the number of studies on UF-RO systems, there are few studies that reported the efficiency of arsenic removal from these systems together (Guimarães et al., 2022, Tomaszewska; Bodzek, 2013).

However, membranes are subject to fouling, the deposit of organic, inorganic, and biological material on the membrane surface, resulting in lower permeability and greater energy expenditure to maintain performance (Huang et al., 2009). Fouling is determined by several factors, such as feed water characteristics, membrane features, and operation conditions (Yu et al.,, 2020). As the fouling layer development is intrinsic to membrane processes, several fouling mitigation techniques are investigated (Costa et al., 2021), including pretreatments.

Pretreatment and membrane process integration is done recurrently at full scale (Huang et al., 2009). Pretreatments effectively improve the feed quality and impact the membrane performance mainly in three ways: changing the size distribution of potential foulants, modifying the affinity between contaminating species or between them and the membrane surface, and minimizing the growth of microorganisms.

In their consistent review, Huang et al. (2009) emphasize that coagulation is the pretreatment used most successfully to reduce fouling. The coagulation process involves the addition of a coagulating agent that destabilizes the colloidal dispersion, reducing the repulsive charges between the particles. The aggregation of these destabilized particles to form flocs that settle at a faster rate is named flocculation. When applied before membrane filtration, these processes provide less foulant feed water.

Shen et al. (2020) observed that coagulation and flocculation alleviated UF fouling since organic matter was efficiently removed, and larger flocs, more resistant to shear force, were produced. Thus, a porous cake layer made the membrane pores less obstructed. In addition to less pore blockage and lower fouling layer resistance, coagulation and flocculation increase backwash efficiency (Barbot et al., 2008). Malkoske et al. (2020) investigated three types of pretreatment configuration for microfiltration and UF: coagulation and no/incidental flocculation, coagulation and flocculation, and conventional coagulation (coagulation, flocculation, and sedimentation). It was observed that coagulation and flocculation before UF was the pretreatment configuration that provided a smaller cake layer and a lower resistance of the fouling layer. In contrast, conventional coagulation provided a greater reduction in fouling rate since the mass flux to the membrane surface was reduced.

Assessing coagulation and flocculation as pretreatment for UF is particularly strategic since conventional drinking water treatment often involves this process. In addition, many water treatment plants (WTP) apply pre-oxidation before coagulation since it is widely known to improve coagulation performance in removing natural organic matter, inorganic colloids, and algae (Xie et al., 2016).

In this way, several plants can implement membrane systems, requiring as few modifications as possible to the existing structure and process, so the system pre-oxidation - coagulation/flocculation can act as an efficient pretreatment of the feed of the membrane process.

Besides, the RO permeate physicochemical quality is very high, so mixtures of the permeates can be made, furnishing a blend that meets potability standards. It is an attractive strategy, considering it reduces the volume of water to be treated by RO and the energy costs related to its operation. Guimarães et al. (2022) found that coupling UF and RO to conventional water treatment could enable the formulation of blends that meet the drinking standards, even with feeds containing high concentrations of arsenic. In this 2022 paper, the authors have evaluated already consolidated technologies; however, they brought the novelty of integrating them into the conventional water treatment process to guarantee the removal of arsenic and safe water. However, this study was carried out using a bench-scale system.

Thus, given the promising results found and the entire scenario described, the primary objective of the present study was to investigate, for the first time on a pilot scale, the performance of pre-oxidation, coagulation, and flocculation as pretreatment for the UF- RO system treating surface water with a focus on removing arsenic. The study validates the performance of membrane separation processes reported on a bench scale. In addition to the fact that no other paper that evaluates the integration of UF-RO into conventional treatment on a pilot scale with this objective has yet been found, the authors have also not found any work that analyzes the effect of pre-oxidation, coagulation, and flocculation on UF-RO performance.

Therefore, in the present study, the performance of UF-RO with and without pretreatment was evaluated, and permeate quality was compared to the potability standard parameters. Strategies for concentration management were also discussed. In addition to standing out for being a pilot-scale study, real water matrices in different periods (dry and rainy) were treated, representing real conditions of water quality along the operation of a drinking water treatment plant.

In a broader context, considering that many water treatment plants in the world apply pre-oxidation, coagulation, and flocculation and that the waters of several countries naturally have concentrations of arsenic higher than those recommended by WHO, it may be interesting to install membranes to guarantee the removal of arsenic and other behaviors persistent to conventional treatment. Therefore, this work is especially relevant as it provides interesting information about how these conventional processes affect the performance of membranes when used to generate safe drinking water.

3.2 Methodology

3.2.1 Surface water

The UF-RO test was conducted with raw surface water from the Velhas River basin (latitudes: 17°15′S and 20°25′S and longitudes 43°25′W and 44°50′W, Minas Gerais, Brazil). The Velhas River drains an area of 27,867 km2, and it is the main tributary of the São Francisco River, one of the largest Brazilian rivers. Velhas River receives industrial and domestic wastewater. This basin includes the iron quadrangle, a region well known because of its gold and iron deposits and where there is intensive mining activity. Therefore, arsenic and iron, besides other contaminants such as manganese, pose a challenge to water treatment plants (WTP) from this basin. The most recent monitoring data (from 2023) on arsenic, iron, and manganese, provided by environmental agencies, is summarized in Figure 3.1. Data for dissolved manganese were unavailable; however, it is noteworthy that all three elements occur in high concentrations in surface water and could threaten the drinking water quality provided by conventional drinking water treatment plants. The total concentration value for arsenic varied from 0.5 to 183.8 µg/L; for iron and manganese, that were also monitorated, the values corresponded to 0.03 to 15.08 mg/L and 0.007 to 4.193 mg/L, respectively.

Figure 3.1. Monitoring data (obtained during 2023) on arsenic, iron, and manganese, provided by environmental agencies (IGAM, 2023). Data for dissolved manganese was not available.

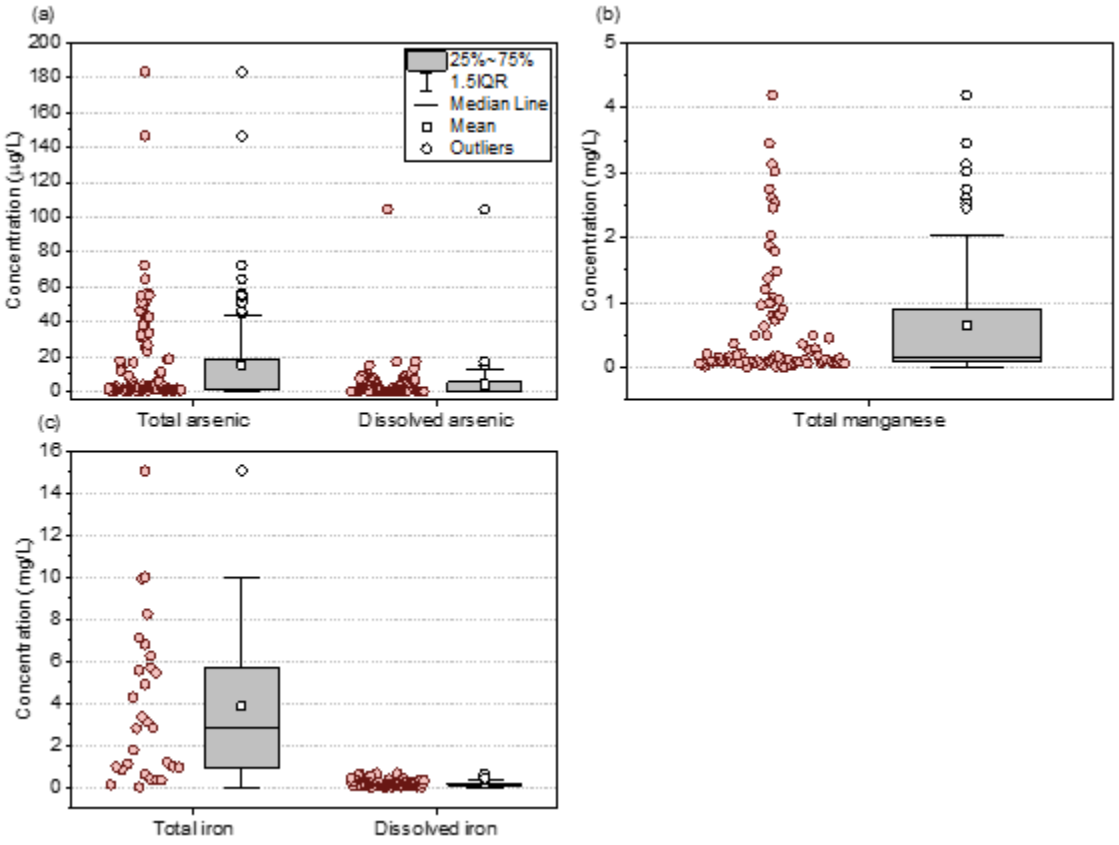

The river water that fed ultrafiltration was enriched with varying dosages of arsenic (13, 15, 18, and 20 µg/L) using a stock solution prepared with deionized water ($Na_2HAsO_4 \cdot 7H_2O$; 1 g/L). These values were observed in water previously treated by conventional process. These other physicochemical characteristics of the raw water used in this study are shown in Table 3.1, which exhibited high values of turbidity and manganese.

Table 3.1. Characterization of water from the Velhas River (UF feed during period without pretreatment) and the settle water (UF feed during period with pretreatment). Sampling occurred in August 2022, when tests were carried out. The minimum sampling frequency was 12 times a day, except for iron, which was 6 times a day.

Parameter	Velhas river				Settled water			
	Average	Median	Minimum	Maximum	Average	Median	Minimum	Maximum
Turbidity (NTU)	71.03 ± 80.97	32.2	10.3	333	2.25 ± 0.44	2.11	1.69	3.92
Color (Uh)*	179.46 ± 338.07	50	15	1200	29.86 ±6.7	30	20	40
pH	7.72 ± 0.33	7.69	6.81	8.59	8.96 ± 0.17	9.01	8.23	9.22

Conductivity (µS/cm)	74.87 ± 0.81	75.01	73.62	76.21	135.77 ± 1.32	135.7	133.2	139.2
Arsenic (µg/L)	18 ± 5	18	9	33	19 ± 5	2	8	30
Iron (mg/L)	6.2 ± 14.87	0.81	0.07	55	0.75 ± 0.15	0.8	0.52	1.05
Manganese (mg/L)	0.32 ± 0.36	0.16	0.03	1.44	0.06 ± 0.01	0.06	0.04	0.08

Due to the UF-RO pilot plant's connection to an existing water treatment facility, intentionally introducing arsenic into raw surface water, risking water quality, was deemed inappropriate. Besides, the occurrence of As is seasonal, increasing mainly during the rainy season. Therefore, adding arsenic solution in the water for a more extended operation was necessary to guarantee arsenic supply for this study.

3.2.2 Pilot-plant description

The feed system consisted of 3 interconnected feed tanks with a capacity of 20 m^3. Feed pumps, piping, and valves were arranged to recirculate feed into the tank and promote mixing.

The UF system operated with ZeeWeed 500d modules (Figure 3.2) with a polymeric membrane with nominal pore size of 0.04 µm and area of 40.9 m^2. The treatment capacity is 1 - 2.25 m^3/h in direct filtration mode. The main skid contained the membrane tank, cleaning-in-place (CIP) tank, chemical cleaning pumps, control panel, air compressor, and other minor components used to operate the membranes.

Figure 3.2. Pilot-scale Ultrafiltration - ZeeWeed 500d modules

The membranes operated under a small negative pressure (0.15 – 0.20 bar) created by pumping permeate through the hollow fiber. Part of the permeate was stored in a process tank for back pulse and backwash. The permeate pump was also used to perform backwash and maintenance cleaning of the membranes. During operation, the pump flow rate was controlled to maintain the desired filtration rate. Membrane aeration occurred intermittently through the bottom of the membranes to create turbulence. Aeration was provided only as part of the backwash step in low solids loading applications (feed turbidity < 10 NTU). System operation included back pulse backwashing, aeration, and draining of the membrane tank to eliminate solids. The UF plant was positioned downstream of the WTP settlers.

The reverse osmosis plant operated with three 4” elements in a 2:1 arrangement, as shown in Figure 3.3. The area of each membrane module was 8.4 m^2. The main skid contains the membrane modules, pumps, CIP tank, control panel, and most other components used to operate the membranes. RO was fed with UF permeate stored in the RO feed tank. The feed water from the RO pilot plant was previously filtered using 5 µm cartridge filters to remove suspended solids that could damage the membrane elements.

Both UF and RO units had instruments that enabled remote operation and online monitoring of permeate flux, pressure, temperature, and pH, with the UF unit including turbidity and the RO unit electrical conductivity and total dissolved solids (TDS).

3.2.3 Pilot-plant operation

To assess pretreatment effects on UF-RO system performance, UF was fed with water from a real Water Treatment Plant (WTP). The water treatment plant has a nominal treatment capacity of approximately 7.5 m^3/s. The treatment sequence applied in this WTP was: pre-oxidation (NaOCl), coagulation-flocculation (two fast mixing chambers, 24 hydraulic and mechanized flocculators with four chambers each; coagulant: $FeCl_3$), settlers (six pool-type settlers), sand filtration, disinfection, fluoridation, and stabilization. The settled water was pumped to the pilot plant feed tanks. The quality of the settled water produced by the WTP is shown in Table 3.1.

The operation with pretreatment lasted 129 h. The UF operated with a constant permeate flux of 39 $L/m^2.h$ and a water recovery of 95%. Every 14 min, a backwash was performed for one minute. Once a day, the membrane was cleaned with a 200 mg/L solution of sodium hypochlorite, and once a week, maintenance cleaning was performed by applying a citric acid solution (800 mg/L). The cleaning procedure followed the steps: backwash (15 seconds), aeration of the membranes (600 seconds), concentrate drainage, filling the tank with the cleaning solution via backwash and internal recirculation, resting for contact with the solution (900 seconds), cleaning solution drainage, backwash flushing (30 seconds), membranes resting (10 seconds), filling with raw water, and returning to operation. The RO unit operated with a constant permeate flux of approximately 17 $L/m^2.h$ and the element recovery of 11.7%.

The operation without pretreatment was conducted for 223 h, similar to that described previously, except that the UF permeate recovery was 92% when the feed had turbidity from 10 to 100 UT and 87% when turbidity of about 300 NTU was observed. In addition, it was necessary to dose sodium hypochlorite (0.5 mg/L) in the UF feed to prevent biofouling in the UF-RO system (which was not

necessary when the pretreatment was applied since the feed was decanted water containing enough residual chlorine to control biofouling). Figure 3.3 provides an infographic with an overview of operational conditions.

Figure 3.3. Operational conditions during UF-RO test with (1) and without (2) pretreatment

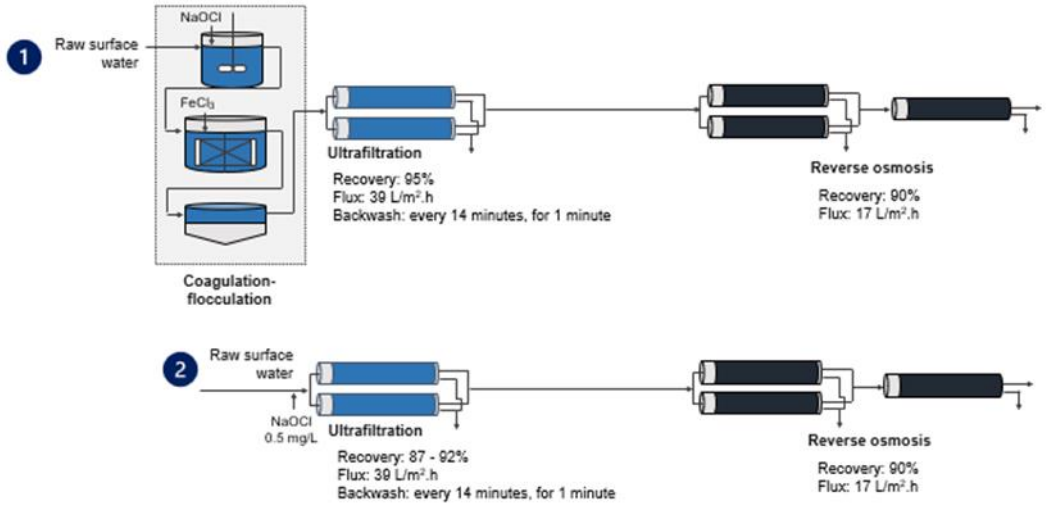

Flux, pressure, temperature, turbidity, and pH of the feed and permeate were monitored using the pilot unit instruments. Color, iron, manganese, and arsenic concentrations of currents were also monitored. Daily, a sample of the permeates from both UF and RO was collected to verify the effective compliance of the treated water with the Brazilian potability standards established by Ordinance GM/MS nº 888/2021. A sample of the RO concentrate was also collected daily to assess whether the quality of the RO concentrate meets the Brazilian release standards in accordance with COPAM/CERH-MG Resolution No. 08 of November 21, 08/2022.

Sampling, conservation of samples, and physicochemical analyses were carried out following the recommendations of the Standard Methods for the Examination of Water and Wasterwater (APHA, 2017). The samples were characterized in terms of their turbidity (Hach 2100Q), pH (MS Tecnopon mPA-210), color (Hach DR3900), and conductivity (MS Tecnopon mCA-150). Iron, manganese, aluminum, calcium, magnesium, and arsenic concentration values were determined by inductively coupled plasma mass spectrometry (Agilent ICP-MS

7700; method 3125B). The analyses to verify compliance with current legislation were conducted in an external laboratory according to the Standard Methods for The Examination of Water and Wastewater (APHA, 2017).

The total resistance to filtration (R) was obtained through the permeability data monitored and using equation 1:

$$R(1/m) = 1/(k \cdot \mu_{25^{o}C}) \quad (1)$$

In which k is the membrane permeability in (m^3/m^2.s.Pa) and μ is the dynamic viscosity of water at 25 ºC (8.9 x 10^{-4} Pa.s).

Specific energy consumption (SEC) for UF was calculated according to Moreira et al. (2022) and for RO was calculated according to Kim and Hong (2023) and Kim et al. (2024).

3.2.4 Blends

While operating the pilot plant with pretreatment, the feasibility of treating only a portion of the settled water in the UF-RO system was assessed. The fraction of settled water not treated by the UF-RO system underwent filtration in sand filters. The permeates and filtered water were blended. This strategy can reduce energy costs while maintaining acceptable water quality. Two blend formulation strategies were evaluated. Strategy I involved the mixture of WTP-filtered water and RO permeate in a 1:1 ratio, while strategy II consisted of the mixture of UF permeate, RO permeate, and WTP-filtered water in a 1:1:1 ratio. The filtered water used in the blends was also fortified with arsenic to have the same concentration as the UF feed water. The water quality leaving the sand filters is shown in Table 3.2. The blends were formulated and characterized daily according to the parameters mentioned in item 3.2.3.

Table 3.2. Characterization of the WTP filtered water.

Parameter	Value
Color (uH)	5
pH	8.8
Turbidity (NTU)	< 0.1
Temperature (ºC)	19.8

Iron (mg/L)	< 0.001
Manganese (mg/L)	< 0.001
Total Arsenic (mg/L)	< 0.0005
Dissolved As (mg/L)	< 0.0005
Condutivity (µS/cm)	143
Calcium (mg/L)	13.8
Magnesium (mg/L)	2.29

3.2.5 Statistical analysis

Microsoft Excel and Statistica 13.3 were used for statistical and data analysis. Mann-Whitney U Test and Spearman were used to compare two independent groups and correlation. Non-parametric statistical tests were applied due to the number of replicates and for better confidence in comparing two independent groups and correlation. A confidence level of 95% was set for all statistical analyses performed.

3.2.6 Economic analysis

The economic analysis was carried out in order to: (i) assess how much more it costs for the WTP of the present study to operate the UF-RO system treating its entire flow, considering 15 years of operation and excluding expenses with concentrate; (ii) assess the capital expenditures for the WTP related to the implementation of the UF-RO system operating treating the entire flow and considering the adoption of blending strategies; (iii) assess the OpEX related to the operation of the treatment system for different communities, from 1,500 inhabitants to 540,000. The economic analysis was conducted similarly to that described in Moreira et al. (2021). Concerning the values of the parameters used in the calculations, the membrane's flux, recovery, operating pressure, and cleaning frequency were based on values obtained in this study. Annual correction index and currency were obtained according to the time of writing, and other parameters were obtained from Moreira et al. (2021). The parameters used for the calculations are found in Table 3.3.

Table 3.3. Values of the parameters considered for the economic analysis

Parameters	
UF permeate flux (L/m^{2}h)	39
UF recovery (%)	95
UF operating pressure (bar)	0.2
RO permeate flux (L/m^{2}h)	17
RO recovery (%)	19
RO operating pressure (bar)	90
Plant lifespan (year)	15
Pump Eficiency	0.75
Membrane lifespan (year)	7
Annual correction index (%)	10.7
Currency (September 21th, 2024)	US$ 1.00 = R$ 5.50
Membrane cleaning Frequency	6 a week

3.3 Results and discussion

3.3.1 Membranes performance and compliance with potability standards

The turbidity and color results are presented in Figure 3.4 and show the high efficiency of UF and RO with and without pretreatment. Even with a feed with high turbidity and color, permeates have high quality (<0.25 NTU). During the pilot plant operation without pretreatment, a marked increase in color (>2100 uH) and turbidity (>300 NTU) in the feed for this test was observed. The increase in both parameters marked the beginning of the rainy season, which promotes higher turbulence in water streams and increases the concentration of suspended particles. However, even in this scenario, the high quality of the permeate was evident, attesting to the efficiency of the membranes in removing solids and other compounds that generate turbidity and color.

UF membranes usually remove suspended solids with efficiencies greater than 90% (Cano; Moulin, 2022; Bourgeous et al., 2001; Elgamarnah et al., 2023; Czuba et al., 2022). The main removal mechanism involved is size exclusion, retaining particles with an average size greater than the membrane pores. Previous studies also demonstrated their efficiency in terms of color removal [(Moreira et al., 2023). Furthermore, in a system that integrates UF and RO membranes, the first acts as a pretreatment, preventing severe fouling in RO membranes (Cano; Moulin, 2022).

Figure 3.4. (a) Turbidity and (b) color in the feed (F) stream, ultrafiltration permeate (UFp), and reverse osmosis permeate (ROp) in a scenario with (n=68) and without pretreatment (n=58).

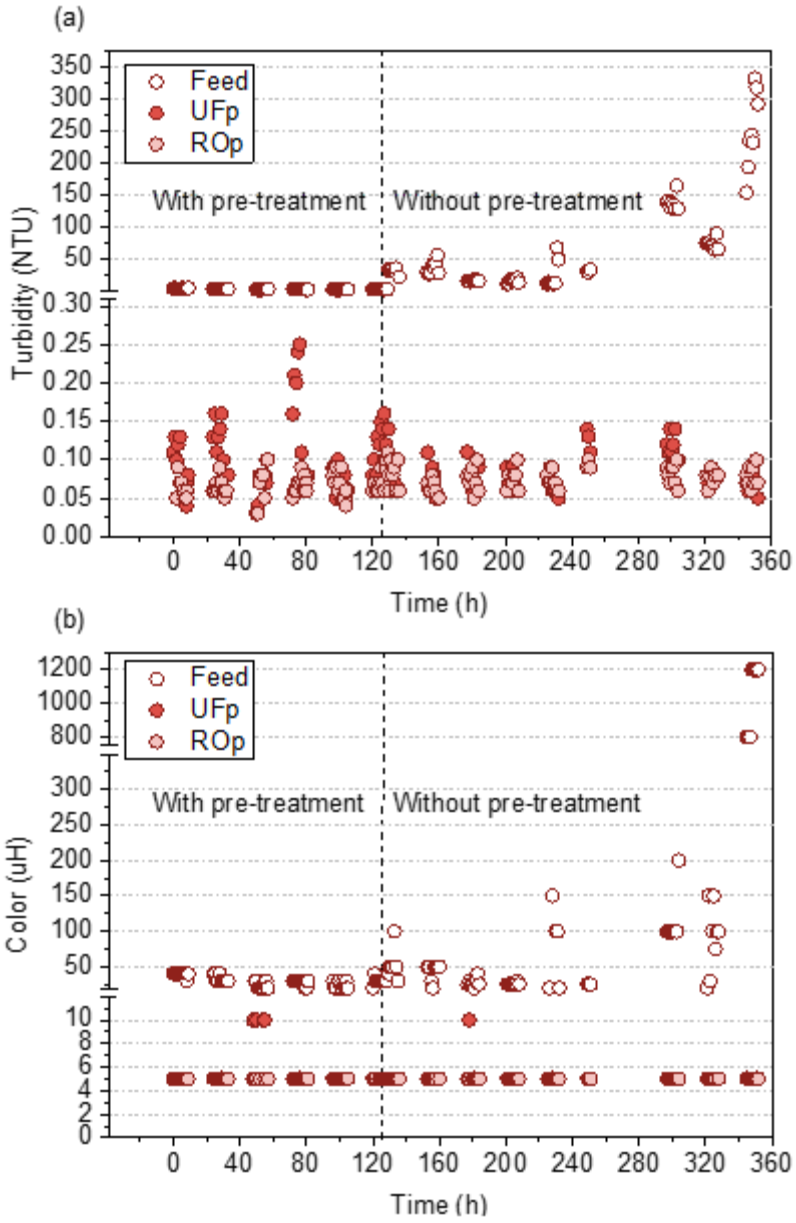

Mann-Whitney test was applied for color with and without pretreatment, and it is notable that the pretreatment did not affect the turbidity and color values, and all of them remained within the national limits for potability (15 uH for color; (Brasil, 2021)). Regarding turbidity, UF permeates from both tests did not present significative difference (p=0.054), while RO permeates were significantly different (p=0.00), even the average values of turbidity in RO permeates being very close (0.077 ± 0.015 and 0.066 ± 0.016).

Figure 3.5 shows the arsenic concentration in the feed, UF permeate, and RO permeate during the pilot plant operation. The arsenic concentration in the UF feed varied between 8 and 30 µg/L during operation with pretreatment, and 9.3 to 33.2 µg/L during operation without pretreatment. UF was not effective in removing As, and the mean removal values were 27±17% and 36 ± 26% with and without pretreatment, respectively. The UF permeate had arsenic values higher than national and international potability standards (maximum value of 10 µg/L) in 60% (with pretreatment) and 63% (without pretreatment) of the samples.

It is noteworthy that UF membranes are porous and have larger pores (0.01 µm) than arsenic in its dissolved form (0.0002 µm (Yang et al., 2019)). In this way, only the arsenic associated with solids in suspension or its colloidal form is removed by UF. Arsenic and its association with suspended solids were confirmed by the significant and negative relationship between the values of dissolved arsenic and turbidity in the UF feed (RSpearman: -0.6685, $p < 0.001$ for system with pretreatment and RSpearman: -0.4797, $p = 0.00131$ for system without pretreatment). In other words, the greater the concentration of suspended solids (indirectly monitored as turbidity), the lower the concentration of dissolved arsenic.

In addition to the interaction of arsenic with other suspended species present in the feed, arsenic co-precipitation with iron oxidation may have occurred due to the residual chlorine. Previous studies (Moreira et al., 2021a, Moreira et al., 2021b) demonstrated an oxidant agent's contribution to converting dissolved iron in the raw water into its non-soluble form (e.g., colloids and complexes). The compounds formed entrapped the dissolved species of arsenic and manganese, leading to their indirect removal. This hypothesis is reinforced by the moderate and negative relationship between dissolved arsenic and iron concentration values in the UF feed during the operation with pretreatment (RSpearman: -0.502, $p < 0.05$).

Even so, the residual concentration of arsenic in the UF permeate corresponded to 15 and 12 µg/L on average for systems with and without pretreatment. UF permeates were similar in terms of arsenic ($p=0.055$). Notably, the removal

efficiency decreases as the concentration of arsenic increases in the UF feed, an expected result given the lower contribution of UF membranes to arsenic removal. Under such circumstances, it is possible to verify the importance of RO to promote the effective removal of arsenic, generating permeates with concentrations below the maximum potability value (10 µg/L, Ordinance GM/MS nº 888/2021 and WHO (Brasil, 2021; WHO, 2011)). Even with arsenic concentration variations in UF permeates (5 to 24.4 µg/L with pretreatment and 1.83 to 23.6 µg/L without pretreatment), RO permeates always had arsenic concentrations below 0.5 µg/L.

Figure 3.5. Arsenic concentration in the feed stream (F), ultrafiltration permeate (UFp) and reverse osmosis permeate (ROp) with (n=69) and without pretreatment (n=66).

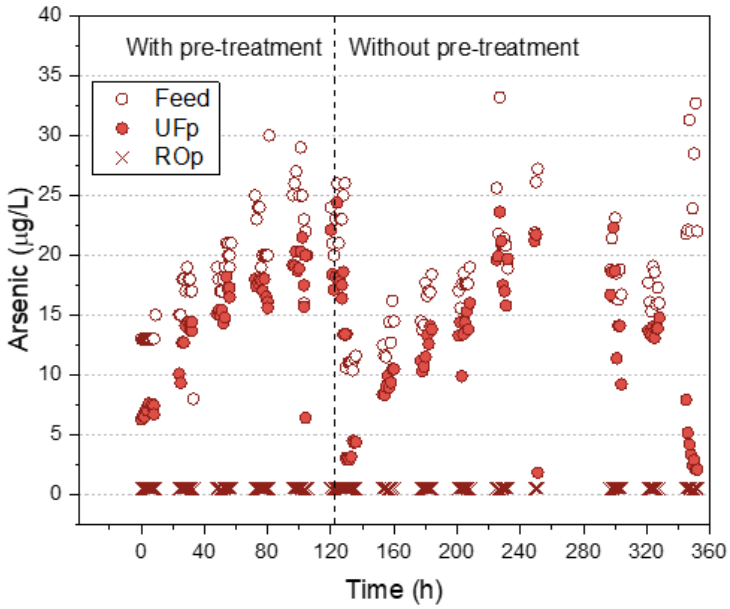

Another point of attention is the removal of iron and manganese (Figure 3.6). When pretreatment was applied, UF feed showed manganese concentrations between 0.044 and 0.079 mg/L. It is noted that the pretreatment had already provided water that meets the standards of the GM/MS 888/2021 (Brasil, 2021) ordinance (maximum allowed value of 0.1 mg/L) and the provisional guideline value of 80 µg/L recommended by WHO (WHO, 2011) for manganese.

High removals of manganese by the membranes were observed, even when there was no pretreatment - only 6.8% of UF permeates did not meet national and international potability standards for manganese. The permeates from the

test without pretreatment had higher manganese concentrations. It can be explained by the higher manganese concentration in the non-pretreated UF feed (it varied from 0.028 to 1.44 mg/L without pretreatment). These higher values are due to the beginning of the rainy season. Besides, when there was no pretreatment and no oxidation step, UF could not remove the fraction of magnesium that was dissolved. In this way, RO permeates in the two systems showed significantly different manganese values ($p<0.00$). The inclusion of an oxidation step before UF would be an option to increase manganese retention by the UF in cases where the UF-RO system would operate receiving raw water.

Figure 3.6. Concentration of (a) iron and (b) manganese in the feed stream (F), ultrafiltration permeate (UFp) and reverse osmosis permeate (ROp) with (n=31) and without pretreatment (n=59).

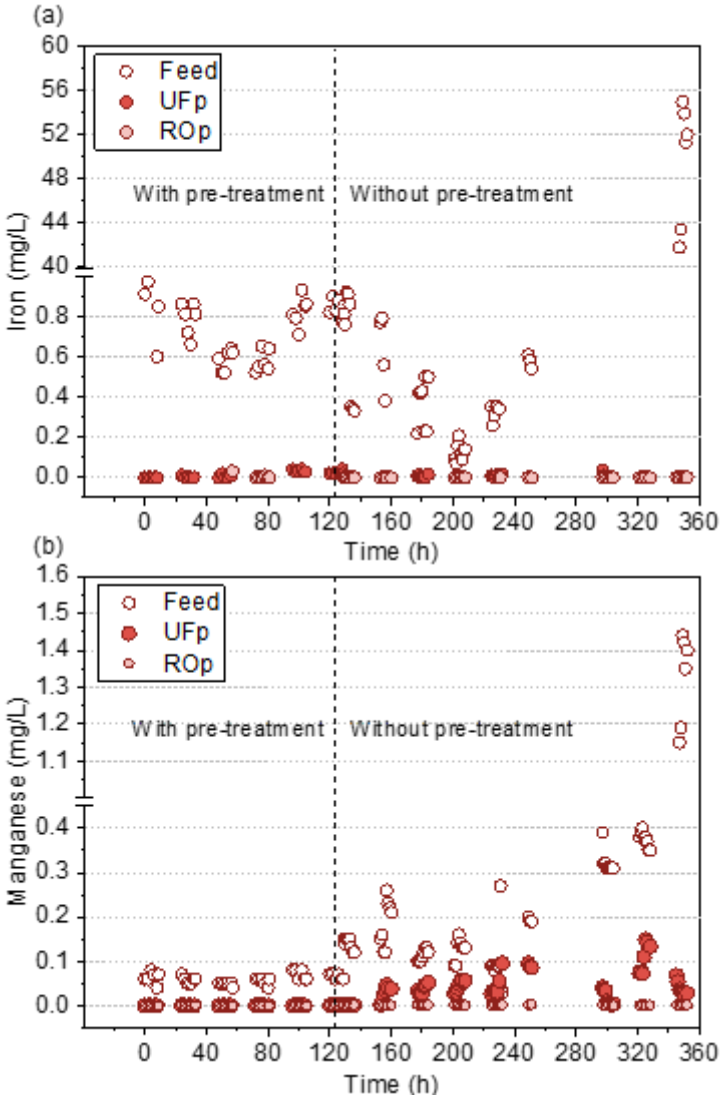

Iron levels in UF feed varied from 0.071 to 55 mg/L when there was no pretreatment and from 0.22 to 1.05 mg/Lwhen pretreatment was applied. Iron effective removal was verified using membranes, even when the UF feed had a notably higher iron concentration during the rainy season. The iron concentration in permeates was lower than the established maximum value for potability (0.3 mg/L - GM/MS 888/2021 (Brasil, 2021); no guideline is proposed for iron by WHO (WHO, 2011)). UF and RO permeates showed no significant difference in iron concentration (p=0.36 and 0.30, respectively). The effective removal of iron by UF membranes is expected since most of the iron is found in its insoluble form. In addition, as manganese and arsenic are associated with iron complexes, their removal also contributes to the removal of other chemical elements (Zhang et al., 2020). As with iron and manganese, UF is a barrier to both contaminants. Besides, UF prevented fouling of RO membranes by iron and manganese.

In addition to color, turbidity, iron, manganese, and arsenic, pH, temperature, conductivity, residual chlorine, calcium, magnesium, TSS, alkalinity, and hardness were monitored, whose average values are shown in Table 3.4.

Table 3.4**. Additional physicochemical characterization of the feed stream, ultrafiltration permeate (UFp), and reverse osmosis permeate (ROp) during periods with pretreatment (C/F-UF-RO) and without pretreatment (UF-RO). Table B1 (Appendix) contains all the potability parameters required by Brazilian legislation for blends formulated in the UF-RO test with and without pretreatment.**

Parameter	Sample		Mean ± standard deviation	Median	Min.	Max.
pH	C/F-UF-RO	Feed	8.96 ± 0.17	9.01	8.23	9.22
		UF_P	8.95 ± 0.13	8.97	8.51	9.17
		RO_P	8.17 ± 0.74	8.34	6.25	9.13
	UF-RO	Feed	7.72 ± 0.33	7.69	6.81	8.59
		UF_P	7.54 ± 0.33	7.46	6.87	8.47
		RO_P	6.73 ± 0.41	6.74	5.85	8.10
Temperature (ºC)	C/F-UF-RO	Feed	22.3 ± 1.8	22.1	18.3	26.1
		UF_P	21.9 ± 1.7	22.1	18.4	25.1
		RO_P	24.5 ± 2.1	24.7	19.5	27.6
	UF-RO	Feed	20.9 ± 2.0	20.5	18.2	26.3
		UF_P	20.8 ± 1.7	20.4	17.9	26.1
		RO_P	24.0 ± 1.1	23.9	22.0	29.3
Conductivity (µS/cm)	C/F-UF-RO	Feed	135.77 ± 1.32	135.70	133.2	139.2
		UF_P	135.46 ± 3.0	134.90	132.40	153.30
		RO_P	4.48 ± 1.57	4.43	2.10	16.26
	UF-RO	Feed	74.87 ± 0.81	75.01	73.62	76.21

		UF_P	76.42 ± 5.69	74.71	70.25	102
		RO_P	3.01 ± 0.74	2.60	2.31	5.30
		Feed	0.81 ± 0.27	0.80	0.40	1.50
	C/F-UF-RO	UF_P	0.65 ± 0.25	0.60	0.40	1.80
Residual chlorine (mg/L)		RO_P	-	-	-	-
		Feed	0.17 ± 0.07	0.20	0.10	0.30
	UF-RO	UF_P	0.45 ± 0.18	0.40	0.20	1.50
		RO_P	<0.10	-	-	-
		Feed	-	-	-	-
	C/F-UF-RO	UF_P	16.71 ± 2.39	16.00	13.40	21.50
		RO_P	<0.10	-	-	-
Calcium (mg/L)		Feed	-	-	-	-
	UF-RO	UF_P	5.99	5.88	0.20	1.50
		RO_P	<0.10	-	-	-
		Feed	-	-	-	-
	C/F-UF-OI	UF_P	2.54 ± 0.34	2.43	2.05	3.18
		RO_P	<0.10	-	-	-
Magnesium (mg/L)		Feed	-	-	-	-
	UF-RO	UF_P	2.59 ± 0.27	2.55	2.18	3.46
		RO_P	<0.10	-	-	-
		Feed	<5.00	-	-	-
	C/F-UF-RO	UF_P	<5.00	-	-	-
		RO_P	-	-	-	-
TSS (mg/L)		Feed	54.43 ± 87.84	23.00	8.00	252.00
	UF-RO	UF_P	<5.00	-	-	-
		RO_P	-	-	-	-
		Feed	-	-	-	-
	C/F-UF-RO	UF_P	33.41 ± 1.74	32.95	30.80	39.50
		RO_P	<5.00	-	-	-
Alkalinity (mg/L)		Feed	-	-	-	-
	UF-RO	UF_P	28.09 ± 2.10	27.70	24.80	34.20
		RO_P	5.56 ± 3.49	5.00	5.00	26.80
		Feed	-	-	-	-
	C/F-UF-RO	UF_P	51.67 ± 6.74	49.80	41.80	66.90
		RO_P	5.94 ± 5.26	5.00	5.00	44.30
Hardness (mg/L)		Feed	-	-	-	-
	UF-RO	UF_P	25.56 ± 2.13	24.95	22.20	30.50
		RO_P	5.49 ± 3.11	5.00	5.00	24.70

Overall, UF and RO membranes generated a high-quality permeate in both tests. The concentrations of magnesium were similar in UF permeate in both periods ($p = 0.53$), whereas conductivity, residual Cl, Calcium, alkalinity, and hardness were statistically different (all p values <0.00). When pretreatment was applied,

UF feed came from the WTP, where salts, alkalizers, and pre-oxidants were used. Because of this, pretreatment with coagulation and flocculation increased these parameters in UF permeate. On the other hand, the RO permeates in both periods showed no significant difference concerning calcium ($p=0.80$), alkalinity ($p=0.84$), and hardness ($p=0.45$), which is justified by the effectiveness of RO in removing these ions.

Given the high quality of the permeates, blend formulation strategies were carried out. Different proportions of filtered water, ultrafiltration permeate, and reverse osmosis permeate were evaluated, with a focus on arsenic as the target element owing to its toxicity and the stringent drinking water standards it necessitates. The formulations were designed to meet the prescribed arsenic standards for potable water, and subsequent validation encompassed the compliance assessment for other evaluated elements. Strategy I involved mixing filtered water (FW) and RO permeate, and strategy II involved mixing filtered water, UF permeate, and RO permeate. It was considered that the sand filter would not remove dissolved arsenic, and arsenic was added to the filtered water at the same concentration as the decanted water. Figure 3.7 shows the necessary proportions of each stream to reach the arsenic concentration allowed for drinking water (10 µg/L), considering arsenic concentrations of 13, 15, 18, and 20 µg/L in filtered water.

Figure 3.7. Strategies (a) I and (b) II related to blend ratios in the treatment of waters with different initial arsenic concentrations in scenarios with (C/F-UF-RO) and without (UF-RO) pretreatment. The values denote the contributions of filtered water (FW),

ultrafiltration permeate (UF), and reverse osmosis permeate (RO) to the overall volume of treated water.

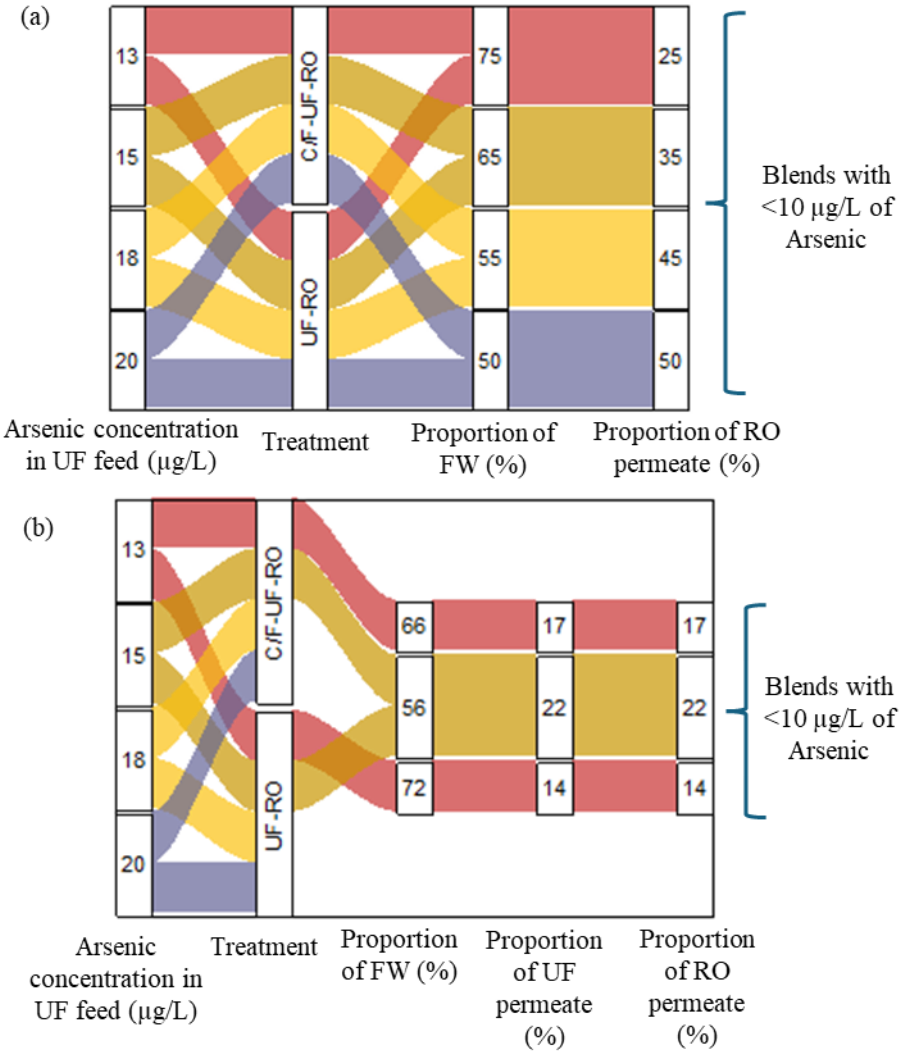

The higher the concentration of arsenic in the filtered water, the more RO permeate is necessary for the blend to meet potability standards. For both with and without pretreatment tests, the strategy of including UF permeate in the blend to reduce the required proportion of RO permeate is viable for concentrations of 13 and 15 µg/L of arsenic in the filtered water. However, it is worth emphasizing that strategy II enabled the reduction of RO permeate in the blend from 25 to 17 (with pretreatment) and to 14% (without pretreatment) when the filtered water has 13 µg/L of arsenic and 35 to 22% when filtered water has 15 µg/L of arsenic.

Regarding the effects of pretreatment on the costs of blending strategies, Table 3.5 shows the membrane area and specific energy consumed (SEC) by the UF-RO system in each blending strategy. It can be observed that pretreatment had

little effect on the specific energy required by UF-RO, regardless of the blending strategy adopted. However, pretreatment reduces the required UF membrane area by 8.4%, reducing cleaning costs and membrane replacement costs. It is important to highlight that a detailed economic assessment is necessary to fully understand the impact of pretreatment on costs.

Table 3.5. Effect of pretreatment on membrane area and specific energy consumed by the UF-RO system in each blending strategy. In the system without pretreatment, operation in the rainy season was considered, with feed with higher turbidity. (Considering a flow rate of 10 m^3/s, UF flux of 39 L/m^2h, and RO flux of 17 L/m^2h).

	With pretreatment		Without pretreatment	
Blend strategy	I	II	I	II
UF recovery rate (%)	95	95	87	87
UF membrane area (m^2)	485830	647773	530504	707339
UF membrane area reduction (%)	8.4	8.4	-	-
RO membrane area (m2)	1176471	784314	1176471	784314
SEC UF (kWh/m3)	0,005848	0,005848	0,006386	0,006386
SEC RO (kWh/m3)	0,284791	0,286488	0,284791	0,286488

In addition to reducing the amount of RO water and, therefore, reducing costs, blending strategies are interesting since the RO permeate is deficient in ions, so this strategy enables water mineralization and minimizes the requirement for chemicals.

Moreover, the comprehensive assessment of various parameters, as depicted in Table B1 of the appendix, reveals that the formulations devised to meet drinking water standards for arsenic successfully achieved compliance across the spectrum of evaluated elements. The results affirm the efficacy of the formulated approach in ensuring the attainment of stringent standards for multiple contaminants in the treated water. This outcome underscores the reliability of the proposed methodology in delivering potable water quality across a range of critical parameters.

Besides, during intense rainfall season, settling units from the WTP present an increase in water turbidity, affecting sand filter performance. Turbidity values in settling units varied between 2.32 and 24.1 NTU during this season, which may affect sand filter performance. Therefore, the blend strategy can be applied,

reducing the fraction of water that would pass through the sand filters and increasing the amount of water to be treated by the UF. Adjusting the blending strategy can reduce the load of suspended particles on the sand filters and enhance the overall water quality. In more extreme situations, the entire flow can be treated by UF membranes to guarantee the quality of the treated water.

3.3.2 Membrane fouling

The UF and RO fluxes were maintained, by increasing pressure, at around 39 L/m^2.h and 17 L/m^2.h, respectively. However, the UF membrane permeability (L/m^2.h.bar) during the period without pretreatment was lower than during the period with pretreatment (Figure 3.7), when the permeability of the UF membrane was also more constant.

The higher turbidity of the non-pretreated feed contributed to the drop in permeability (Figure B1), as the feed with more foulant content could worsen fouling conditions. Over time, the foulant material present in the feed deposited on the membrane surface, further fouling the membrane surface throughout the operation and increasing the total resistance to filtration (Figure 3.8). Therefore, although daily cleaning with sodium hypochlorite solution immediately increased permeability, it progressively decreased over time.

Furthermore, fouling conditions also aggravated during the UF-RO operation without pretreatment due to the increase in feed turbidity caused by the beginning of the rainy season after 150 hours of operation. Thus, another contribution of pretreatment is evident: maintaining a higher membrane permeability throughout the operation and ensuring greater performance robustness in the face of variations in feed quality, which in some places may occur periodically with the rainy season, among other factors. A lower membrane permeability directly impacts operational expenses, as it is necessary to increase pressure to maintain flux, having an even greater impact on long-term operations.

Figure 3.8 also shows a decline in the flux during the period without pretreatment in the first hours of operation. Although the turbidity values in this initial period without pretreatment were similar to the turbidity values in the period with

pretreatment (Fig B1), the non-pretreated feed was more foulant since the beginning, which is evidenced by the average concentration of algae (193 cell/mL) and cyanobacteria (27 cell/mL) in the feed. In contrast, the pretreated feed presented an average concentration of algae and cyanobacteria of 2 and 3 cell/mL, respectively. Therefore, the membrane needed to retain more algae and bacteria, which would be precursors to biofouling development in the period without pretreatment. Furthermore, the determination of absorbance in UV-254 light, which is a measure of organic matter (Albrektiene et al., 2012), also indicated that the feed in the period without pretreatment was more foulant since it had an average absorbance of 77.6 UVA/cm, while the pretreated feed had 3.8 UVA/cm. In this way, more organic matter contacted the membrane in the period without pretreatment, aggravating the fouling conditions.

Figure 3.8. Permeability and total resistance to filtration for ultrafiltration (UF) and reverse osmosis (RO) in scenarios with and without pretreatment. PUF = UF permeability; RUF = total resistance to filtration for UF; PRO = RO permeability; RRO = total resistance to filtration for RO (Resistance of UF and RO membranes were 1,81x 10^{12} and 79 x 10^{14}, respectively).

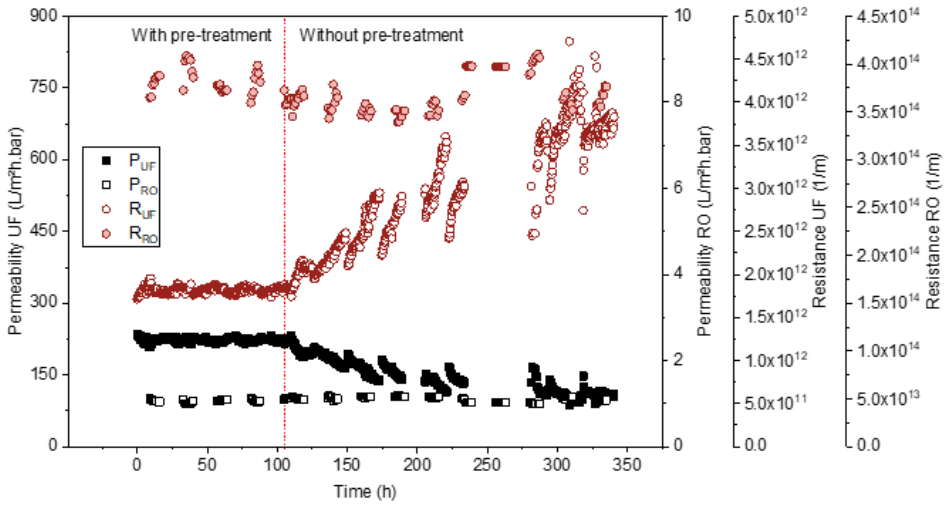

In RO, both flux and permeability remained without major variations. It attests to the efficiency of the UF membrane in removing foulants from the water that feeds RO, ensuring that fouling does not compromise the system performance during the study period.

Figure 3.8 and Figure B2 also show the effect of the cleaning procedure in the two periods of operation. When pretreatment was applied, daily cleaning was crucial to maintain the flux as it was sufficient to reestablish permeability, which varied from 222.25 ± 6.95 (average permeability value in the period from the beginning of the operation until the first cleaning) to 218.50 ± 9.04 (average in the period between the last cleaning of the period with pretreatment and the end of the operation in this way). In the period without pretreatment, daily cleaning was not able to totally reestablish membrane permeability, which varied from 187.03 ± 11.68 (average from the beginning of the period without pretreatment until the first cleaning) to 109.53 ± 6.53 (average from the last cleaning to the end of the operation). It is seen in Figure B2, in which the flux values after the cleaning procedure were compared with the initial ones, with a decay in the ratio for the period without pretreatment. In this second period, maintenance cleaning could not prevent the effects of irreversible fouling and maintain the flux. However, it still managed to increase permeability until the final moments of the operation, when cleaning was no longer able to reestablish permeability well due to the established fouling layer.

More frequent cleaning may be required to maintain the system performance when pretreatment is not applied. Besides the maintenance cleaning of the present study, a deeper cleaning may be necessary to restore the membrane. This cleaning must be done at a specific frequency in long-term operations and would certainly impact the membrane lifespan.

3.3.3 Concentrate management

Firstly, it is worth highlighting that the pilot plant operation was carried out to guarantee high water recovery. In the period with pretreatment, UF recovery was 95%, and without pretreatment, when turbidity values were higher, it varied between 87 and 92%. Concentrate generation was around 1.2 L/m^{2}h during the pretreatment period. During the period without pretreatment, with low turbidity at the beginning of the operation, concentrate generation was around 2 L/m^{2}h . At the beginning of the rainy season, with high turbidity in the feed, concentrate generation was approximately 3.4 L/m^{2}h . Thus, relatively little concentrate was

generated, and this reduced water loss facilitates concentrate management, as will be discussed in this section.

Table 3.6 shows the physicochemical characteristics of the concentrates generated by UF and RO. Concerning turbidity, when there was no pretreatment, the UF concentrate showed significantly higher values, which is explained by the higher turbidity feed that fed this system. The RO concentrates were significantly different in relation to some physicochemical parameters. Color, iron, and manganese were lower in RO concentrates when the pretreatment was applied, which is consistent with the fact that the UF permeate presented lower values for these parameters in this period. The pH, conductivity, and TDS of the RO concentrate in the period with pretreatment were significantly higher, also according to the higher values of these parameters in the UF permeate in this period, when UF feed came from the WTP, where salts, alkalizers, and pre-oxidants are used. Because of this, pretreatment with coagulation and flocculation increased the concentration of dissolved solids, pH, and conductivity of currents generated in membrane processes.

Table 3.6. Physicochemical characterization of UF and RO concentrates

Parameter	Sample		Mean	Median	Min.	Max.	COPAM 08/2022
Color (uH)	C/F-UF-RO	UF_C	375 ± 253	325	50	1000	-
		RO_C	5.9 ± 3.1	5.0	0.0	13.8	
	UF-RO	UF_C	411 ± 581	200	30	2000	
		RO_C	7.6 ± 2.3	7.6	5	13.3	
pH	C/F-UF-RO	UF_C	8.9 ± 0.2	8.9	8.5	9.2	6 -9
		RO_C	8.4 ± 0.4	8.5	7.4	9.0	
	UF-RO	UF_C	7.8 ± 0.3	7.7	7.4	8.6	
		RO_C	7.9 ± 0.1	7.8	7.7	8.2	
Turbidity (NTU)	C/F-UF-RO	UF_C	26.8 ± 15.7	22.7	8.3	57.2	
		RO_C	0.2 ± 0.3	0.1	0.1	1.0	
	UF-RO	UF_C	208 ± 294	160	41	1010	
		RO_C	0.2 ± 0.2	0.1	0,1	1.3	
Temperature (ºC)	C/F-UF-RO	UF_C	22 ± 2.8	21.6	18.9	29.3	-
		RO_C	25 ± 1.5	25.3	21.2	27.7	
	UF-RO	UF_C	20.4 ± 1.5	20.3	18.1	24.2	
		RO_C	24.2 ± 1.2	24.4	22.5	27	
Total Iron (mg/L)	C/F-UF-RO	UF_C	11.1 ± 7.8	9.7	1.8	27	15*
		RO_C	0.010 ± 0.001	0.010	0.010	0.016	

	UF-RO	UF_C	14.4 ± 18.9	3.7	0	63.5	
		RO_C	0.07 ± 0.14	0.01	0.01	0.52	
Total Manganese (mg/L)	C/F-UF-RO	UF_C	0.84 ± 0.64	0.58	0.13	2.29	1
		RO_C	< 0.010	-	-	-	
	UF-RO	UF_C	1.6 ± 2.1	0.6	0.3	6.9	
		RO_C	0.23 ± 0.25	0.14	0.01	0.98	
Total Arsenic (mg/L)	C/F-UF-RO	UF_C	0.051 ± 0.033	0.042	0.011	0.131	0.2
		RO_C	0.047 ± 0.014	0.051	0.020	0.062	
	UF-RO	UF_C	0.035 ± 0.019	0.026	0.019	0.087	
		RO_C	0.06 ± 0.04	0.048	0.009	0.179	
Conductivity (µS/cm)	C/F-UF-RO	UF_C	137 ± 1	137	134	138	-
		RO_C	420 ± 70	440	244	516	
	UF-RO	UF_C	74.8 ± 0.1	74.8	74.7	74.9	
		RO_C	249 ± 34	251	175	347	
Residual chlorine (mg/L)	C/F-UF-RO	UF_C	0.95 ± 0.31	0.9	0.6	1.5	-
		RO_C	0.1 ± 0.1	0.1	0.1	0.2	
	UF-RO	UF_C	0.45 ± 0.07	0.45	0.4	0.5	
		RO_C	0.2 ± 0.1	0.2	0.2	0.2	
TDS (mg/L)	C/F-UF-RO	UF_C	87.3 ± 0.6	87.5	86.1	88	-
		RO_C	297 ± 30	296	227	364	
	UF-RO	UF_C	47.6 ± 0.2	47.6	47.5	47.8	
		RO_C	164 ± 20	164	126	230	

*Maximum value allowed for iron

From all parameters in Table 3.6, only iron in UF concentrated when the pretreatment was not applied exceeded the threshold values for disposal in surface water. Since the concentrate could not be disposed of directly, it would be necessary to apply a treatment. However, aiming to avoid the generation of a waste stream from the UF, an alternative is the concentrate recirculation at the beginning of the treatment carried out in the WTP. It would be feasible since the UF operates with a permeate recovery of 95%, so the concentrate flow is much lower than the flow of the Velhas river. Even if the UF is considered operating at its maximum capacity, the input of pollutants is minimal compared to the total that enters the WTP. For example, when considering the mass balance for pollutants such as arsenic, iron, and manganese, the contribution of the recirculation of the UF concentrate would represent less than 0.001% of the total amount that enters these pollutants per hour in the UF-RO systems, except for manganese when

pretreatment is not applied, whose contribution from the recirculation of the UF concentrate would mean just over 0.001% of the total input. It is important to highlight that this recirculation is safer when pretreatment is adopted. The recirculation of the concentrate directly in the UF feed may be critical. Part of the contaminants that will be returned to the system can be removed by conventional treatment, which may not lead to operational problems in the membrane system.

Furthermore, the effect of recirculating the UF concentrate on conventional treatment and membrane polishing performance has been previously investigated on a bench scale (Guimarães et al., 2022). The results revealed that the recirculation of the concentrate did not contribute to the accumulation of solids and ions in the UF and RO concentrates, nor did it increase fouling potential. It occurred due to the treatment applied before membranes, which included oxidation, coagulation/flocculation, and sedimentation. Thus, the feasibility of recirculating the UF concentrate is related to the performance of these processes. Concentrate recirculation can also lead to the accumulation of microorganisms if coagulation/flocculation, and sedimentation performance are not adequate. This point may be critical to the system without pretreatment.

Regarding the RO concentrate, in the two periods, the quality of the stream was within the parameters of COPAM 08/2022, which concerns release standards (Table 3.7). In this way, RO concentrates can be safely disposed of in the river.

Table 3.7. Characterization of RO concentrates in the C/F-UF-RO and UF-RO tests and comparison with the maximum values allowed for release (COPAM-CERH Resolution No. 08/2022)

Parameters	C/F-UF-RO		UF-RO		VMP
	Mean	Median	Mean	Median	
Total arsenic (mg/L)	0.05 ± 0.02	0.04	0.05 ± 0.02	0.04	0.2
Barium (mg/L)	0.05 ± 0.01	0.05	0.05 ± 0.01	0.05	5
Boron (mg/L)	< 0.01	-	0.01 ± 0.00	0.01	5
Cadmium (mg/L)	< 0.001	-	< 0.001	-	0.1
Lead (mg/L)	< 0.01	-	< 0.01	-	0.1
Free cyanide (mg/L)	< 0.01	-	< 0.01	-	0.2
Dissolved copper (mg/L)	0.006 ± 0.001	0.006	0.006 ± 0.001	0.006	1
Chrome (mg/L)	< 10	-	< 10	-	-
DBO (mg/L)	2,20 ± 0.05	2.20	2.20 ± 0.05	2.20	60
DQO (mg/L)	10,0 ± 5.6	8.8	10.0 ± 5.6	8.8	80
Dissolved iron (mg/L)	0,03 ± 0.06	0.01	0.03 ± 0.06	0.01	15
Fluoride (mg/L)	0.15 ± 0.06	0.15	0.15 ± 0.06	0.15	10
Phenol index (mg/L)	0.04 ± 0.04	0.02	0.04 ± 0.04	0.02	0.5

Manganese (mg/L)	0.17 ± 0.016	0.11	0.17 ± 0.016	0.11	1
Floating materials	V.A	-	V.A	-	V.A.
Mercury (µg/L)	< 0.075	-	< 0.075	-	0.01
Nickel (mg/L)	0.01	-	0.01	-	1
Ammonia nitogen (mg/L)	0.26 ± 0.14	0.27	0.26 ± 0.14	0.27	20
Mineral oils and greases (mg/L)	< 5	-	< 5	-	20
Animal and vegetable oils and greases (mg/L)	< 5	-	< 5	-	50
pH	7.8 ± 0.2	7.7	7.8 ± 0.2	7.7	6-9
Silver (mg/L)	< 0.01	-	< 0.01	-	0.1
Selenium (mg/L)	0.006 ± 0.002	0.005	0.006 ± 0.002	0.005	0.3
Total dissolved solids (mg/L)	161 ± 18	166	161 ± 18	166	-
Total suspended solids (mg/L)	< 5	-	< 5	-	100
Sulfide (mg/L)	< 0.05	-	<0.05	-	1
Surfactants (mg/L)	<0.2	-	<0.2	-	2
Carbon tetrachloride (µg/L)	< 0.5	-	< 0.5	-	1
Trichloroethene (µg/L)	< 0.5	-	< 0.5	-	1
Zinc (mg/L)	0.02 ± 0.01	0.02	0.02 ± 0.01	0.02	5

Table 3.8 summarizes the findings of this study. The quality of the UF permeates generated in both periods with and without pretreatment was high concerning many parameters, even when receiving a much higher pollutant load, as during the rainy season. The RO permeates generated in the two tests had practically no differences. It attests to the robustness of the assessed membrane processes for treating surface water. Pretreatment did not affect UF-RO removal of color and turbidity, which were less than 15 uH and 0.1 NTU, respectively, for the final permeate. Effective iron removal was verified using membranes and permeates had concentrations lower than 0.3 mg/L, even in the period without pretreatment during the rainy season, when concentrations as high as 55 mg/L of iron were observed in the feed. Pretreatment increased manganese removal, and UF-RO provided water that met the national (0.1 mg/L) and international (80 µg/L WHO guideline) standards. Concerning arsenic, RO was crucial to remove it, generating water with arsenic concentrations lower than 0.5 µg/L, a much lower value at 10 µg/L from WHO guidelines.

Table 3.8. Summary of the main findings of the present study, comparing UF-RO with and without pretreatment.

	With pretreatment	Without pretreatment
Water quality: Color, Turbidity, Iron, Manganese, and Arsenic values.	High quality: < 15 uH, < 0.1 NTU, < 0.3 mg/L, < 0.1 mg/L, 0.5 µg/L	High quality, even during rainy season: < 15 uH, < 0.1 NTU, < 0.3 mg/L, < 0.1 mg/L, 0.5 µg/L
Process resilience	High resilience	High resilience, even during rainy season
Water recovery	UF recovery: 95%	UF recovery: 87 - 92% (with higher turbidity)
UF concentrate	Concentrate recirculation is suggested - Concentrate generation was around 1.2 L/m^2	Concentrate recirculation may be critical - Concentrate generation was around 2 - 3.4 L/m^2
RO concentrate	Can be safely disposed of	Can be safely disposed of
Operational effect	Higher UF membrane permeability	More severe fouling conditions
Residue generation	More residue due to pretreatment steps	Less residue

Considering the system with the pretreatment, the recirculation of the UF concentrate is suggested at the beginning of the treatment carried out in the water treatment plant. The RO concentrate can be safely disposed of according to Brazilian legislation. In this way, the concentrates generated in the two tests would require little effort in their management.

A remarkable impact of pretreatment with pre-oxidation, coagulation, and flocculation observed on the performance of the membrane system was the effect on membrane permeability. The UF membrane permeability with pretreatment was greater and more stable. When there was no pretreatment, there was a worse fouling condition in the UF membrane surface, mainly when the rainy season started, and the turbidity of the feed increased a lot. Therefore, it can be observed that pretreatment has a direct impact on operational expenses when treating real matrices, especially those that are subject to major changes in quality and long-term operations.

3.3.4 Economic analysis

The operating cost (OpEX) of the UF-RO plant for treating the entire WTP flow considered in this study is shown in Figure 3.9. The OpEX would vary between

1.05 and 4.34 US$/m^3, depending on the years of operation of the plant, with the membrane system accounting for 29.8% of the total cost (conventional system + UF-RO) and RO accounting for 17.8% of the total cost. The factor contributing most to the operating costs is the replacement of membranes, which in this analysis considered a lifespan of 7 years, given that the system would be fed with water that underwent conventional treatment. It is also worth mentioning that the recirculation of the UF concentrate and the fact that the RO concentrate can be safely disposed of in the water body contributed to a lower OpEX value.

Figure 3.9. Operating Cost of the UF-RO plant treating the entire WTP flow (Membrane lifespan of 7 years)

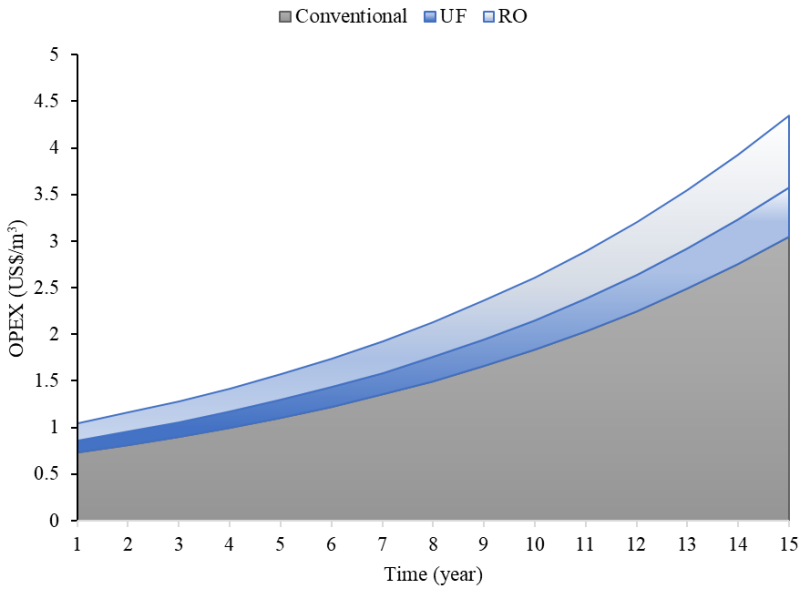

Regarding CapEX, the variation in value would be quite different if the blending strategies were adopted (Figure 3.10). If strategy I were adopted, a membrane unit could be implemented that treated only half of the WTP flow, while for strategy II, 66% of the flow would pass through the UF and 33% through the RO.

Figure 3.10. CapEX of the UF-RO plant according to different treatment strategies

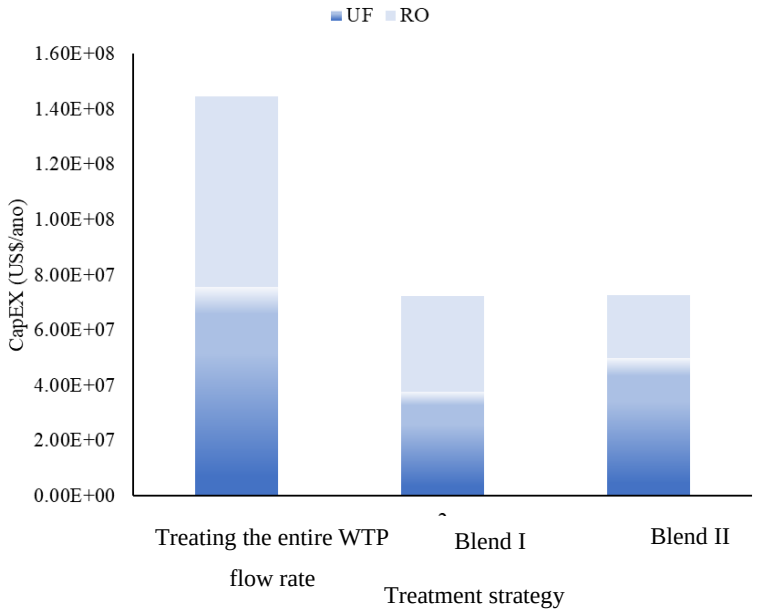

Regarding the UF-RO system operating without pretreatment, a cost analysis was performed for communities of different populations, considering real cities in the same state where the WTP of this study is located and a comparison with the operating costs of the conventional system (Figure 3.11). The operating costs of the membrane system for the smallest (1,500 inhabitants) and largest (540,000 inhabitants) evaluated community ranged from 0.47-0.49 US$/m^3. The CapEX ranged from 47,902 - 17,296,037 US$/m^3 for the smallest and largest communities, respectively.

Figure 3.11. Costs for implementing UF-RO treatment systems considering different communities. Treatment of all estimated required flow was considered.

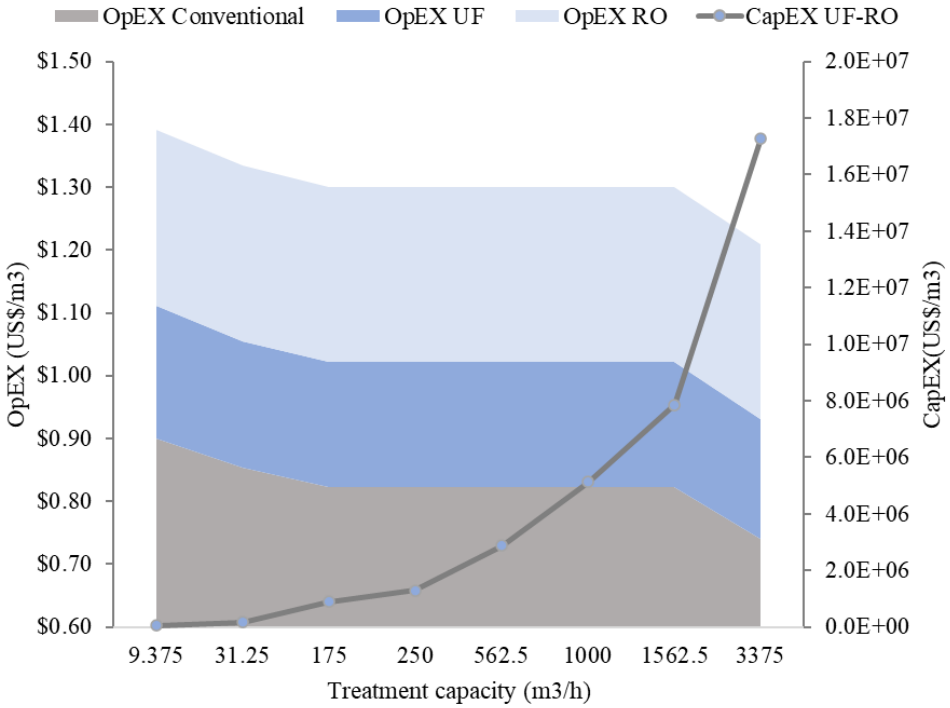

For larger communities already served by WTP, adopting the membrane system is recommended, considering the adoption of the blending strategy with recirculation of the UF concentrate if the quality of the same allows it. For smaller communities that do not have WTP, treating the concentrate stream, which was considered in the calculations, will be necessary. Even so, the costs of the membrane system are competitive, in addition to being a robust and efficient alternative for locations known to have high concentrations of arsenic in their drinking water source.

When considering the costs involved in implementing and operating a membrane system to remove arsenic and improve the quality of drinking water, one should not only consider the amount that will be spent. It is also necessary to consider the environmental and human health consequences, which also have an economic impact (Moreira et al., 2020 For example, it is estimated that each µg/L As in drinking water can cause 51 extra cases of lung cancer. Considering health costs, approximately US$11.9 million per year can be saved by reducing As concentrations in drinking water to values below 1 µg/L (Ahmad et al., 2020).

3.4 Final considerations

The pilot-scale UF-RO membrane system generated high-quality water when treating surface water with or without pretreatment, although fouling conditions were more attenuated during the period with the application of pretreatment. RO was essential to ensure arsenic removal and compliance with potability standards. The application of pretreatment increases the membrane permeability, and in this configuration, the recirculation of the concentrate generated in the UF for the beginning of the WTP, together with the raw water, can be done. The RO concentrate can be disposed of safely. The UF-RO system increased the resilience of the real WTP, effectively contributing to the high-quality water supplied to the population.

4 CHAPTER 4: LONG-TERM PERFORMANCE OF PILOT SCALE UF-RO FOR ARSENIC REMOVAL FROM SURFACE WATER: IMPACT OF OPERATING CONDITIONS

Abstract

In the present study, the performance of a pilot-scale ultrafiltration – reverse osmosis (UF-RO) system was assessed in an operation that lasted more than 2000 hours, focusing on operational aspects, such as the mode of operation, namely, Feed and Bleed and Full Drain, feed turbidity, and backwashing flux. The compliance with the potability standards of the permeates generated and the management of the concentrates were also evaluated. The operating conditions of different RO modules were investigated: the first modules of the first stage, which operate in a milder condition concerning feed characteristics; the last modules of the first stage and the first modules of the second stage, which operate in an intermediate condition; and the last modules of the second stage, which operate in the most severe condition. Regarding the operational aspects of the UF, it was observed that Full Drain operation mode, flux during backwashing/flux after backwashing ratio (J_{DBW}/J_{ABW}) equal to 0.91, and the lower turbidity in the supply significantly increase the permeability of the membrane. A model – developed with gradient boosting machine technique - that can predict membrane permeability with 84.4% accuracy was developed from the generated data. Significant differences were only observed in the conductivity and calcium concentration of the permeate produced during the two operating modes. Regardless of the mode of operation, UF produced a permeate with turbidity < 0.25 NTU, color < 10 uC, iron < 0.012 mg/L, and manganese < 0.006 mg/L. The arsenic removal rate was around 19%, reinforcing the need to apply RO. RO permeates had a maximum arsenic concentration of 0.5 µg/L. All the RO concentrates generated could be safely disposed of in surface water, despite the variations in RO feed characteristics, as turbidity (0.036-0.182 NTU), arsenic (18.5-48.7 µg/L), iron (0.007-0.020 mg/L), and manganese (0.002-0.01 mg/L). It is expected that this paper will provide a relevant contribution to the advances in the studies of the UF-RO system, enabling its application on a full scale and providing greater security for the population supplied with this drinking water.

4.1 Introduction

The presence of arsenic in water is naturally expected in several localities (Costa et al., 2023; Khosravi-Darani et al., 2022; Genchi et al., 2022). In addition, several anthropogenic activities, such as mining, contribute to releasing arsenic into water resources (Chandio et al., 2021). It is an alarming situation, as exposure to arsenic through contaminated water can cause several adverse health effects and, in the long term, diseases such as arsenicosis.

In this context, the World Health Organization (WHO) has established that the maximum concentration of arsenic in water considered safe for human consumption is 10 µg/L (WHO, 2003). However, adhering to the precautionary principle, the WHO recommends that As concentrations be kept as low as possible (WHO, 2011), considering that there are indications that concentrations below 10 µg/L can cause injury to health. In fact, some countries adopted lower As maximum concentration. Denmark adopts a maximum value of 5 µg/L; in the Netherlands, there is a voluntary limit of 1 µg/L (Ramsay et al., 2021). Therefore, applying technologies that efficiently remove arsenic becomes imperative.

Ultrafiltration (UF) is a low-pressure driven membrane process that can act as a barrier to bacteria, viruses, colloids, and precipitated species when applied to treating surface water (Shen et al., 2020). It is an economically competitive process compared to conventional techniques, often generating water of higher quality than the conventional process is capable of (Xu et al., 2024). UF has relatively higher fluxes when compared to other membrane processes, such as RO, lower energy requirements, and is less susceptible to fouling development consequences (Singh et al., 2021). Given these reasons, the remarkable growth of the application of full-scale UF in recent decades has been observed. Yu et al. (2020) investigated the performance of a full-scale UF System, acting as polishing for a water treatment plant with a capacity of 100,000 m^3/day. The integration of the UF was successful, improving the performance of the water treatment plant.

Although it is an efficient and consolidated process, as the main UF separation mechanism is size exclusion, and its average pore size is 0.01 µm (Moreira et al.,

2023), pollutants smaller than this are not expected to be efficiently removed. Therefore, UF is not expected to remove arsenic efficiently, and arsenic removals equal to or less than 14% have already been reported (Hsieh et al. 2011). Guimarães et al. (2022) observed arsenic removal efficiencies by UF that varied between approximately 14 and 80%, and the higher efficiencies were related to a higher presence of arsenic in its colloidal form.

In this context, reverse osmosis (RO) is a technology recognized for removing arsenic with efficiencies greater than 90% (Yoon et al., 2009). This membrane technology has already been studied as a post-treatment to remove arsenic from surface waters, and, even with the application of other processes previously, RO was responsible for ensuring the reduction of arsenic concentration to meet potability standards (Schimidt et al., 2016). Despite being a recognized effective process to remove arsenic and generate a high-quality permeate, the energy demand of RO is higher, and it is a membrane process more susceptible to fouling. Therefore, an alternative that has already proven to be attractive to overcome the respective limitations of UF and RO is to combine the advantages of the two processes, integrating the UF and RO systems (Costa et al., 2024).

Other studies assessed membrane technology for As removal from groundwater (Algiere et al., 2022). However, water scarcity has forced the use of surface water with higher As concentrations in areas of mining activity or with sediments containing As (Komorowicz; Barałkiewicz, 2016). In these cases, the main objective of applying RO may be As removal, although there are other additional improvements, such as removing co-occurring emerging pollutants (Chen et al., 2020). Given this, studies aimed at optimizing these processes when treating surface water containing arsenic to provide greater sustainability to their operation are crucial.

Costa et al. (2024) evaluated the performance of a pilot-scale UF-RO system treating surface water containing arsenic. The authors reported that the integrated system generated high-quality water with or without previous application of conventional water treatment. Moreira et al. (2025) also found that the UF-RO system increased the robustness of conventional treatment, being an

alternative that ensures arsenic removal and safe drinking water even during critical feeding conditions, such as in cases of dam failure. Although this is a promising system, further studies on its operational conditions are needed since they may ensure the process is efficient and economically viable considering long-term operations. The operating mode, the backwashing force, and the system's ability to adapt to changes in the feed given seasonality can be highlighted as operational aspects that deserve attention to ensure a sustainable operation.

Besides being directly associated with its permeability and useful life, the membrane's operating mode is a determinant of the recovery rate, quantity, and quality of the concentrate generated – which directly impacts the management of the concentrate in its environmental, technological, and economic aspects. Thus, it is possible to have operations with minimal concentrate disposal, with high recovery rates, but with a greater tendency to place the membrane operating under more critical conditions, even operations with frequent drainage of the membrane tank, which, despite reducing recovery, favors the operation of the membrane under less demanding conditions, which is beneficial for its useful life, in addition to generating concentrates that are easier to manage.

Another crucial operational procedure for ensuring the long-term performance of UF is Backwashing. This commonly employed method for membrane fouling control involves reversing the filtration flux to unclog membrane pores and clean the membrane. The proper backwashing procedure is of utmost importance for the sustainable operation of the membrane process, as it is a physical cleaning technique that, when appropriately applied, maintains flux and efficiency, thereby minimizing the need for chemical cleaning (Chang et al., 2017).

While more frequent backwashing and higher backwashing strength (the ratio between backwashing flux and permeate flux) can effectively mitigate membrane fouling, they also reduce water recovery, increase operational costs, and present challenges to sustainable operation. On the other hand, less frequent backwashing may lead to increased fouling buildup, ultimately decreasing net water production. Studies have shown that optimal backwash strength should be

between 1.5-2.5 (Chang et al., 2017). However, it is recognized that the application of pretreatment can alter this parameter, favoring the application of a lower backwashing strength (Chang et al., 2017), which should be evaluated on a case-by-case basis.

Furthermore, it is imperative that the treatment system be able to adapt to variations in water quality due to seasonality, such as during the rainy/dry season. Changes in feed quality can pose a challenge to the success of the treatment applied (Vasyukova et al., 2012). In the case of membrane application, seasonal variation in feed quality has been shown to impact UF performance and retention (Aschermann et al., 2016). Costa et al. (2024) demonstrated that even during the rainy season and the consequent increase in surface water turbidity, the UF-RO system produced high-quality water irrespective of the variations of the initial feed water characteristics, such as turbidity, iron, and manganese concentration. However, the consequences of increased turbidity on membrane performance were not evaluated, which is crucial to maintain safe and high-quality water production in the long-term in a sustainable manner.

As RO is crucial to ensure the supply of safe, arsenic-free water, it is necessary to ensure the robustness of the process. In this sense, one strategy is to operate RO in two stages, which increases recovery. Kim et al. (2020) found that two-stage RO consumed less energy than single-stage RO when more membrane modules were used. In addition, applying two stages is more attractive for applications with higher recovery rates. Thus, evaluating the performance of the different modules of the different stages of RO becomes necessary for adopting this configuration since ensuring the robustness of the process in long-term operations is an essential factor to consider when aiming for sustainable full-scale applications.

The main objective of this article was to evaluate the performance of a UF-RO system on a pilot scale treating arsenic-containing water in a long-term operation, which has not yet been reported in the literature, with emphasis on the evaluation of operational aspects of the system. Thus, in the present study, the performance of the membranes, the compliance with the potability standards of the permeates

generated, and the management of the concentrates were evaluated. The effect of two modes of operation of the UF, namely, Feed and Bleed (FB) and Full Drain (FD), backwashing strength impact, and resilience to different feed turbidities were investigated. In addition, the operating conditions of different RO modules were investigated: the first modules of the first stage, which operate in a milder condition in terms of the feed features that fed the RO module (such as lower turbidity values in RO feed); the last modules of the first stage and the first modules of the second stage, which operate in an intermediate condition; and the last modules of the second stage, which operate in the most severe condition. By evaluating important operational aspects, it is expected that this paper will make a relevant contribution to the advances in the studies of the UF-RO system on a pilot scale, addressing important aspects to enable its application on a full scale, which will increase the sustainability and resilience of the water treatment plant (WTP) and the safety of the water supplied to the population.

4.2 Methodology

4.2.1 Feed water

The UF system was fed with water from a real water treatment plant (WTP). The WTP treats water from the Velhas River basin (latitudes 17°15′S and 20°25′S and longitudes 43°25′W and 44°50′W, Minas Gerais, Brazil), which receives industrial and domestic wastewater. This basin includes the iron quadrangle, a region known for its gold and iron deposits and where there is intensive mining activity. Therefore, arsenic, iron, and manganese may be challenging for water treatment plants from this basin. The monitoring data from 2023 reveals that the arsenic concentration varied from 0.5 to 183.8 µg/L, and for iron and manganese, the values corresponded to 0.03 to 15.08 mg/L and 0.007 to 4.193 mg/L, respectively (IGAM, 2023).

The WTP has a nominal treatment capacity of approximately 9 m^3/s. The treatment sequence applied in this WTP is: pre-oxidation (NaOCl), coagulation-flocculation (two fast-mixing chambers, 24 hydraulic and mechanized flocculators with four chambers each; coagulant: $FeCl_3$), settlers (six pool-type settlers), sand filtration, disinfection, fluoridation, and stabilization. The decanted water was

pumped to the pilot plant feed tanks. The quality of the settled water produced by the WTP is shown in Table B1.

The UF feedwater was enriched with dosages of arsenic (13, 15, 18, and 20 µg/L) using a stock solution prepared with deionized water ($Na_2HAsO_4 \cdot 7H_2O$; 1 g/L). Due to the UF-RO pilot plant's connection to an existing water treatment facility, intentionally introducing arsenic into raw surface water, risking water quality, was deemed inappropriate. Besides, As occurrence is seasonal, increasing mainly during the rainy season. Therefore, adding arsenic solution to the water for a more extended operation was necessary to guarantee the arsenic supply for this study. For similar reasons and aiming to simulate the system's operation with a more critical feed, a fine fraction of tailings was dosed during the last two weeks of operation to maintain a feedwater turbidity of around 10 NTU.

4.2.2 Ultrafiltration description and operation

The feed system consisted of 3 interconnected feed tanks with a capacity of 20 m^3. Feed pumps, piping, and valves were arranged to recirculate feed into the tank and promote mixing. The UF system operated with three ZeeWeed 500d modules with a polymeric membrane with nominal pore size of 0.04 µm and a membrane area of 40.9 m^2 in each module. The treatment capacity is 1 - 2.25 m^3/h in direct filtration mode. The main skid contained the membrane tank, cleaning-in-place (CIP) tank, chemical cleaning pumps, control panel, air compressor, and other minor components used to operate the membranes.

The membranes operated under a small negative pressure (0.15 – 0.20 bar) created by pumping permeate through the hollow fiber. Part of the permeate was stored in a process tank for back pulse and backwash operations. The permeate pump was also used to perform backwash and maintenance cleaning of the membranes. During operation, the pump flow rate was controlled to maintain the desired filtration rate. Membrane aeration occurred intermittently through the bottom of the membranes to create turbulence. System operation included back pulse backwashing, aeration, and draining of the membrane tank to eliminate solids. The UF plant was positioned downstream of the WTP settlers.

The UF presented a constant permeate flux of 37-39 L/m^2.h during the first 1630 hours of operation. After this period, the flux reduced to about 29 L/m^2.h due to the changes in the way of operating the RO, as specified in item 2.3, which started to demand less water, resulting in a reduction in the permeate flux of the UF.

The ultrafiltration pilot plant operated in two distinct modes (Figure 4.1). First, the Feed and Bleed operation was carried out. This operation mode consisted of continuous permeation without discarding concentrate. It lasted 129 hours, and the recovery rate was 99%. In this mode of operation, every 14 minutes of filtration, about 1 minute of backwashing was performed without draining the tank. Once a day, the membrane was cleaned with a 200 mg/L solution of sodium hypochlorite, and once a week, maintenance cleaning was performed by applying a citric acid solution (800 mg/L). The cleaning procedure followed the steps: backwash (15 seconds), aeration of the membranes (600 seconds), concentrate drainage, filling the tank with the cleaning solution via backwash and internal recirculation, resting for contact with the solution (900 seconds), cleaning solution drainage, backwash flushing (30 seconds), membranes resting (10 seconds), filling with raw water, and returning to operation.

Figure 4.1- Operational modes of UF: Feed and Bleed (a) and Full Drain (b)

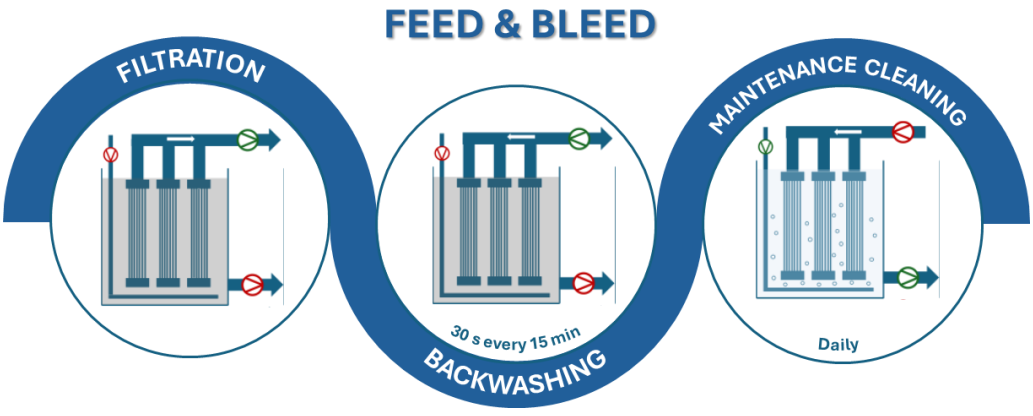

(a)

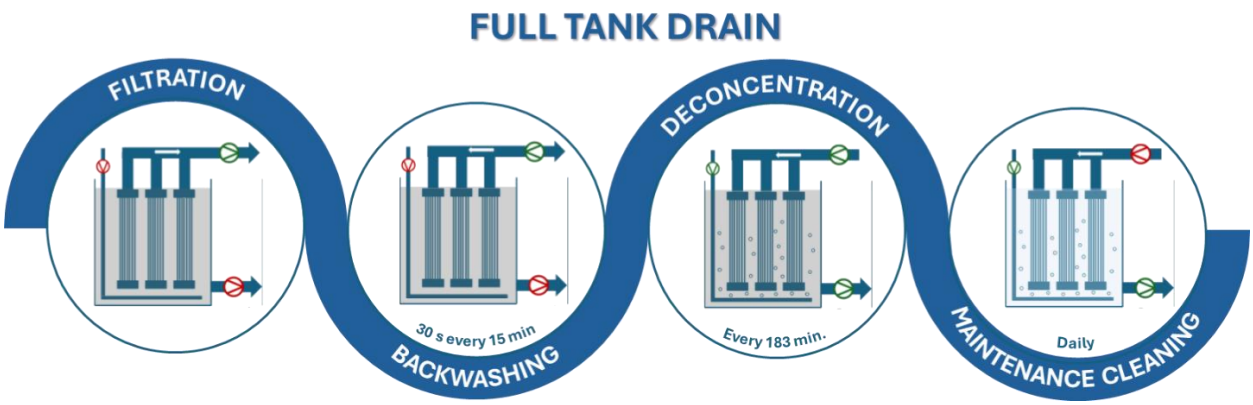

(b)

The other mode of operation was Full Drain. In this mode, the membrane tank was drained at each backwash to limit the accumulation of solids. The filtration time was 183 minutes, and the tank draining and filling time was 12 minutes. First, the membrane system operated in this condition for the same operating time as in the Feed and Bleed mode. Since Full Drain was selected for long-term operation, UF operated in this mode for a total of 1930 hours. Permeate recovery during this operation was around 95% due to the higher volume of concentrate disposal with the frequent draining of the membrane tank.

Maintenance cleaning was performed similarly to that described for the Feed and Bleed mode of operation. Membrane recovery cleaning was performed monthly with sodium hypochlorite solution (800 mg/L) and citric acid (5000 mg/L). Recovery cleaning solutions were heated up to 40 °C. The recovery cleaning followed the steps: aeration of the membranes (600 seconds), backwash flushing (15 seconds), concentrate drainage, filling the tank with the cleaning solution, resting for contact with the solution (18000 seconds), cleaning solution drainage, backwash flushing (30 seconds), membranes resting (10 seconds), filling with raw water, and returning to operation.

The data from the long-term operation of the UF were separated into sets to allow the evaluation of the effect of the operational aspects on the membrane permeability since the operation underwent changes beyond the operating mode, namely backwashing flux rate and the turbidity of the UF feed.

4.2.3 Reverse Osmosis description and operation

The area of each membrane module of RO was 8.4 m^2. The main skid contains the membrane modules, pumps, CIP tank, control panel, and most of the other components used to operate the membranes. RO was fed with UF permeate stored in the RO feed tank. The feed water from the RO pilot plant was previously filtered using 5 µm cartridge filters to remove suspended solids that could damage the membrane elements.

During the pilot scale operation, the operating conditions of the different RO modules were simulated (Figure 4.2): operating condition of the first modules of the 1st stage, where only one module operated; the condition of the last modules of the first stage and the first modules of the second stage, where five modules operated in the 3:2 configuration; and the condition of the last modules of the 2nd stage, in which the three modules operated in a 2:1 arrangement. In addition to the operation of different numbers of modules, the operational conditions were adjusted for the simulation of the different scenarios, as shown in Figure 4.2.

Figure 4.2 – Operation scheme of the reverse osmosis (RO) pilot plant. Qa: feed flow rate. Qp: permeate flow rate. Qc: concentrate flow rate.

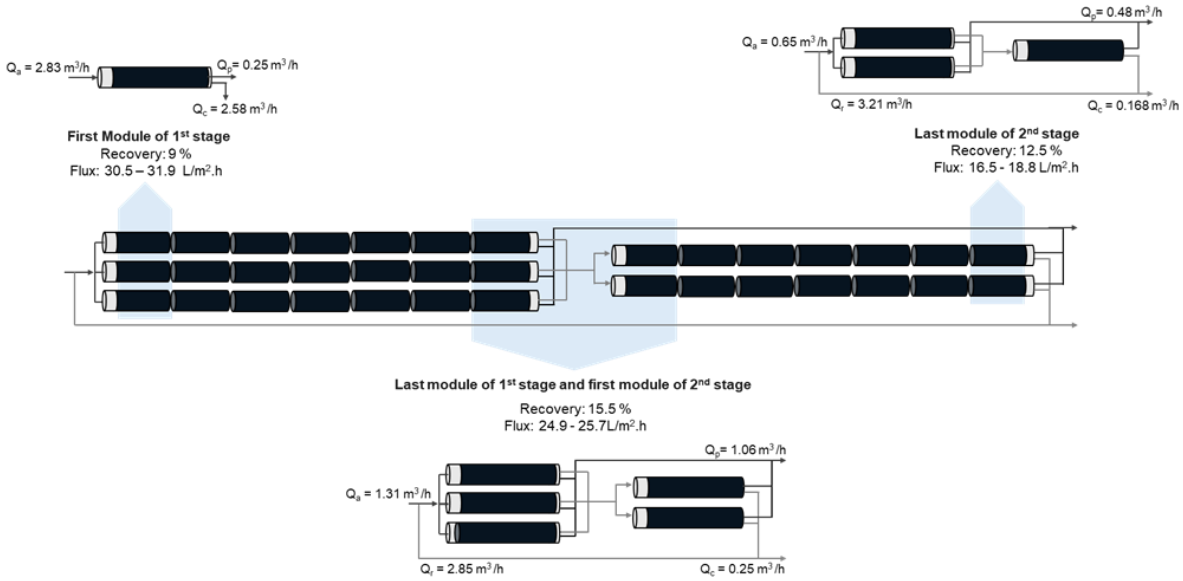

No chemical cleaning of the RO membrane was performed during the operation period. Both UF and RO units had instruments that enabled remote operation and online monitoring of permeate flux, pressure, temperature, and pH, with the UF unit including turbidity and the RO unit electrical conductivity and total dissolved solids (TDS).

4.2.4 UF-RO Monitoring

Flux, pressure, temperature, turbidity, and pH of the feed and permeate were monitored using the pilot unit instruments. Color, iron, manganese, and arsenic concentrations of currents were also monitored following the Standard Methods for the Examination of Water and WasteWater (APHA, 2017). During the first 129 hours of operation, a sample of the permeates from both UF and RO was collected daily to verify the effective compliance of the treated water with the Brazilian potability standards established by Ordinance GM/MS nº 888/2021. After this period, samplings for this purpose were carried out weekly.

A sample of the RO concentrate was also collected daily to assess whether the quality of the RO concentrate meets the Brazilian release standards, in accordance with COPAM/CERH-MG Resolution No. 08 (2022).

Sampling, conservation of samples, and physicochemical analyses were carried out following the recommendations of the Standard Methods for the Examination of Water and Wastewater (APHA, 2017). The samples were characterized in terms of their turbidity (Hach 2100Q), pH (MS Tecnopon mPA-210), color (Hach DR3900), and conductivity (MS Tecnopon mCA-150). Iron, manganese, aluminum, calcium, magnesium, and arsenic concentration values were determined by inductively coupled plasma mass spectrometry (Agilent ICP-MS 7700; method 3125B).

Ultrafiltration membrane samples, after experiments, were analyzed using Scanning Electron Microscopy (Jeol JSM 3630LV) coupled with Energy Dispersive X-ray Spectroscopy (EDS) to map the distribution of chemical elements on the membrane surface. Additional characterizations were performed by external laboratories, adhering to standardized protocols. Fluorescence

Excitation-Emission Matrices (EEMs) were recorded over a range of 250 to 600 nm, with a 3 nm interval for excitation and a 3.23 nm interval for emission. Emission signals were detected using a medium gain setting with a 2-second integration time (Aqualog®, Horiba). Corrections were applied to remove the influence of second-order Rayleigh scattering.

4.2.5 Data modeling

To predict permeability before backwashing (BBW) based on raw water turbidity, temperature, and the ratio of permeability during (DBW) and after backwashing (ABW), a gradient boosting machine was used. Gradient boosting is a machine learning technique that combines gradient-based optimization with boosting. Gradient-based optimization minimizes a model's loss function by using gradient calculations on the training data. Boosting, on the other hand, creates a robust predictive system by sequentially combining an ensemble of weak models, each one improving upon the previous ones (https://doi.org/10.3389/fnbot.2013.00021, https://docs.h2o.ai/h2o/latest-stable/h2o-docs/booklets/GBMBooklet.pdf). In this implementation of the algorithm, decision trees were used.

The model was built in R using the h2o package (https://docs.h2o.ai/h2o/latest-stable/h2o-docs/index.html). Data were filtered to remove observations where BBP permeability exceeded 240 L/m².h.bar, as these indicated that the system had not yet stabilized after backwashing. The original dataset contained 1,991 observations, which were reduced to 1,976 after removing the outliers with BBW permeability above 240 L/m².h.bar. The dataset was split into training and test sets, comprising 70% and 30% of the observations, respectively. Cross-validation was performed using 4 folds during model training. The learning rate was set at 0.1, and 50 trees were used to build the model.

4.2.6 Statistical analysis

Microsoft Excel and Statistica 13.3 were used for statistical and data analysis. Mann-Whitney U Test and Spearman were used for comparison between two independent groups and correlation. Kruskal-Wallis test was conducted for

comparison between multiple groups independents. A confidence level of 95 or 99% was set for statistical tests.

4.3 Results and discussion

4.3.1 Impact of operating mode on UF performance

In the Feed and Bleed operating mode, water is continuously bled from the system during the permeation cycle. Backwashing was conducted without removing solids from the membrane tank, and the contents of the membrane tank were de-concentrated only once per day during the maintenance chemical cleaning. In contrast, in the tank drain operating mode, water is drained from the membrane tank at the end of each permeation cycle, during the backwash-aeration step, to de-concentrate solids and eliminate foulants. The permeate flux was maintained at 38.7 ± 1.8 L/m²h, and the membrane permeability (k) profiles for both the Feed and Bleed and Full Drain operating modes are presented in Figure 4.3. The membrane permeability in Full Drain mode (231.5 L/m²h.bar) was significantly higher (10.5%) than in Feed and Bleed mode (207.2 L/m²h.bar), despite the feed exhibiting lower turbidity values during the Feed and Bleed phase (Table 4.1).

Figure 4.3. **Effect of operating mode on ultrafiltration membrane permeability.**

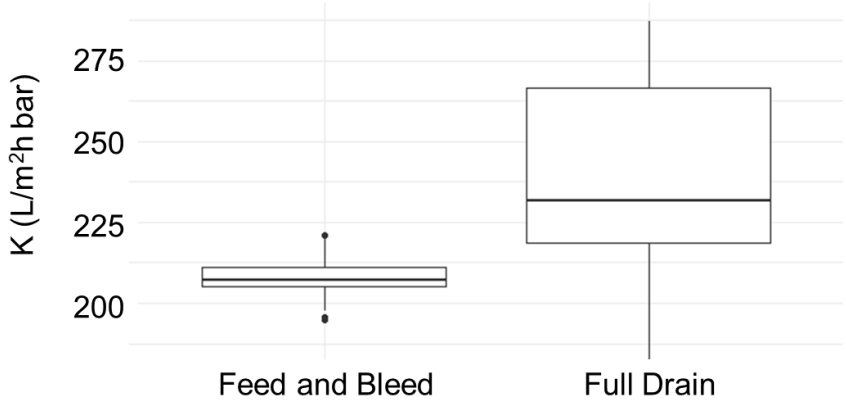

.

Regarding the daily water production in each operating mode, in the Feed and Bleed mode, the average value was 34,503 L/day (permeate recovery rate of 99%), while in the Full Drain mode, the production was 32,397 L/day (permeate

recovery rate of 95%). This difference was expected since the periodic drainage of the membrane tank involves a period in which no permeation occurs. Furthermore, the daily concentrate volume in Full Drain mode (1.71 m^3/day) was higher compared to Feed and Bleed mode (0.35 m^3/day). However, the Full Drain mode offers energy savings, primarily due to lower membrane fouling and reduced aeration requirements. In the Feed and Bleed mode, membrane aeration occured during the backwashing for 15 seconds every 15 minutes, whereas in the Full Drain mode, aeration occured only during backwashing at the end of each 183-minute permeation cycle. This reduction in aeration and the operation of the ultrafiltration system under lower transmembrane pressure results in at least 92% of energy savings related to operational aspects of aeration in the Full Drain mode compared to the Feed and Bleed mode. Moreover, the Full Drain mode allows for the removal of accumulated solids from the membrane tank, enabling operation at a lower average solids concentration. Combined with the reduced aeration per production cycle, the membranes experience less wear and tear, potentially extending their operational lifespan.

The physicochemical quality of the permeate obtained in each mode was also compared (Table 4.1). In Full Drain mode, the UF feed exhibited higher turbidity, along with significantly elevated levels of color, iron, manganese, and conductivity ($p < 0.05$). However, statistically significant differences were only observed in the conductivity and calcium concentration of the permeate produced during the two operating modes. Regardless of the mode of operation or the quality of the feed, ultrafiltration was able to produce a permeate with turbidity < 0.25 NTU, color < 10 uC, iron <0.012 mg/L and manganese < 0.006 mg/L, being the last ones concerning elements due to their frequent high concentrations in the surface water in study. The concentration of manganese on permeates was always lower than the provisional guideline value of 80 µg/L recommended by WHO for manganese. The iron concentration in permeates was lower than the national value for potability (0.3 mg/L - GM/MS 888/2021; no guideline is proposed for iron by WHO).

Although unexpected, the UF membrane achieved an arsenic removal rate of 19%, with no significant difference in the membrane performance for arsenic

retention between the two operating modes. Therefore, UF could not guarantee a safe arsenic concentration in the permeate (10 µg/L). Arsenic removal by UF may be related to removing suspended particles, which may act as carriers for other contaminants. For instance, during the Feed and Bleed operation, a significant negative correlation was observed between dissolved arsenic and turbidity in the UF feed (Spearman's R: -0.630, $p<0.05$), indicating an association between arsenic and suspended solids. Another mechanism that enables arsenic removal by UF is arsenic co-precipitation with oxidated iron due to the residual chlorine. It was demonstrated that oxidant agents may contribute to converting dissolved iron into non-soluble forms, such as colloids and complexes, that can entrap dissolved arsenic and manganese, leading to their indirect removal (Moreira et al., 2021).

Table 4.1. Physicochemical characterization of the feed (UFF) and permeate (UFp) streams during Feed and bleed and Full Drain operation modes.

Parameter	Operation mode	Sample	Mean ± standard deviation	Median	Min.	Max.
Color (uH)	Feed and Bleed	UF_F	29.86 ± 6.70	30	20	40
		UF_P	5.34 ± 1.33	5	5	10
	Full Drain	UF_F	57.20 ± 15.17	58	33	71
		UF_P	5 ± 0	5	5	5
Turbidity (NTU)	Feed and Bleed	UF_F	2.25 ± 0.44	2.11	1.69	3.92
		UF_P	0.10 ± 0.04	0.08	0.04	0.25
	Full Drain	UF_F	6.40 ± 1.56	6.65	4.56	9.8
		UF_P	0.08 ± 0.03	0.09	0.03	0.12
Iron (mg/L)	Feed and Bleed	UF_F	0.75 ± 0.15	0.8	0.52	1.05
		UF_P	0.01 ± 0.01	0	0	0.04
	Full Drain	UF_F	0.95 ± 0.22	0.94	0.61	1.27
		UF_P	0.005 ± 0.003	0.004	0.004	0.012
Manganese (mg/L)	Feed and Bleed	UF_F	0.06 ± 0.01	0.06	0.04	0.08
		UF_P	ND	ND	ND	ND
	Full Drain	UF_F	0.09 ± 0.01	0.1	0.08	0.11
		UF_P	0.002 ± 0.002	0.001	0.001	0.006
Arsenic (mg/L)	Feed and Bleed	UF_F	0.018 ± 0.006	0.02	0	0.03
		UF_P	0.014 ± 0.007	0.02	0	0.02
	Full Drain	UF_F	0.016 ± 0.002	0.016	0.01	0.019
		UF_P	0.011± 0.004	0.011	0.004	0.015
pH	Feed and Bleed	UF_F	8.96 ± 0.17	9.01	8.23	9.22
		UF_P	8.95 ± 0.13	8.97	8.51	9.17

	Full Drain	UF_F	8.67 ± 0.42	8.76	8.05	9.23
		UF_P	8.82 ± 0.31	8.9	8.26	9.22
Conductivity (µS/cm)	Feed and Bleed	UF_F	135.77 ± 1.32	135.7	133.2	139.2
		UF_P	135.46 ± 3.0	134.9	132.4	153.3
	Full Drain	UF_F	148.16 ± 2.23	147.8	144.7	151.1
		UF_P	148.24 ± 2.45	147.6	143.8	152.2
Residual chlorine (mg/L)	Feed and Bleed	UF_F	0.81 ± 0.27	0.8	0.4	1.5
		UF_P	0.65 ± 0.25	0.6	0.4	1.8
	Full Drain	UF_F	-	-	-	-
		UF_P	0.67 ± 0.25	0.76	0.2	1.02
Calcium (mg/L)	Feed and Bleed	UF_F	-	-	-	-
		UF_P	16.71 ± 2.39	16	13.4	21.5
	Full Drain	UF_F	-	-	-	-
		UF_P	20.20 ± 3.02	18.7	18.1	25.3
Magnesium (mg/L)	Feed and Bleed	UF_F	-	-	-	-
		UF_P	2.54 ± 0.34	2.43	2.05	3.18
	Full Drain	UF_F	-	-	-	-
		UF_P	2.74 ± 0.17	2.78	2.54	2.95

*ND: Not detected; *-: not meansured

When managing the concentrate stream, it is important to consider not only the volume produced but also the quality of the concentrate. Table 4.2 presents the physicochemical characterization of the UF-generated concentrate streams. Although the Feed and Bleed mode produced a lower volume of concentrate than the Full Drain mode, the concentrate generated during the Feed and Bleed operation mode was more concentrated.

No significant differences were found between the UF concentrates for most parameters, except for iron and manganese ($p<0.05$), whose concentrations were higher in the Feed and Bleed operation even though concentrations in the UF feed for this mode were significantly lower.

This can be attributed to the greater accumulation of these ions in the UF concentrate during the Feed and Bleed operation. In some cases, the concentrations of iron and manganese in the UF concentrate exceeded the maximum levels allowed for surface water disposal, highlighting the impact of the operation mode on concentrate management. The maximum concentration observed for iron in the Feed and Bleed concentrate corresponded to 27 mg/L,

which is greater than the maximum contaminant level of 15 mg/L established by national regulation. In contrast, the iron concentrations for the concentrate generated in the Full Drain mode remained within the established limits (Table 4.2). For manganese, 29% of the concentrate samples generated in the Feed and Bleed mode had concentrations above the limit of 1 mg/L (maximum value of 2.29 mg/L), while only 10% of the concentrate samples generated in the Full Drain mode had manganese concentrations above 1 mg/L (maximum value of 1.08 mg/L). It is worth mentioning that although the conductivity and TDS values for the concentrate generated in the Full Drain mode were significantly higher, these parameters, in addition to not presenting critical values, do not compromise the safe disposal of the concentrate generated in this mode.

Table 4.2. UF concentrate physical-chemical characterization. *Maximum contaminant level established by local guidelines for wastewater discharge in receiving bodies. **Maximum value allowed for iron

Parameter	Operation mode	Mean	Median	Min.	Max.	COPAM 01/2008*
Color (uH)	Feed and Bleed	375 ± 253	325	50	1000	-
	Full Drain	188 ± 96	145	90	351	
pH	Feed and Bleed	8.9 ± 0.2	8.9	8.5	9.2	6 - 9
	Full Drain	8.9 ± 0.3	9.0	8.3	9.2	
Turbidity (NTU)	Feed and Bleed	26.8 ± 15.7	22.7	8.3	57.2	
	Full Drain	31.2 ± 7.3	32.0	19.9	40.1	
Total Iron (mg/L)	Feed and Bleed	11.1 ± 7.8	9.7	1.8	27	15**
	Full Drain	5.2 ± 4.0	3.8	1.4	12.5	
Total Manganese (mg/L)	Feed and Bleed	0.84 ± 0.64	0.58	0.13	2.29	1
	Full Drain	0.38 ± 0.32	0.25	0.11	1.08	
Total Arsenic (mg/L)	Feed and Bleed	0.051 ± 0.033	0.042	0.011	0.131	0.2
	Full Drain	0.031 ± 0.026	0.029	0.014	0.084	
Conductivity (µS/cm)	Feed and Bleed	137 ± 1	137	134	138	-
	Full Drain	179 ± 35	171	148	271	
Residual chlorine (mg/L)	Feed and Bleed	1.0 ± 0.3	0.9	0.6	1.5	-
	Full Drain	0.8 ± 0.4	0.9	0.1	1.3	
TDS (mg/L)	Feed and Bleed	87.3 ± 0.6	87.5	86.1	88	-
	Full Drain	107.5 ± 10.1	109.0	94.2	123.1	

As previously discussed by Costa et al. (2024), one alternative to avoid generating a concentrate stream that requires treatment would be to recirculate the UF concentrate back to the beginning of the WTP process. Due to the high

recovery rates, the contribution of UF concentrate recirculation to the total contaminant load (arsenic, iron, and manganese) entering the UF-RO system would be minimal—less than 0.003%, even in Full Drain mode, where concentrate generation is higher. Furthermore, studies by Moreira et al. (2023) confirmed that recirculating the UF concentrate did not lead to the accumulation of solids or ions in the system's concentrates, nor did it worsen membrane fouling. Most solids would be removed by the coagulation-flocculation process already employed by the WTP (Moreira et al., 2023).

The permeability, permeate quality, and concentrate management results suggest that Full Drain mode offers superior operational and technical performance in water treatment (Figure 4.4). Consequently, this configuration was selected for the long-term operation of the membrane system. The following sections will focus on the results obtained during this mode of operation.

Figure 4.4. Summary of comparison between feed and bleed and full drain operating modes

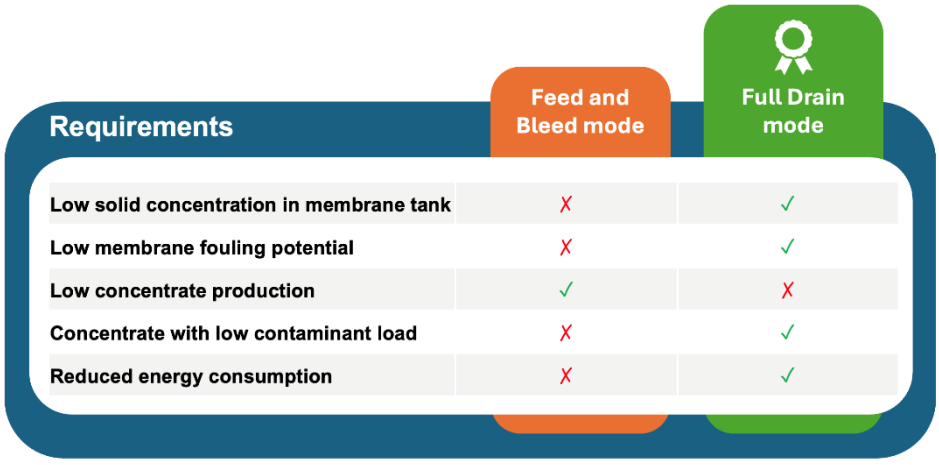

4.3.2 Long-term effects of operational variables in Full-Drain mode

In the long-term operation, the contribution of parameters such as backwashing flow rate, feed characteristics (specifically turbidity), and the robustness of the process in consistently providing water that meets drinking water standards were evaluated. The results of these assessments for the system operating in Full Drain mode are discussed below.

During the UF operation, different backwash strengths (ratio between backwashing and permeate flux) were evaluated (Figure 4.5). Aiming to verify the influence of this variable on the permeability of the UF membrane, the data were separated into three groups according to the ratio J_{DBW}/J_{ABW}: 0.76, 0.91, and 1.09. It was previously verified that there was no significant difference between the turbidity of the feed during UF operation corresponding to these groups (p=0.781), which would affect the permeability. Permeate flux and operation mode were also the same.

Figure 4.5. Permeability (K) of UF membrane before (BBW), during (DBW), and after (ABW) backwashing and boxplots showing significant difference (p<0.001) between backwash strength practiced in each period.

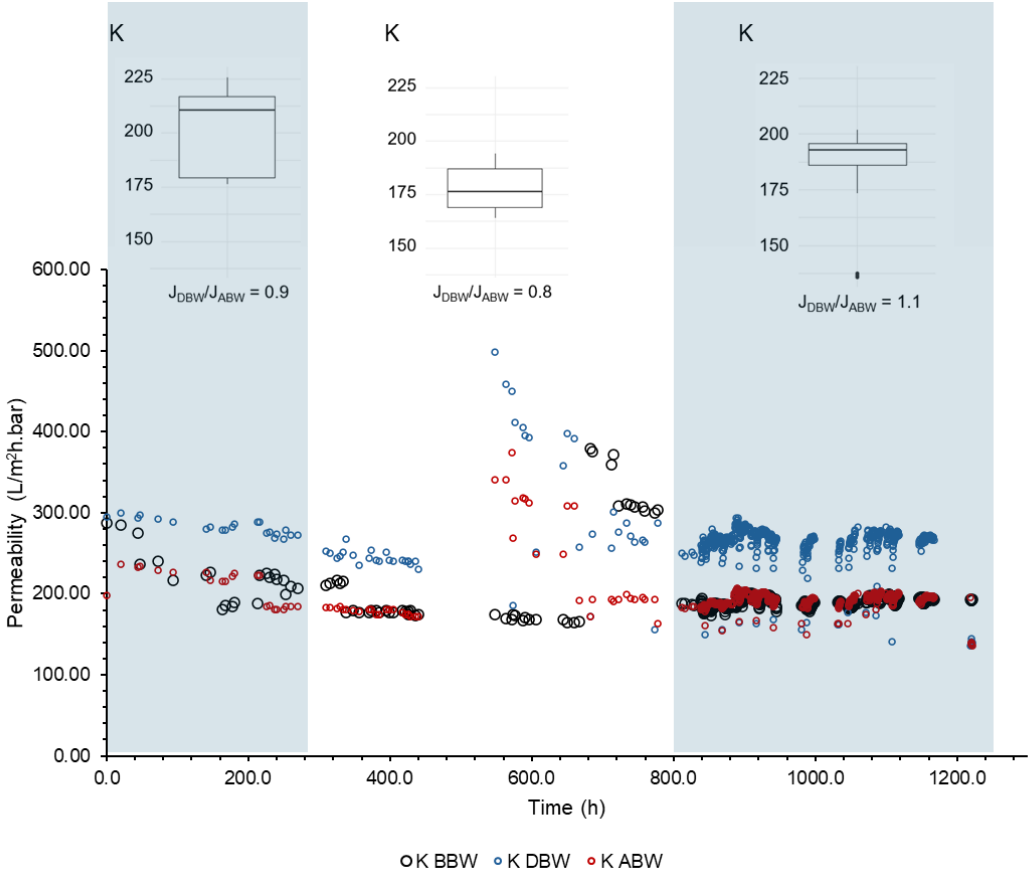

There was no statistically difference between the permeability before and after backwashing, indicating the low fouling potential of the UF feed, which can be attributed to the use of conventional drinking water process as pretreatment. Due to the low membrane fouling potential, a high backwashing strength could be dispensed. The membrane permeability increased from 180 to 216 L/m^{2}h.bar with the increase of the backwashing strength from 0.8 to 0.9 times of permeate flux.

A higher backwashing strength (1.1) of permeate flux did not result in an increase in permeability, which was 194 L/m^{2}h.bar. Thus, adopting a 0.9 ratio would be sufficient to ensure the adequate performance of the UF in this case without the need for higher rates, which would lead to excessive permeate consumption for backwashing, reducing net water production. It emphasizes the importance of evaluating the operational aspects of each case since adopting a backwashing strength sufficient to maintain the membrane permeability rather than higher values favors a process with more sustainable costs, which is especially important considering long-term operations.

The effect of turbidity on permeability was also assessed (Figure 4.6). During the first 140 hours of operation, the UF system was fed with water with an average turbidity lower than 10 NTU (turbidity ranges from 5.5 to 12.8 NTU). After this period, the UF feed had an average turbidity exceeding 10 NTU (turbidity range from 8.6 to 22.0 NTU) during 210 hours of operation. Throughout the entire period, the UF system was operated at a constant flux of 37 L/m^2.h) and with the J_{DBP}/J_{ABP} ratio of 0.9. As expected, the higher turbidity significantly reduces the permeability of the UF membrane due to the more severe fouling.

Figure 4.6. Permeability (K) of UF membrane before (BBW), during (DBW), and after (ABW) backwashing and boxplots showing significant difference (p<0.001) between the feed turbidity in each period.

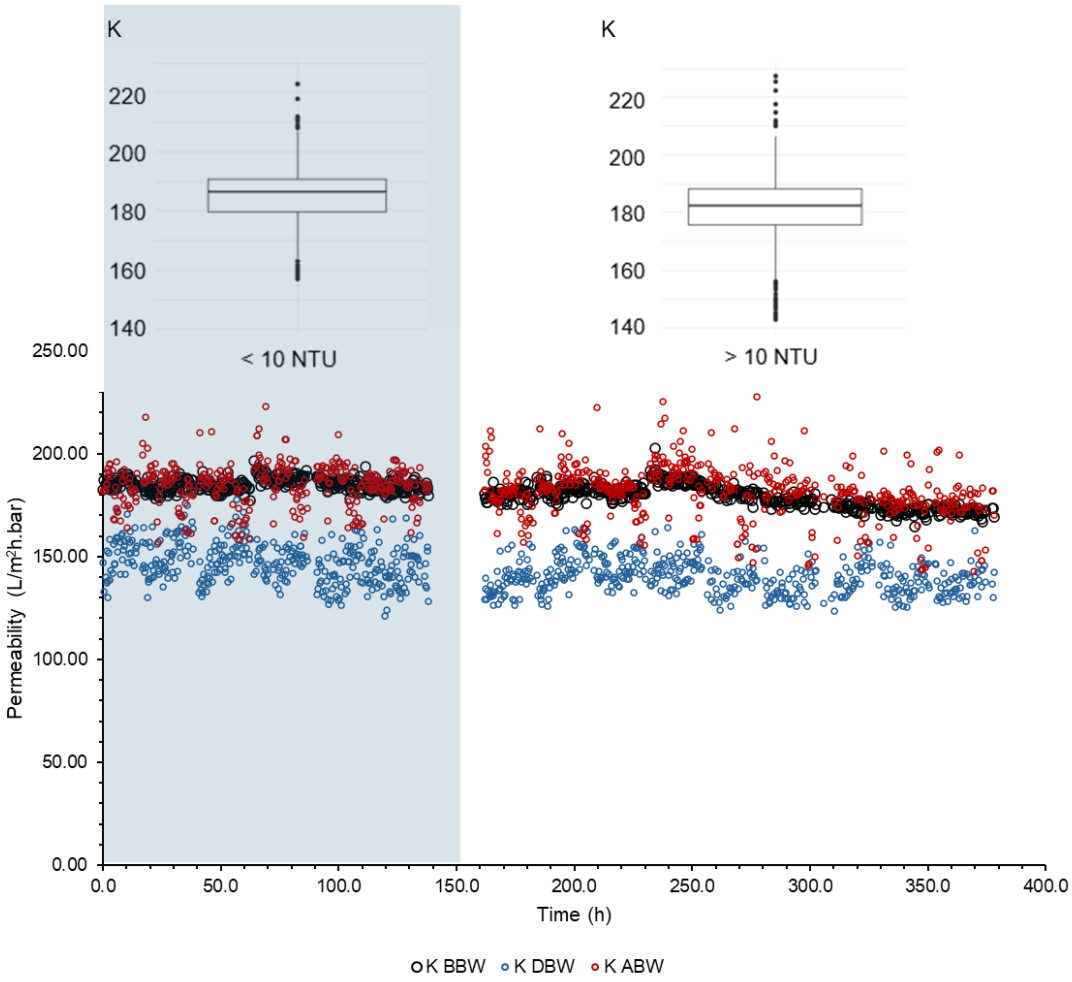

There was no statistical difference between the permeability before and after backwashing, indicating the low fouling potential of the UF feed, which can be attributed to greater membrane fouling observed during operation with high-turbidity water, could have been mitigated by using a higher backwashing strength. These results suggest the importance of optimizing backwashing strength, considering seasonal variations in water to achieve a balance between fouling control and permeate water consumption. A potential solution is to implement data-driven modeling to predict key operational parameters and optimize backwashing using stochastic dynamic programming techniques.

In this context, a model was developed to predict the permeability of the UF membrane. After tests with different input parameters, the turbidity and

temperature of the feed, as well as the J_{DBW} and J_{ABW} ratio, were selected. These parameters were selected due to their influence on permeability. Temperature changes water viscosity; feed turbidity is related to the presence of solids that can reduce permeability due to fouling formation, as verified in this study; and the J_{DBW}/J_{ABW} ratio was chosen because of the contribution of the backwashing flux to cleaning the membranes and resuming flux, as also highlighted in the previous item. The model's performance on the test set achieved an R^2 of 84.4%, an RMSE of 4.94, and an MAE of 3.27. A plot of the predicted versus actual values shows a good fit, indicating that the model is suitable for prediction (Figure 4.7). Due to the low membrane fouling potential, a consequence of the conventional drinking water process as pretreatment, a high backwashing strength could be dispensed. The membrane permeability increased from 180 to 216 $L/m^2h.bar$ with the increase of the backwashing strength from 0.8 to 0.9 times of permeate flux. A higher backwashing strength (1.1) of permeate flux did not result in an increase in permeability, which was 194 $L/m^2h.bar$. Thus, adopting a 0.9 ratio would be sufficient to ensure the adequate performance of the UF in this case without the need for higher rates, which would lead to excessive permeate consumption for backwashing, reducing net water production. It emphasizes the importance of evaluating the operational aspects of each case since adopting a backwashing strength sufficient to maintain the membrane permeability rather than higher values favors a process with more sustainable costs, which is especially important considering long-term operations.

Figure 4.7. Scatter plots between actual and predicted values for Permeability BBW

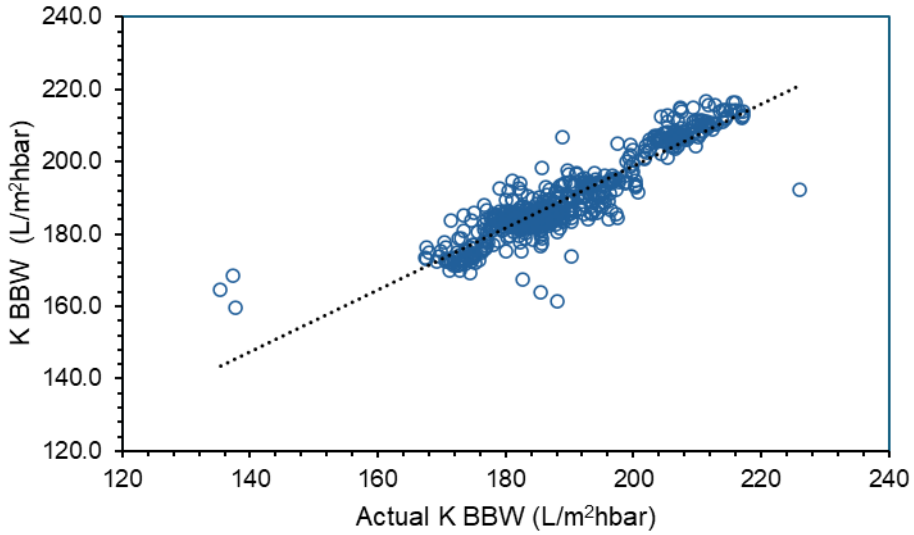

If a variable is important, permuting its values is expected to degrade the model's performance. The greater the impact on performance, the more significant the variable is (REF: https://www.amazon.de/-/en/Przemyslaw-Biecek/dp/0367135590). For this model, the variable that contributes the most to explaining BBP permeability is turbidity (Figure 4.8), as expected according to operational results.

Figure 4.8. Contribution of each variable to the permeability value

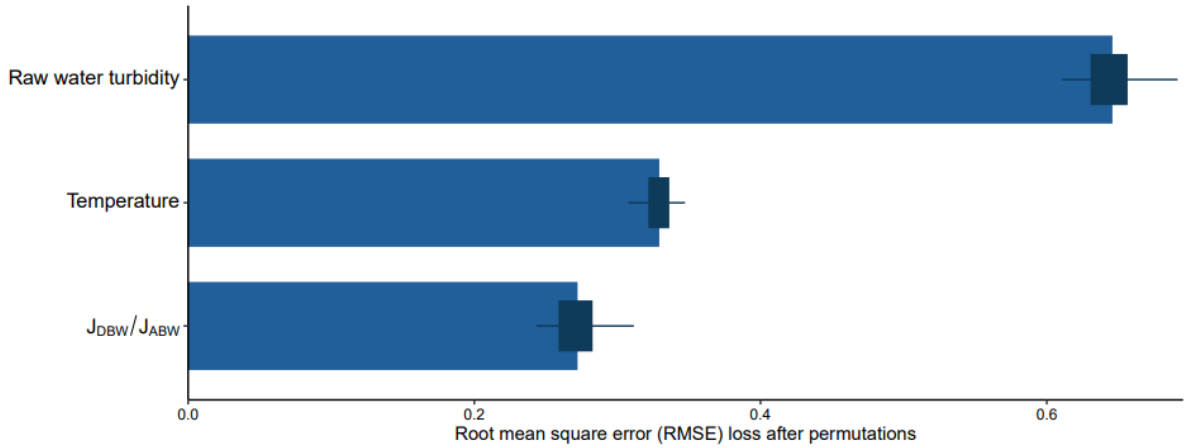

4.3.3 Consistency of UF permeate quality in the long-term operation

The integration of UF into conventional water treatment processes and reverse osmosis RO systems provides an opportunity to produce water with a lower fouling potential for RO, as well as the option to blend UF permeate with RO permeate. This blending can reduce the volume of water requiring RO treatment, improving system efficiency. In both cases, it is crucial that the UF permeate consistently maintains high water quality. Turbidity and color of the UF feed and permeate during the 1,900 h of operation of the system are presented in Figure 4.9, highlighting the high efficiency of UF throughout the entire operation to remove them. UF permeate consistently exhibited turbidity and color values lower than 0.25 NTU and 10 uH, respectively. All permeates remained within the Brazilian limits for potability (15 uH for color; - GM/MS 888/2021), even when UF feed had higher color and turbidity values. The periodic draining of the tank at each cycle allowed the membrane to operate under a less critical condition by minimizing the concentration of solids that remained in contact with its surface. The main mechanism for removing solids in UF is size exclusion, and previous studies have also demonstrated UF efficiency in terms of color and turbidity removal (Costa et al., 2024).

Figure 4.9. (a) Turbidity and (b) color in the feed and permeate from UF during the long-term operation.

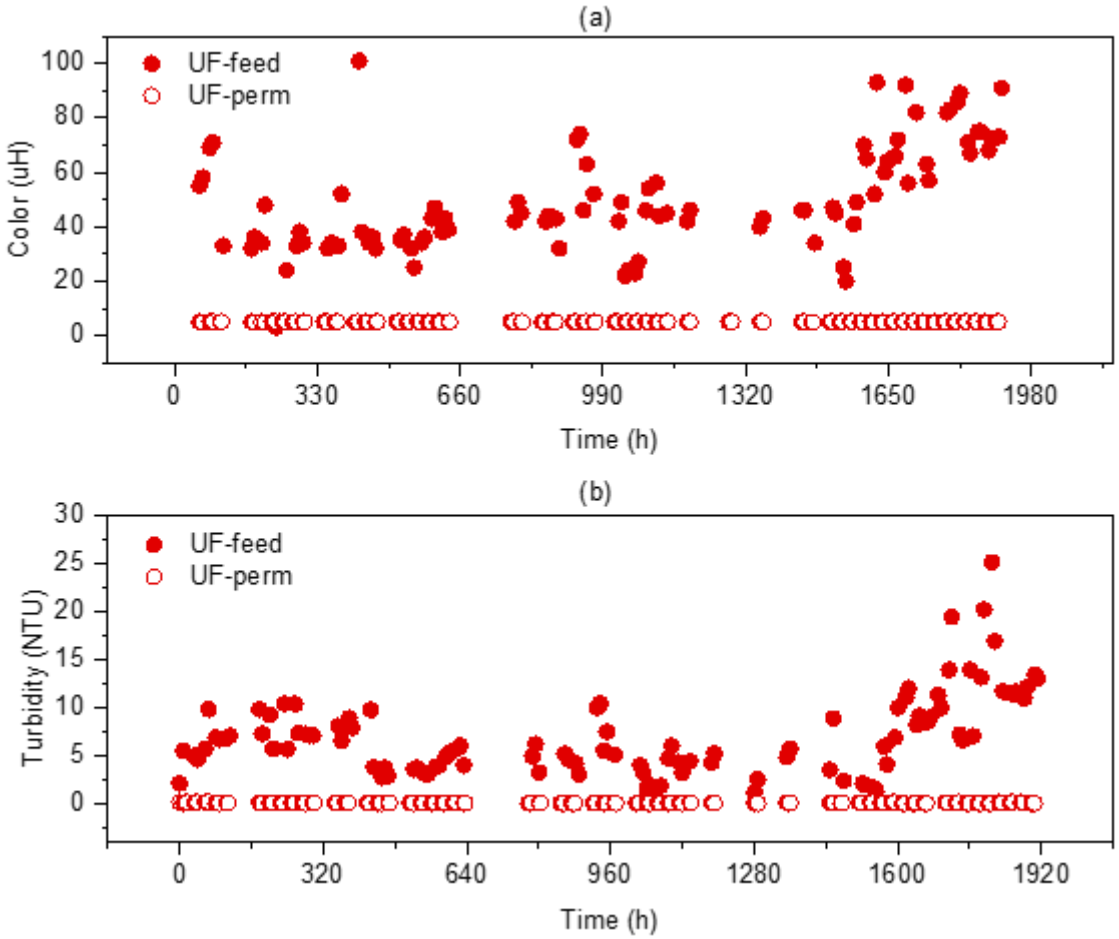

Figure 4.10 shows the concentrations of iron and manganese in the UF feed and permeate. The iron and manganese concentrations in the UF feed range from 0.007 to 2.278 and 0.005 to 0.187 mg/L, respectively, evidencing the importance of the UF as a pretreatment of RO membranes. Both iron and manganese are potential fouling agents. Furthermore, residual oxidants like hypochlorite and chloramine in the membrane feed water, catalyzed by iron and manganese on the membrane surface, can lead to free-radical reactions that severely damage the typically RO polyamide layer. UF effectively reduced the iron and manganese concentrations to below 0.086 and 0.028 mg/L, respectively. These values meet the provisional guideline for iron (0.3 mg/L -GM/MS 888/2021 and United States Environmental Protection Agency (EPA, 2024), no guideline is proposed for iron by WHO (WHO, 2011)) and manganese (80 µg/L - WHO (2011); 50 µg/L - EPA (2024)) for potable water. Moreover, the iron and manganese levels observed in

the UF permeate are within the typical limits recommended by RO manufacturers (1 mg/L for iron and 0.05 mg/L for manganese).

Figure 4.10. (a) Iron and (b) manganese in the feed and permeate from UF during during the long-term operation

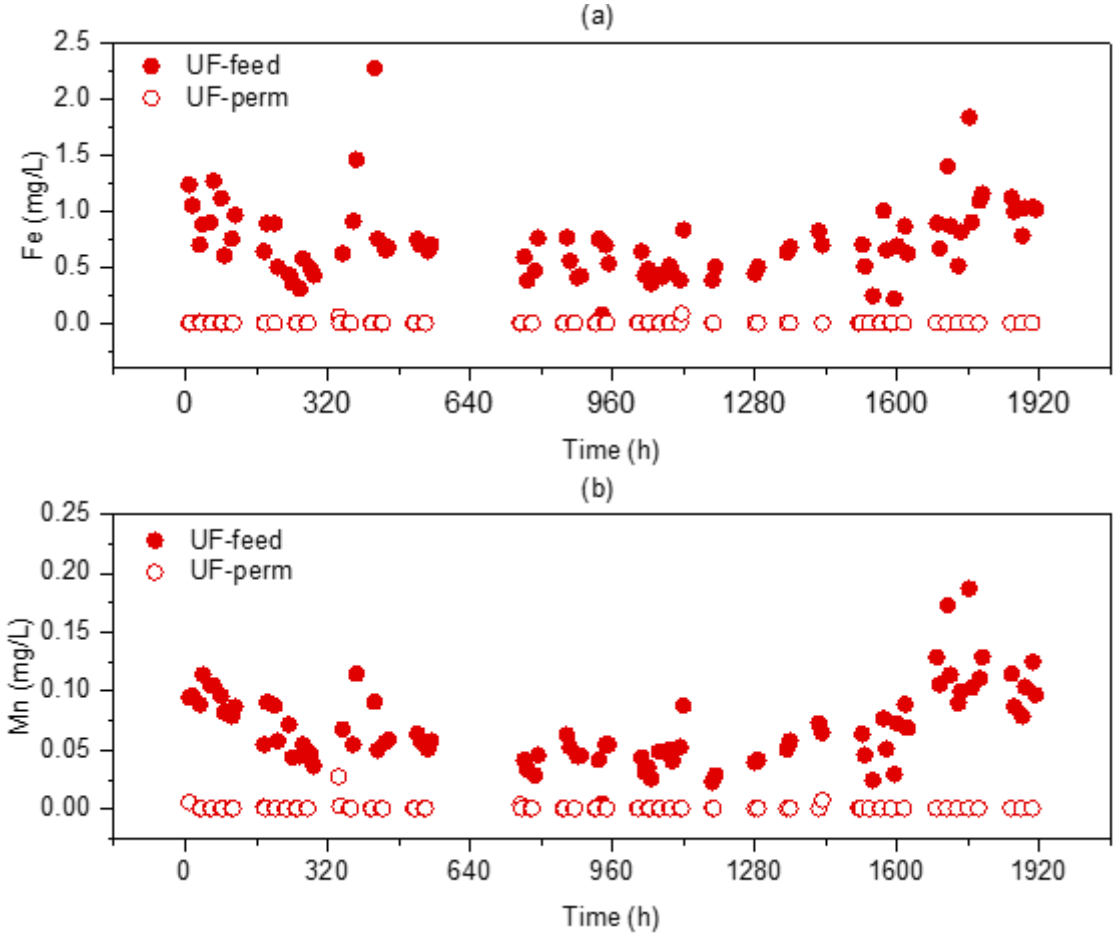

The arsenic concentration in the UF feed ranged from 2.15 to 35.1 µg/L (Figure 4.11). UF was not effective in removing As, present in its soluble form, with an average removal efficiency of 22.9 ± 45.5%. As shown in Figure 4.11, higher As concentration in the UF feed led to higher concentration in the UF permeate, and it explains the variations in As concentration during the operation. As discussed previously, it was expected that UF membranes porous (0.01 µm) are larger than arsenic in its dissolved form (0.0002 µm) (Yang et al., 2019). The mean concentration of arsenic in the UF permeate was 14.6 ± 6.1 µg/L. The presence of arsenic in UF permeates demonstrates the importance of integrating RO into the treatment system to meet the potability standards (10 µg/L, Ordinance

GM/MS No. 888/2021 and WHO (2011)) and ensure the production of safe drinking water. UF acts only on the arsenic fraction associated with suspended solids or in colloidal form.

Figure 4.11. Arsenic concentration in the feed and permeate from UF during the long-term operation.

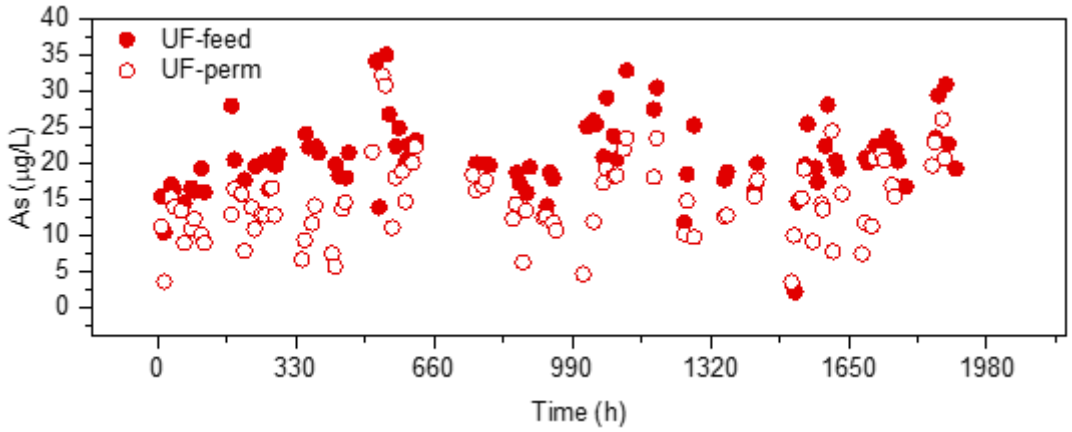

Table 4.3 contains other parameters that were monitored throughout the long-term pilot plant operation, allowing verification of the high quality of the permeates. The Silt Density Index (SDI) of the UF effluent was consistently below 1.4, making it suitable for further treatment by RO. The water exhibited low hardness (< 73 mg/L) and organic matter content (TOC < 1.1 mg/L), conditions that are favorable for RO application. Although UF alone was insufficient to achieve arsenic removal to meet drinking water standards, it effectively prepared the water for a more sustainable and efficient RO operation. During the 1.960-hour operation, the UF process demonstrated consistent removal rates of turbidity, iron, and manganese, and the flux of UF remained relatively stable, showing low membrane fouling potential.

Table 4.3. Additional parameters for characterization of UF permeate during the long-term operation

Parameter	Mean ± standard deviation	Median	Min.	Max.
pH	8.85 ± 0.38	8.91	7.45	9.48
Conductivity	172.31 ± 30.55	170.85	141.80	298.10
Residual chlorine (mg/L)	0.51 ± 0.26	0.57	0.01	1.60
Algae (cell/mL)	< 1	-	-	-
Cyanobacteria (cell/mL)	< 3	-	-	-

SDI	1.14 ± 0.36	1.24	0.11	1.39
TOC (mg/L)	1.01 ± 0.04	1	< 1	1.1
Magnesium (mg/L)	2.51 ± 0.28	2.52	1.97	3.00
Calcium (mg/L)	21.67 ± 2.11	21.20	17.80	27.60
Alkalinity (mg/L)	33.4 ± 1.7	32.9	30.8	39.5
Hardness (mg/L)	58.78 ± 20.13	64.80	10.60	73.00

4.3.4 Reverse Osmosis

The RO system operated for 1,900 hours, with modules and recirculation streams arranged to simulate typically two-stage RO conditions: (I) the first modules of the 1st stage, (II) the last modules of the first stage, and the first modules of the second stage; and (III) last modules of the 2nd stage. The system was operated at a recovery rate of 80% without adding antiscalant or biocide. No chemical cleaning was carried out during the period. Table 4.4 shows the physicochemical characterization of the RO permeate for the three conditions evaluated. In all simulated conditions, the RO permeate met the potability parameters, attesting to the efficiency of the process. All modules in a two-stage RO system could produce water with similar concentrations in terms of color, iron, manganese, and arsenic ($p>0.05$).

Table 4.4. Physicochemical characterization of reverse osmosis currents during the simulation of different conditions. Sample N is found in Table C1 of the supplementary material

Parameter	First module of 1st stage 			Last module of 1st stage and first of 2nd stage 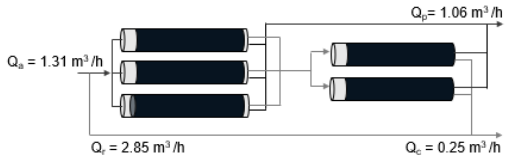				Last modules of 2nd stage 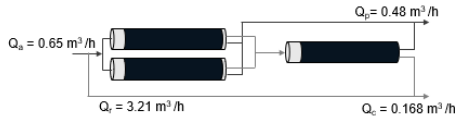			
	UF permeate	**RO Permeate**	**RO Concentrate**	**UF permeate**	**RO Feed***	**RO Permeate**	**RO Concentrate**	**UF permeate**	**RO Feed***	**RO Permeate**	**RO Concentrate**
Turbidty (NTU)	0.036 ± 0.021	0.031 ± 0.025	0.06 ± 0.05	0.048 ± 0.034	0.068 ± 0.064	0.032 ± 0.024	0.08 ± 0.05	0.099 ± 0.045	0.182 ± 0.216	0.068 ± 0.019	0.199 ± 0.250
Color (uH)	5.00 ± 0.00	5.00 ± 0.00	5.0 ± 0.0	5.00 ± 0.00	5.15 ± 0.33	5.00 ± 0.00	5.2 ± 0.4	5.38 ± 1.33	5.81 ± 2.78	5.00 ± 0.00	5.9 ± 3.1
Arsenic (µg/L)	18.51 ± 8.25	< 0.5	18 ± 7	18 ± 2	48.69 ± 22.61	< 0.5	60 ± 30	16 ± 5	43 ± 13	< 0.5	47 ± 14
Iron (mg/L)	0.007 ± 0.013	0.004 ± 0.002	0.004 ± 0.000	0.004 ± 0.000	0.020 ± 0.011	0.004 ± 0.000	0.026 ± 0.015	0.012 ± 0.015	0.011 ± 0.005	0.006 ± 0.011	0.010 ± 0.001
Manganese (mg/L)	0.002 ± 0.004	0.0010 ± 0.0001	< 0.001	0.001 ± 0.000	0.004 ± 0.003	0.004 ± 0.000	0.005 ± 0.005	<0.010	<0.010	<0.001	< 0.010
Calcium (mg/L)	21.74 ± 2.27	0.07 ± 0.07	-	21.49 ± 1.69	-	0.17 ± 0.06	-	16.71 ± 2.39	-	0.10 ± 0.01	-
Magnesium (mg/L)	2.514 ± 0.284	0.004 ± 0.003	-	-	-	0.032 ± 0.054	-	2.54 ± 0.34	-	0.100 ± 0.000	-
EC (µS/cm)	171 ± 12	3.34 ± 1.27	195 ± 28	175 ± 31	536 ± 101	8.23 ± 1.74	670 ± 127	135.46 ± 2.92	372 ± 57	4.48 ± 1.57	420 ± 70
pH	8.92 ± 0.39	7.52 ± 0.87	8.3 ± 0.9	8.71 ± 0.31	8.10 ± 0.23	6.64 ± 0.25	7.9 ± 0.3	8.95 ± 0.13	8.42 ± 0.68	8.17 ± 0.74	8.4 ± 0.4
TDS (mg/L)	107.14 ± 7.87	2.11 ± 0.84	124.7 ± 16.6	108.6 ± 19.4	349.6 ± 5.3	5.14 ± 1.01	439.1 ± 86.1	86.35 ± 1.41	262 ± 25	2.87 ± 1.06	297 ± 30

*Combined UF permeate and concentrate recycle

When comparing the quality of the RO permeates during the different simulated conditions, it was observed that there was no significant difference for the parameters: color, iron, manganese, and arsenic ($p>0.05$). Although UF permeate during the two operating modes did not present a significant difference ($p>0.05$) for residual chlorine and magnesium values, there was a significant difference between these parameters in the RO permeates. The permeates were also different regarding conductivity, TDS, and calcium concentration.

Notably, RO consistently ensured that the arsenic concentration remained within potability limits (10 µg/L, Ordinance GM/MS No. 888/2021 and WHO (WHO, 2011)). Additionally, RO achieved even stricter limits, such as 5 µg/L, which have been enforced in regions like New Jersey and Denmark, respectively, and the ultra-low limit of 1 µg/L in the Netherlands (Ersboll et al., 2018; Ramsay et al., 2021). This performance was maintained throughout the entire operation (Figure 4.12), even when the arsenic concentration in the RO feed was as high as 60 µg/L. This included all evaluated modules, even the last module of the second stage, which operated under more critical conditions. The RO permeate had a maximum arsenic concentration of 0.5 µg/L.

Figure 4.12. Arsenic concentration in the feed and permeate from RO during the long-term operation

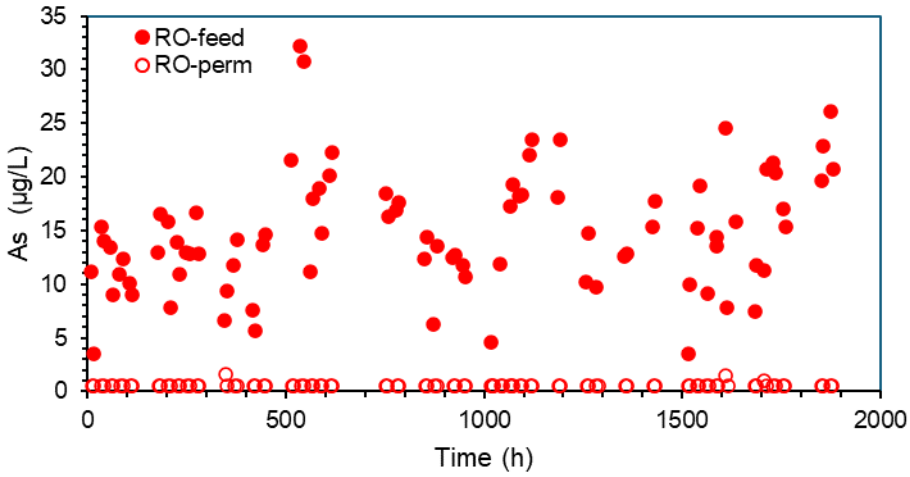

The low arsenic concentrations in the permeate present a valuable opportunity for blending reverse osmosis (RO) permeate with ultrafiltration (UF) permeate. This approach reduces the flow rate of water requiring treatment in the RO system, leading

to decreased energy demand and increased water recovery. Blending UF and RO permeates, ensuring the production of safe water, particularly concerning arsenic concentrations, also serves as a strategy for standardizing the quality of treated water, as RO permeate exhibits low ion concentrations (calcium, magnesium, and total dissolved solids concentrations were, respectively, 0.10 ± 0.08, 0.03 ± 0.01, and 2.11 ± 1.92 mg/L). According to the World Health Organization (WHO, 2017), public acceptance of water hardness levels can vary significantly across different communities. Water with hardness levels below 100 mg/L may possess low buffering capacity, potentially rendering it more corrosive to plumbing infrastructure. However, WHO does not propose a minimum hardness value (WHO, 2017). It is important to note that blending is a widely practiced strategy in various RO membrane installations around the world (Brião et al., 2013; Elazhar et al., 2021). This approach allows for the adjustment of treated water quality, thereby preventing excessive demineralization and reducing the need for chemical additives in post-treatment processes aimed at mitigating corrosivity and enhancing buffering capacity.

The greater conductivity and TDS levels in the RO permeate during the simulation of the last modules of the first stage and the first modules of the second stage could be associated with the higher values at the RO input during the simulation of the operation of these modules than in the other simulations. It can be explained by the recycling practiced in each of them, which caused the contribution of TDS and conductivity through the recirculation of concentrate to be greater in this condition than in the others.

Regarding the permeate turbidity values, there was no difference between the operation of the first module of the first stage, and the last modules from the first stage and the first modules from the second stage. However, there was a difference between these operations and the operation that simulated the last module of the second stage. The differences in turbidity between RO permeates are related to the performance of the UF in each mode of operation since there was a significant difference between the turbidity values of the UF permeates ($p<0.05$) and in the feed and bleed mode - corresponding to the simulation of the last modules of the second stage of the RO - the values were higher. It can be explained by the more severe operating conditions of the feed and bleed mode since solids were not removed from the membrane tank.

Therefore, the RO concentrate also had higher turbidity values, and given the recycling conditions, the turbidity values at the RO entrance in this condition were higher.

Concerning RO concentrate management, color, pH, and chlorine were not significantly different in RO concentrates. As expected, for the parameters in which there was a significant difference, the values of the RO concentrate of the first modules of the first stage were lower, given the less demanding feeding conditions.

Given that the water has a low total dissolved solids (TDS) concentration, as it is surface water pre-treated by a conventional process integrated with ultrafiltration (UF), the concentrate produced, even with high permeate recovery, exhibits low TDS levels, differing from RO concentrate generated in desalination processes. Despite variations in the concentrate produced across different modules, Table 4.3 indicates that all streams of reverse osmosis (RO) concentrate met the quality standards required for direct discharge into surface water, in compliance with Brazilian regulations (COPAM 01/2008), including for the critical elements iron, manganese and arsenic, whose maximum concentrations (respectively 0.044, 0.012, and 0.105 mg/L) always remained within the levels permitted for direct disposal (15, 1, and 0.2 mg/L).

The higher turbidity of the RO feed during the simulation of the last modules of the second stage may also be related to the lower permeability of the membrane when simulating these conditions (Figure 4.13 (c)). The RO system was operated with constant permeate flux. The permeate flux adopted in each scenario was determined based on the Winflows design software simulation, considering the feed water quality. During the simulation of the first modules of the first stage, it is possible to perceive the stability in the performance of the RO membrane in long-term operation. Therefore, the UF membrane successfully acted as a barrier to potential foulants, allowing RO to avoid problems with fouling throughout the operation. It is worth mentioning that during the entire period of RO operation, chemical cleaning was not necessary on the membranes, which represents another advantage of coupling the UF-RO membranes. In addition to saving on chemicals, the useful life of the membrane is prolonged.

Figure 4.13. Flux (a), TMP (b) and Permeability (c) in the RO membrane during the simulation of different modules

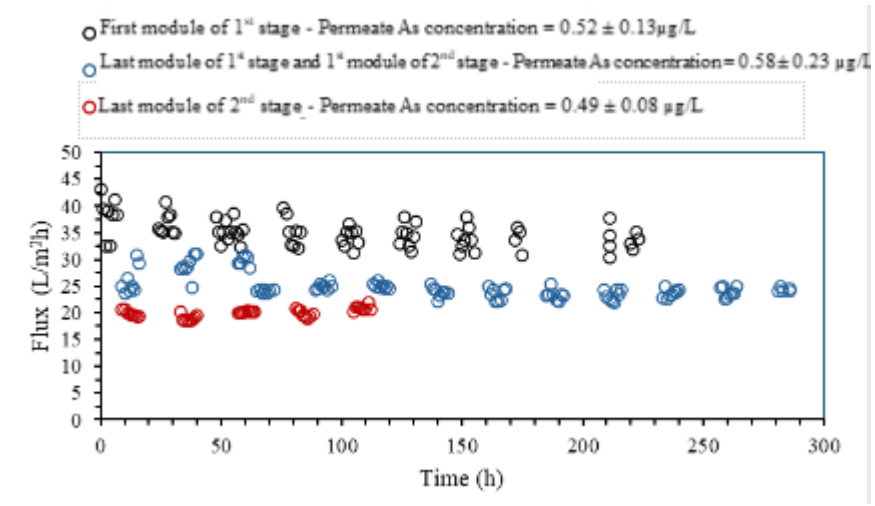

(a)

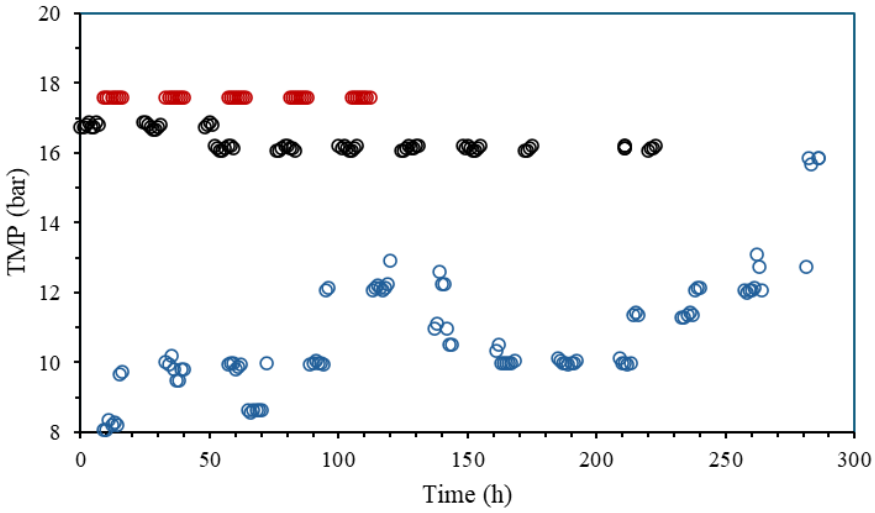

(b)

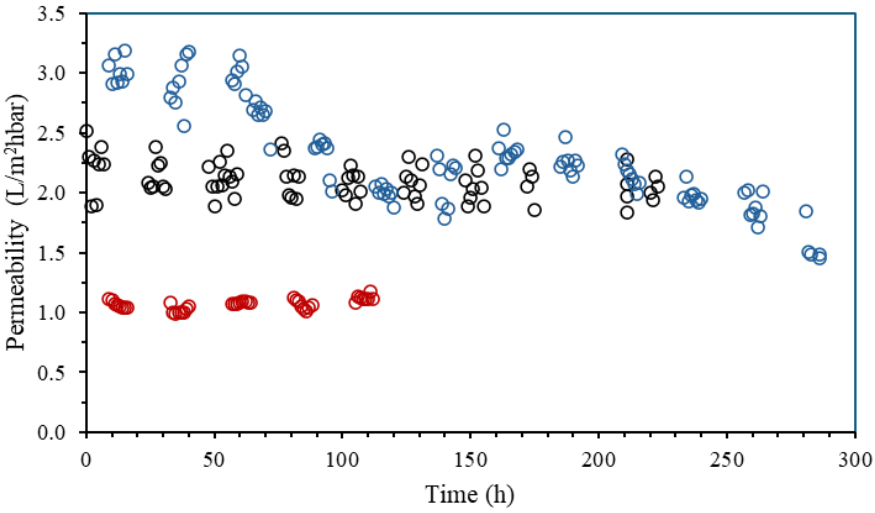

(c)

During the simulation of conditions of the last modules of the first stage and the first modules of the second stage, there was a deliberate reduction in the flux and, consequently, in the pressure applied, which has already been discussed. However, the membrane permeability also decreased due to the feeding condition of the RO elements being more critical in terms of TDS and conductivity (Table 4.3).

4.3.5 Membrane fouling characterization and chemical cleaning effectiveness

The maintenance of a constant permeate flux in the UF-RO system during the long-term pilot plant operation, with reduced pressure values, suggests that the operational protocols (such as de-concentration mode, backwashing procedure, daily maintenance cleaning, and monthly recovery) efficiently maintained membrane permeability. Pressure peaks or other events that could indicate a severe membrane fouling development were not observed.

Scanning electron microscopy (SEM) images (Figure 4.14 (a)) show the fouling layer on the surface of the UF membrane, which was formed mainly by inorganic components, with a notable presence of iron, aluminum, arsenic, and manganese. Despite the relatively low arsenic removal by the UF membrane, the images show some degree of As retention in the UF fouling layer.

In addition to inorganic components, the presence of dissolved organic matter from both UF and RO on the fouling layer can be noted (Figure 4.15). A distinct region can be observed in λexc 270-330 and λemi 320-380 for the UF fouling layer. Sen-Kavurmaci et al. (2015) related this region to the presence of dissolved organic carbon derived from microbial byproducts in natural waters. It may be related to the presence of residual chlorine in the medium, which leads microorganisms to death – and can cause the release of microbiological byproducts. A consequence of the residual chlorine is the prevention of biofouling development. In the RO fouling layer, the region λexc 250 - 380 and λemi 340 – 440 can be observed, which may correspond to humic-like substances (Sen-Kavurmaci et al., 2015).

Given the fouling characterization, it can be concluded that the UF membrane successfully provided a low fouling potential feed to the RO during long-term operation, which had a much lower fouling extent on its surface (Figure 4.14 (b)). In fact, UF significantly reduced the presence of iron and manganese on the surface of the RO membrane. Furthermore, UF appears to have successfully blocked the passage of microbiological byproducts into the RO feed since this form of dissolved organic carbon was not found in the RO membrane fouling.

Chemical cleaning of the UF was performed three times during the study period. The membrane permeability before and after each cleaning was 192 and 243 (cleaning 1), 166 and 182 (cleaning 2), and 192 and 195 L/m^{2}h.bar (cleaning 3). Therefore, it can be observed that the cleaning procedure adopted was adequate to recover the membrane permeability and can even be performed less frequently depending on the quality of the system feed, as in the case of cleaning 3, when no important gain in permeability was observed.

The characterization of membrane fouling attests that UF effectively contributed to the fact that chemical cleaning was not necessary to apply to the RO throughout the period. Besides, it did not impair RO performance; it preserved the integrity of the RO membrane, increasing its lifespan and reducing chemical costs. These are essential factors to ensure the long-term operational and economic sustainability of the membrane process.

Figure 4.14. Scanning electron microscopy and elemental mapping (iron – Fe, manganese – Mn, arsenic – As, and aluminum – Al) of (a) ultrafiltration and (b) reverse osmosis membranes.

(a) (b)

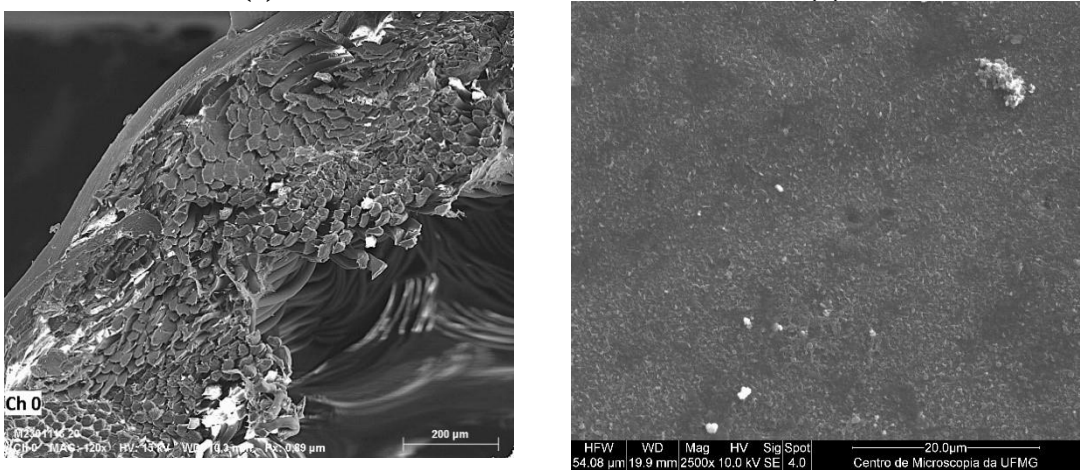

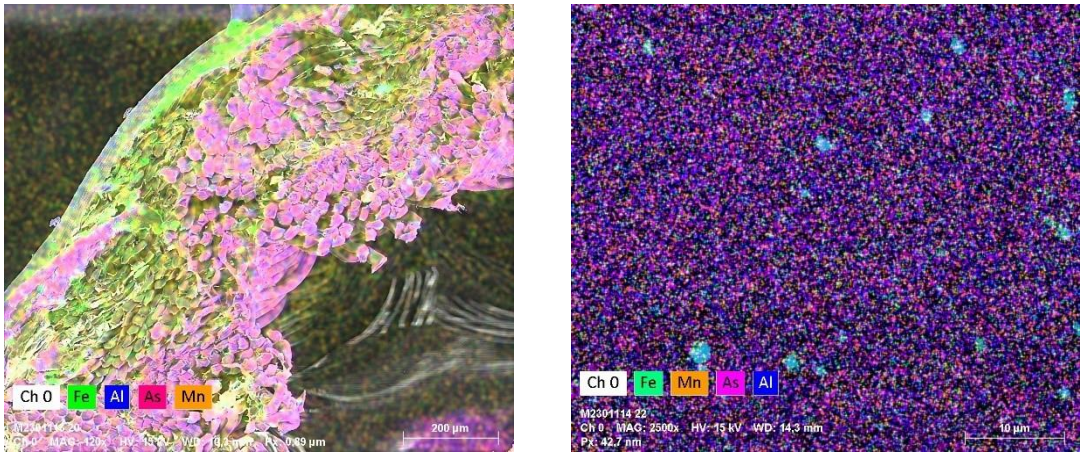

Figure 4.15. Excitation Emission Matrix (EEM) for the (a) ultrafiltration and (b) reverse osmosis membrane.

(a)

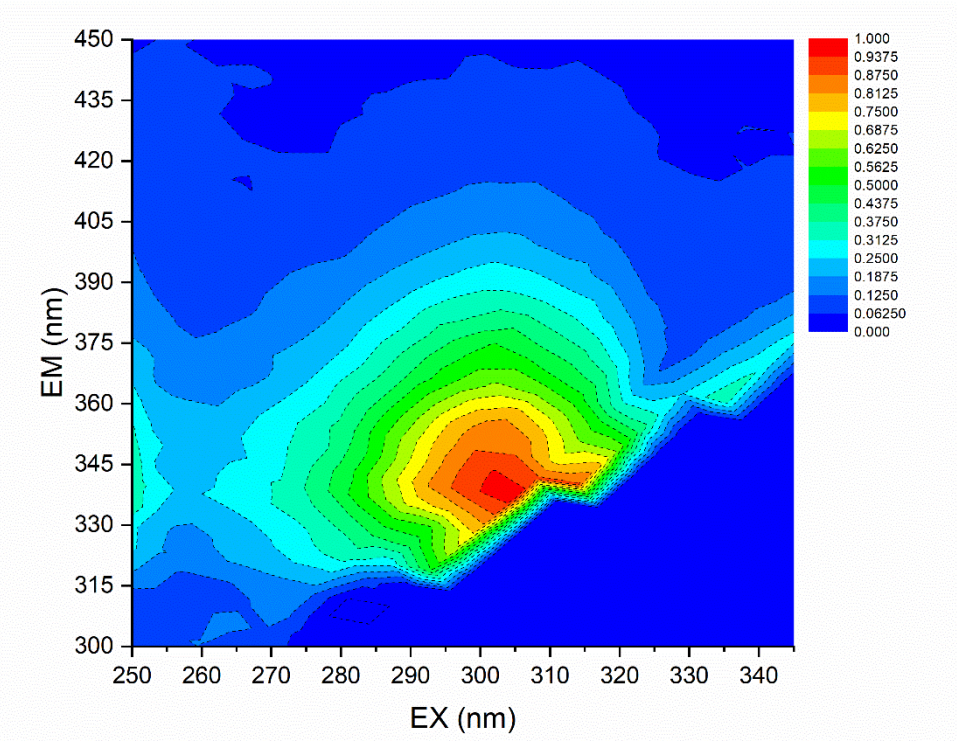

(b)

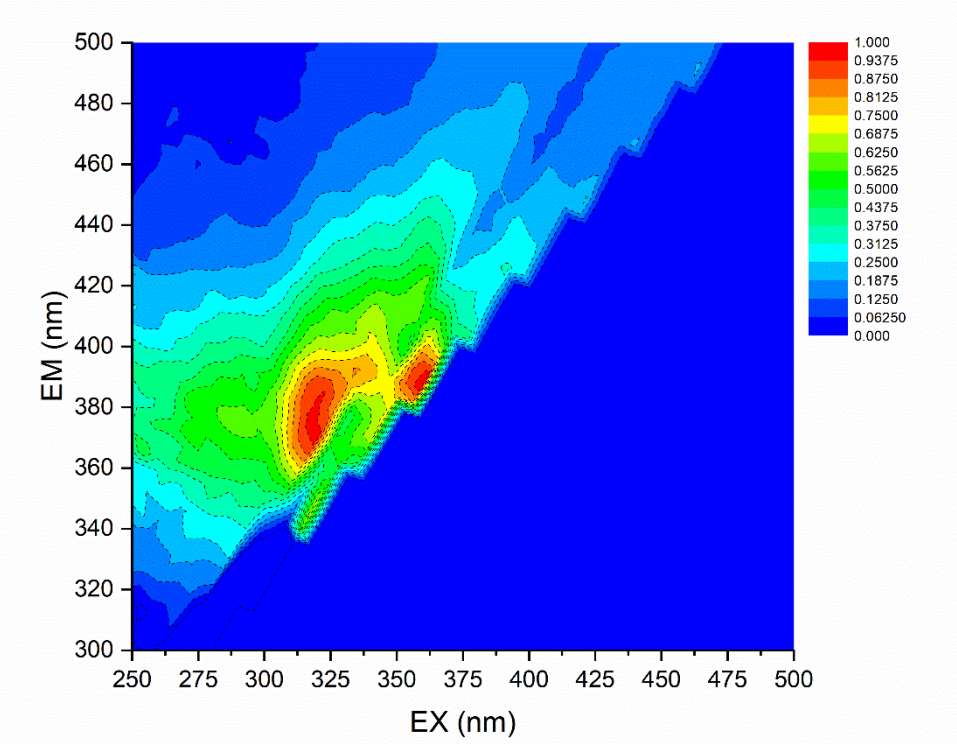

4.4 Conclusion

In the present study, the performance of a pilot-scale UF-RO system was evaluated in a long-term operation. Regarding the UF operational aspects, it was observed that: (i) when operated in Full Drain mode, the UF membrane had a higher permeability; (ii) regarding the backwashing flux, the J_{DBW}/J_{ABW} ratio significantly impacted the membrane permeability, with a ratio of 0.9 being sufficient to provide the best UF performance observed during the tests; (iii) turbidity had a great impact on permeability. From the generated data, a model was developed that, with turbidity, temperature, and J_{DBW}/J_{ABW} ratio values, can predict the membrane permeability with 84.4% accuracy.

Regarding the quality of the UF permeate, the potability standards were consistently met for most parameters, including for manganese (<0.028 mg/L) and iron (<0.086 mg/L). Arsenic removals ranged from 2.15 to 45.5%, reinforcing the need for RO application. Furthermore, the operating mode can impact concentrate management, and more than 80% of the UF concentrates generated during the Full Drain operating mode could be safely disposed of.

Regarding RO, all permeates met the potability standards with arsenic concentrations. The RO permeate had a maximum arsenic concentration lower than 0.5 µg/L. There was no difference in the permeates regarding color, iron, manganese, and arsenic when comparing the operating conditions of the different modules. All RO concentrates generated can be safely disposed of in surface water.

5 CHAPTER 5: ULTRAFILTRATION WITH IN-LINE COAGULATION ($FeCl_3$) TO ENHANCE ARSENIC REMOVAL AND IMPROVE DRINKING WATER QUALITY: FROM BENCH TO PILOT-SCALE

Abstract

This chapter discusses the use of ultrafiltration membranes aided by in-line coagulation with $FeCl_3$ (0.086 – 0.172 mg/L) to improve the resilience of drinking water treatment plants. The process was considered after the settling units and was first studied on a bench scale, later validated in a pilot plant that operated continuously for approximately 31 days. In experiments without an in-line dose of $FeCl_3$, the average flux values corresponded to 189.9 ± 11.8 L/m^{2}h, compared with 193.4 ± 5.3 L/m^{2}h for experiments when the coagulant was considered. The flux decay was lower in experiments with an in-line dose of $FeCl_3$ (J/J0 > 0.95) and analysis of particle sizes revealed that the average diameter increased from 24.1 to 29.2 µm after the coagulant was added. Consequences related to a greater particle size were a fouling layer more porous permeable, and with a lower hydraulic resistance. The additional coagulant dosage also acts on the residual natural organic matter, monitored by excitation-emission matrices. Furthermore, the results show that the concentrate recirculation to the beginning of the water treatment plant did not affect its overall performance. In fact, concentrate recycling would increase the recovery rate of ultrafiltration membranes and reduce losses during water treatment. Similar observations were obtained in pilot-scale operations, that validated the in-line dose on a more representative system that is closer to the full-scale treatment process.

5.1 Introduction

Water is a crucial natural resource, and ensuring water security is a top priority worldwide. Water security encompasses quantity and quality, and both aspects are interconnected. While conventional water treatment processes have been used for decades to treat water, they have proven to be less robust in handling current and future water quality challenges. These are generally physicochemical technologies, such as coagulation-flocculation and sand filtration, which are effective in turbidity and color removal, but generally present lower efficiency for the removal of trace contaminants (organic and inorganic) (Couto et al., 2019; Moreira et al., 2021a).

In a previous study (Moreira et al., 2021a), it was assessed the performance of these processes for surface water treatment characterized by high turbidities (≤1000 NTU) and concentrations of arsenic, iron, and manganese. Depending on the watershed, these characteristics are commonly observed in rainy seasons (Trindade et al., 2016) and water treatment plants are required to adjust their processes to guarantee a water supply within the threshold values for contaminants. As demonstrated by Moreira et al. (2021), the removal efficiency of trace contaminants tends to decrease as the initial water turbidity or the initial contaminants concentration increases.

To address these challenges, there has been a growing interest in the use of ultrafiltration membranes in water treatment plants (Chang et al., 2022; Ma et al., 2019). Ultrafiltration is porous membranes (Ø 0.01 µm) that act as a physical barrier to the remaining colloids and suspended solids. It is a process driven by hydraulic pressure (0.1–0.5 bar) with a capacity to produce, on average, 0.010–10 m^3 L/m^2h.bar (Liao et al., 2020) (volume of water produced per hour for one square meter of membrane and one unit of pressure applied (Huisman et al., 2007)). From all membrane separation processes driven by hydraulic pressure (which includes nanofiltration and reverse osmosis), they generally present the lowest pressure requirement and still offer a high water quality, being highly effective in removing various contaminants from water (Ma et al., 2019; Jacquet et al., 2021).

In a concept of multiple barriers for water treatment, ultrafiltration would contribute with an additional barrier to high molecular-weight organics, algae cells resulting from seasonal algae population, and viruses, which may pass unaltered through conventional treatment processes, including sand filters, but are effectively retained by ultrafiltration membranes (Jacquet et al., 2021; Yu et al., 2020). However, there are no expectations that ultrafiltration membranes would act on the dissolved fraction of inorganic contaminants due to their size, smaller than the equivalent diameter of the membrane pores.

Arsenic, a naturally occurring compound, is one of the contaminants found in freshwater sources. Depending on the geological characteristics, manganese and iron tends to occur concomitantly as all three species could derive from the same rock matrix. Their concentration in freshwater is often intensified due to anthropogenic

activities, thereby posing a significant threat to both human health and the environment (Moreira et al., 2021b). For arsenic and manganese, conventional water treatment plants exhibit a low removal efficiency (Guimarães et al., 2022), further worsening the issue and leaving communities susceptible to their detrimental effects. Considering the implications of their occurrence, it is imperative to promptly address this matter through the implementation of effective treatment strategies. Such measures are essential to ensure the provision of safe drinking water that is free from arsenic, iron, and manganese contamination.

One alternative previously investigated to control the occurrence of inorganic contaminants in drinking water, especially metals and some metalloids, was a pre-oxidation process before coagulation-flocculation (Moreira et al., 2021c). Under an oxic environment, most dissolved species are converted to oxides, which are insoluble and greater in size. Manganese, however, is thermodynamically more stable in its dissolved form (Mn^{2+}) and high oxidant dosages are required to oxidate this specie (Moreira et al., 2021c). When formed, manganese oxides have an equivalent diameter smaller than the pores of conventional sand filters. In this process, manganese oxides gradually coat the filter media, while bacteria settle and proliferate on them. Therefore, the removal observed comes from contributions of both chemical catalytic oxidation and biological oxidation (Yang et al., 2020), whereas size exclusion would play a minor role in this process.

If iron is present in surface water, it may also form complexes with other contaminants, including manganese and arsenic. Iron complexes, which are easily formed under the pH and redox potential in which water treatment occurs, can adsorb and entrap other contaminants even though they are in their dissolved form (Zhang et al., 2014). The synergistic effect between iron oxides and other contaminants in their removal was suggested in previous papers that observed a positive relationship between their occurrence and removal (Moreira et al., 2021a) and empirically demonstrated by observing the complexes formed by spectroscopy techniques (Zhang et al., 2014). Indeed, arsenic adsorption on metal oxides, such as iron and manganese complexes, plays an important role in the mobility and bioavailability of arsenic in aquatic environments (Zhang et al., 2014).

As a second alternative, in-line coagulation with iron-based coagulants seems to be a logical approach when the remaining dissolved species are intended to be removed by ultrafiltration. The idea was explored by other authors to improve the removal of organic (natural humic acid) (Wang et al., 2006) and inorganic (silica) (Cheng et al., 2009) contaminants by ultrafiltration. The authors reported improvements in irreversible fouling prevention due to the aggregation and settling of suspended and dissolver particles, obtaining flocs with a greater size that were loosely bound to the membrane surface (Cheng et al., 2009). Whereas reversible fouling is easily removed (e.g.: through backwash), irreversible ones require periodical chemical cleaning protocols to prevent it or mitigate its effects.

To the best of the author's knowledge, this study represents the first investigation into the utilization of $FeCl_3$-assisted in-line coagulation in conjunction with ultrafiltration membranes to improve the removal efficiency of arsenic. The bench-scale results were validated in a pilot ultrafiltration system that operated continuously for approximately 31 days. The pilot-sacle membranes system was integrated after the settling units of an existing water treatment plant accounted with conventional treatment processes. Their permeate quality was then compared with the stream leaving the sand filters to demonstrate possible improvements in water quality provided by ultrafiltration membranes. By analyzing these topics, it is expected to provide a comprehensive understanding of the challenges facing water treatment plants and offer potential solutions for improving water security.

5.2 Materials and methods

5.2.1 Water and sediments sampling

Surface water was collected in the Velhas river basin (latitudes: 17°15′S and nd 20°25′S and longitudes 43°25′W and 44°50′W), located in the central region of Minas Gerais (Brazil). Water treatment plants located on the basin were generally designed with conventional technologies, e.g.: coagulation-flocculation, settlers, sand-filters, or sand-filters followed by disinfection, intended mainly for solids removal from raw surface water.

The basin also embraces the iron quadrangle, one of the largest and most well-known iron and gold deposits in the world (Varejão et al., 2011). The geochemical background of these areas suggests a high concentration of iron, arsenic, manganese, and aluminum, which are intensified by the mining activities located in the iron quadrangle. (Varejão et al., 2011). These are major contaminants that threaten the water supply and tend to be at higher concentrations during rainy seasons. To better represent the challenges faced in the basin, water and sediments were collected nearby the catchment point of a water treatment plant.

Once collected, the water samples were stored in the absence of light at temperatures below 4 °C and brought to room temperature before their use and characterization. The surface water and samples collected in this study were characterized in terms of their turbidity (Hach 2100Q), pH (MS Tecnopon mPA-210), color (Hach DR3900), conductivity (MS Tecnopon mCA-150), metals and metalloids (Hach DR3900). Iron, manganese, aluminum, and arsenic concentration values were also determined by inductively coupled plasma mass spectrometry (Agilent ICP-MS 7700; method 3125B). The particles' average diameter was monitored on a laser dispersion particle size distribution analyzer (Model LA-950, Horiba). Fluorescence excitation-emission matrices were obtained from 250 to 600 nm using 3 nm for excitation intervals and 3.23 nm for emissions using a medium gain and 2 s integration for emission detection (Aqualog®, Horiba). The data were corrected by masking the second-order Rayleigh scatter.

5.2.2 Pre-oxidation, coagulation-flocculation, and sand filtration

Surface water samples (2 L) were spiked with aluminum (0.632 mg/L; salt used: $Al_2(SO_4)_3$), arsenic (0.017 mg/L; salt used: Na_2HAsO_4), iron (1.1 mg/L; salt used: $FeCl_3$), and manganese (1.7 mg/L; salt used: $MnSO_4$). The metal species and arsenic were pipetted from stock solutions prepared with deionized water of 1 g/L (for aluminum, iron, and manganese) and 10 g/L (for arsenic). The concentration values refer to the total content of each specie, accounting for dissolved and non-dissolved species, and are representative of the water quality during rainy seasons according to the water quality monitoring (Trindade et al., 2017). Previous studies demonstrated the decrease in efficiency of coagulation-flocculation and sand-filtration as the contaminant’s concentration increases (Moreira et al., 2021a). Under such

circumstances, violations of drinking water is more prone to occur and reinforcements in drinking water treatment process would be required to guarantee its safety.

The waters were pre-oxidized (NaOCl; 7.7 mg/L) for 1 h in a Jar test under constant agitation (120 rpm). Following the pre-oxidation, the medium pH was adjusted before coagulation-flocculation using a 0.01 mol/L sodium hydroxide (NaOH) solution to achieve a pH value of 8. Iron chloride ($FeCl_3$; 3 mg/L) was used as the coagulant agent, and the paddles were operated at rapid mixing (100 rpm; 1 min), followed by 68, 44, 37, and 26 rpm, each held for 4 min. The media were allowed to settle for 5 min, and the supernatant was collected for physicochemical characterization and further sand filtration. The oxidant and coagulant concentrations were based on previous studies that investigated their contribution to metals, metalloids (arsenic) (Moreira et al., 2021c), and solids removal (Moreira et al., 2023).

A down-flow sand filtration system with a height of 240 mm and an inner diameter of 19 mm was used, filled with conventional sand with an average particle diameter of 0.297–1.18 µm (depth: 150 mm). Before each test, the filters were compacted using deionized water (500 mL).

The physicochemical parameters were compared in raw surface water, after the settling unit, and after the sand filters to assess the performance of these processes in water treatment.

5.2.3 Ultrafiltration: Bench-scale

A storage tank with a capacity of 2 L received treated water from the settling unit through a Zeeweed ultrafiltration module provided by Suez Water Technologies & Solutions. The module had a membrane made of polyetherimide with an average pore diameter of 0.04 µm and a filtration area of 0.047 m^2. The experiments were carried out at a constant temperature of 25 ± 1 °C and pressure of 0.20 ± 0.05 bar, with a permeate recovery rate of up to 90%. Aeration was used to reduce membrane fouling, with an airflow rate of 0.5 Nm^3/h continuously provided to the ultrafiltration tank. After the filtration tests, physical cleaning was performed by recirculating water for 5 min at a rate of 2 L/min, followed by backwashing with distilled water for 5 min. The permeate

flux (J, L/m^{2}h) and the efficiency of contaminant rejections were monitored during these experimental trials.

If the water permeability was not restored, chemical cleaning was carried out using an ultrasonic bath with NaOH (0.2 wt%) and citric acid (pH = 2.5) solutions for 20 min each.

Four different concentrations of $FeCl_3$ were tested during the in-line dose experiments: 0.086, 0.103, 0.138, and 0.172 mg/L. They considered the value already recommended by the membrane manufacturer (0.086 mg/L) to prevent fouling from fine particles, and greater values (0.103–0.172 mg/L) to verify their contribution in terms of arsenic removal. The coagulant contact time was 5 s for these experiments. This value was estimated based on the residence time of the feed on the pilot system, considering the flow rate and the point of application of the coagulant. A schematic of the surface water treatment setup, including the processes of coagulation-flocculation and sand filtration, can be found in Figure 5.1.

Figure 5.1. Schematic of the surface water treatment setup, including the processes of coagulation-flocculation, sand filtration, and ultrafiltration.

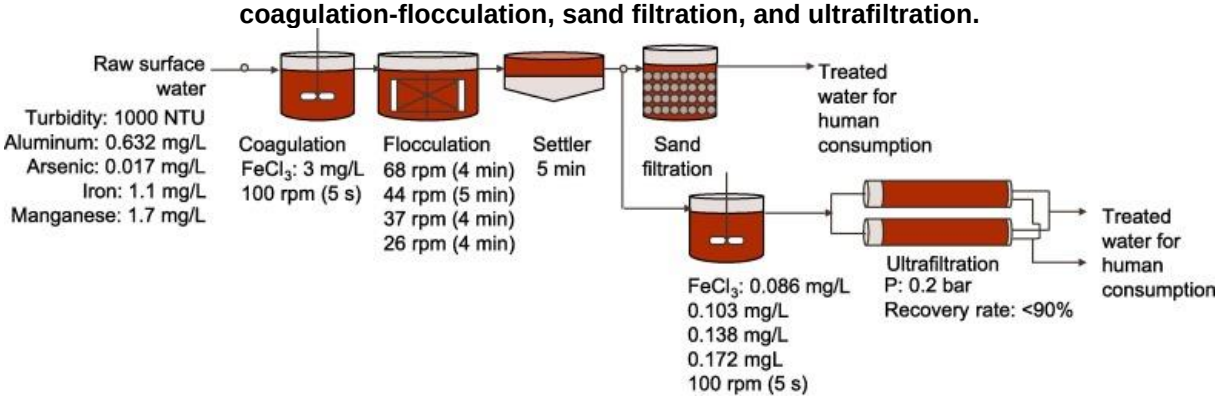

5.2.4 Pilot-scale ultrafiltration

The pilot scale ultrafiltration system was integrated into a water treatment facility currently equipped with stages of pre-oxidation, coagulation-flocculation (two fast mixing chambers, 24 hydraulic and mechanized flocculators with four chambers each; coagulant: $FeCl_3$), settlers (six pool-type settlers equipped with automated sludge scrapers), and sand-filtration (24 units filled with sand and operated with a descending flow), designed with a treatment capacity of approximately 7.5 m^3/s. The ultrafiltration membranes were positioned downstream of the settlers, a decision guided by several considerations. Notably, during periods of heavy rainfall, the settling units may

experience an increase in water turbidity, which can detrimentally affect the performance of the sand filters. To mitigate this issue, ultrafiltration membranes can be employed to process either a fraction or the entire flow rate, thereby reducing the load of suspended particles on the sand filters. Conversely, in situations where the water turbidity at the outlet of the settlers adheres to the recommended levels for sand filtration, the ultrafiltration permeate can be blended with the effluent leaving the sand filters, thus enhancing the overall water quality.

To demonstrate the influence of rainy seasons on water quality, Table 5.1 showcases the principal physicochemical parameters of raw surface water during the operational period of the pilot plant. Notably, the table highlights turbidity values of up to 3,128 NTU for raw surface water, highlighting the significant impact of rainy seasons on water quality.

Table 5.1. Descriptive statistics of the key physicochemical parameters obtained from the raw surface water within the basin where the water treatment plant is situated. *Refers to true color values. Data were obtained from local environmental agency responsible to monitor the water quality [17].

Parameter	Average	Standard deviation	Median	Minimum	Maximum
Turbidity (NTU)	201.18	321.23	105.5	1.34	3128
Color (uH)*	47	31	43	10	162
pH	6.60	0.60	6.60	4.80	8.10
Electrical conductivity (µS/cm)	127.0	132.6	73.1	3.1	744.8
Aluminum (mg/L)	0.193	0.154	0.147	0.024	0.554
Arsenic (mg/L)	0.005	0.014	0.008	0.0005	0.090
Iron (mg/L)	7.65	5.93	8.17	0.08	22.25
Manganese (mg/L)	0.272	0.638	0.100	0.003	6.270

The ultrafiltration pilot plant (ZeeWeed 500d pilot) consists of 3 feeding tanks with a capacity of 20 m^3 each, equipped with three ZeeWeed 500d modules. The plant has the flexibility to isolate each of the modules, thus being able to operate with one, two, or three modules. The membrane area of each module is 40.9 m^2, and the system has a treatment capacity of 1 to 2.25 m^3/h in direct filtration mode. The unit also has instruments that enable remote operation and online monitoring of permeate flow,

pressure, temperature, pH, and turbidity, and includes the application of $FeCl_3$ in the ultrafiltration feeding via chemical injectors of the quill injection type.

The membranes operated under a small negative pressure (0.15 – 0.20 bar) created by pumping permeate through the hollow fiber. Part of the permeate is stored in a process tank for the back pulse and backwash operations. The system operates with a constant permeate flux (37 L/m^2h) and a permeate recovery rate of 95%. Membrane aeration occurs intermittently from the bottom of the membranes to create turbulence. System operation includes back pulse (at 15-minute intervals for 30 s), permeation, backwash, and draining of the membrane tank to remove solids (at 183-minute intervals for 15 s). The system operated continuously for approximately 31 days, with and without an in-line dose of $FeCl_3$ for comparison purposes.

5.2.5 Statistical analysis

Microsoft Excel and OriginPro were used for statistical analysis. Although the results had a trend for a normal distribution ($n \leq 792$), verified by the Shapiro-Wilk's test and Levene's test for homogeneity, Kruskal-Wallis post-hoc with Dunn's tests were preferred given the number of replicates and for better confidence on the hypothesis tested. For similar reasons, Mann-Whitney U Test and Spearman were preferred for comparison between two independent groups and correlation, respectively. A confidence level of 95% was set for all statistical analyses performed.

5.3 Results and discussions

5.3.1 Coagulation-flocculation and sand filtration

Table 5.2 shows the results for raw surface water, after the settling unit, and after the sand filters obtained on a bench scale. The settling unit was responsible for removing the suspended solids from surface water that were formed after the processes of coagulation-flocculation. This is evident from the decrease in turbidity and apparent color after the settling unit, from 979 NTU to 2.23 NTU and 3360 uH to 7 uH, indicating that the settling unit removed a large portion of the suspended solids and color-causing compounds. The use of conventional coagulation and flocculation to treat surface water with high turbidity is not a major issue as long as the coagulant is added in the appropriate concentration.

Table 5.2. Physicochemical parameters during conventional water treatment. Results refer to averages ± standard deviation (n ≥ 3).

Parameter	Raw surface water	After settling unit	After sand filters
Turbidity (NTU)	979 ± 27	2.23 ± 0.41	0.38 ± 0.05
Apparent color (uH)	3360 ± 238	7 ± 1	1 ± 1
pH	6.99 ± 0.10	7.49 ± 0.05	7.41 ± 0.13
Conductivity (µS/cm)	153.4 ± 4.1	164.5 ± 17.8	71.1 ± 5.1
Aluminum (mg/L)	0.591 ± 0.014	0.006 ± 0.002	<0.001
Arsenic (mg/L)	0.020 ± 0.001	0.015 ± 0.001	0.011 ± 0.002
Iron (mg/L)	1.10 ± 0.12	0.68 ± 0.05	0.14 ± 0.01
Manganese (mg/L)	1.76 ± 0.13	0.076 ± 0.021	0.10 ± 0.01

Studies suggest that the greater concentration of suspended particles increases the collision frequencies and favors the formation of flocs of higher density that easily settle (Li et al., 2013). Two possible mechanisms would explain the results observed, the particle destabilization promoted by the coagulant and also a reduction of the effective surface charge. The high concentration of suspended solids results in a lower surface charge influence and a lower number of water molecules adsorbed around a given particle. In this case, the adjacent particles, so far remaining apart principally due to electrostatic repulsion and to a certain extent to the ordered water structure around them, are now able to approach close enough together so that Van der Waal forces of attraction can hold them together (Moreira et al., 2023; Bratby, 2006). To a lesser extent, the settling unit also removed some of the dissolved substances such as aluminum, arsenic, iron, and manganese, whereas the pH and conductivity remained relatively unchanged after the settling unit.

Sand filters remove most suspended solids and some of the dissolved substances that are not removed by the settling unit. This is evident from the further decrease in turbidity and apparent color after the sand filters. The turbidity decreased from 2.23 NTU to 0.38 NTU, whereas the color values decreased from 7 uH to 1 uH, indicating further removal of color-causing compounds.

The concentration of aluminum and iron were within the recommended values for drinking water after the sand filters (aluminum: <0.2 mg/L and iron: <0.3 mg/L),

whereas manganese violated the maximum contaminant level (manganese: <0.1 mg/L) in some replicates and arsenic were above the threshold values for all of them (0.01 mg/L). Even so, the concentration values differed significantly for settling units and sand filters (p-valueAl: 0.0099, p-valueAs: 0.0200, and p-valueFe: 0.0116, p-valueMn > 0.05), suggesting that sand filters still had a contribution to their removal.

The speciation diagram for manganese that correlates the pH and redox potential suggests that manganese would be predominantly in its dissolved form (see Fig. C1 – appendix C). In that case, physical adsorption would be the prevailing mechanism in its removal, whereas other phenomena such as precipitation, co-precipitation, and size exclusion would have minor contributions, limiting the efficiency of sand filters in manganese removal. For arsenic, previous studies suggested that the complexes formed would present an average diameter of 0.04 µm (Moreira et al., 2021a), smaller in size than the pore sizes of sand filters (10–100 µm) (Brandt et al., 2017). As for manganese, the removal by size exclusion would also have minor contributions, limiting the efficiency of sand filters. The results emphasize the limitations of conventional treatment processes in arsenic and manganese removal. As an alternative to sand filters, ultrafiltration membranes were investigated first on a bench scale before being validated in a pilot scale.

5.3.2 Performance of ultrafiltration membranes: Bench-scale

The performance of ultrafiltration was compared in experiments with and without an in-line dose of coagulant and the results for permeate flux were shown in Figure 5.2. The results from experiment one was obtained with the same feed solution, differing only by the additional dose of coagulant. As for the first experiment, the same protocol was employed for experiments two, three, and four represented in Figure 5.2.

Figure 5.2. Normalized ultrafiltration permeate flux (J/J_0) for experiments without and with an in-line dose of $FeCl_3$. J: final permeate flux, J_0: initial permeate flux. Transmembrane pressure 0.2 bar. J/J_0 values < 1 represents flux decay. Three experiments were performed in each condition and the error bars refer to the standard deviation of the replicates.

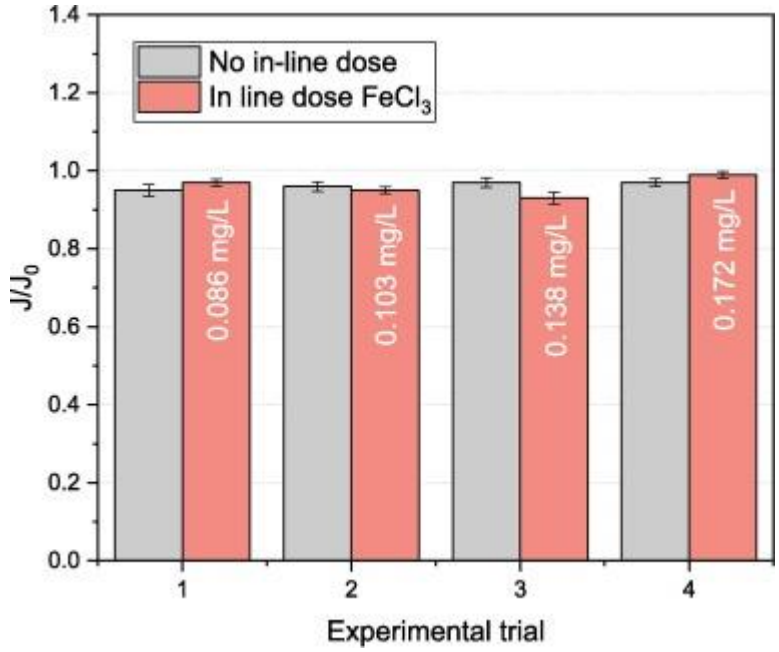

In experiments without an in-line dose of $FeCl_3$, the average flux values corresponded to 189.9 ± 11.8 L/m^{2}h, compared with 193.4 ± 5.3 L/m^{2}h for experiments when the coagulant was considered. Even at high recovery rates (90%), the flux decay was lower than 6% in experiments without coagulant or lower than 5% in experiments with an in-line dose of $FeCl_3$. The values suggest that the ultrafiltration membrane was favored by an additional coagulant dosage that resulted in a higher permeate flux and lower decays. The differences observed were also statistically significant (see Table D1) and the Mann-Whitney tests pointed out that the final permeate flux was higher for experiments with an in-line dose of $FeCl_3$ except for the fourth experimental trial. The benefits of using the coagulant can be even greater in a longer-term operation, resulting in an extended lifespan of the membrane. By reducing fouling, it prevents frequent chemical cleaning protocols that are capable to compromise the membrane integrity (Lebron et al., 2021; Gul et al., 2021).

On the other side, when experiments with different doses were compared in a Kruskal-Wallis statistical test, the difference in final flux values was considered non-significant (p-value: 0.1160; see Table D2), suggesting that a lower coagulant dosage (0.086 mg/L) would already improve the ultrafiltration performance without an excessive

dosage. For that reason, this dosage was chosen for subsequential experiments, later justified in the manuscript by the improvements in arsenic as well.

The first explanation for the lower fouling rate in experiments with an in-line dose is the increase in floc sizes. Analysis of particle sizes for samples collected before ultrafiltration in experiments without and the addition of a coagulant revealed that the particles average diameter increased from 24.1 to 29.2 µm (Figure 5.3). Consequences related to greater particle size are a fouling layer more porous and permeable, and with a lower hydraulic resistance (Guigui et al., 2002), leading to higher permeate fluxes as observed. The increase in floc sizes also prevents pore blocking in the early stages of filtration, a dominant fouling mechanism in ultrafiltration processes that compromises their performance (Costa et al., 2006). Although not investigated in this study, other authors as Shen et al. (2020) demonstrated a shift in pore blocking to cake layer formation when a coagulant is dosed prior to ultrafiltration, which resulted in a loosely fouling layer that is easier to be removed under physical cleaning procedures.

Figure 5.3. Analysis of particle sizes for two aqueous samples from ultrafiltration feed before (UF) and after (UF-$FeCl_3$) the in-line dosing of $FeCl_3$.

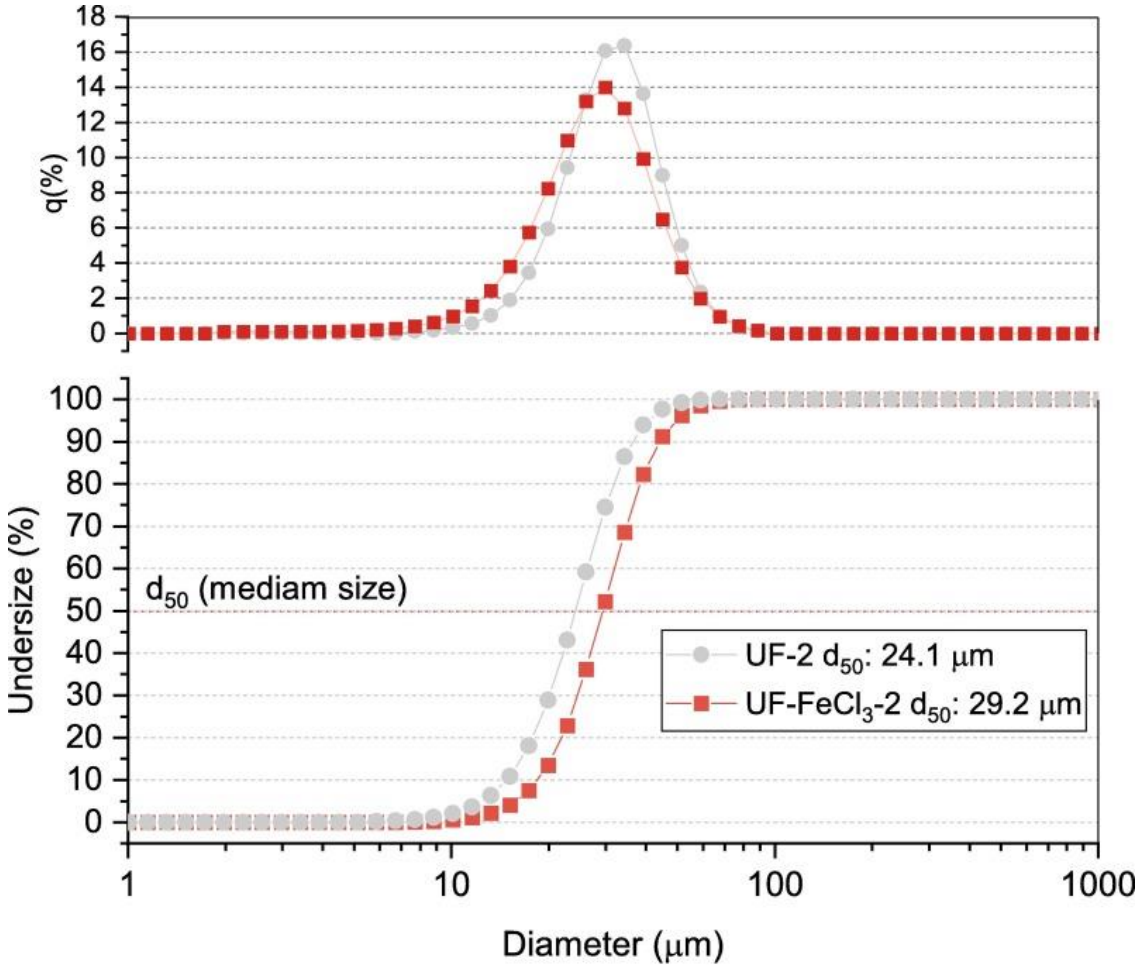

The additional coagulant dosage also acts on the residual natural organic matter leaving the settler unit. These are defined as a complex matrix of organic materials, often recalcitrant, commonly present in natural waters. As for turbidity and the other contaminants considered in this study, the natural organic matter is also subjected to seasonality, tending to occur at higher concentrations in rainy seasons. As their concentration increases, the efficiency of coagulation-flocculation processes tends to decrease (Sharp et al., 2006), suggesting that ultrafiltration membranes would be subjected to a higher concentration of foulant material during these events. In that case, the residual concentration of dissolved organic matter observed is expected and tends to increase after the process of coagulation-flocculation, ultimately reaching the ultrafiltration membranes (Li et al., 2020).

The contribution of an additional removal of natural organic matter is seen in the excitation-emission matrices shown in Figure 5.4. The results for feed samples without

and with an in-line dose of $FeCl_3$ were shown in Figure 5.4(a) and (c), respectively, and the results for ultrafiltration permeate obtained from experiments without and with an inline dose of $FeCl_3$ were shown in Figure 5.4(b) and (d), respectively. Two distinct regions are observed in Figure 5.4, the first one between λexc: 220–250 and λemi: 280 – 380, followed by a region at λexc: 280–380 and λemi: 260–470. Sen-Lavurmaci et al. (2016) correlated them with the presence of aromatic proteins, fulvic-like substances, and humic-like substances. Notably, the process in which an in-line dose was considered had a lower concentration of these compounds entering the system, and consequently leaving in the permeate, seen by the lower intensities observed in Figure 5.4 (b) and (d). In a previous study, the colloidal fraction of natural organic matter was found to be a major fouling component of ultrafiltration (Costa et al., 2006; Howe et al., 2002), moreover, their occurrence could favor the formation of disinfection byproducts depending on the disinfection procedure used (e.g.: disinfection with free chlorine). Therefore, an in-line dose could lower the fouling rate of ultrafiltration membranes and reduce the risks of disinfection by-product formation, in both cases resulting from an additional removal of the remaining dissolved organic matter.

.

Figure 5.4. Excitation Emission Matrix (EEM) for ultrafiltration feed samples (a) before and (b) after the in-line dose of $FeCl_3$ (0.086 mg/L), and for ultrafiltration permeate of experiments (c) without and (d) with an in-line dose of $FeCl_3$.

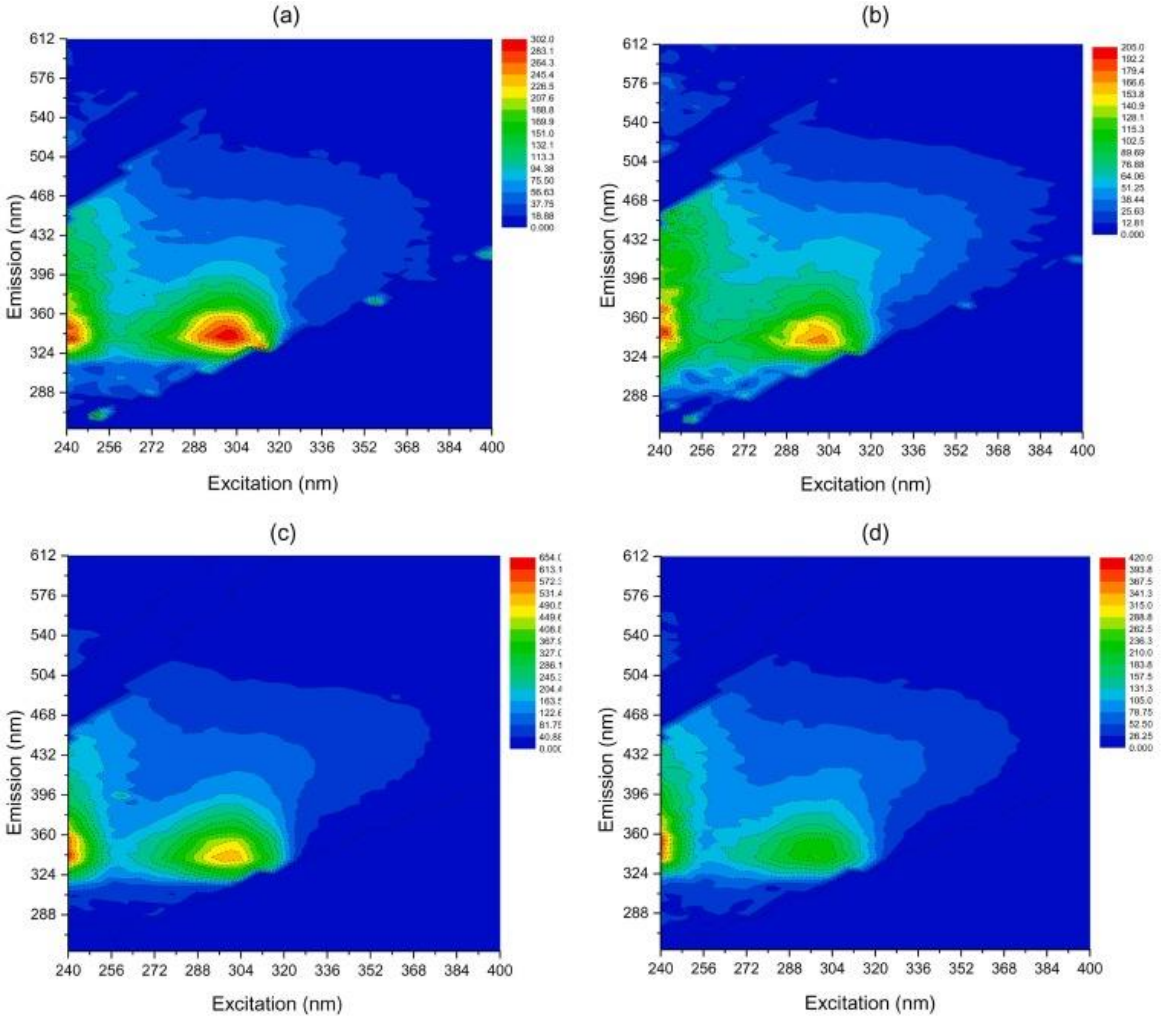

The physicochemical characteristics of streams leaving the settling units and the ultrafiltration membranes were presented in Table 5.3 and Figure 5.5. Among the parameters presented in Table 5.3, color was the one favored by an additional dose of coagulant starting at lower dosages (0.086 mg/L). Differences observed between the turbidity values were considered non-significant (p-value: 0.0717). The removal of all metallic (aluminum and manganese) species and arsenic was favored by the in-line dose except for iron, which tended to be at higher concentrations in ultrafiltration permeate (Figure 5.5). Despite the greater concentration, the residual iron remaining in the ultrafiltration permeate was still lower than the maximum contaminant level for drinking water (0.3 mg/L). As for iron, all other species were within the threshold values. Another observation to be made is the contribution to arsenic removal, even considering the lowest dosage of $FeCl_3$ (0.086 mg/L).

Table 5.3. Comparison between the parameters of turbidity, apparent color, pH, and conductivity after the settling unit, ultrafiltration (UF) permeate, and UF permeate aided by an in-line dose of FeCl3 (UF-FeCl3). Results refer to averages ± standard deviation (n = 3).

Parameter	$FeCl_3$ dose (mg/L)	Settling	UF permeate – without $FeCl_3$	UF permeate – with $FeCl_3$
Turbidity (NTU)	0.086	3.66 ± 0.75	0.08 ± 0.02	0.08 ± 0.01
	0.103	4.19 ± 0.61	0.08 ± 0.02	0.07 ± 0.01
	0.138	4.07 ± 0.52	0.07 ± 0.02	0.06 ± 0.01
	0.172	4.14 ± 0.41	0.07 ± 0.01	0.07 ± 0.01
Apparent color (uH)	0.086	31 ± 4	4 ± 2	<1
	0.103	33 ± 4	2 ± 1	<1
	0.138	34 ± 2	<1	<1
	0.172	36 ± 1	3 ± 1	<1
pH	0.086	7.18 ± 0.07	7.21 ± 0.11	7.15 ± 0.04
	0.103	7.20 ± 0.04	7.26 ± 0.04	7.18 ± 0.12
	0.138	7.40 ± 0.06	7.36 ± 0.07	7.41 ± 0.39
	0.172	6.75 ± 0.06	7.31 ± 0.03	7.50 ± 0.05
Conductivity (µS/cm)	0.086	153.1 ± 4.4	149.5 ± 11.1	157.2 ± 3.2
	0.103	139.5 ± 0.7	146.2 ± 2.3	143.7 ± 3.8
	0.138	142.8 ± 1.65	147.6 ± 2.8	146.9 ± 2.7
	0.172	139.9 ± 6.5	151.4 ± 5.0	150.5 ± 1.4

Note: Table 2, Table 3 renumbere from 1 to 3.

Figure 5.5. Comparison between the parameters of (a) aluminum, (b) arsenic, (c) iron, and (d) manganese after the settling unit, UF permeate, and UF permeate aided by an in-line dose of $FeCl_3$ (UF-$FeCl_3$). Results refer to averages ± standard deviation (n = 3). Effect of concentrate recirculation: bench-scale. Note: the errors were minimal for the aluminum concentration in experiments that involved an inline dose of $FeCl_3$. As a result, the error bars were not visible in the corresponding bars on the graph (a).

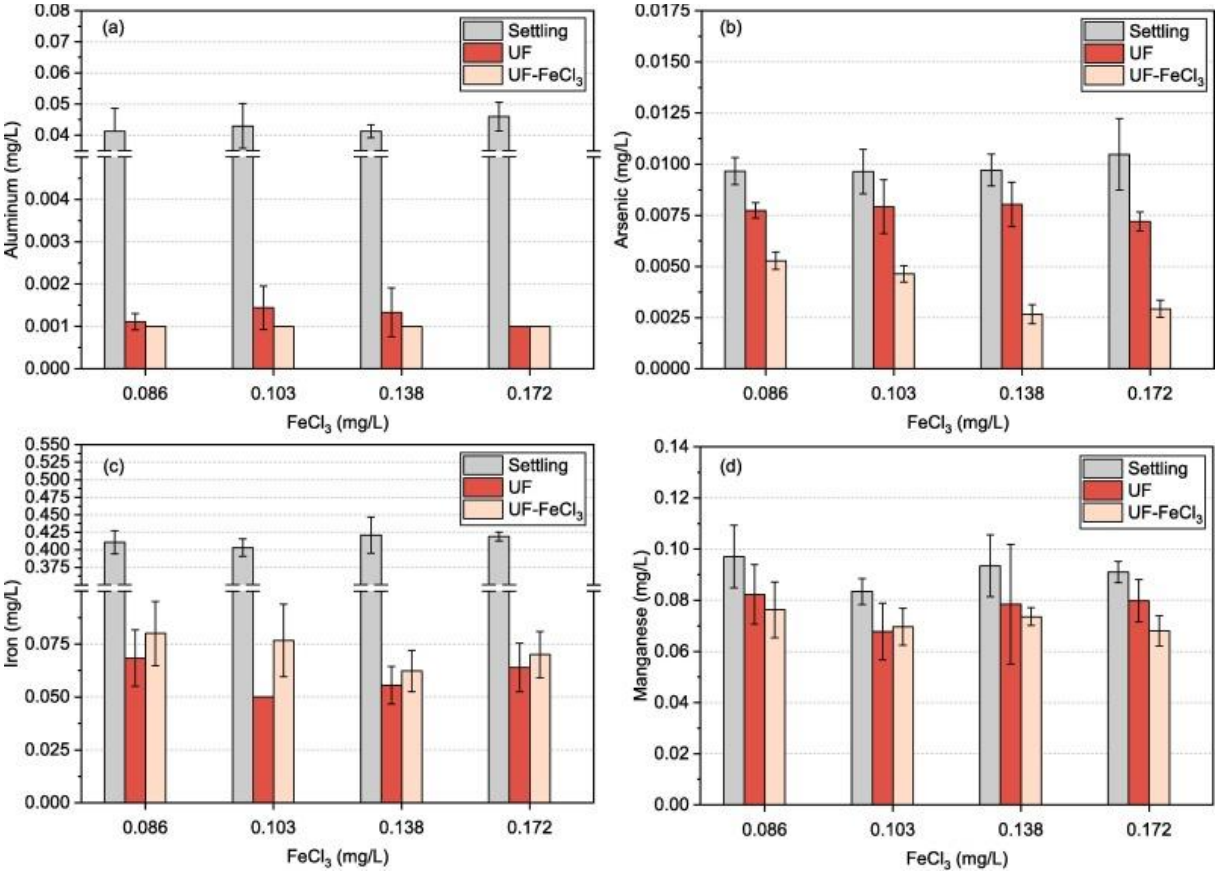

Previous studies demonstrated that the co-occurrence of iron contributes positively to arsenic, aluminum, and manganese removal (Moreira et al., 2021a; Vries et al., 2017). In addition to favoring an appropriate formation of flocs through the destabilized colloidal particles, the higher concentrations of $FeCl_3$ would also lead to the formation of amorphous metal hydroxide flocs, in which arsenic, manganese, and aluminum would be entrapped by the flocs formed and therefore removed. For arsenic, in specific, insoluble precipitates such as ferric arsenate ($AsFeO_4$) might be formed in a wide pH range (3–8) in cases where both elements, arsenic and iron, coexists in the medium (Hering et al., 1996; Krause, Ettel, 1989). That would explain the favored contribution of iron the removal of the metallic species and arsenic.

Even so, an important observation to note is that conventional treatment processes, which comprises coagulation-flocculation, settling, and sand filtration, exhibit limited

resilience in water treatment. As a result, variations in water quality are expected, including variations in arsenic concentrations. One example is the results for arsenic reported in Figure 5.5. The bars represent average values, but when considering the minimum and maximum values, the arsenic concentrations ranged from 0.004 mg/L to 0.014 mg/L after the settling units. These findings align with previous studies (Moreira et al., 2021a) and emphasize the need for robust technologies like ultrafiltration to ensure the quality of drinking water.

When the characterizations obtained after sand filters (Table 5.2) are compared with ultrafiltration permeate (Table 5.3 and Figure 5.5) it is possible to see the improvements in water quality, especially in terms of residual concentrations of arsenic and manganese. Ultrafiltration would then be an effective reinforcement strategy to guarantee water safety, acting as an effective barrier to contaminants.

The study also addressed the issue of concentrate disposal by recycling it back to the coagulation-flocculation processes. The strategy increases the recovery rate of ultrafiltration membranes and lowers the water losses during its treatment. The experiments were made considering an in-line dose of $FeCl_3$ (0.086 mg/L). As demonstrated in the previous results, it was sufficient to observe improvements in ultrafiltration performance, ensuring that its permeate would attain the drinking water standards for aluminum (0.1 mg/L), arsenic (0.01 mg/), iron (0.3 mg/L) and manganese (0.1 mg/L). The results were summarized in Figure 5.6, which illustrates the impact on the parameters of surface water, decanted water (after settlers), filtered water (after sand filters), and ultrafiltration permeate.

Figure 5.6. Comparison of physicochemical characteristics at different stages of the treatment process along the four stages of ultrafiltration concentrate recycling. In-line dose of $FeCl_3$ before ultrafiltration (UF): 0.086 mg/L. Note: numbers 1 to 4 relate to water treatment repetitions, while recirculation of the concentrate stream in the specified proportions began from repetition 2 onwards.

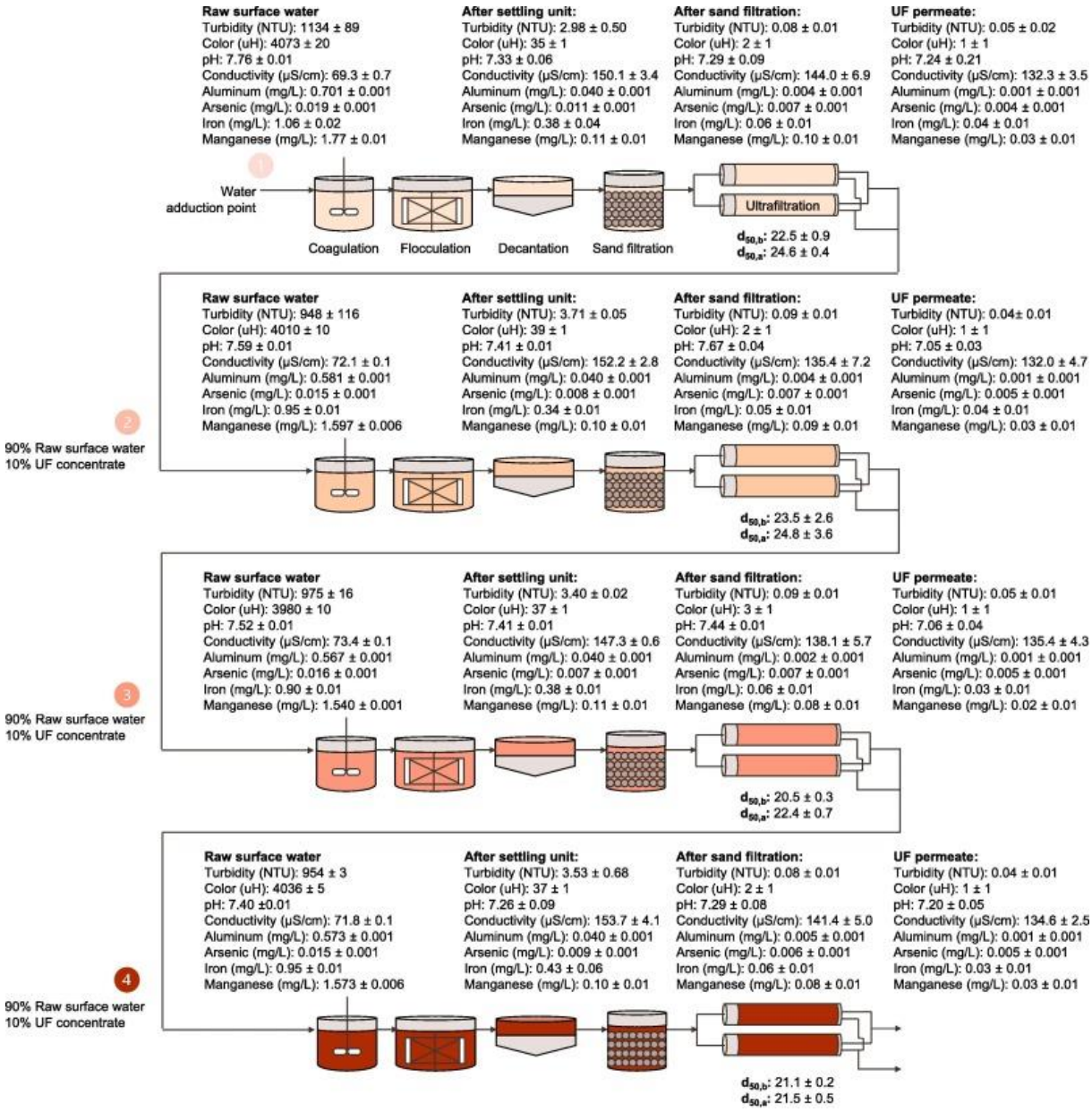

The results show that the concentrate recirculation did not significantly affect the quality of the decanted water, filtered water, and ultrafiltration permeate in terms of turbidity, as there were no significant differences observed between the turbidity values. However, the surface water showed a reduction in turbidity from 1134 ± 89 NTU to around 959 NTU for the experiments in which the concentrate, with a turbidity

of around 26 NTU, was recycled. The low coagulant dosage used in the ultrafiltration feed (0.086 mg/L) and the high permeate recovery (90%) reduced the negative impact on the coagulation/flocculation process due to the residual coagulant fraction in the concentrate stream. Similar to the turbidity values, recirculation of the ultrafiltration concentrate did not affect the quality of the decanted water, filtered water, and ultrafiltration permeate in terms of color, conductivity, metals, and arsenic as there were no significant differences observed for the values of each current.

Membrane fouling was also monitored during the cycles of ultrafiltration concentrate recirculation. This is important given the build-up potential of fouling elements, whether natural compounds or even the additional dose of coagulant. However, the results indicate that even with high permeate recovery, the permeate flux decay was minimal, and the recirculation of the ultrafiltration concentrate did not aggravate the membrane fouling (see Fig. C2). There were no significant differences observed for flow values normalized (J/J_0) between the three sequential experiments that received the ultrafiltration concentrate (p-value: 0.1038). The values corresponded to 0.85 ± 0.10, for the first experiment without ultrafiltration concentrate, and 0.96 ± 0.02 (#2), 0.86 ± 0.01 (#3), 0.93 ± 0.03 (#4) for the following experiments in which the concentrate was recirculated.

Even so, it was observed the presence of natural organic compounds, similar to the ones previously described (aromatic proteins, fulvic-like substances, humic-like substances), persisted in the water treatment process. Although the decanted water samples from experiments #2 to #4 showed more intense peaks associated with residual organic carbon (Figure 5.7), there was no tendency for organic compounds to accumulate in ultrafiltration permeate as noted by the intensity values. In that case, the potential for disinfection by-products obtainment remains low, however, complementary investigations are required to better comprehend their build-up potential and possible impacts on ultrafiltration performance in terms of fouling. Matilainen et al. (2010) suggested that the optimum pH value for ferric-based coagulation varied between 4.5 and 6, achieving removals of up to 70% of natural organic matter. Intended to improve the performance of coagulation-flocculation, the dosage could be revised as well.

Figure 5.7. Excitation Emission Matrix (EEM) for samples collected after the settling unit and for ultrafiltration permeate.

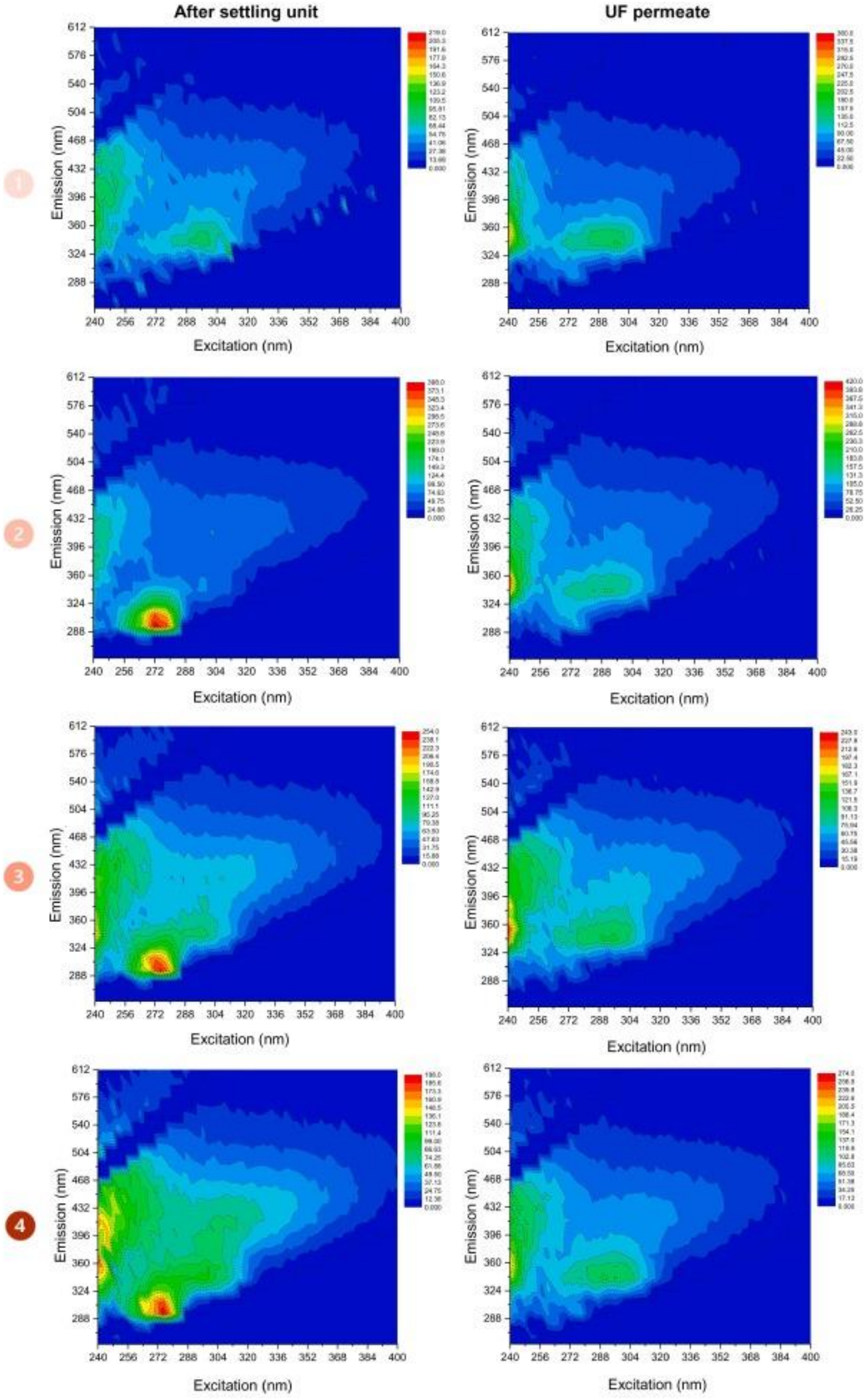

Note: numbers 1 to 4 relate to water treatment repetitions, while recirculation of the concentrate stream in the specified proportions began from repetition 2 onwards.

Sieliechi et al. (2008) suggested that concentrations of ferric chloride can yield more compact flocs due to the interaction between anionic humic substances and the cationic coagulant species. The authors associated a neutralization mechanism as the main responsible for humic acid removal during coagulation. Upon increasing the coagulant concentration, the number of colloids formed also increases and ultimately leads to a higher collision rate of destabilized colloids. In addition to neutralization, complexation destabilization was also suggested by the authors as a mechanism contributing to humic acid removal, leading to a greater performance of coagulation-flocculation processes.

In the broader context of our investigation, significant improvements were observed in ultrafiltration performance through the implementation of in-line $FeCl_3$ dosing. This novel approach not only yielded higher removal efficiencies for arsenic and manganese but also holds promising potential for the removal of other contaminants. Notably, Cheng et al. (2009) demonstrated the advantages of in-line dosing in effectively mitigating silica-induced membrane fouling, elucidating its practical benefits. Moreover, Wang et al. (2006) focused on the prevention of fouling induced by natural humic acids, providing valuable insights into fouling mechanisms. Building upon these studies, the current research expands the scope of fouling prevention to encompass broader improvements in water quality and the resilience of drinking water treatment plants. Additionally, the collective findings from these studies and the current research contribute to an essential discourse on extending membrane lifespan and broadening their utilization in drinking water treatment plants. Based on the positive outcomes, the process was validated on a pilot scale defining 0.086 mg/L as the coagulant concentration to be considered in experimental trials with an in-line dose.

5.3.3 Performance of ultrafiltration membranes: Pilot-scale

The pilot-scale tests were carried out under constant flux and the transmembrane pressure was adjusted to account for the increase in membrane resistance caused by fouling. Figure 5.8 illustrates the profiles of permeate flux and transmembrane pressure obtained from tests conducted without dosing and with in-line coagulant dosing. The

operation did not consider an intermediate chemical cleaning between the scenarios (without and with in-line dosing of $FeCl_3$).

Figure 5.8. Comparison between the ultrafiltration (a) permeate flux (J) in L/m²h (LMH), (b) transmembrane pressure (TMP), and (c) normalized flux (J/J_0) in pilot-scale operated without and with in-line dosing of $FeCl_3$ (0.086 mg/L).

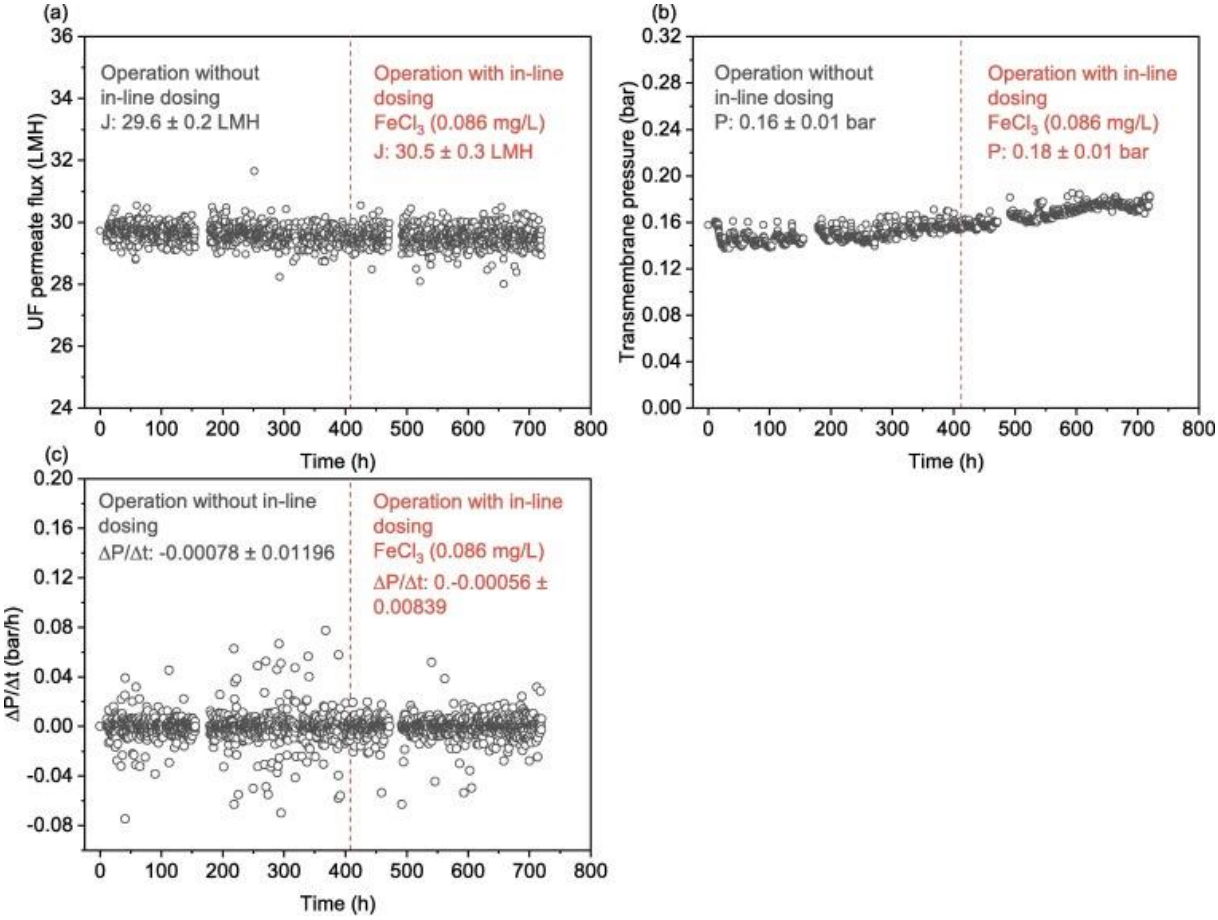

The average flux results before and after the physical cleaning process via back pulse were 29.6 ± 0.3 L/m²h and 27.1 ± 1.8 L/m²h, respectively, for the first part of the pilot plant operation. For the second part, where coagulant was added to the ultrafiltration feed, the corresponding values were 29.5 ± 0.2 and 26.5 ± 1.2 L/m²h. Notably, the mean values were similar and within the same standard deviation when comparing different scenarios before and after the back pulse process. In both scenarios, an increase in operating pressure was required to ensure system operational capacity (Figure 5.8b).

The need to operate at higher transmembrane pressures was not related to the additional iron dosage in the second scenario (with an in-line dose of $FeCl_3$) since the same adjustment was necessary when the plant was operated without the coagulant. As a comparison, for the first scenario, the transmembrane pressure increased, on average, from 0.13 to 0.15 bar, compared with an increase from 0.15 to 0.18 bar for the second scenario. Additional evidence of this fact is that the increase in transmembrane pressure over time remained the same throughout the entire operation (Figure 5.8c), without statistical difference between both periods ($p = 0.0744$). It is important to highlight that no chemical cleaning was conducted between scenarios, and the dosage was initiated with the already fouled membrane. These findings underscore the significance of implementing a comprehensive cleaning protocol to preserve and restore membrane permeability, thus preventing undesired pressure build-up in ultrafiltration processes, as observed in this study.

The pilot-scale experiments revealed an increase in floc sizes from 10.3 ± 0.5 to 18.1 ± 0.3 µm, validating the observations made in bench-scale, which contributed to the stable performance of ultrafiltration membranes and enhanced removal efficiency of other parameters such as turbidity, color, metals, and arsenic. These findings were presented in Figure 5.9, Figure 5.10, which compare the operation with and without an additional dose of $FeCl_3$. The robustness of ultrafiltration membranes observed in bench-scale studies was also observed in pilot-scale experiments. Despite the variations in physicochemical (Moreira et al., 2021a; Moreira et al., 2021b) characteristics in the ultrafiltration feed, the permeate quality remained relatively similar and within the recommended maximum levels for drinking water except for arsenic in experiments without in-line dosing.

Figure 5.9. Comparison between the values of turbidity and color in ultrafiltration (UF) feed and permeate in pilot-scale operated without and with in-line dosing of $FeCl_3$ (0.086 mg/L).

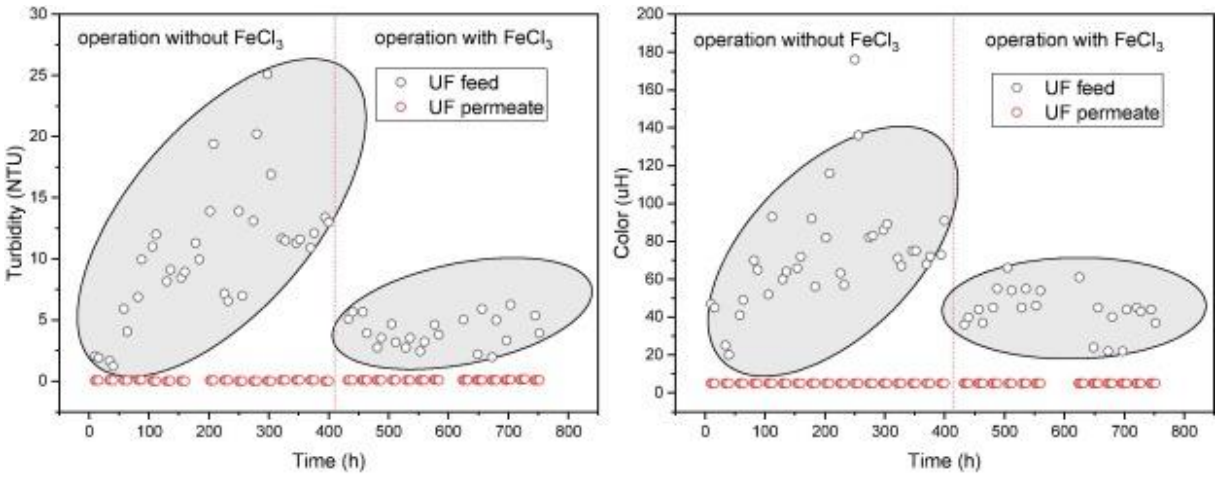

Figure 5.10. Comparison between the concentrations of arsenic in ultrafiltration (UF) feed and permeate in pilot-scale operated without and with in-line dosing of $FeCl_3$ (0.086 mg/L). MCL: maximum contaminant level according to national standards for drinking water.

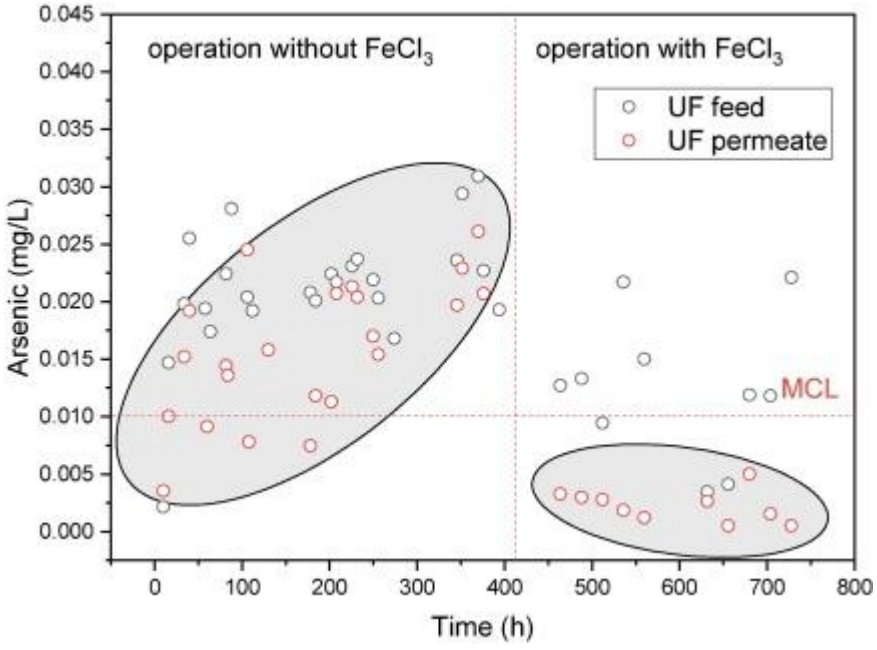

It is seen in Fig. 9, Fig. 10 that the additional dose of $FeCl_3$ alleviated the contaminant load entering the ultrafiltration system, as demonstrated by lower values of turbidity, color, and arsenic in the second scenario. In previous investigations with a similar surface water composition in terms of aluminum, arsenic, iron, and manganese, it was shown that conventional processes for water treatment effectively removed aluminum, iron, and manganese, but had limitations specifically with arsenic (Moreira et al., 2021a; Moreira et al., 2021b). Ultrafiltration successfully retained manganese when its concentrations exceeded acceptable levels, as a result, the frequency of monitoring

manganese was not the same as arsenic. Among these contaminants, the in-line dose had a particular impact on arsenic removal and attainment of drinking water standards.

In contrast to the findings of bench-scale studies, violations in terms of maximum contaminant levels occurred more frequently in the ultrafiltration permeate and the in-line dose was necessary to meet the required standards. The contribution of iron to form complexes with arsenic (e.g.: $AsFeO_4$), readily formed within the prevailing pH (3–8) and redox conditions of water treatment processes, is seen by the lower concentrations of arsenic in the ultrafiltration permeate. A previous investigation has established that under such water quality conditions, there is a favorable prevalence of colloidal fractions of iron and arsenic, characterized by sizes exceeding 0.04 µm. This finding elucidates the observed higher removal efficiencies for arsenic during pilot-scale operations (Moreira et al., 2021a). Additionally, Table S3 presents a concise overview of physical, chemical (including aluminum, iron, and manganese), and biological parameters associated with the ultrafiltration permeate when operated with the in-line dosage of $FeCl_3$. These parameters align with the regulations set by local agencies to ensure the suitability of water for human consumption. Notably, all parameters were successfully met, thereby reinforcing the significant role of ultrafiltration membranes in providing a reliable and safe water supply.

5.4 Final considerations

Comparing bench and pilot scale studies is crucial while proposing reinforcements of drinking water treatment plants. In the current study, the in-line dose defined on a bench scale was validated when the process was scaled-up to a more representative system that is closer to the full-scale production process. The additional dose of FeCl3 contributed to higher removal rates of turbidity, color, metals (aluminum, iron, and manganese), and arsenic by ultrafiltration, without necessarily contributing to membrane fouling. The increase in floc size observed in the pilot scale when the coagulant was added could have favored the formation of a more porous and permeable fouling layer, reducing its impact on the permeate flux. Future studies should complement the impact of natural organic matter on the ultrafiltration membranes on a pilot scale. In addition to arsenic, it is recommended the monitoring other species that exceeded the threshold values after sand filtration in pilot-scale experiments, such as manganese. Although they tended to be removed, the bench

scale results suggested their potential to build up along the treatment process, especially in cases where the ultrafiltration concentrate is recycled back to the initial processes of the water treatment plant. In any case, the ultrafiltration membrane demonstrated an effective alternative to reinforce water treatment plants and guarantee water safety under critical water quality conditions.

6 CHAPTER 6: GENERAL CONCLUSIONS

The urgent issue of arsenic in water, with concentrations exceeding the WHO's recommended limit of 10 µg/L, poses a noteworthy health risk. Many regions lack the resources for adequate monitoring and treatment. Addressing this issue, a comprehensive survey of arsenic levels in water sources across Latin American countries was conducted, along with a risk assessment. This survey was done to enhance comprehension of the implications of arsenic contamination in these natural water sources. The findings are as follows:

- Arsenic was often detected in surface and groundwater concentrations above 10 µg/L in Latin American countries. Waters considered potable also presented higher concentrations of arsenic.
- Although the problems related to arsenic in water in some places, such as Argentina and Chile, are well known, little investigation has been conducted in other Latin American countries, raising doubts about the risks related to arsenic in water.
- In the worst scenario considered, if directly consumed, most waters offer non-carcinogenic risks (HQ>1), and median carcinogenic risk values were classified as unacceptable. It is crucial that the monitoring and treatment of water containing arsenic be effective.
- Many places in Latin America face challenges such as the availability of qualified labor, resource limitations, and logistical difficulties, which may render effective monitoring and treatment unfeasible.
- Tests that are easy to perform, do not require expensive equipment, and can be used in situ, such as colorimetric methods, should be adopted. These methods are not intended to replace tests performed to verify compliance with legislation, but they can enable frequent monitoring in diverse locations.

Furthermore, among the techniques capable of effectively removing arsenic from water, membrane separation processes stand out as promising solutions to be adopted by communities, from small to large ones. Larger communities can integrate membrane systems as a polishing step for WTPs already in operation. Therefore, the coupling of ultrafiltration and reverse osmosis (UF-RO) membranes, on a pilot-scale,

to a conventional WTP was evaluated with a focus on arsenic removal. The main conclusions of this study were:

- The pilot-scale UF-RO membrane system generated high-quality water when treating surface water with or without the treatment previously applied in the WTP. RO was essential to guarantee safe water with arsenic concentrations below 0.5 µg/L and compliance with potability standards.
- The treatment applied in the WTP increased the membrane permeability.
- When evaluating the possibility of integrating UF-RO into a WTP, it is suggested that the UF concentrate be recirculated at the beginning of conventional treatment, and the RO concentrate could be disposed of safely. Thus, concentrate management costs would be minimal.
- The UF-RO system increased the resilience of the real WTP, effectively contributing to the high-quality water supplied to the population.
- If a WTP of the dimensions of this study adopts the UF-RO system under the conditions evaluated, the OpEX of the membrane system would be equivalent to 29.8% of the total OpEX (conventional treatment + UF-RO). The OpEX of RO is equivalent to 17.8% of the total. The factor that contributes most to operational costs is membrane replacement. The adoption of the blend strategy can greatly reduce CapEX.
- In the case of the UF-RO system operating without pretreatment, the OpEX ranged from 0.47-0.49 US$/m^3 for communities with 1,500 to 540,000 inhabitants. Considering the quality of the permeate produced, this is a competitive and attractive alternative for smaller and larger communities.

Given the performance of the UF-RO system, a long-term operation was carried out, totaling more than 2000 hours of operation. Long-term operations on a pilot scale system are an essential step in enabling the implementation of a full-scale system. In UF, the main objective was to evaluate the influence of operational aspects on the system performance. In RO, the operating conditions of the different membrane modules were evaluated. The main conclusions were:

- The UF membrane had a higher permeability when it was operated in the Full Drain mode and a J_{DBW}/J_{ABW} ratio of 0.91 was applied. Feed turbidity had a great impact on membrane permeability.
- With turbidity, temperature, and J_{DBW}/J_{ABW} ratio values as input, a model that can predict membrane permeability with 84.4% accuracy was developed.
- Comparing UF permeates generated during Feed and Bleed and Full Drain modes of operation, it was observed that there was a significant difference regarding color and turbidity, with the highest values in the permeates generated during the Feed and Bleed mode. However, the potability standards were consistently met for these parameters, as well as for manganese (<0.028 mg/L) and iron (<0.086 mg/L). However, arsenic concentration averaged 8-30 µg/L, reinforcing the need for RO application.
- The operating mode can impact concentrate management.
- Regarding RO, all permeates met the potability standards, with arsenic concentrations < 0.5 µg/L. There was no difference in the permeates regarding color, iron, manganese, and arsenic when comparing the operating conditions of the different modules. All RO concentrates generated can be safely disposed of in surface water.

Finally, as membrane manufacturers suggest dosing the coagulant at the UF inlet, it was decided to investigate whether an in-line coagulant dose could improve the UF performance of the system in the present study, for example, by increasing arsenic removal. The main conclusions of this stage were:

- The in-line dosage of $FeCl_3$ contributed to higher removal rates of turbidity, color, aluminum, iron, manganese, and arsenic by ultrafiltration.
- The UF permeate obtained on the pilot scale system achieved all potable standards.
- When the coagulant was added, greater particle size was obtained, leading to a fouling layer that was more porous and permeable.
- Concentrate recirculation to the beginning of the WTP did not affect its overall performance.

Therefore, dosing in-line coagulant ($FeCl_3$) in the ultrafiltration feed is another alternative for As removal that can provide water with arsenic concentration lower than 10 µg/L for UF feeds with up to approximately 23 µg/L of As. In this scenario, it is advantageous to adopt this alternative since it is a process with low energy demand. It is worth mentioning that it is not an alternative that has the robustness of the UF-RO process, so it would be necessary to reinforce monitoring As concentration in permeate. In fact, RO is a robust process that will ensure high arsenic removal even when there are variations in the feed, such as higher arsenic concentrations or turbidity, which are known to affect coagulation performance. These variations may happen due to factors such as the rainy season.

On the other hand, with higher As concentrations in the feed, the application of RO is necessary, as even with the in-line coagulant dosage in UF, a permeate considered safe for consumption will not be obtained. Furthermore, arsenic concentrations in RO permeate were lower than 0.5 µg/L, which can enable (i) the formulation of blends, in order to meet the limit of 10 µg/L, (ii) meet WHO advice to keep arsenic levels as low as possible. In fact, several countries have already adopted lower maximum arsenic values in their legislation, and the application of the RO can guarantee compliance with stricter legislation. In addition to health and environmental benefits, economic benefits offset the costs of implementing and operating technologies such as the UF-RO system.

Based on all of the above, the thesis objective was achieved, and the efficiency of treating water with high concentrations of arsenic using a UF-RO system on a pilot scale can be confirmed. In a broader context, the results are expected to further contribute to ensuring water safety, mainly when supplied for human consumption, and to achieving UN Sustainable Development Goal 6: ensuring the availability and sustainable management of water and sanitation for all.

REFERENCES

Abdul, K.S.M., Jayasinghe, S.S., Chandana, E.P., Jayasumana, C., De Silva, P.M.C., 2015. Arsenic and human health effects: A review. Environmental toxicology and pharmacology, 40, 828-846. https://doi.org/10.1016/j.etap.2015.09.016

Abejón, A., Garea, A., Irabien, A., 2015. Arsenic removal from drinking water by reverse osmosis: Minimization of costs and energy consumption, Sep Purif Technol 144, 46–53. https://doi.org/10.1016/j.seppur.2015.02.017.

Alarcón-Herrera, M.T., Martin-Alarcon, D.A., Gutiérrez, M., Reynoso-Cuevas, L., Martín-Domínguez, A., Olmos-Márquez, M.A., Bundschuh, J., 2020. Co-occurrence, possible origin, and health-risk assessment of arsenic and fluoride in drinking water sources in Mexico: Geographical data visualization. Science of The Total Environment 698, 134168. https://doi.org/10.1016/j.scitotenv.2019.134168

Albrektienė, R., Rimeika, M., Zalieckienė, E., Šaulys, V., Zagorskis, A., 2012. Determination of organic matter by uv absorption in the ground water / organinių medžiagų požeminiame vandenyje nustatymas taikant uv bangų absorbciją, Journal of Environmental Engineering and Landscape Management 20, 163–167. https://doi.org/10.3846/16486897.2012.674039.

Alonso, D.L., Latorre, S., Castillo, E., Brandão, P.F.B., 2014. Environmental occurrence of arsenic in Colombia: A review. Environmental Pollution 186, 272–281. https://doi.org/10.1016/j.envpol.2013.12.009

Amaral, M.C.S., Grossi, L.B., Ramos, R.L., Ricci, B.C., Andrade, L.H., 2018. Integrated UF–NF–RO route for gold mining effluent treatment: From bench-scale to pilot-scale. Desalination 440, 111–121. https://doi.org/10.1016/j.desal.2018.02.030

APHA, A.P.H.A., 2019. Standard Methods for the Examination of Water and Wastewater.

Armienta, M.A., Segovia, N., 2008. Arsenic and fluoride in the groundwater of Mexico. Environ Geochem Health 30, 345–353. https://doi.org/10.1007/s10653-008-9167-8

Ayers, R.S., Westcot, D.W., 1994. Water quality for agriculture.

Ayerza, A., 1917. Arsenicismo regional endemico. Bol Acad Nac Med de Buenos Aires, 11-24.

Barbot, E., Moustier, S., Bottero, J., Moulin, P., 2008. Coagulation and ultrafiltration: Understanding of the key parameters of the hybrid process, J Memb Sci 325, 520–527. https://doi.org/10.1016/j.memsci.2008.07.054.

Bidone, E., Cesar, R., Santos, M.C., Sierpe, R., Silva-Filho, E.V., Kutter, V., Dias da Silva, L.I., Castilhos, Z., 2018. Mass balance of arsenic fluxes in rivers impacted by gold mining activities in Paracatu (Minas Gerais State, Brazil), Environmental Science and Pollution Research 25, 9085–9100. https://doi.org/10.1007/s11356-018-1215-z.

Borba, R.P., Figueiredo, B.R., Rawlins, B., Matschullat, J., 2003. Geochemical distribution of arsenic in waters, sediments and weathered gold mineralized rocks from Iron Quadrangle, Brazil. Environmental Geology 44, 39–52. https://doi.org/10.1007/s00254-002-0733-6

Brandhuber, P., Amy, G., 2001. Arsenic removal by a charged ultrafiltration membrane — influences of membrane operating conditions and water quality on arsenic rejection, Desalination 140, 1–14. https://doi.org/10.1016/S0011-9164(01)00350-2.

Brandt, M.J., Johnson, K.M., Elphinston, A.J., Ratnayaka D.D., 2017. Twort's Water Supply, Elsevier, pp. 367-406

Bratby, J. Coagulation and flocculation with emphasis on water and wastewater treatment IWA Publishing (2006)

Brazil, Ministério da Saúde, Portaria GM/MS n° 888, Brazil, 2021. https://www.in.gov.br/en/web/dou/-/portaria-gm/ms-n-888-de-4-de-maio-de-2021-318461562.

Bundschuh, J., Litter, M.I., Parvez, F., Román-Ross, G., Nicolli, H.B., Jean, J.-S., Liu, C.-W., López, D., Armienta, M.A., Guilherme, L.R.G., Cuevas, A.G., Cornejo, L., Cumbal, L., Toujaguez, R., 2012. One century of arsenic exposure in Latin America: A

review of history and occurrence from 14 countries. Science of The Total Environment 429, 2–35. https://doi.org/10.1016/j.scitotenv.2011.06.024

Cano, G., Moulin, P., 2022. Treatment of Boiler Condensate by Ultrafiltration for Reuse, Membranes (Basel) 12, 1285. https://doi.org/10.3390/membranes12121285.

Chang, H., Zhu, Y., Yu, H., Qu, F., Zhou, Z., Li, X., Yang, Y., Tang, X., Liang, H., 2022. Long-term operation of ultrafiltration membrane in full-scale drinking water treatment plants in China: Characteristics of membrane performance, Desalination 543, 116122. https://doi.org/10.1016/j.desal.2022.116122.

Cheng, H.-H., Chen, S.-S., Yang, S.-R., 2009. In-line coagulation/ultrafiltration for silica removal from brackish water as RO membrane pretreatment Sep Purif Technol., 70, pp. 112-117, 10.1016/j.seppur.2009.09.001.

Costa, A.R., de Pinho, Elimelech M., 2006. Mechanisms of colloidal natural organic matter fouling in ultrafiltration J. Memb. Sci., 281, pp. 716-725, 10.1016/j.memsci.2006.04.044

Costa, F.C.R., Ricci, B.C., Teodoro, B., Koch, K., Drewes, J.E., Amaral, M.C.S., 2021. Biofouling in membrane distillation applications - a review, Desalination 516, 115241. https://doi.org/10.1016/j.desal.2021.115241.

Couto, C.F., Lange, L.C., Amaral M.C.S., 2019. Occurrence, fate and removal of pharmaceutically active compounds (PhACs) in water and wastewater treatment plants—a review J. Water Process Eng., 32, Article 100927, 10.1016/j.jwpe.2019.100927

De C. Silva, D., Bellato, C.R., De O. Marques Neto, J., Fontes, M.P.F., 2018. Arsenic and trace metals in water and sediment of the velhas river, southeastern iron quadrangle region, minas gerais, BRAZIL. Quim Nova 41, 1011–1018. https://doi.org/10.21577/0100-4042.20170275

de Figueiredo, B.R., Borba, R.P., Angélica, R.S., 2007. Arsenic occurrence in Brazil and human exposure. Environ Geochem Health 29, 109–118. https://doi.org/10.1007/s10653-006-9074-9

de Souza, A.C.M., de Almeida, M.G., Pestana, I.A., de Souza, C.M.M., 2019. Arsenic Exposure and Effects in Humans: A Mini-Review in Brazil. Arch Environ Contam Toxicol 76, 357–365. https://doi.org/10.1007/s00244-018-00586-6

Dhar, R.K., Zheng, Y., Rubenstone, J., van Geen, A., 2004. A rapid colorimetric method for measuring arsenic concentrations in groundwater. Anal Chim Acta 526, 203–209. https://doi.org/10.1016/j.aca.2004.09.045

Diaz, O., Arcos, R., Tapia, Y., Pastene, R., Velez, D., Devesa, V., Montoro, R., Aguilera, V., Becerra, M., 2015. Estimation of Arsenic Intake from Drinking Water and Food (Raw and Cooked) in a Rural Village of Northern Chile. Urine as a Biomarker of Recent Exposure. Int J Environ Res Public Health 12, 5614–5633. https://doi.org/10.3390/ijerph120505614

Foureaux, A.F.S., Lebron, Y.A.R., Moreira, V.R., Grossi, L.B., Santos, L.V.S., Amaral, M.C.S., 2020. Technical and economic potential of high-temperature NF and DCMD for gold mining effluent reclamation. Chemical Engineering Research and Design 162, 149–161. https://doi.org/10.1016/j.cherd.2020.08.003

Frisbie, S. H., Mitchell, E. J., 2022. Arsenic in drinking water: An analysis of global drinking water regulations and recommendations for updates to protect public health. PLoS One, 17(4), e0263505. https://doi.org/10.1371/journal.pone.0263505

George, C.M., Sima, L., Arias, M.H.J., Mihalic, J., Cabrera, L.Z., Danz, D., Checkley, W., Gilman, R.H., 2014. Arsenic exposure in drinking water: an unrecognized health threat in Peru. Bull World Health Organ 92, 565–572. https://doi.org/10.2471/BLT.13.128496

Gibbon-Walsh, K., Salaün, P., Uroic, M.K., Feldmann, J., McArthur, J.M., van den Berg, C.M.G., 2011. Voltammetric determination of arsenic in high iron and manganese groundwaters. Talanta 85, 1404–1411. https://doi.org/10.1016/j.talanta.2011.06.038

Glade, S., Bandaru, S.R., Nahata, M., Majmudar, J., Gadgil, A., 2021. Adapting a drinking water treatment technology for arsenic removal to the context of a small, low-

income California community. Water Res 204. https://doi.org/10.1016/j.watres.2021.117595

Guigui, C., Rouch, J.C., Durand-Bourlier, L., Bonnelye, V., Aptel, P., 2002. Impact of coagulation conditions on the in-line coagulation/UF process for drinking water production Desalination, 147, 95-100, 10.1016/S0011-9164(02)00582-9

Guimarães, R.N., Moreira, V.R., Amaral, M.C.S., 2022. Membrane technology as an emergency response against drinking water shortage in scenarios of dam failure. Chemosphere 309, 136618. https://doi.org/10.1016/j.chemosphere.2022.136618

Gul, A., Hruza, J., Yalcinkaya, F., 2021. Fouling and chemical cleaning of microfiltration membranes: a mini-review Polymers (Basel)., 13, 846, 10.3390/polym13060846

He, Y., Zheng, Y., Ramnaraine, M., Locke, D.C., 2004. Differential pulse cathodic stripping voltammetric speciation of trace level inorganic arsenic compounds in natural water samples. Anal Chim Acta 511, 55–61. https://doi.org/10.1016/j.aca.2004.01.036

Hering, J.G., Chen, P.-Y., Wilkie, J.A., Elimelech, M., 1997. Arsenic Removal from Drinking Water during Coagulation. Journal of Environmental Engineering 123, 800–807. https://doi.org/10.1061/(ASCE)0733-9372(1997)123:8(800)

Hering, J.G., Chen, P.-Y., Wilkie, J.A., Elimelech, M., Liang, S., 1996. Arsenic removal by ferric chloride. J Am Water Works Assoc 88, 155–167. https://doi.org/10.1002/j.1551-8833.1996.tb06541.x

Howe, K.J., Clark, M.M., 2002. Fouling of microfiltration and ultrafiltration membranes by natural waters Environ. Sci. Technol., 36, 3571-3576, 10.1021/es025587r

Hsieh, L.-H.C., Weng, Y.-H., Huang, C.-P., Li, K.-C., 2008. Removal of arsenic from groundwater by electro-ultrafiltration, Desalination 234, 402–408. https://doi.org/10.1016/j.desal.2007.09.110.

Huang, H., Schwab, K., Jacangelo, J.G., 2009. Pretreatment for Low Pressure Membranes in Water Treatment: A Review, Environ Sci Technol 43, 3011–3019. https://doi.org/10.1021/es802473r.

IGAM, Séries históricas de monitoramento da qualidade das águas superficiais no estado de Minas Gerais (3° TRIM e 4° TRIM - 2022) (Historical series of surface water quality monitoring in the state of Minas Gerais (3rd TRIM and 4th TRIM - 2022)), (2022). http://repositorioigam.meioambiente.mg.gov.br/handle/123456789/4302.

IGAM, Séries históricas de monitoramento da qualidade das águas superficiais no estado de Minas Gerais (1° TRIM e 2° TRIM - 2023) (Historical series of surface water quality monitoring in the state of Minas Gerais (3rd TRIM and 4th TRIM - 2022)), (2023). http://repositorioigam.meioambiente.mg.gov.br/handle/123456789/4302.

IRIS, I.R.I.S., 1991a. Arsenic, inorganic; CASRN 7440-38-2.

Jacquet, N., Wurtzer, S., Darracq, G., Wyart, Y., Moulin, L., Moulin P., 2021. Effect of concentration on virus removal for ultrafiltration membrane in drinking water production J Memb Sci., 634, 119417, 10.1016/j.memsci.2021.119417

Kabir, F., Chowdhury, S., 2017. Arsenic removal methods for drinking water in the developing countries: technological developments and research needs. Environmental Science and Pollution Research 24, 24102–24120. https://doi.org/10.1007/s11356-017-0240-7

Kearns, J.K., Edson, C.B., 2018. Expanding Quantification of Arsenic in Water to 0 µg L−1 with a Field Test Kit: Substituting 0.4% M/V Silver Nitrate as the Colorimetric Reagent; Employing Digital Image Analysis. Water Air Soil Pollut 229, 75. https://doi.org/10.1007/s11270-018-3717-1

Krause, E., Ettel, V.A., 1989. Solubilities and stabilities of ferric arsenate compounds. Hydrometallurgy 22, 311–337. https://doi.org/10.1016/0304-386X(89)90028-5

Kumar, A., Kumar, V., Pandita, S., Singh, S., Bhardwaj, R., Varol, M., Rodrigo-Comino, J., 2023. A global meta-analysis of toxic metals in continental surface water bodies. Journal of Environmental Chemical Engineering, 109964. https://doi.org/10.1016/j.jece.2023.109964

Kumar, R., Patel, M., Singh, P., Bundschuh, J., Pittman, C.U., Trakal, L., Mohan, D., 2019. Emerging technologies for arsenic removal from drinking water in rural and peri-

urban areas: Methods, experience from, and options for Latin America. Science of The Total Environment 694, 133427. https://doi.org/10.1016/j.scitotenv.2019.07.233

Kumar, R., Rauwel, P., Kriipsalu, M., Rauwel, E., 2022. A colorimetric method of As 3+ ion detection and quantification using hand-held Lovibond photometers. J Phys Conf Ser 2315, 012031. https://doi.org/10.1088/1742-6596/2315/1/012031

Kundu, S., Ghosh, S.K., Mandal, M., Pal, T., Pal, A., 2002. Spectrophotometric determination of arsenic via arsine generation and in-situ colour bleaching of methylene blue (MB) in micellar medium. Talanta 58, 935–942. https://doi.org/10.1016/S0039-9140(02)00434-4

Lebron, Y.A.R., Moreira, V.R., da Costa, P.R., Alkmin, A.R., de França Neta, L.S., Cerqueira, A.C., Amaral, M.C.S., 2021. Chemical cleaning procedures on permeability recovery and lifespan of MBR membranes treating petroleum refinery wastewater: from bench- to pilot-scale applications J. Water Process. Eng., 44, Article 102411, 10.1016/j.jwpe.2021.102411

Leupin, O.X., Hug, S.J., 2005. Oxidation and removal of arsenic (III) from aerated groundwater by filtration through sand and zero-valent iron. Water Res 39, 1729–1740. https://doi.org/10.1016/j.watres.2005.02.012

Li, J, Jiao, S., Zhong, L., Pan, J., Ma Q., 2013. Optimizing coagulation and flocculation process for kaolinite suspension with chitosan Colloids Surf. A Physicochem. Eng. Asp., 428, 100-110, 10.1016/j.colsurfa.2013.03.034

Li, L., Wang, Y., Zhang, W., Yu, S., Wang, X., Gao, N., 2020. New advances in fluorescence excitation-emission matrix spectroscopy for the characterization of dissolved organic matter in drinking water treatment: a review Chem. Eng. J., 381, 122676, 10.1016/j.cej.2019.122676

Litter, M.I., Ingallinella, A.M., Olmos, V., Savio, M., Difeo, G., Botto, L., Farfán Torres, E.M., Taylor, S., Frangie, S., Herkovits, J., Schalamuk, I., González, M.J., Berardozzi, E., García Einschlag, F.S., Bhattacharya, P., Ahmad, A., 2019. Arsenic in Argentina:

Occurrence, human health, legislation and determination. Science of The Total Environment 676, 756–766. https://doi.org/10.1016/j.scitotenv.2019.04.262

Lu, T.H., Su, C.C., Chen, Y.W., Yang, C.Y., Wu, C.C., Hung, D.Z., Chen, C.H., Cheng, P.W., Liu, S.H., Huang, C.F., 2011. Arsenic induces pancreatic β-cell apoptosis via the oxidative stress-regulated mitochondria-dependent and endoplasmic reticulum stress-triggered signaling pathways. Toxicology letters, 201, 15-26. https://doi.org/10.1016/j.toxlet.2010.11.019

Ma, B., Xue, W., Hu, C., Liu, H., Qu, J., Li, L., 2019. Characteristics of microplastic removal via coagulation and ultrafiltration during drinking water treatment Chem. Eng. J., 359, 159-167, 10.1016/j.cej.2018.11.155

Malkoske, T.A., Bérubé, P.R., Andrews, R.C., 2020. Coagulation/flocculation prior to low pressure membranes in drinking water treatment: a review, Environ Sci (Camb) 6, 2993–3023. https://doi.org/10.1039/D0EW00461H.

Marcillo, C.E., García Prado, G., Copeland, N., Krometis, L.H., 2020. Drinking water quality and consumer perceptions at the point-of-use in San Rafael Las Flores, Guatemala. Water Pract Technol 15, 374–385. https://doi.org/10.2166/wpt.2020.025

Matilainen, A., Vepsäläinen, M., Sillanpää, M., 2010. Natural organic matter removal by coagulation during drinking water treatment: a review Adv. Colloid Interface Sci., 159, 189-197, 10.1016/j.cis.2010.06.007

Mohan, D., Pittman, C.U., 2007. Arsenic removal from water/wastewater using adsorbents—A critical review. J Hazard Mater 142, 1–53. https://doi.org/10.1016/j.jhazmat.2007.01.006

Moreira, V.R., Costa, F.C.R., Moser, P.B., Guimarães, R.N., Santos, L.V.S., de Paula, E.C., Amaral, M.C.S., 2023a. Ultrafiltration with in-line coagulation (FeCl3) to enhance arsenic removal and improve drinking water quality: From bench to pilot-scale. Chemical Engineering Journal 472, 145063. https://doi.org/10.1016/j.cej.2023.145063

Moreira, V.R., Guimarães, R.N., Moser, P.B., Santos, L.V.S., de Paula, E.C., Lebron, Y.A.R., Silva, A.F.R., Casella, G.S., Amaral, M.C.S., 2023b. Restrictions in water

treatment by conventional processes (coagulation, flocculation, and sand-filtration) following scenarios of dam failure. Journal of Water Process Engineering 51, 103450. https://doi.org/10.1016/j.jwpe.2022.103450

Moreira, V.R., Lebron, Y.A.R., de Paula, E.C., Santos, L.V. de S., Amaral, M.C.S., 2021a. Recycled reverse osmosis membrane combined with pre-oxidation for improved arsenic removal from high turbidity waters and retrofit of conventional drinking water treatment process. J Clean Prod 312, 127859. https://doi.org/10.1016/j.jclepro.2021.127859

Moreira, V.R., Lebron, Y.A.R., Lange, L.C., Santos, L.V.de S., 2019. Simultaneous biosorption of Cd(II), Ni(II) and Pb(II) onto a brown macroalgae Fucus vesiculosus: Mono- and multi-component isotherms, kinetics and thermodynamics. J Environ Manage 251, 109587. https://doi.org/10.1016/j.jenvman.2019.109587

Moreira, V.R., Lebron, Y.A.R., Santos, L.V. de S., Amaral, M.C.S., 2022. Low-cost recycled end-of-life reverse osmosis membranes for water treatment at the point-of-use. J Clean Prod 362, 132495. https://doi.org/10.1016/j.jclepro.2022.132495

Moreira, V.R., Lebron, Y.A.R., Santos, L.V. de S., Amaral, M.C.S., 2021b. Dead-end ultrafiltration as a cost-effective strategy for improving arsenic removal from high turbidity waters in conventional drinking water facilities. Chemical Engineering Journal 417, 128132. https://doi.org/10.1016/j.cej.2020.128132

Moreira, V.R., Lebron, Y.A.R. , Santos, L.V.S., de Paula, E.C., Amaral, M.C.S., 2021. Arsenic contamination, effects and remediation techniques: a special look onto membrane separation processes Process Saf. Environ. Prot., 148, 604-623, 10.1016/j.psep.2020.11.033

Motalebizadeh, A., Bagheri, H., Asiaei, S., Fekrat, N., Afkhami, A., 2018. New portable smartphone-based PDMS microfluidic kit for the simultaneous colorimetric detection of arsenic and mercury. RSC Adv 8, 27091–27100. https://doi.org/10.1039/C8RA04006K

Namgung, U. K., Xia, Z., 2001. Arsenic induces apoptosis in rat cerebellar neurons via activation of JNK3 and p38 MAP kinases. Toxicology and applied pharmacology, 174(2), 130-138. https://doi.org/10.1006/taap.2001.9200

NCH-409/1, 2005. Norma Chilena Oficial NCH 409/1 of 2005: Agua potable - Parte 1 - Requisitos. Chile.

Nicolau, C., Reich, M., Lynne, B., 2014. Physico-chemical and environmental controls on siliceous sinter formation at the high-altitude El Tatio geothermal field, Chile. Journal of Volcanology and Geothermal Research 282, 60–76. https://doi.org/10.1016/j.jvolgeores.2014.06.012

Ning, R.Y., 2002. Arsenic removal by reverse osmosis, Desalination 143, 237–241. https://doi.org/10.1016/S0011-9164(02)00262-X.

Olmos, V., Antolini, L., Choque, D., Colussi, C., Luxardo, R., Martos y Mula, Ana; Quiroga, A.María., 2016. Exposure to arsenic in drinking water and association with cancer and CKD, genotoxicity and neurocognitive damage in Argentina. Portal Regional da BVS.

Parvez, F., Chen, Y., Yunus, M., Zaman, R.U., Ahmed, A., Islam, T., Maria, A., Rabiul, H., Vesna, S., Joseph, G., Ahsan, H., 2011. Associations of arsenic exposure with impaired lung function and mortality from diseases of the respiratory system: findings from the health effects of Arsenic Longitudinal Study (HEALS). Epidemiology, 22, S179. https://doi.org/10.1097/01.ede.0000392225.89379.73

Perkin-Elmer-Coorporation, 1996. Analytical methods for atomic absorption spectroscopy.

Pinto, C.C., Calazans, G.M., Oliveira, S.C., 2019. Assessment of spatial variations in the surface water quality of the Velhas River Basin, Brazil, using multivariate statistical analysis and nonparametric statistics. Environ Monit Assess 191, 164. https://doi.org/10.1007/s10661-019-7281-y

Pronk, W., Ding, A., Morgenroth, E., Derlon, N., Desmond, P., Burkhardt, M., Wu, B., Fane, A.G., 2019. Gravity-driven membrane filtration for water and wastewater

treatment: A review. Water Res 149, 553–565. https://doi.org/10.1016/j.watres.2018.11.062

Ramsay, L., Petersen, M.M., Hansen, B., Schullehner, J., van der Wens, P., Voutchkova, D., Kristiansen, S.M., 2021. Drinking Water Criteria for Arsenic in High-Income, Low-Dose Countries: The Effect of Legislation on Public Health. Environ Sci Technol 55, 3483–3493. https://doi.org/10.1021/acs.est.0c03974

Reis, B.G., Araújo, A.L.B., Amaral, M.C.S., Ferraz, H.C., 2018. Comparison of Nanofiltration and Direct Contact Membrane Distillation as an alternative for gold mining effluent reclamation. Chemical Engineering and Processing - Process Intensification 133, 24–33. https://doi.org/10.1016/j.cep.2018.08.020

Rockafellow-Baldoni, M., Spayd, S.E., Hong, J.-Y., Meng, Q., Ohman-Strickland, P., Robson, M.G., 2018. Arsenic exposure and cancer risk reduction with local ordinance requiring whole-house dual-tank water treatment systems. Human and Ecological Risk Assessment: An International Journal 24, 1256–1267. https://doi.org/10.1080/10807039.2017.1411779

Rodriguez, R., Armienta, M.A., Mejia Gómez, J.A., 2005. Arsenic contamination of the Salamanca aquifer system in Mexico: A risk analysis, Natural Arsenic in Groundwater: Occurrence, Remediation and Management - Proceedings of the Pre-Congress Workshop “Natural Arsenic in Groundwater (BWO 06)”, 32nd International Geological Congress. https://doi.org/10.1201/9780203970829-15

Ruffino, B., Campo, G., Crutchik, D., Reyes, A., Zanetti, M., 2022. Drinking Water Supply in the Region of Antofagasta (Chile): A Challenge between Past, Present and Future. Int J Environ Res Public Health 19, 14406. https://doi.org/10.3390/ijerph192114406

Salaün, P., Gibbon-Walsh, K.B., Alves, G.M.S., Soares, H.M.V.M., van den Berg, C.M.G., 2012. Determination of arsenic and antimony in seawater by voltammetric and chronopotentiometric stripping using a vibrated gold microwire electrode. Anal Chim Acta 746, 53–62. https://doi.org/10.1016/j.aca.2012.08.013

Sanyal, K., Chappa, S., Bahadur, J., Pandey, Ashok.K., Mishra, N.L., 2020. Arsenic quantification and speciation at trace levels in natural water samples by total reflection X-ray fluorescence after pre-concentration with N -methyl- d -glucamine functionalized quartz supports. J Anal At Spectrom 35, 2770–2778. https://doi.org/10.1039/D0JA00385A

S., Sen-Kavurmaci, Birben, N.C., Tomruk, A., Bekbolet, M., 2016. Characterization of organic matter in natural waters by EEM fluorescence properties, desalination Water Treat., 57, 2428-2436, 10.1080/19443994.2015.1022804

Sharp, E.L., Parsons, S.A., Jefferson, B., 2006. Seasonal variations in natural organic matter and its impact on coagulation in water treatment Sci. Total Environ., 363, 183-194, 10.1016/j.scitotenv.2005.05.032

Shen, X., Gao, B., Guo, K., Yue Q., 2020. Characterization and influence of floc under different coagulation systems on ultrafiltration membrane fouling Chemosphere, 238, 124659, 10.1016/j.chemosphere.2019.124659

Sidhu, M., Mahajan, P., Bhatt, S.M., 2014. Highly sensitive & low cost colorimetric method for quantifying arsenic metal in drinking water of Malwa Punjab and comparison with ICAP-AES. Ann Biol Res 5, 105–109.

Siéliéchi, J.-M., Lartiges, B.S., Kayem, G.J., Hupont, S., Frochot, C., Thieme, J., Ghanbaja, J., d'Espinose de la Caillerie, J.B., Barrès, O., Kamga, R., Levitz, P., Michot L.J., 2008. Changes in humic acid conformation during coagulation with ferric chloride: implications for drinking water treatment Water Res., 42, 2111-2123, 10.1016/j.watres.2007.11.017

Skoog, D.A., West, D.M., Holler, F.J., 2013. Fundamentals of analytical chemistry. https://doi.org/10.1016/b978-0-323-85208-1.00006-1

Smith, A.H., Hopenhayn-Rich, C., Bates, M.N., Goeden, H.M., Hertz-Picciotto, I., Duggan, H.M., Wood, R., Kosnett, M.J., Smith, M.T., 1992. Cancer risks from arsenic in drinking water. Environ Health Perspect 97, 259–267. https://doi.org/10.1289/ehp.9297259

Stocker, J., Balluch, D., Gsell, M., Harms, H., Feliciano, J., Daunert, S., Malik, K.A., van der Meer, J.R., 2003. Development of a Set of Simple Bacterial Biosensors for Quantitative and Rapid Measurements of Arsenite and Arsenate in Potable Water. Environ Sci Technol 37, 4743–4750. https://doi.org/10.1021/es034258b

Tapia, J., Mukherjee, A., Rodríguez, M.P., Murray, J., Bhattacharya, P., 2022. Role of tectonics and climate on elevated arsenic in fluvial systems: Insights from surface water and sediments along regional transects of Chile. Environmental Pollution 314, 120151. https://doi.org/10.1016/j.envpol.2022.120151

Tapia, J., Murray, J., Ormachea, M., Tirado, N., Nordstrom, D.K., 2019. Origin, distribution, and geochemistry of arsenic in the Altiplano-Puna plateau of Argentina, Bolivia, Chile, and Perú. Science of The Total Environment 678, 309–325. https://doi.org/10.1016/j.scitotenv.2019.04.084

Tapia, J., Schneider, B., Inostroza, M., Álvarez-Amado, F., Luque, J.A., Aguilera, F., Parra, S., Bravo, M., 2021. Naturally elevated arsenic in the Altiplano-Puna, Chile and the link to recent (Mio-Pliocene to Quaternary) volcanic activity, high crustal thicknesses, and geological structures. J South Am Earth Sci 105, 102905. https://doi.org/10.1016/j.jsames.2020.102905

Teixeira, M.C., Santos, A.C., Fernandes, C.S., Ng, J.C., 2020. Arsenic contamination assessment in Brazil – Past, present and future concerns: A historical and critical review. Science of The Total Environment 730, 138217. https://doi.org/10.1016/j.scitotenv.2020.138217

Trindade, A.L.C., Almeida, K.C.d.B., Barbosa, P.E., Oliveira S.M.A.C., 2016. Tendências temporais e espaciais da qualidade das águas superficiais da sub-bacia do Rio das Velhas, estado de Minas Gerais Engenharia Sanitaria e Ambiental., 22 (1), 13-24.

Vahidnia, A., Van der Voet, G. B., De Wolff, F. A., 2007. Arsenic neurotoxicity—a review. Human & experimental toxicology, 26(10), 823-832. https://doi.org/10.1177/0960327107084539

Valente-Campos, S., Nascimento, E.D.S., Umbuzeiro, G.D.A., 2014. Water quality criteria for livestock watering – a comparison among different regulations. Acta Sci 36, 1. https://doi.org/10.4025/actascianimsci.v36i1.21853

Varejão, E.V.V., Bellato, C.R., Fontes, M.P.F., Mello, J.W.V., 2011. Arsenic and trace metals in river water and sediments from the southeast portion of the Iron Quadrangle, Brazil Environ. Monit Assess., 172, 631-642, 10.1007/s10661-010-1361-3

Varol, M. 2019. Arsenic and trace metals in a large reservoir: Seasonal and spatial variations, source identification and risk assessment for both residential and recreational users. Chemosphere, 228, 1-8. https://doi.org/10.1016/j.chemosphere.2019.04.126

Varol, M.; Tokatli, C., 2022. Seasonal variations of toxic metal (loid)s in groundwater collected from an intensive agricultural area in northwestern Turkey and associated health risk assessment. Environmental Research, 204, 111922, 2022. https://doi.org/10.1016/j.envres.2021.111922

Vries, D., Bertelkamp, C., Schoonenberg Kegel, F., Hofs, B., Dusseldorp, J., Bruins, J.H., de Vet, W., van den Akker, B., 2017. Iron and manganese removal: recent advances in modelling treatment efficiency by rapid sand filtration Water Res., 109, 35-45, 10.1016/j.watres.2016.11.032

Wang, J., Wang, X.C., 2006. Ultrafiltration with in-line coagulation for the removal of natural humic acid and membrane fouling mechanism J. Environ. Sci. (China)., 18, 880-884, 10.1016/S1001-0742(06)60008-9

WHO, Arsenic, metals, fibres and dust, 1st ed., Lyon, France, 2009. https://www.ncbi.nlm.nih.gov/books/NBK304375/pdf/Bookshelf_NBK304375.pdf.

WHO, 2001a. Arsenic and arsenic compounds. Genova.

WHO, 2001b. Arsenic and arsenic compounds. Genova.

WHO, Arsenic, Drinking-water and Health Risks Substitution in Arsenic Mitigation: a discussion paper, Geneva, 2003.https://cdn.who.int/media/docs/default-source/wash-documents/water-safety-and- quality/wsh03.06fulltext.pdf?sfvrsn=3e67a751_3.

WHO, Arsenic, Https://Www.Who.Int/News-Room/Fact-Sheets/Detail/Arsenic (2022).

WHO, W.H.O., 2011. Guidelines for Drinking-water Quality. Genebra. https://doi.org/10.1016/S1462-0758(00)00006-6

Xie, P., Chen, Y., Ma, J., Zhang, X., Zou, J., Wang, Z., 2016. A mini review of preoxidation to improve coagulation, Chemosphere 155, 550–563. https://doi.org/10.1016/j.chemosphere.2016.04.003.

Yang, H., Yan, Z., Du, X., Bai, L., Yu, H., Ding, A., Li, G., Liang, H., Aminabhavi T.M., 2020. Removal of manganese from groundwater in the ripened sand filtration: biological oxidation versus chemical auto-catalytic oxidation Chem. Eng. J., 382, 123033, 10.1016/j.cej.2019.123033

Yang, Q., Lau, C.H., Ge, Q., 2019. Novel Ionic Grafts That Enhance Arsenic Removal via Forward Osmosis, ACS Appl Mater Interfaces 11, 17828–17835. https://doi.org/10.1021/acsami.9b03991.

Yoon, J., Amy, G., Chung, J., Sohn, J., Yoon, Y., 2009. Removal of toxic ions (chromate, arsenate, and perchlorate) using reverse osmosis, nanofiltration, and ultrafiltration membranes, Chemosphere 77, 228–235. https://doi.org/10.1016/j.chemosphere.2009.07.028. .

Yu, H., Li, X., Chang, H., Zhou, Z., Zhang, T., Yang, Y., Li, G., Ji, H., Cai, C., Liang, H., 2020. Performance of hollow fiber ultrafiltration membrane in a full-scale drinking water treatment plant in China: a systematic evaluation during 7-year operation J. Memb. Sci., 613, 118469, 10.1016/j.memsci.2020.118469

Zhang, G., Liu, F., Liu, H., Qu, J., Liu, R., 2014. Respective role of fe and mn oxide contents for arsenic sorption in iron and manganese binary oxide: an x-ray absorption spectroscopy investigation Environ. Sci. Technol., 48, 10316-10322, 10.1021/es501527c

Zhang, Z., Xiao, C., Adeyeye, O., Yang, W., Liang, X., 2020. Source and Mobilization Mechanism of Iron, Manganese and Arsenic in Groundwater of Shuangliao City, Northeast China, Water (Basel) 12, 534. https://doi.org/10.3390/w12020534.

LIST OF PUBLICATIONS:

1. COSTA, F.C.R.; MOREIRA, V.R.; GUIMARÃES, R.N.; MOSER, P.B.; SANTOS, L.V.S.; DE PAULA, E.C.; AMARAL, M.C.S. Pre-oxidation and coagulation-flocculation as a pretreatment to UF-RO applied for surface water treatment and arsenic removal. **Desalination**, v. 586, p. 117855, 2024.
2. MOREIRA, V.R.; COSTA, F.C.R.; MOSER, P.B.; GUIMARÃES, R.N.; SANTOS, L.V.S.; DE PAULA, E.C.; AMARAL, M.C.S. Ultrafiltration with in-line coagulation (FeCl3) to enhance arsenic removal and improve drinking water quality: From bench to pilot-scale. **Chemical Engineering Journal**, v. 472, p. 145063, 2023.
3. COSTA, F.C.R.; MOREIRA, V.R.; GUIMARÃES, R.N.; MOSER, P.B.; AMARAL, M.C.S. Arsenic in natural waters of Latin-American countries: occurrence, risk assessment, low-cost methods, and technologies for remediation. **Process Safety And Environmental Protection**, v. 184, p. 116-128, 2023.

SUBMITTED PAPER:

1. COSTA, F.C.R.; MOREIRA, V.R.; GUIMARÃES, R.N.; MOSER, P.B.; SANTOS, L.V.S.; DE PAULA, E.C.; QUEIROZ, M.M.; OLIVEIRA, S.M.A.C.; AMARAL, M.C.S. Long-term performance of pilot scale UF-RO for arsenic removal from surface water: impact of operating conditions and machine learning prediction for membrane performance.

OTHER EXPERIENCES:

2. COSTA, F.C.R.; DOS SANTOS, C.R.; AMARAL, M.C.S. Trace organic contaminants removal by membrane distillation: a review on mechanisms, performance, applications, and challenges. **Chemical Engineering Journal**, v. 464, p. 142461, 2023.
3. AMARAL, M.C.S.; COSTA, F.C.R.; SANTOS, C.R. **Nanofiltration and Emerging and Trace Organic Contaminants Wastewater**. Nanofiltration for Sustainability. 1ed., p. 85-112, 2023.
4. FARIA, C. V.; COSTA, F.C.R.; JORGE, A.E.L.; MELO, A.L.P.; SILVA, U.C.M.; SANTOS, V.L.; AMARAL, M.C.S.; FONSECA, F.V. Effects of pharmaceuticals compounds and calcium on granulation, microbiology, and performance of anaerobic granular sludge systems. **Water Science and Technology**, v. 85, p. 3184-3195, 2022.

APPENDIX A

Table A1. Occurrence of arsenic in water resources in Latin American countries

Country	Location	Water matrix	As (µg/L)	Reference
Argentina	Península Valdés, Patagonia	Groundwater	10-400	(Alvarez and Carol, 2019)
	Chaco-Pampean	Groundwater	13-621	(Mariño et al., 2020)
	Patagonia	Surface water	<3-950	(Lamela et al., 2019)
	Buenos Aires	Groundwater	10.70-90.20	(Heredia and Cirelli, 2009)
	Cordoba province	Groundwater	<0.10-1800	(Francisca and Carro Perez, 2009)
	Southern Pampean plain	Groundwater	15.3-144	(Sosa et al., 2019)
	Tucumán Province	Groundwater	12.2-1660	(Nicolli et al., 2012b)
	Buenos Aires	Drinking water	37-76	(Vázquez et al., 2016)
	Rafaela	Groundwater	16-2000	(Siegfried et al., 2015)
	Santa Fé province	Groundwater	32.4-216.0	(Sigrist et al., 2011)
	Santa Fé province	Groundwater	0.009-1600	(Panigatti et al., 2014)
	Several areas	Drinking water supply from wells and from units of transportation and storage (aqueducts, cisterns, tanks, etc	0-1660	(Litter et al., 2019)
	Chaco province	Groundwater	0.7-1990	(Giménez et al., 2014)
	Chaco–Pampean Plain	Several water sources	51-850	(Pérez-Carrera and Fernández Cirelli, 2010)
	San Juan and La Pampa	Surface and Groundwater	3-1326	(O'Reilly et al., 2010)
	Northern Argentina	Surface and groundwater	0.5-250	(Concha et al., 2006)
	Salta Province	Drinking water	3.5-322	(Concha et al., 2010)
	Chaco-pampean plain	Groundwater	5.51-37	(Gomez et al., 2009)
	San Juan Province	Surface water	192.3-1437.9	(Funes Pinter et al., 2018)
	La Pampa Province	Groundwater	<4-5300	(Smedley et al., 2002)
	Bahía Blanca district	Surface and groundwater	7-302	(Paoloni et al., 2009)
	Santiago del Estero Province	Groundwater	2.0-4780	(Paoloni et al., 2009)
	Pampa Plain	Surface water	73-1134	(Rosso et al., 2011)
	Chaco-Pampean plain	Groundwater	<10-5300	(Nicolli et al., 2012a)
	Santiago del Estero Province	Groundwater	7.0-14969	(Bhattacharya et al., 2006)
	Eastern Tucuman Province	Groundwater	<5.0-1079	(García et al., 2007)
Bolivia	Central Bolivian Altiplano	Surface and Groundwater	0-623	(Muñoz et al., 2014)
	Cochabamba	Groundwater	<3-581	(Zhao and Guo, 2012)
	Central Bolivian Altiplano	Surface and groundwater	3.5-623	(Muñoz et al., 2014)

	El Molino, Tasapampa, Tuero Chico, Sotomayor and Cota communities	Surface water	0.9-12800	(Archer et al., 2005)
	Bolivian Altiplano	Groundwater	< 5.6–233.2	(Ormachea Muñoz et al., 2015)
	Central Andean highland	Surface and groundwater	< 10 - 1450	(García et al., 2005)
	Oruro department	Groundwater	< 1 - 964	(Van Den Bergh et al., 2010)
	Oruro department	Water from rainwater harvesting tanks	30-750	(Van Den Bergh et al., 2010)
	Cochabamba area	Groundwater	<3-582	(Quaghebeur et al., 2019)
Brazil	Minas Gerais state	Surface and groundwater	<0.8-2980	(Borba et al., 2003)
	Vitória Bay	Seawater	<5	(Vieira et al., 2021)
	Minas Gerais state	Surface water	0.5-29.1	(Bidone et al., 2018)
	Minas Gerais state	Surface water	15-400	(Moreira et al., 2021b)
	Minas Gerais state	Drinking water	<10	(Moreira et al., 2021a)
	Minas Gerais state	Drinking water	<5	(Guimarães et al., 2022)
	Minas Gerais state	Groundwater	1	(Moreira et al., 2022)
	Minas Gerais state	Surface water	57.7-414	(Costa et al., 2015)
	Minas Gerais state	Drinking water	<1	(Moreira et al., 2022)
	Minas Gerais state	Groundwater and spring water	<0.08-12.0	(Ferreira et al., 2017)
	Minas Gerais state	Surface and Groundwater	9-224	(Gonçalves et al., 2007)
	Mato Grosso state	Surface and groundwater	0.2-2337.5	(Viana et al., 2022)
	Patos lagoon estuary	Groundwater and Rainwater	1.23-35.6	(Mirlean and Roisenberg, 2006)
	Minas Gerais state	Surface water	<1-26.1	(Gontijo et al., 2016)
	Rio de Janeiro state	Groundwater	5->600	(Mirlean et al., 2014)
	São Paulo state	Groundwater	130-170	(Campos, 2002)
	Minas Gerais state	Surface water	36.7-68.3	(Varejão et al., 2011)
	Rio de Janeiro state	Groundwater	0.13-38.8	(Meneguelli-Souza et al., 2020)
	Minas Gerais state	Surface water	78.1-85.3	(De C. Silva et al., 2018)
Chile	Antofagasta	Drinking water supply	10-1240	(Ruffino et al., 2022)
	The Second Region of Chile	Surface and geothermal water	1400	(Romero et al., 2003)
	Northern Chile	Surface water	30-2600	(Guerra et al., 2016)
	Northern Chile	Acidic saline lake	0.00-23974.91	(Escudero et al., 2013)
	El Tatio geothermal field	Thermal Waters	16000-32000	(Nicolau et al., 2014)
	Several areas	Surface water	150-2500	(Pérez-Carrera and Fernández Cirelli, 2010)

	Northern, central and southern Chile	Surface water	0.2-8795	(Tapia et al., 2022)
	Arica and Parinacota region	Several water sources	<1-21300	(Pincetti-Zúniga et al., 2022)
	Atacama desert	Groundwater	2.8-278	(Leybourne and Cameron, 2008)
	Altiplano-Puna	Saline and brackish water	7-24800	(Tapia et al., 2022)
	Agricultural village of Socaire	Drinking water	247-357	(Diaz et al., 2015)
	Antofagasta region	Surface water	0.01-3	(Queirolo, 2000)
Colombia	Santurbán paramo	Surface water	0.6-52.3	(Alonso et al., 2020)
	Marmato	Surface warer	0.4-3521	(Torrance et al., 2021)
	Chinú and Corozal cities	Drinking water	1.76-2.19	(Vesga Ferreira et al., 2015)
Costa Rica	Northwest Costa Rica	Groundwater	20-80	(Zimmerman et al., 2021)
	San José	Groundwater	40.1	(Kunz et al., 2018)
	Cartago	Surface water	<10	(Montero Campos et al., 2010)
	Alajuela Province	Drinking water	>10	(Aguilar et al., 2019)
	Bagaces and Los Chiles districts	Groundwater	16-43.6	(Arias-Barrantes et al., 2018)
Cuba	Mine of Santa Lucia, in western Cuba	Surface water	4.0-24	(Romero et al., 2010)
Ecuador	Guayas and Los Ríos provinces	Surface and groundwater	0.49-5.84	(Otero et al., 2016)
	North-central Andean region	Geothermal sources	2-969	(Cumbal et al., 2010)
	Southeast Ecuador	Surface and groundwater	16-135	(Villa-Achupallas et al., 2018)
	Quito, Ibarra and Guayaquil	Sources for drinking water	<9.67	(Cipriani-Avila et al., 2020)
	Cuenca and Azogues cities	Surface and groundwater	0.0-28.04	(Pauta-Calle et al., 2021)
El Salvador	Central El Salvador	Surface water	150-770	(Bundschuh et al., 2008)
Guatemala	Guatemala city	Tap water	0.3-29.3	(Hoponick Redmon et al., 2022)
	Chimaltenango	Groundwater	<0.40-49.0	(Lotter et al., 2014)
	Mixco	Groundwater	134.1-167.1	(Garrido Hoyos et al., 2013)
	San Rafael Las Flores	Drinking water	<2-17.87	(Marcillo et al., 2020)
	Lemoa	Surface and groundwater	<10	(Elmore et al., 2005)
Haiti	Eastern Haiti	Groundwater	<40	(Eisen-Cuadra et al., 2013)
Honduras	Platanares and Azacualpa area	Several sources	17 - 842	(Barberi et al., 2013)
Mexico	Semiarid basin in Mexican Altiplano / Sierra Madre Oriental in central Mexico	Groundwater	0.01-128	(Cauich-Kau et al., 2022)
	Durango city	Groundwater	0.2-188	(Robledo-Peralta et al., 2021)
	Several areas	Drinking, surface and groundwater	0.01-16000	(Osuna-Martínez et al., 2021)

	Yaqui Valley	Groundwater	6.0-75	(Navarro-Espinoza et al., 2021)
	Southern part of Zacatecas state	Groundwater	3.3-75.4	(Navarro et al., 2017)
	San Luis Potosí state	Groundwater	2.5-30	(Fernández-Macias et al., 2020)
	Sonora state	Groundwater	2.7-98.7	(García-Rico et al., 2019)
	Several areas	Surface and Groundwater	~0 - ~40	(Alarcón-Herrera et al., 2020)
	Durango state	Groundwater	24.48	(López-Guzmán et al., 2019)
	Guanajuato state	Groundwater	3.0-46	(Morales et al., 2015)
	Guanajuato state	Groundwater	26	(Castañeda et al., 2022)
	Lerma-Chapala basin	Groundwater	25-120	(Adrian Ortega-Guerrero, 2009)
	Region of Zimapán Hidalgo	Groundwater	360-530	(Flores et al., 2009)
	Chihuahua state	Groundwater	0->100	(Hermosillo-Muñoz and Valles-Aragón, 2016)
	Cerro Prieto geothermal field	Groundwater	318-5179	(Armienta et al., 2014)
	Chihuahua state	Groundwater	Nd-39	(Reyes-Gómez et al., 2013)
	Chihuahua state		110-191	(Flores-Tavizón et al., 2003)
	Chihuahua state	Groundwater	75-134	(Piñón et al., 2003)
Nicaragua	É uma revisão, muitas regiões do país	Drinking water	10-1320	(Delgado Quezada et al., 2020)
	Sébaco valley	Groundwater	10-122	(Bundschuh et al., 2008)
	San Juan de Limay	Groundwater	<2.02-115.45	(Bundschuh et al., 2008)
	North of the active Telica volcano	Groundwater	43-50	(Gonzalez et al., 2019)
	Several areas		10-1200	(Gonzalez Rodriguez et al., 2019)
Panama	Herrera and Los Santos provinces	Surface water	~1	(Gonzalez Rodriguez et al., 2019)
Peru	Arequipa	Surface water	356	(Ccamerccoa et al., 2022)
	Western Amazon	Groundwater	<0.5-700	(de Meyer et al., 2019, 2017)
	Central Andes	Surface water	0.0-26.2	(Custodio et al., 2020b)
	Western Amazonia	Groundwater	<0.5-715	(de Meyer et al., 2017)
	Several areas	Groundwater	0.1-93.1	(George et al., 2014)
	Tacna, Moquegua, Cerro de Pasco, and Chiclayo		3-1100	(Bolisetty et al., 2021)
	Central Andes	Surface water	5- 38	(Condor et al., 2021)
	Department of Puno	Surface water	0-29	(Belizario Quispe et al., 2019)
	Central Andes	Surface water	2.6-229	(Custodio et al., 2020a)
Triple border of Argentine,	South domain of Guarani Aquifer System	Groundwater	<10-94	(Gastmans et al., 2010)

Brazil, and Uruguay				
Uruguay	Several areas	Groundwater	1.72-120.48	(Machado et al., 2019)
	South-western Uruguay	Groundwater	0.1-58.0	(Manganelli et al., 2007)

References

Adrian Ortega-Guerrero, M., 2009. Occurrence, distribution, hydrochemistry and origin of arsenic, fluoride and other trace elements dissolved in groundwater at basin scale in central Mexico. Rev. Mex. Ciencias Geol. 26, 143–161. https://doi.org/10.1612/inf.tecnol.4098it

Aguilar, G., Riddle, D.D., Knappett, P.S.K., Zapata, M., Weatherby, K.M., Brumbelow, J.K., Moore, G.W., 2019. Hydro-geochemical Processes Driving Arsenic Concentrations in Springs in the Highlands of Costa Rica. AGU Fall Meet. Abstr.

Alarcón-Herrera, M.T., Martin-Alarcon, D.A., Gutiérrez, M., Reynoso-Cuevas, L., Martín-Domínguez, A., Olmos-Márquez, M.A., Bundschuh, J., 2020. Co-occurrence, possible origin, and health-risk assessment of arsenic and fluoride in drinking water sources in Mexico: Geographical data visualization. Sci. Total Environ. 698, 134168. https://doi.org/10.1016/j.scitotenv.2019.134168

Alonso, D.L., Pérez, R., Okio, C.K.Y.A., Castillo, E., 2020. Assessment of mining activity on arsenic contamination in surface water and sediments in southwestern area of Santurbán paramo, Colombia. J. Environ. Manage. 264, 110478. https://doi.org/10.1016/j.jenvman.2020.110478

Alvarez, M. del P., Carol, E., 2019. Geochemical occurrence of arsenic, vanadium and fluoride in groundwater of Patagonia, Argentina: Sources and mobilization processes. J. South Am. Earth Sci. 89, 1–9. https://doi.org/10.1016/j.jsames.2018.10.006

Archer, J., Hudson-Edwards, K.A., Preston, D.A., Howarth, R.J., Linge, K., 2005. Aqueous exposure and uptake of arsenic by riverside communities affected by mining contamination in the Río Pilcomayo basin, Bolivia. Mineral. Mag. 69, 719–736. https://doi.org/10.1180/0026461056950283

Arias-Barrantes, B., Urbina, A., Alvarado-Gámez, A.L., 2018. Determinación de As(III) y As(V) en los pozos de las plantas de remoción de arsénico de Costa Rica. Rev. Tecnol. en Marcha 31, 136. https://doi.org/10.18845/tm.v31i2.3631

Armienta, M.A., Rodríguez, R., Ceniceros, N., Cruz, O., Aguayo, A., Morales, P., Cienfuegos, E., 2014. Groundwater quality and geothermal energy. The case of Cerro Prieto Geothermal Field, México. Renew. Energy 63, 236–254. https://doi.org/10.1016/j.renene.2013.09.018

Barberi, F., Carapezza, M.L., Cioni, R., Lelli, M., Menichini, M., Ranaldi, M., Ricci, T., Tarchini, L., 2013. New geochemical investigations in Platanares and Azacualpa geothermal sites (Honduras). J. Volcanol. Geotherm. Res. 257, 113–134. https://doi.org/10.1016/j.jvolgeores.2013.03.011

Belizario Quispe, G., Capacoila Coila, J., Huaquisto Ramos, E., Cornejo Olarte, D.A., Chui Betancur3, H.N., 2019. DETERMINACIÓN DEL CONTENIDO DE FÓSFORO Y ARSÉNICO, Y DE OTROS METALES CONTAMINANTES DE LAS AGUAS SUPERFICIALES DEL RÍO COATA, AFLUENTE DEL LAGO TITICACA, PERÚ. Rev. Boliv. Química 36. https://doi.org/10.34098/2078-3949.36.5.4

Bhattacharya, P., Claesson, M., Bundschuh, J., Sracek, O., Fagerberg, J., Jacks, G., Martin, R.A., Storniolo, A. del R., Thir, J.M., 2006. Distribution and mobility of arsenic in the Río Dulce alluvial aquifers in Santiago del Estero Province, Argentina. Sci. Total Environ. 358, 97–120. https://doi.org/10.1016/j.scitotenv.2005.04.048

Bidone, E., Cesar, R., Santos, M.C., Sierpe, R., Silva-Filho, E.V., Kutter, V., Dias da Silva, L.I., Castilhos, Z., 2018. Mass balance of arsenic fluxes in rivers impacted by gold mining activities in Paracatu (Minas Gerais State, Brazil). Environ. Sci. Pollut. Res. 25, 9085–9100. https://doi.org/10.1007/s11356-018-1215-z

Bolisetty, S., Rahimi, A., Mezzenga, R., 2021. Arsenic removal from Peruvian drinking water using milk protein nanofibril–carbon filters: a field study. Environ. Sci. Water Res. Technol. 7, 2223–2230. https://doi.org/10.1039/D1EW00456E

Borba, R.P., Figueiredo, B.R., Rawlins, B., Matschullat, J., 2003. Geochemical distribution of arsenic in waters, sediments and weathered gold mineralized rocks from Iron Quadrangle, Brazil. Environ. Geol. 44, 39–52. https://doi.org/10.1007/s00254-002-0733-6

Bundschuh, J., Armienta, M.A., Birkle, P., Bhattacharya, P., Matschullat, J., Mukherjee, A.B., 2008. Natural Arsenic in Groundwaters of Latin America.

Campos, V., 2002. Arsenic in groundwater affected by phosphate fertilizers at São Paulo, Brazil. Environ. Geol. 42, 83–87. https://doi.org/10.1007/s00254-002-0540-0

Castañeda, L.F., Coreño, O., Nava, J.L., 2022. Simultaneous removal of arsenic, fluoride, and hydrated silica from deep well water by electrocoagulation using hybrid Al-Fe electrodes. Process Saf. Environ. Prot. 166, 290–298. https://doi.org/10.1016/j.psep.2022.08.025

Cauich-Kau, D., Rüde, T.R., Cardona-Benavides, A., Castro-Larragoitia, J., 2022. Natural occurrence and controls of arsenic in groundwater in a semiarid basin in the Mexican Altiplano. Hydrogeol. J. 30, 2459–2477. https://doi.org/10.1007/s10040-022-02562-w

Ccamerccoa, M.H., Falcon, N.L.T., Félix, L.L., Pacheco-Salazar, D.G., Aragón, F.F.H., Coaquira, J.A.H., Garnier, J., Vera-Gonzales, C., 2022. High efficiency of magnetite nanoparticles for the arsenic removal from an aqueous solution and natural water taken from Tambo River in Peru. J. Environ. Heal. Sci. Eng. 20, 849–860. https://doi.org/10.1007/s40201-022-00825-y

Cipriani-Avila, I., Molinero, J., Jara-Negrete, E., Barrado, M., Arcos, C., Mafla, S., Custode, F., Vilaña, G., Carpintero, N., Ochoa-Herrera, V., 2020. Heavy metal assessment in drinking waters of Ecuador: Quito, Ibarra and Guayaquil. J. Water Health 18, 1050–1064. https://doi.org/10.2166/wh.2020.093

Concha, G., Broberg, K., Grandér, M., Cardozo, A., Palm, B., Vahter, M., 2010. High-Level Exposure to Lithium, Boron, Cesium, and Arsenic via Drinking Water in the Andes of Northern Argentina. Environ. Sci. Technol. 44, 6875–6880. https://doi.org/10.1021/es1010384

Concha, G., Nermell, B., Vahter, M., 2006. Spatial and temporal variations in arsenic exposure via drinking-water in Northern Argentina. J. Heal. Popul. Nutr. 24, 317–326.

Condor, A., Custodio, M., Chanamé, F., Cuadrado, W., Peñaloza, R., 2021. Heavy Metals and Arsenic in Water, Sediment and the Muscle of Oncorhynchus mykiss from the Tishgo river in the Central Andes of Peru. J. Ecol. Eng. 22, 156–166. https://doi.org/10.12911/22998993/134045

Costa, R. de V.F. da, Leite, M.G.P., Mendonça, F.P.C., Nalini Jr., H.A., 2015. Geochemical mapping of arsenic in surface waters and stream sediments of the Quadrilátero Ferrífero, Brazil. Rem Rev. Esc. Minas 68, 43–51. https://doi.org/10.1590/0370-44672015680077

Cumbal, L., Vallejo, P., Rodriguez, B., Lopez, D., 2010. Arsenic in geothermal sources at the north-central Andean region of Ecuador: concentrations and mechanisms of mobility. Environ. Earth Sci. 61, 299–310. https://doi.org/10.1007/s12665-009-0343-7

Custodio, M., Álvarez, D., Cuadrado, W., Montalvo, R., Ochoa, S., 2020a. Potentially toxic metals and metalloids in surface water intended for human consumption and other uses in the Mantaro River watershed, Peru. Soil Water Res. 15, 237–245. https://doi.org/10.17221/152/2019-SWR

Custodio, M., Cuadrado, W., Peñaloza, R., Montalvo, R., Ochoa, S., Quispe, J., 2020b. Human Risk from Exposure to Heavy Metals and Arsenic in Water from Rivers with Mining Influence in the Central Andes of Peru. Water 12, 1946. https://doi.org/10.3390/w12071946

De C. Silva, D., Bellato, C.R., De O. Marques Neto, J., Fontes, M.P.F., 2018. Arsenic and trace metals in water and sediment of the velhas river, southeastern iron quadrangle region, minas gerais, BRAZIL. Quim. Nova 41, 1011–1018. https://doi.org/10.21577/0100-4042.20170275

de Meyer, C.M.C., Berg, M., Rodriguez, J., Carpio, E., Garcia, P., Wahnfried, I., 2019. Exploring arsenic and other geogenic groundwater contaminants in the vast and scarcely studied Amazon Basin, in: Environmental Arsenic in a Changing World. CRC Press, London, pp. 50–51. https://doi.org/10.1201/9781351046633-18

de Meyer, C.M.C., Rodríguez, J.M., Carpio, E.A., García, P.A., Stengel, C., Berg, M., 2017. Arsenic, manganese and aluminum contamination in groundwater resources of Western Amazonia (Peru). Sci. Total Environ. 607–608, 1437–1450. https://doi.org/10.1016/j.scitotenv.2017.07.059

Delgado Quezada, V., Altamirano Espinoza, M., Bundschuh, J., 2020. Arsenic in geoenvironments of Nicaragua: Exposure, health effects, mitigation and future needs. Sci. Total Environ. 716, 136527. https://doi.org/10.1016/j.scitotenv.2020.136527

Diaz, O., Arcos, R., Tapia, Y., Pastene, R., Velez, D., Devesa, V., Montoro, R., Aguilera, V., Becerra, M., 2015. Estimation of Arsenic Intake from Drinking Water and Food (Raw and Cooked) in a Rural Village of Northern Chile. Urine as a Biomarker of Recent Exposure. Int. J. Environ. Res. Public Health 12, 5614–5633. https://doi.org/10.3390/ijerph120505614

Eisen-Cuadra, A., Christian, A.D., Dorval, E., Broadaway, B., Herron, J., Hannigan, R.E., 2013. Metal Geochemistry of a Brackish Lake: Étang Saumâtre, Haiti, in: Medical Geochemistry. Springer Netherlands, Dordrecht, pp. 149–166. https://doi.org/10.1007/978-94-007-4372-4_9

Elmore, A.C., Miller, G.R., Parker, B., 2005. Water quality in Lemoa, Guatemala. Environ. Geol. 48, 901–907. https://doi.org/10.1007/s00254-005-0028-9

Escudero, L. V., Bijman, J., Chong, G., Pueyo, J.J., Demergasso, C., 2013. Geochemistry and Microbiology in an Acidic, High Altitude (4,000 m) Salt Flat — High Andes, Northern Chile. Adv. Mater. Res. 825, 28–32. https://doi.org/10.4028/www.scientific.net/AMR.825.28

Fernández-Macias, J.C., Ochoa-Martínez, Á.C., Orta-García, S.T., Varela-Silva, J.A., Pérez-Maldonado, I.N., 2020. Probabilistic human health risk assessment associated with fluoride and arsenic co-occurrence in drinking water from the metropolitan area of San Luis Potosí, Mexico. Environ. Monit. Assess. 192, 712. https://doi.org/10.1007/s10661-020-08675-7

Ferreira, C.A., L Palmieri, H.E., Ângela de C Menezes, M.B., L A Auler, L.M., 2017. Hydrochemical Assessment of Spring Waters from the Iron Quadrangle Region, Minas Gerais, Brazil , SiO. Am. J. Water Resour. 5, 29–40.

Flores-Tavizón, E., Alarcón-Herrera, M.T., González-Elizondo, S., Olguín, E.J., 2003. Arsenic Tolerating Plants from Mine Sites and Hot Springs in the Semi-Arid Region of Chihuahua, Mexico. Acta Biotechnol. 23, 113–119. https://doi.org/10.1002/abio.200390016

Flores, E., Armienta, A., Micete, S., Valladares, M.R., 2009. Water treatment for human consumption with high arsenic content: A study case in zimapán hidalgo- Mexico. Inf. Tecnol. 20, 85–93. https://doi.org/10.1612/inf.tecnol.4098it.08

Francisca, F.M., Carro Perez, M.E., 2009. Assessment of natural arsenic in groundwater in Cordoba Province, Argentina. Environ. Geochem. Health 31, 673–682. https://doi.org/10.1007/s10653-008-9245-y

Funes Pinter, I., Salomon, M.V., Gil, R., Mastrantonio, L., Bottini, R., Piccoli, P., 2018. Arsenic and trace elements in soil, water, grapevine and onion in Jáchal, Argentina. Sci. Total Environ. 615, 1485–1498. https://doi.org/10.1016/j.scitotenv.2017.09.114

García-Rico, L., Meza-Figueroa, D., Jay Gandolfi, A., del Rivero, C.I., Martínez-Cinco, M.A., Meza-Montenegro, M.M., 2019. Health Risk Assessment and Urinary Excretion of Children Exposed to Arsenic through Drinking Water and Soils in Sonora, Mexico. Biol. Trace Elem. Res. 187, 9–21. https://doi.org/10.1007/s12011-018-1347-5

García, M.E., Bundschuh, J., O., R., J., Q., Persson, K.M., Bengtsson, L., Berndtsson', R., C., 2005. Heavy Metals in Aquatic Plants and Their Relationship To Concentrations in Surface Water, Groundwater and Sediments — a Case Study of Poopó Basin, Bolivia. Rev. Boliv. Química 22, 11–18.

García, M.G., Sracek, O., Fernández, D.S., Hidalgo, M. del V., 2007. Factors affecting arsenic concentration in groundwaters from Northwestern Chaco-Pampean Plain, Argentina. Environ. Geol. 52, 1261–1275. https://doi.org/10.1007/s00254-006-0564-y

Garrido Hoyos, S., Avilés Flores, M., Ramírez Gonzalez, A., Grajeda Fajardo, C., Cardoso Zoloeta, S., Velásquez Orozco, H., 2013. Comparing Two Operating Configurations in a Full-Scale Arsenic Removal Plant. Case Study: Guatemala. Water 5, 834–851. https://doi.org/10.3390/w5020834

Gastmans, D., Veroslavsky, G., Chang, H.K., Marmisolle, J., Oleaga, A., 2010. Influência do arcabouço hidroestratigráfico nas ocorrências de arsênio em águas subterrâneas ao longo do corredor termal do rio Uruguai (Argentina - Brasil - Uruguai). Geociencias 29, 105–120.

George, C.M., Sima, L., Arias, M.H.J., Mihalic, J., Cabrera, L.Z., Danz, D., Checkley, W., Gilman, R.H., 2014. Arsenic exposure in drinking water: an unrecognized health threat in Peru. Bull. World Health Organ. 92, 565–572. https://doi.org/10.2471/BLT.13.128496

Giménez, M., Osicka, R., Blanes, P., Morisio, Y., Farías, S., 2014. Heavy metal concentration in arsenic contaminated groundwater of the Chaco Province, Argentina. pp. 135–137. https://doi.org/10.1201/b16767-51

Gomez, M.L., Blarasin, M.T., Martínez, D.E., 2009. Arsenic and fluoride in a loess aquifer in the central area of Argentina. Environ. Geol. 57, 143–155. https://doi.org/10.1007/s00254-008-1290-4

Gonçalves, J.A.C., de Lena, J.C., Paiva, J.F., Nalini, H.A., Pereira, J.C., 2007. Arsenic in the groundwater of Ouro Preto (Brazil): its temporal behavior as influenced by the hydric regime and hydrogeology. Environ. Geol. 53, 785–793. https://doi.org/10.1007/s00254-007-0691-0

Gontijo, E.S.J., Watanabe, C.H., Monteiro, A.S.C., Tonello, P.S., da Silva, G.A., Friese, K., Roeser, H.M.P., Rosa, A.H., 2016. Distribution and bioavailability of arsenic in natural waters of a mining area studied by ultrafiltration and diffusive gradients in thin films. Chemosphere 164, 290–298. https://doi.org/10.1016/j.chemosphere.2016.08.107

Gonzalez, B., Heijman, S.G.J., Rietveld, L.C., van Halem, D., 2019. Arsenic removal from geothermal influenced groundwater with low pressure NF pilot plant for drinking water production in Nicaraguan rural communities. Sci. Total Environ. 667, 297–305. https://doi.org/10.1016/j.scitotenv.2019.02.222

Gonzalez Rodriguez, B., Rietveld, L.C., Longley, A.J., van Halem, D., 2019. Arsenic contamination of rural community wells in Nicaragua: A review of two decades of experience. Sci. Total Environ. 657, 1441–1449. https://doi.org/10.1016/j.scitotenv.2018.12.168

Guerra, P., Gonzalez, C., Escauriaza, C., Pizarro, G., Pasten, P., 2016. Incomplete Mixing in the Fate and Transport of Arsenic at a River Affected by Acid Drainage. Water, Air, Soil Pollut. 227, 73. https://doi.org/10.1007/s11270-016-2767-5

Guimarães, R.N., Moreira, V.R., Amaral, M.C.S., 2022. Membrane technology as an emergency response against drinking water shortage in scenarios of dam failure. Chemosphere 309, 136618. https://doi.org/10.1016/j.chemosphere.2022.136618

Heredia, O.S., Cirelli, A.F., 2009. Trace elements distribution in soil, pore water and groundwater in Buenos Aires, Argentina. Geoderma 149, 409–414. https://doi.org/10.1016/j.geoderma.2008.12.020

Hermosillo-Muñoz, M., Valles-Aragón, M., 2016. Arsenic determination in agricultural water in Chihuahua, Mexico. pp. 252–253. https://doi.org/10.1201/b20466-123

Hoponick Redmon, J., Mulhern, R.E., Castellanos, E., Wood, E., McWilliams, A., Herrera, I., Liyanapatirana, C., Weber, F., Levine, K., Thorp, E., Bynum, N., Amato, K., Najera Acevedo, M.A., Baker, J., Van Houtven, G., Henry, C., Wade, C., Kondash, A., 2022. A Participatory Science Approach to Evaluating Factors Associated with the Occurrence of Metals and PFAS in Guatemala City Tap Water. Int. J. Environ. Res. Public Health 19, 6004. https://doi.org/10.3390/ijerph19106004

Kunz, S., Romero-Esquivel, L.G., Otter, P., Feistel, U., Grischek, T., Valverde-Cerdas, J., Feller, J., 2018. Treatment of arsenic-contaminated water using in-line electrolysis, co-precipitation and filtration in Costa Rica. Water Supply 18, 40–48. https://doi.org/10.2166/ws.2017.089

Lamela, P.A., Navoni, J.A., Pérez, R.D., Pérez, C.A., Vodopivez, C.L., Curtosi, A., Bongiovanni, G.A., 2019. Analysis of occurrence, bioaccumulation and molecular targets of arsenic and other selected volcanic elements in Argentinean Patagonia and Antarctic ecosystems. Sci. Total Environ. 681, 379–391. https://doi.org/10.1016/j.scitotenv.2019.05.096

Leybourne, M.I., Cameron, E.M., 2008. Source, transport, and fate of rhenium, selenium, molybdenum, arsenic, and copper in groundwater associated with porphyry–Cu deposits, Atacama Desert, Chile. Chem. Geol. 247, 208–228. https://doi.org/10.1016/j.chemgeo.2007.10.017

Litter, M.I., Ingallinella, A.M., Olmos, V., Savio, M., Difeo, G., Botto, L., Farfán Torres, E.M., Taylor, S., Frangie, S., Herkovits, J., Schalamuk, I., González, M.J., Berardozzi, E., García Einschlag, F.S., Bhattacharya, P., Ahmad, A., 2019. Arsenic in Argentina: Occurrence, human health, legislation and determination. Sci. Total Environ. 676, 756–766. https://doi.org/10.1016/j.scitotenv.2019.04.262

López-Guzmán, M., Alarcón-Herrera, M.T., Irigoyen-Campuzano, J.R., Torres-Castañón, L.A., Reynoso-Cuevas, L., 2019. Simultaneous removal of fluoride and arsenic from well water by electrocoagulation. Sci. Total Environ. 678, 181–187. https://doi.org/10.1016/j.scitotenv.2019.04.400

Lotter, J.T., Lacey, S.E., Lopez, R., Socoy Set, G., Khodadoust, A.P., Erdal, S., 2014. Groundwater arsenic in Chimaltenango, Guatemala. J. Water Health 12, 533–542. https://doi.org/10.2166/wh.2013.100

Machado, I., Bühl, V., Mañay, N., 2019. Total arsenic and inorganic arsenic speciation in groundwater intended for human consumption in Uruguay: Correlation with fluoride, iron, manganese and sulfate. Sci. Total Environ. 681, 497–502. https://doi.org/10.1016/j.scitotenv.2019.05.107

Manganelli, A., Goso, C., Guerequiz, R., Fernández Turiel, J.L., García Vallès, M., Gimeno, D., Pérez, C., 2007. Groundwater arsenic distribution in South-western Uruguay. Environ. Geol. 53, 827–834. https://doi.org/10.1007/s00254-007-0695-9

Marcillo, C.E., García Prado, G., Copeland, N., Krometis, L.H., 2020. Drinking water quality and consumer perceptions at the point-of-use in San Rafael Las Flores, Guatemala. Water Pract. Technol. 15, 374–385. https://doi.org/10.2166/wpt.2020.025

Mariño, E.E., Ávila, G.T., Bhattacharya, P., Schulz, C.J., 2020. The occurrence of arsenic and other trace elements in groundwaters of the southwestern Chaco-Pampean plain, Argentina. J. South Am. Earth Sci. 100, 102547. https://doi.org/10.1016/j.jsames.2020.102547

Meneguelli-Souza, A.C., Pestana, I.A., Azevedo, L.S., de Almeida, M.G., Alves, M. da G., Oliveira, D.F.C., Dupim, M.O., Gonçalves, R.A., Godoy, J.M. de O., de Souza, C.M.M., 2020. Arsenic in groundwater in Paraíba do Sul river, Brazil: sources, hydrogeochemistry, and correlation with redox parameters. Environ. Earth Sci. 79, 194. https://doi.org/10.1007/s12665-020-08934-3

Mirlean, N., Baisch, P., Diniz, D., 2014. Arsenic in groundwater of the Paraiba do Sul delta, Brazil: An atmospheric source? Sci. Total Environ. 482–483, 148–156. https://doi.org/10.1016/j.scitotenv.2014.02.138

Mirlean, N., Roisenberg, A., 2006. The effect of emissions of fertilizer production on the environment contamination by cadmium and arsenic in southern Brazil. Environ. Pollut. 143, 335–340. https://doi.org/10.1016/j.envpol.2005.11.022

Montero Campos, V., Quesada Kimsey, J., Ledezma Espinoza, A., Sandoval Mora, J.A., 2010. Determinación de arsénico en abastecimientos de agua para consumo humano de la provincia de Cartago, Costa Rica. Acta Med. Costarric. 52. https://doi.org/10.51481/amc.v52i2.642

Morales, I., Villanueva-Estrada, R.E., Rodríguez, R., Armienta, M.A., 2015. Geological, hydrogeological, and geothermal factors associated to the origin of arsenic, fluoride, and groundwater temperature in a volcanic environment "El Bajío Guanajuatense", Mexico. Environ. Earth Sci. 74, 5403–5415. https://doi.org/10.1007/s12665-015-4554-9

Moreira, V.R., Lebron, Y.A.R., de Paula, E.C., Santos, L.V. de S., Amaral, M.C.S., 2021a. Recycled reverse osmosis membrane combined with pre-oxidation for improved arsenic removal from high turbidity waters and retrofit of conventional drinking water treatment process. J. Clean. Prod. 312, 127859. https://doi.org/10.1016/j.jclepro.2021.127859

Moreira, V.R., Lebron, Y.A.R., Santos, L.V. de S., Amaral, M.C.S., 2022. Low-cost recycled end-of-life reverse osmosis membranes for water treatment at the point-of-use. J. Clean. Prod. 362, 132495. https://doi.org/10.1016/j.jclepro.2022.132495

Moreira, V.R., Lebron, Y.A.R., Santos, L.V. de S., Amaral, M.C.S., 2021b. Dead-end ultrafiltration as a cost-effective strategy for improving arsenic removal from high turbidity waters in conventional drinking water facilities. Chem. Eng. J. 417, 128132. https://doi.org/10.1016/j.cej.2020.128132

Muñoz, M., Huallpara, L., Coariti, E., Aróstegui, J., Kohfahl, C., Estévez, M., Bhattacharya, P., 2014. Natural arsenic occurrence in drinking water and assessment of water quality in the southern part of the Poopó lake basin, Bolivian Altiplano. pp. 154–156. https://doi.org/10.1201/b16767-58

Navarro-Espinoza, S., Angulo-Molina, A., Meza-Figueroa, D., López-Cervantes, G., Meza-Montenegro, M., Armienta, A., Soto-Puebla, D., Silva-Campa, E., Burgara-Estrella, A., Álvarez-Bajo, O., Pedroza-Montero, M., 2021. Effects of Untreated Drinking Water at Three Indigenous Yaqui Towns in Mexico: Insights from a Murine Model. Int. J. Environ. Res. Public Health 18, 805. https://doi.org/10.3390/ijerph18020805

Navarro, O., González, J., Júnez-Ferreira, H.E., Bautista, C.-F., Cardona, A., 2017. Correlation of Arsenic and Fluoride in the Groundwater for Human Consumption in a Semiarid Region of Mexico. Procedia Eng. 186, 333–340. https://doi.org/10.1016/j.proeng.2017.03.259

Nicolau, C., Reich, M., Lynne, B., 2014. Physico-chemical and environmental controls on siliceous sinter formation at the high-altitude El Tatio geothermal field, Chile. J. Volcanol. Geotherm. Res. 282, 60–76. https://doi.org/10.1016/j.jvolgeores.2014.06.012

Nicolli, H.B., Bundschuh, J., Blanco, M. del C., Tujchneider, O.C., Panarello, H.O., Dapeña, C., Rusansky, J.E., 2012a. Arsenic and associated trace-elements in groundwater from the Chaco-Pampean plain, Argentina: Results from 100years of research. Sci. Total Environ. 429, 36–56. https://doi.org/10.1016/j.scitotenv.2012.04.048

Nicolli, H.B., García, J.W., Falcón, C.M., Smedley, P.L., 2012b. Mobilization of arsenic and other trace elements of health concern in groundwater from the Salí River Basin, Tucumán Province, Argentina. Environ. Geochem. Health 34, 251–262. https://doi.org/10.1007/s10653-011-9429-8

O'Reilly, J., Watts, M.J., Shaw, R.A., Marcilla, A.L., Ward, N.I., 2010. Arsenic contamination of natural waters in San Juan and La Pampa, Argentina. Environ. Geochem. Health 32, 491–515. https://doi.org/10.1007/s10653-010-9317-7

Ormachea Muñoz, M., Bhattacharya, P., Sracek, O., Ramos Ramos, O., Quintanilla Aguirre, J., Bundschuh, J., Maity, J.P., 2015. Arsenic and other trace elements in thermal springs and in cold waters from drinking water wells on the Bolivian Altiplano. J. South Am. Earth Sci. 60, 10–20. https://doi.org/10.1016/j.jsames.2015.02.006

Osuna-Martínez, C.C., Armienta, M.A., Bergés-Tiznado, M.E., Páez-Osuna, F., 2021. Arsenic in waters, soils, sediments, and biota from Mexico: An environmental review. Sci. Total Environ. 752, 142062. https://doi.org/10.1016/j.scitotenv.2020.142062

Otero, X.L., Tierra, W., Atiaga, O., Guanoluisa, D., Nunes, L.M., Ferreira, T.O., Ruales, J., 2016. Arsenic in rice agrosystems (water, soil and rice plants) in Guayas and Los Ríos provinces, Ecuador. Sci. Total Environ. 573, 778–787. https://doi.org/10.1016/j.scitotenv.2016.08.162

Panigatti, M., Boglione, R., Griffa, C., Schierano, M., 2014. Groundwater arsenic in the central-west of the Santa Fe Province, Argentine. pp. 159–161. https://doi.org/10.1201/b16767-60

Paoloni, J.D., Sequeira, M.E., Espósito, M.E., Fiorentino, C.E., Blanco, M. del C., 2009. Arsenic in Water Resources of the Southern Pampa Plains, Argentina. J. Environ. Public Health 2009, 1–7. https://doi.org/10.1155/2009/216470

Pauta-Calle, G., Velasco, M., Vázquez, G., Abril, A., Torres, S., 2021. Analysis and risk assessment of arsenic in the water sources of the cities Cuenca and Azogues, Ecuador. MASKANA 12, 71–79. https://doi.org/10.18537/mskn.12.02.08

Pérez-Carrera, A., Fernández Cirelli, A., 2010. Arsenic and Water Quality Challenges in South America, in: Water and Sustainability in Arid Regions. Springer Netherlands, Dordrecht, pp. 275–293. https://doi.org/10.1007/978-90-481-2776-4_17

Pincetti-Zúniga, G.P., Richards, L.A., Daniele, L., Boyce, A.J., Polya, D.A., 2022. Hydrochemical characterization, spatial distribution, and geochemical controls on arsenic and boron in waters from arid Arica and Parinacota, northern Chile. Sci. Total Environ. 806, 150206. https://doi.org/10.1016/j.scitotenv.2021.150206

Piñón, M.M., Bautista, M.R.G., Pérez, H.A., 2003. Removal of arsenic and fluoride from drinking water with cake alum and a polymeric anionic flocculent. Fluoride 36, 122–128.

Quaghebeur, W., Mulhern, R.E., Ronsse, S., Heylen, S., Blommaert, H., Potemans, S., Valdivia Mendizábal, C., Terrazas García, J., 2019. Arsenic contamination in rainwater harvesting tanks around Lake Poopó in Oruro, Bolivia: An unrecognized health risk. Sci. Total Environ. 688, 224–230. https://doi.org/10.1016/j.scitotenv.2019.06.126

Queirolo, F., 2000. Total arsenic, lead, cadmium, copper, and zinc in some salt rivers in the northern Andes of Antofagasta, Chile. Sci. Total Environ. 255, 85–95. https://doi.org/10.1016/S0048-9697(00)00451-4

Reyes-Gómez, V.M., Alarcón-Herrera, M.T., Gutiérrez, M., López, D.N., 2013. Fluoride and Arsenic in an Alluvial Aquifer System in Chihuahua, Mexico: Contaminant Levels, Potential Sources, and Co-occurrence. Water, Air, Soil Pollut. 224, 1433. https://doi.org/10.1007/s11270-013-1433-4

Robledo-Peralta, A., López-Guzmán, M., Morales-Amaya, C.G., Reynoso-Cuevas, L., 2021. Arsenic and Fluoride in Groundwater, Prevalence and Alternative Removal Approach. Processes 9, 1191. https://doi.org/10.3390/pr9071191

Romero, F.M., Prol-Ledesma, R.M., Canet, C., Alvares, L.N., Pérez-Vázquez, R., 2010. Acid drainage at the inactive Santa Lucia mine, western Cuba: Natural attenuation of arsenic, barium and lead, and geochemical behavior of rare earth elements. Appl. Geochemistry 25, 716–727. https://doi.org/10.1016/j.apgeochem.2010.02.004

Romero, L., Alonso, H., Campano, P., Fanfani, L., Cidu, R., Dadea, C., Keegan, T., Thornton, I., Farago, M., 2003. Arsenic enrichment in waters and sediments of the Rio Loa (Second Region, Chile). Appl. Geochemistry 18, 1399–1416. https://doi.org/10.1016/S0883-2927(03)00059-3

Rosso, J.J., Puntoriero, M.L., Troncoso, J.J., Volpedo, A. V., Fernández Cirelli, A., 2011. Occurrence of Fluoride in Arsenic-Rich Surface Waters: A Case Study in the Pampa Plain, Argentina. Bull. Environ. Contam. Toxicol. 87, 409–413. https://doi.org/10.1007/s00128-011-0358-0

Ruffino, B., Campo, G., Crutchik, D., Reyes, A., Zanetti, M., 2022. Drinking Water Supply in the Region of Antofagasta (Chile): A Challenge between Past, Present and Future. Int. J. Environ. Res. Public Health 19, 14406. https://doi.org/10.3390/ijerph192114406

Siegfried, K., Hahn-Tomer, S., Koelsch, A., Osterwalder, E., Mattusch, J., Staerk, H.-J., Meichtry, J., De Seta, G., Reina, F., Panigatti, C., Litter, M., Harms, H., 2015. Introducing Simple Detection of Bioavailable Arsenic at Rafaela (Santa Fe Province, Argentina) Using the ARSOlux Biosensor. Int. J. Environ. Res. Public Health 12, 5465–5482. https://doi.org/10.3390/ijerph120505465

Sigrist, M., Albertengo, A., Beldoménico, H., Tudino, M., 2011. Determination of As(III) and total inorganic As in water samples using an on-line solid phase extraction and flow injection hydride generation atomic absorption spectrometry. J. Hazard. Mater. 188, 311–318. https://doi.org/10.1016/j.jhazmat.2011.01.126

Smedley, P.., Nicolli, H.., Macdonald, D.M.., Barros, A.., Tullio, J.., 2002. Hydrogeochemistry of arsenic and other inorganic constituents in groundwaters from La Pampa, Argentina. Appl. Geochemistry 17, 259–284. https://doi.org/10.1016/S0883-2927(01)00082-8

Sosa, N.N., Kulkarni, H. V., Datta, S., Beilinson, E., Porfido, C., Spagnuolo, M., Zárate, M.A., Surber, J., 2019. Occurrence and distribution of high arsenic in sediments and groundwater of the Claromecó fluvial basin, southern Pampean plain (Argentina). Sci. Total Environ. 695, 133673. https://doi.org/10.1016/j.scitotenv.2019.133673

Tapia, J., Mukherjee, A., Rodríguez, M.P., Murray, J., Bhattacharya, P., 2022. Role of tectonics and climate on elevated arsenic in fluvial systems: Insights from surface water and sediments along regional transects of Chile. Environ. Pollut. 314, 120151. https://doi.org/10.1016/j.envpol.2022.120151

Torrance, K.W., Redwood, S.D., Cecchi, A., 2021. The impact of artisanal gold mining, ore processing and mineralization on water quality in Marmato, Colombia. Environ. Geochem. Health 43, 4265–4282. https://doi.org/10.1007/s10653-021-00898-y

Van Den Bergh, K., Du Laing, G., Montoya, J.C., De Deckere, E., Tack, F.M.G., 2010. Arsenic in drinking water wells on the Bolivian high plain: Field monitoring and effect of salinity on removal efficiency of iron-oxides-containing filters. J. Environ. Sci. Heal. Part A 45, 1741–1749. https://doi.org/10.1080/10934529.2010.513262

Varejão, E.V. V., Bellato, C.R., Fontes, M.P.F., Mello, J.W. V., 2011. Arsenic and trace metals in river water and sediments from the southeast portion of the Iron Quadrangle, Brazil. Environ. Monit. Assess. 172, 631–642. https://doi.org/10.1007/s10661-010-1361-3

Vázquez, C., Rodríguez Castro, M.C., Palacios, O., Boeykens, S., 2016. Risk Analysis of Acute Or Chronic Exposure to Arsenic of the Inhabitants in a District of Buenos Aires, Argentina. J. Sustain. Dev. Energy, Water Environ. Syst. 4, 234–241. https://doi.org/10.13044/j.sdewes.2016.04.0019

Vesga Ferreira, J.C., Granados Acuña, G., Sierra Carrillo, J.E., 2015. Optimization of a multi-service network over a PLC cannel under MmQoS. Ing. y Desarro. 33, 260–280. https://doi.org/10.14482/inde.33.2.6368

Viana, J.L.M., Souza, A.F. de, Hernández, A.H., Elias, L.P., Eismann, C.E., Rezende-Filho, A.T., Barbiero, L., Menegario, A.A., Fostier, A.H., 2022. In situ arsenic speciation at the soil/water interface of saline-alkaline lakes of the Pantanal, Brazil: A DGT-based approach. Sci. Total Environ. 804, 150113. https://doi.org/10.1016/j.scitotenv.2021.150113

Vieira, K.S., Crapez, M.A.C., Lima, L.S., Delgado, J.F., Brito, E.B.C.C., Fonseca, E.M., Baptista Neto, J.A., Aguiar, V.M.C., 2021. Evaluation of bioavailability of trace metals through bioindicators in a urbanized estuarine system in southeast Brazil. Environ. Monit. Assess. 193, 18. https://doi.org/10.1007/s10661-020-08809-x

Villa-Achupallas, M., Rosado, D., Aguilar, S., Galindo-Riaño, M.D., 2018. Water quality in the tropical Andes hotspot: The Yacuambi river (southeastern Ecuador). Sci. Total Environ. 633, 50–58. https://doi.org/10.1016/j.scitotenv.2018.03.165

Zhao, K., Guo, H., 2012. Removal of arsenic from aqueous solution by granular modified natural siderite: Characterization and behavior, in: Understanding the Geological and Medical Interface of

Arsenic, As 2012 - 4th International Congress: Arsenic in the Environment. CRC Press, pp. 298–300. https://doi.org/10.1201/b12522-122

Zimmerman, A.J., Gutierrez, D.G., Campos, V.M., Weindorf, D.C., Deb, S.K., Chacón, S.U., Landrot, G., Flores, N.G.G., Siebecker, M.G., 2021. Arsenic speciation in titanium dioxide (TiO2) waste produced via drinking water filtration: Potential environmental implications for soils, sediments, and human health. Environ. Adv. 3, 100036. https://doi.org/10.1016/j.envadv.2021.100036

Figure A1 – Relationship between the values of (a) residue and sample turbidity (n = 65), (b) residue and iron concentration (n = 33), (c) residue and manganese concentration (n = 33). Adapted from: (Guimarães et al., 2022; Moreira et al., 2023b, 2023a; Moreira et al., 2021b, 2021a).

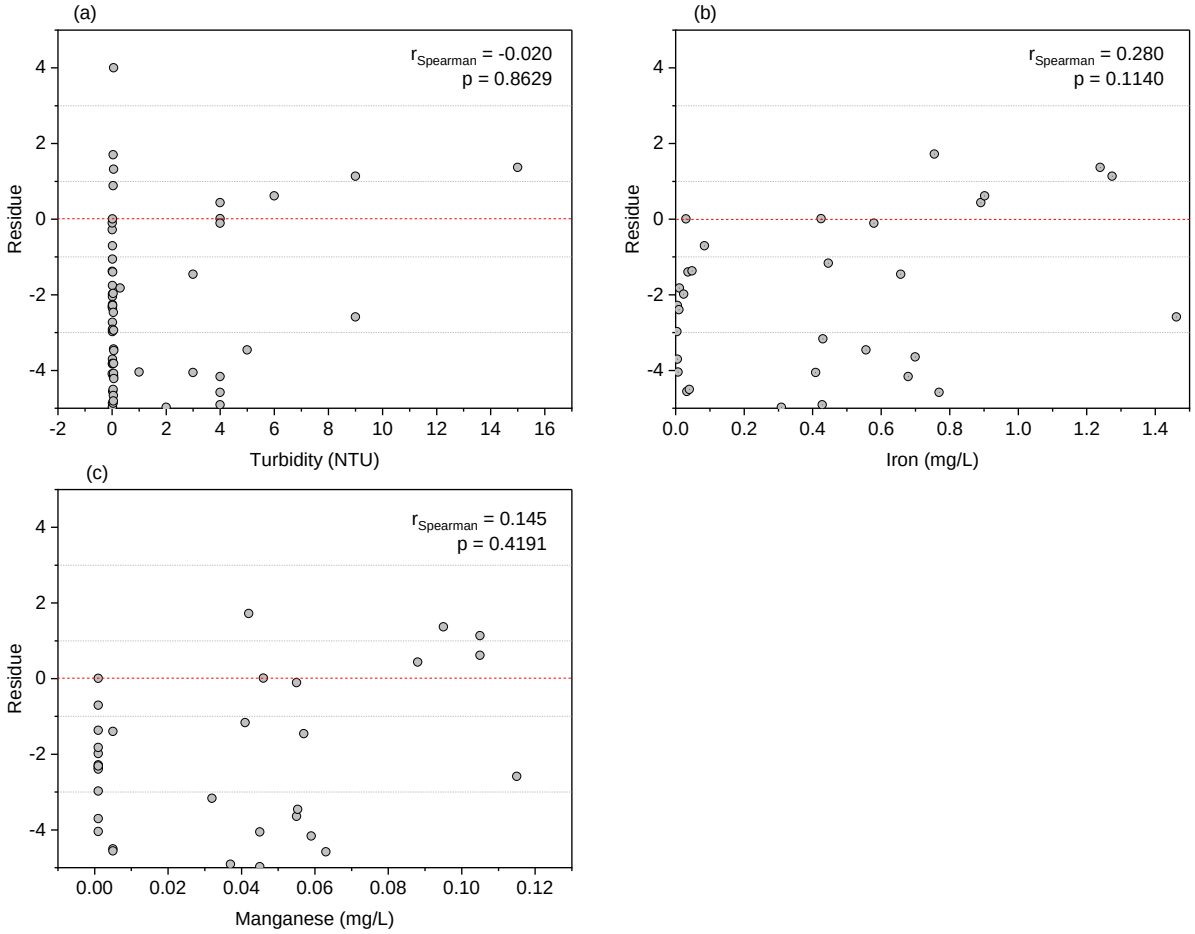

APPENDIX B

Table B1. Potability of blends generated with pretreatment and without pretreatment.

Parameter	Unity	With pretreatment		Without pretreatment		CM/MS n° 888/2021
		Blend I	Blend II	Blend I	Blend II	
Bacteriological standard, cyanotoxins and radioactivity						
Cylindrospermopsins	µg/L	< 0.05	<0.05	<0.05	<0.05	1.0
Microscystin	µg/L	< 0.1	< 0.1	0.088	0.088	1.0
Saxitoxins	µg/L	< 0.02	< 0.02	< 0.02	< 0.02	1.0
Total coliforms	Absence/Presence	Absent	Absent	Absent	Absent	Absence in 100 mL
Escherichia coli	Absence/Presence	Absent	Absent	Absent	Absent	Absence in 100 mL
Alpha radioactivity	Bq/L	< 0.34	< 0.34	< 0.34	< 0.34	0.5
Beta radioactivity	Bq/L	< 0.59	< 0.59	< 0.59	< 0.59	1
Inorganic substances that pose a health risk						
Total antimony	mg/L	0.0006	0.0006	< 0.005	< 0.005	0.006
Total barium	mg/L	0.005	0.007	0.007	0.008	0.700
Bromate	mg/L	< 0.005	< 0.005	< 0.005	< 0.005	0.010
Total cadmium	mg/L	< 0.0005	< 0.0005	< 0.0005	< 0.0005	0.003
Chlorate	mg/L	< 0.020	< 0.020	< 0.020	0.025	0.700
Chlorite	mg/L	< 0.020	< 0.020	< 0.020	< 0.02	0.700
Free residual chlorine	mg/L	0.96	0.92	0.66	0.30	5.00
Total copper	mg/L	<0.00025	<0.00025	0.0016	0.0019	2.00
Total chromium	mg/L	< 0.0005	< 0.0005	< 0.005	< 0,005	0.05
Fluoride	mg/L	0.31	0.430	0.303	0.355	1.500
Total mercury	mg/L	<0.0001	<0.0001	0.5001	0.5001	0.0001
Total nickel	mg/L	<0.001	<0.001	0.003	0.003	0.001
Nitrate	mg/L	0.180	0.036	0.208	0.273	0.438
Nitrite	mg/L	< 0.01	< 0.01	< 0.01	< 0.010	0.01
Total selenium	mg/L	0.005	0.006	< 0.005	< 0.005	0.04
Total uranium	mg/L	< 0.0005	< 0.0005	0.379	0.379	0.03
Organic substances that pose a health risk						
1,2-dichloroethane	µg/L	< 1.0	< 1.0	< 1.0	< 1.0	5.0
1,4-dioxane	µg/L	< 1.0	< 1.0	< 1.0	< 1.0	48.0
2,4-Dichlorophenoxyacetic acid	µg/L	< 0.05	< 0.05	< 0.05	< 0.05	30.0
Total haloacetic acids (9)	mg/L	< 0.036	< 0.036	< 0.036	< 0.036	0.080
Acrylamide	µg/L	< 0.10	< 0.10	< 0.10	< 0.10	0.50
Alachlor	µg/L	< 0.05	< 0.05	< 0.05	< 0.05	20.0
Aldicarb + Aldicarb sulfone + Aldicarb sulfoxide	µg/L	< 9.0	< 9.0	< 9.0	< 9.0	10.0
Aldrin + Dieldrin	µg/L	< 0.02	< 0.02	< 0.02	< 0.02	0.03
Almethrin	µg/L	< 1.0	< 1.0	< 1.0	< 1.0	60.0
Atrazine + S-chlorotriazines	µg/L	< 2.0	< 2.0	< 2.0	< 2.0	2.0

Benzene	µg/L	< 0.50	< 0.50	< 0.50	< 0.50	5.0
Benzo(a)pyrene	µg/L	< 0.01	< 0.01	< 0.01	< 0.01	0.40
Carbendazim	µg/L	< 1.0	< 1.0	< 1.0	< 1.0	120.0
Carbofuran	µg/L	< 1.0	< 1.0	< 1.0	< 1.0	7.0
Cyproconazole	µg/L	< 1.0	< 1.0	< 1.0	< 1.0	30.0
Total chloramines	mg/L	0.076	0.142	0.01	< 0.01	4.0
Vinyl chloride	µg/L	< 0.5	< 0.5	< 0.5	< 0.5	0.5
Chlorothalonil	µg/L	< 0.05	< 0.05	< 0.05	< 0.05	45.0
DDT + DDE + DDD	µg/L	< 0.03	< 0.03	< 0.03	< 0.03	1.0
Di(2-ethylhexyl)phthalate	µg/L	< 1.0	< 1.0	< 1.0	< 1.0	8.0
Dichloromethane	µg/L	< 1.0	< 1.0	< 1.0	< 1.0	20.0
Difenoconazole	µg/L	< 1.0	< 1.0	< 1.0	< 1.0	30.0
Dimethoate + omethoate	µg/L	< 1.05	< 1.05	< 1.05	< 1.05	1.20
Diuron	µg/L	< 1.0	< 1.0	< 1.0	< 1.0	20.0
Epichlorohydrin	µg/L	< 0.10	< 0.10	< 0.10	< 0.10	0.40
Epoxiconazole	µg/L	< 1.0	< 1.0	< 1.0	< 1.0	60.0
Ethylbenzene	µg/L	< 1.0	< 1.0	< 1.0	< 1.0	300.0
Fipronil	µg/L	< 0.05	< 0.05	< 0.05	< 0.05	1.20
Flutriafol	µg/L	< 1.0	< 1.0	< 1.0	< 1.0	30.0
g-Chlordane	µg/L	< 0.01	< 0.01	< 0.01	< 0.01	2.0
Glyphosate + AMPA	µg/L	13.9	13.226	< 15.0	< 15.0	500.0
Hydroxy-Anthrazine	µg/L	< 1.0	< 1.0	< 1.0	< 1.0	120.0
Melathione	µg/L	< 0.05	< 0.05	1.79	1.79	60.0
Mancozeb + Ampa	µg/L	< 7.0	< 7.0	5.250	5.255	8.0
Methamidophos + Acephate	µg/L	< 2.0	< 2.0	1.50	1.50	7.0
Metolachlor	µg/L	< 0.01	< 0.01	0.26	0.26	10.0
Metribuzim	µg/L	< 1.0	< 1.0	0.78	0.78	25.0
Moninate	µg/L	< 0.05	< 0.05	0.038	0.038	6.0
Paraquat	µg/L	< 10.0	< 10.0	< 10.0	< 10.0	13.0
Pentachlorophenol	µg/L	< 0.05	< 0.05	< 0.05	< 0.05	9.0
Picloram	µg/L	< 0.05	< 0.05	< 0.05	< 0.05	60.0
Profenofos	µg/L	< 0.10	< 0.10	< 0.10	< 0.10	0.3
Propargite	µg/L	< 1.0	< 1.0	< 1.0	< 1.0	30.0
Protioconazole + ProticonazolDestio	µg/L	< 3.0	< 3.0	< 3.0	< 3.0	3.0
Simazine	µg/L	< 0.05	< 0.05	< 0.05	< 0.05	2.0
Tebuconazole	µg/L	< 1.0	< 1.0	0.88	0.88	180.0
Terbufos	µg/L	< 0.05	< 0.05	0.11	0.11	1.2
Carbon tetrachloride	µg/L	< 0.5	< 0.5	0.563	0.563	4.0
Tetrachloroethene	µg/L	< 1.0	< 1.0	< 1.0	< 1.0	40.0
Thiamethoxam	µg/L	< 1.0	< 1.0	< 1.0	< 1.0	36.0
Thiodicarb	µg/L	< 1.0	< 1.0	< 1.0	< 1.0	90.0
Toluene	µg/L	< 1.0	< 1.0	0.94	0.94	30.0
Trichloroethene	µg/L	< 0.5	< 0.5	0.444	0.444	4.0
Trifluralin	µg/L	< 0.05	< 0.05	0.045	0.045	20.0
Trihalomethanes	mg/L	0.018	0.025	0.021	0.021	0.100
Xylenes	µg/L	< 3.0	< 3.0	2.63	2.63	500.0

Substances that affect the organoleptic standards						
Total aluminum	mg/L	0.002	0.003	0.001	< 0.001	0.200
Ammonia	mg/L	< 0.10	< 0.10	< 0.10	< 0.0003	1.20
Chloride	mg/L	7.35	10.74	8.7	7.0	250.00
Apparent color	uH	< 5.0	< 5.0	< 5.0	< 5.0	15.0
1,2-Dichlorobenzene	mg/L	< 0.001	< 0.001	< 0.001	< 0.001	0.001
1,4-Dichlorobenzene	mg/L	< 0.0003	< 0.0003	< 0.0003	< 0.0003	0.0003
Total hardness	mg/L	26.42	36.06	25.2	24.6	300.00
Total iron	mg/L	0.024	0.018	0.003	0.004	0.300
Taste and odor	Intensity					6.00
Total manganese	mg/L	< 0.001	0.00102	0.0008	0.0103	0.10
pH	-	8.3	8.6	7.84	7.71	6-9
Total sodium	mg/L	7.7	5.9	3.134	3.373	200.0
Total dissolved solids	mg/L	68	82	50.6	48.8	500
Sulfate	mg/L	2	2.7	1.94	2.56	250.0
Hydrogen sulfide	mg/L	< 0.05	< 0.05	0.17	0.17	0.05
Turbidity	NTU	< 0.1	< 0.1	0.12	0.09	0.5
Total zinc	mg/L	0.002	0.001	0.002	0.008	5.000

Figure B1. Comparison between UF feed turbidity and its permeability in scenarios with and without pretreatment.

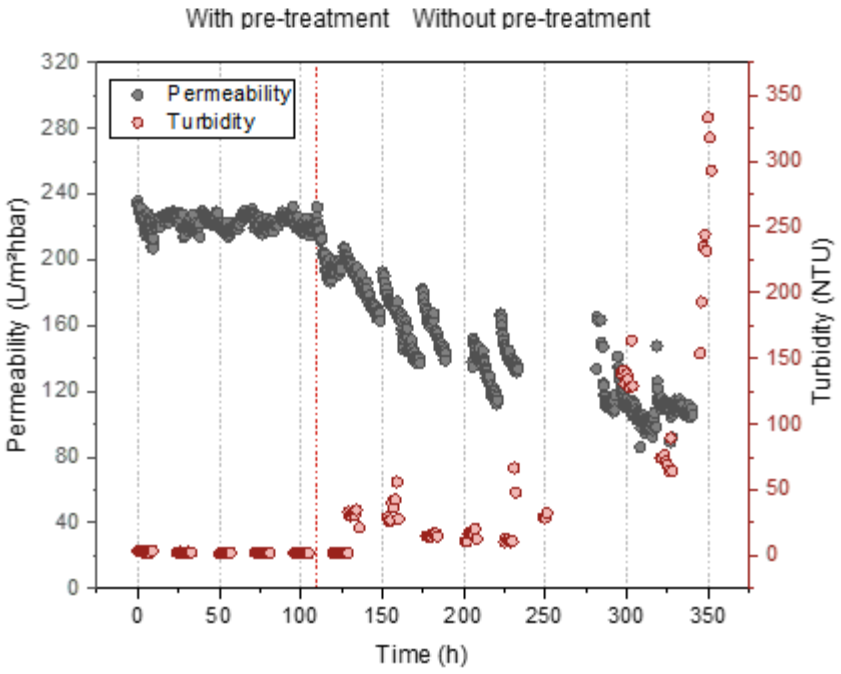

Figure B2. Comparison between ultrafiltration (UF) flux after membrane's cleaning (Jac) and the value at the beginning of the operation (J_0), for different cleaning cycles.

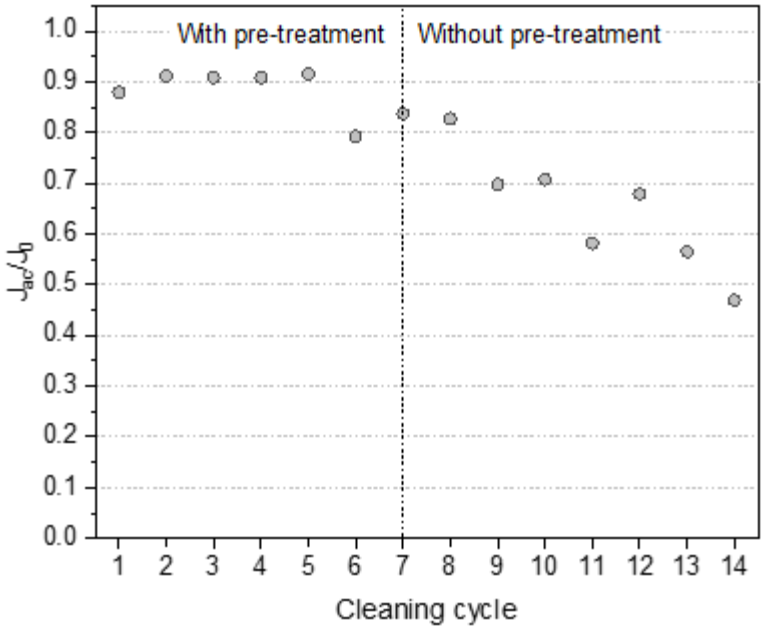

APPENDIX C

Table C1 - Sample N for "Table 4.3. Physicochemical characterization of reverse osmosis currents during the simulation of different conditions"

Parameter	First module of 1st stage 			Last module of 1st stage and first of 2nd stage 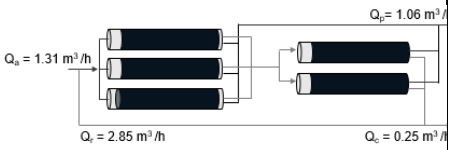			Last modules of 2nd stage 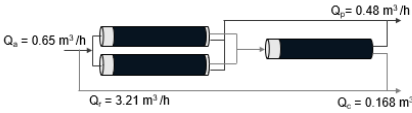		
	UF permeate	**RO Permeate**	**RO Concentrate**	**UF permeate**	**RO Permeate**	**RO Concentrate**	**UF permeate**	**RO Permeate**	**RO Concentrate**
Turbidty (NTU)	112	168	8	46	100	5	69	61	21
Color (uH)	105	206	11	51	102	5	66	66	18
Arsenic (µg/L)	67	72	14	17	26		70	12	34
Iron (mg/L)	58	63	6	17	26	5	31	7	30
Manganese (mg/L)	61	69	6	17	24	5	31	6	29
Calcium (mg/L)	31	31	-	12	18	5	29	25	-
Magnesium (mg/L)	28	25	-	-	13	-	29	25	-
Conductivity (µS/cm)	109	219	13	51	101	-	65	69	34
pH	110	222	12	51	102	5	68	68	29
Total dissolved solids (mg/L)	111	217	11	49	64	5	47	64	34

APPENDIX D

Figure D1. Pourbaix diagram for manganese. In the diagram, the blue dot represents the surface water characteristics: pH = 7.25 and Eh = 0.12 V.

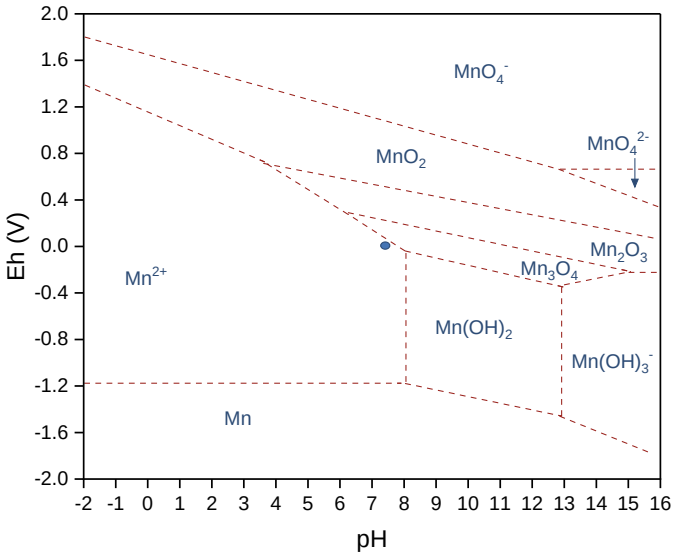

Table D1. Statistics for Mann-Whitney test comparing the final permeate flux in experiment without (J) and with (J_{FeCl3}) an in-line dose of coagulant.

Fe^{3+} (mg/L)	U	Z	p-value	Decision
0.086	0.5	-2.80167	0.99849	$J < J_{FeCl3}$
0.103	12	-0.98638	0.87814	$J < J_{FeCl3}$
0.138	15	-0.43077	0.72677	$J < J_{FeCl3}$
0.172	31.5	2.11141	**0.01737**	$J > J_{FeCl3}$

Table D2. Statistics for Kruskal-Wallis post-hoc with Dunn's test comparing the final permeate flux in experiment at different in-line doses of coagulant.

Fe^{3+} (mg/L)	Mean rank difference	Z	p-value	Decision
0.086 – 0.103	2.5833	0.66318	1.0000	Difference is non-significant
0.086 – 0.138	5.4166	1.39054	0.9861	Difference is non-significant
0.103 – 0.172	9.0000	2.31043	0.1251	Difference is non-significant
0.103 – 0.138	2.8333	0.72736	1.0000	Difference is non-significant
0.103 – 0.172	6.4166	1.64725	0.5970	Difference is non-significant
0.138 – 0.172	3.5833	0.9199	1.0000	Difference is non-significant

Figure D2. Ultrafiltration permeate flux in L/m²h (LMH) for the four stages of ultrafiltration recycling. In-line dose of $FeCl_3$ before ultrafiltration: 0.086 mg/L. J/J_0: the ratio between final permete flux (at 90% recovery rate) and initial permeate flux.*Data not-available

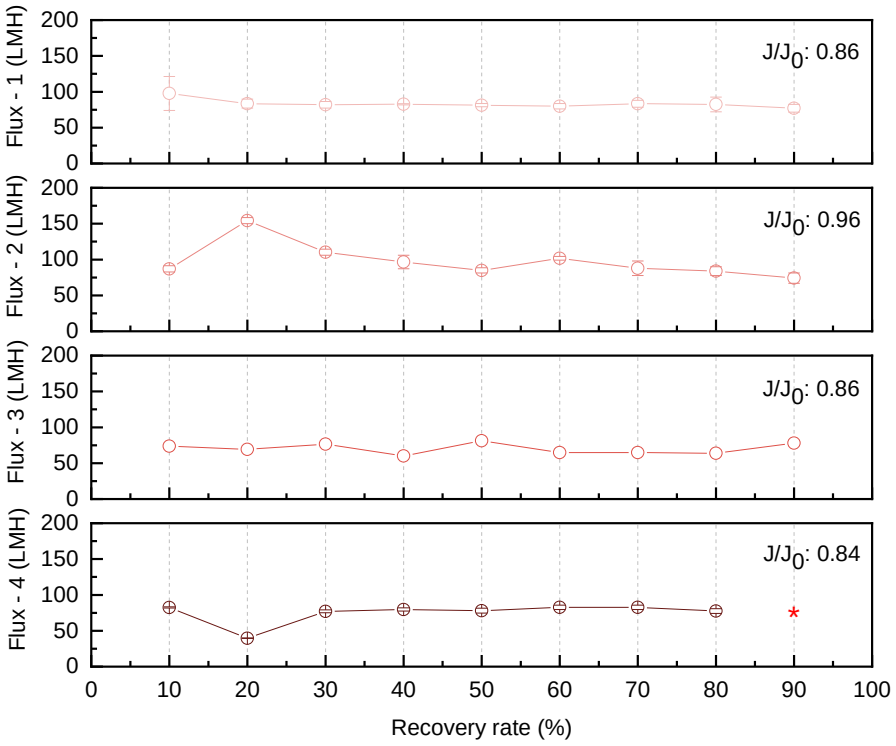

Table D3. Overview of physical, chemical, and biological parameters associated with the ultrafiltration permeate when operated with the in-line dosage of $FeCl_3$. MPV: maximum permitted value.

Parameters	MPV	Average	Standard deviation	Median	Minimum	Maximum
1,2-dichlorobenzene (mg/L)	0.01	<0.001	-	-	-	-
1,4-dichlorobenzene (mg/L)	0.03	<0.0003	-	-	-	-
Total aluminum (mg/L)	0.2	0.0072	0.0046	0.0072	0.0040	0.0105
Ammonia (mg/L)	-	<0.1	-	-	-	-
Chloride (mg/L)	250	27.2	2.0	27.2	25.8	28.6
Apparent color (uH)	15	<5	-	-	-	-
Total hardness (mg/L)	500	57.4	5.7	57.4	53.4	61.4
Total iron (mg/L)	0.3	<0.001	-	-	-	-
Taste (mg/L)	-	None	-	-	-	-
Total manganese (mg/L)	0.1	<0.0010	-	-	-	-
Odor	-	None	-	-	-	-
pH	6 - 9.5	7.78	0.41	7.78	7.49	8.07
Total sodium (mg/L)	200	2.78	0.09	2.78	2.71	2.84
Total dissolved solids (mg/L)	1000	104	45	104	72	136
Sulfate (mg/L)	250	-	-	-	-	-
Hydrogen sulfide (mg/L)	0.1	<0.05	-	-	-	-
Turbidity (NTU)	5	<0.10	-	-	-	-
Total zinc (mg/L)	5	<0.0010	-	-	-	-
(cis+trans) 1,2-Dichloroethene (mg/L)	0.05	-	<1.2	-	-	-
1,4-dioxane (mg/L)	-	-	<1	-	-	-
2,4-D ((2,4-Dichlorophenoxy)acetic acid) (mg/L)	-	-	<0.05	-	-	-
Total Haloacetic Acids (5 compounds) (mg/L)	-	0.035	0.032	0.005	0.032	0.028
Total haloacetic acids (mg/L)	0.08	0.037	0.038	0.002	0.038	0.036
Acrylamide (mg/L)	0.0005	-	<0.1	-	-	-
Alachlor (mg/L)	0.02	-	<0.05	-	-	-
Aldicarb + Aldicarb sulfone + Aldicarb sulfoxide (mg/L)	0.01	-	<3	-	-	-
Aldrin + dieldrin (mg/L)	0.00003	-	<0.02	-	-	-
Ametrine (mg/L)	-	-	<1	-	-	-
Atrazine (mg/L)	0.002	-	<0.25	-	-	-
Atrazine + S- Chlorotriazines (Deethyl-Atrazine - Dea, S- Chlorotriazines (Deethyl-Atrazine - Dea, Deisopropyl Atrazine - Dia and Diaminochlorotriazine - Dact) (mg/L)	-	-	<2	-	-	-
Benzene (mg/L)	0.005	-	<0.5	-	-	-
Benzo(a)pyrene (mg/L)	0.0007	-	<0.01	-	-	-
Carbendazim (mg/L)	-	-	<1	-	-	-
Carbofuran (mg/L)	0.007	-	<0.05	-	-	-
Cyproconazole (mg/L)	-	-	<1	-	-	-
Vinyl chloride (mg/L)	0.002	-	<0.5	-	-	-

Chlorothalonil (mg/L)	-	-	<0.05	-	-	-
DDT + DDE + DDD (mg/L)	0.001	-	<0.03	-	-	-
Di(2-ethylhexyl)phthalate (mg/L)	0.008	-	<1	-	-	-
Dichloromethane (mg/L)	0.02	-	<1	-	-	-
Difenoconazole (mg/L)	-	-	<1	-	-	-
Dimethoate + omethoate (mg/L)	-	-	<1.05	-	-	-
Diuron (mg/L)	0.09	-	<1	-	-	-
Epichlorohydrin (mg/L)	-	-	<0.1	-	-	-
Epoxiconazole (mg/L)	-	-	<1	-	-	-
Ethylbenzene (mg/L)	0.2	-	<1	-	-	-
Fipronil (mg/L)	-	-	<1.2	-	-	-
Flutriafol (mg/L)	-	<0.05	-	-	-	-
G- Chlordane (mg/L)	0.0002	<1	-	-	-	-
Glyphosate + AMPA (mg/L)	0.5	<0.01	-	-	-	-
Hydroxy- atrazine (mg/L)	-	<15	-	-	-	-
Malathion (mg/L)	-	<1	-	-	-	-
Mancozeb(mg/L)	0.18	<0.05	-	-	-	-
Mancozeb + ETU (mg/L)	-	<5	-	-	-	-
Methamidophos(mg/L)	0.012	<7	-	-	-	-
Metolachlor (mg/L)	0.01	<1	-	-	-	-
Metribuzim (mg/L)	-	<0.01	-	-	-	-
Molinate (mg/L)	0.006	<1	-	-	-	-
Paraquat (mg/L)	-	<0.05	-	-	-	-
Pentachlorophenol(mg/L)	0.009	<10	-	-	-	-
Picloram (mg/L)	-	<0.05	-	-	-	-
Profanophos (mg/L)	0.06	<0.05	-	-	-	-
Propargite (mg/L)	-	<0.1	-	-	-	-
Prothioconazole + proticonazoledesthio (mg/L)	-	<1	-	-	-	-
Simazine (mg/L)	0.002	<3	-	-	-	-
Tebuconazole (mg/L)	0.18	<0.05	-	-	-	-
Terbufos (mg/L)	0.0012	<1	-	-	-	-
Carbon tetrachloride (mg/L)	0.004	<0.05	-	-	-	-
Tetrachloroethene (mg/L)	0.04	<0.5	-	-	-	-
Thiamethoxam (mg/L)	-	<1	-	-	-	-
Thiodicarb (mg/L)	-	<1	-	-	-	-
Toluene (mg/L)	0.17	<0.1	-	-	-	-
Trichloroethene (mg/L)	0.02	<1	-	-	-	-
Trifluralin (mg/L)	0.02	<0.3	-	-	-	-
Trihalomethanes (mg/L)	0.1	<0.05	-	-	-	-
Xylenes (mg/L)	0.3	0.034	0.005	0.034	0.030	0.037
Total antimony (mg/L)	0.005	<0.0005	-	-	-	-
Total barium (mg/L)	0.7	0.0110	0.0049	0.0110	0.0075	0.0144
Total cadmium (mg/L)	0.005	<0.0005	-	-	-	-
Chlorate (mg/L)	-	0.05	-	0.05	0.05	0.05

Chlorite (mg/L)	1	<0.02	-	-	-	-
Free residual chlorine (mg/L)	0.2 - 5.0	1.43	-	1.43	1.43	1.43
Total copper (mg/L)	2	<0.00025	-	-	-	-
Total chrome (mg/L)	0.05	0.0013	0.0011	0.0013	0.0005	0.0020
Fluoride (mg/L)	1.5	0.64	0.01	0.64	0.63	0.64
Total mercury (mg/L)	0.001	<0.0001	-	-	-	-
Total nickel (mg/L)	0.07	0.0014	0.0005	0.0014	0.0010	0.0017
Nitrate (as N) (mg/L)	10	0.23	0.08	0.23	0.17	0.29
Nitrite (as N) (mg/L)	1	<0.01	-	-	-	-
Total selenium (mg/L)	0.01	<0.0005	-	-	-	-
Total uranium (mg/L)	0.03	<0.0005	-	-	-	-